

CA 850 8074

A Review of Fusion Breeder Blanket Technology

Part 1 / Review and Findings

Authors

D.P. Jackson	R.A. Verrall	P.M. Garvey
W.N. Selander	R.L. Tapping	W.J. Holtslander
B.M. Townes	J.S. Geiger	I.J. Hastings
T.C. Leung	O.S. Tatone	A.D. Lane
J.N. Miller	E.C. Carlick	

CFFTP GENERAL

CFFTP Report Number
CFFTP-G-84033

Cross Reference Report
AECL-8631

January 1985

The Canadian Fusion Fuels Technology Project represents part of Canada's overall effort in fusion development. The focus for CFFTP is tritium and tritium technology. The project is funded by the governments of Canada and Ontario, and by Ontario Hydro.

The Project is managed by Ontario Hydro.

CFFTP will sponsor research, development and studies to extend existing experience and capability gained in handling tritium as part of the CANDU fission program. It is planned that this work will be in full collaboration and serve the needs of international fusion programs.

A REVIEW OF FUSION BREEDER BLANKET TECHNOLOGY

PART I: REVIEW AND FINDINGS - December 1984

Report No. CFFTP-G-84033
X-Ref Report: AECL-8631

Issue Date: January 1985

by D.P. Jackson, W.N. Selander, B.M. Townes,
T.C. Leung, J.N. Miller, R.A. Verrall, R.L. Tapping
J.S. Geiger, O.S. Tatone, E.C. Carlick, P.M. Garvey
W.J. Holtslander, I.J. Hastings, A.D. Lane

CFFTP GENERAL

'C - Copyright Ontario Hydro, Canada-1984
Enquiries about Copyright and reproduction should be
addressed to the:

Program Manager,CFFTP
2700 Lakeshore Road West
Mississauga, Ontario
L5J 1K3'

Submitted by:

D.P. Jackson
D.P. Jackson, Project Manager
Solid State Science Branch
Atomic Energy of Canada Limited
Chalk River Nuclear Laboratories
Chalk River, Ontario K0J 1J0

W.N. Selander
W.N. Selander

O.S. Tatone
O.S. Tatone

B.M. Townes
B.M. Townes

E.C. Carlick
E.C. Carlick

T.C. Leung
T.C. Leung

P.M. Garvey
P.M. Garvey

J.M. Miller
J.M. Miller

W.J. Holtlander
W.J. Holtlander

R.A. Verrall
R.A. Verrall

I.J. Hastings
I.J. Hastings

R.L. Tapping
R.L. Tapping

A.D. Lane
A.D. Lane

J.S. Geiger
J.S. Geiger

Reviewed by:

for

M.D. Dautovich
D.P. Dautovich
Manager - Technology Development
Canadian Fusion Fuels Technology Project

Approved by:

M.D. Dautovich
T.S. Dautovich
Program Director

PROJECT TEAM

Atomic Energy of Canada Limited Research Company
Chalk River Nuclear Laboratories
Chalk River, Ontario
K0J 1J0
(613) 584-3311

	Branch/Division	Technical Area	Authorship
Project Manager			
D.P. Jackson	Solid State Science	Fusion Systems	0, 1.1, 2, 6, 7, A.1
Project Team			
W.N. Selander	Mathematics & Computation	Liquid Metals	4.1, 4.2
B.M. Townes	Reactor Physics	Neutronics	3.2, 3.4 3.5
T.C. Leung	Reactor Physics	Neutronics	3.1, 3.3 3.5
J.M. Miller	Chemical Engineering	Tritium	4.4, 5.5
R.A. Verrall	Fuel Materials	Solid Breeders	5.
R.L. Tapping	System Materials	Corrosion	4.3
O.S. Tatone	Technical Information	Editorial	-
J.S. Geiger	Nuclear Physics	Fusion Systems	1.2,1.3, A.2,A.3
E.C. Carlick	Maintenance & Construction	Liquid Metals	4.1,4.2
W.J. Holtslander	Chemical Engineering	Tritium	4.4,5.5
I.J. Hastings	Fuel Materials	Solid Breeders	5.
A.D. Lane	Fuel Materials	Solid Breeders	5.6

ACKNOWLEDGEMENTS

We are grateful to the many scientists and engineers in the world fusion community who willingly provided us with information, allowed us to visit their laboratories, welcomed us to symposia and workshops and throughout gave us opportunities for free dialogue with them. Without their cooperation and assistance the work of this study would have been very much more difficult. We would have liked to acknowledge each one of them by name, but there are so many that this is not practical.

We are indebted to CFFTP for sponsoring this project and to AECL for cofunding it. Special thanks are due to Don Dautovich of CFFTP and Bill Seddon of CRNL, who were instrumental in initiating the project, for their support and encouragement throughout.

Finally, our sincere thanks to those upon whom the heavy burden of typing this large report fell: Norma Yeatman, Trudy Ingram, Connie St. Jean, Joan Vaudry, Madeleine Boulanger, Alison Lennard and in particular, to Mary Boland, who had the heaviest typing load of all.

ABSTRACT

This report presents the results of a study of fusion breeder blanket technology. It reviews the role of the breeder blanket, the current understanding of the scientific and engineering bases of liquid metal and solid breeder blankets and the programs now underway internationally to resolve the uncertainties in current knowledge. In view of existing national expertise and experience, a solid breeder R&D program for Canada is recommended.

TABLE OF CONTENTS

	<u>Page</u>
0. EXECUTIVE SUMMARY	0-1
1. INTRODUCTION	1-1
1.1 The Scope and Conduct of the Study	1-1
1.1.1 Scope of the Study	1-1
1.1.2 Conduct of the Study	1-2
1.1.2.1 Phase I	1-3
1.1.2.2 Phase II	1-3
1.1.2.3 Phase III	1-4
1.2 The Thermonuclear Fuel Cycle	1-5
1.3 The Necessity for Breeding	1-5
2. BREEDER BLANKETS	
2.1 Overview of Breeder Blankets	2-1
2.1.1 Liquid Metal Breeders	2-3
2.1.2 Solid Breeders	2-5
2.2 Factors in the Design of a Breeder Blanket	2-7
2.2.1 Materials Selection - Structural Materials	2-8
2.2.2 Neutronics Evaluation of Blankets	2-16
2.2.3 Tritium Breeding Ratios	2-19
2.3 Examples of Blanket Design Concepts	2-22
2.3.1 Fusion Reactor Concepts	2-22
2.3.2 STARFIRE	2-23
2.3.3 DEMO	2-31
2.3.4 MARS	2-34
2.3.5 FPD	2-44
2.3.6 INTOR	2-46
2.3.7 FER	2-47
2.4 Summary	2-48

TABLE OF CONTENTS (continued)

	<u>Page</u>
3. NEUTRONICS ASPECTS OF FUSION BLANKETS	3-1
3.1 Status of Neutronics/Photonics Data	3-1
3.1.1 Introduction	3-1
3.1.2 Neutronics Data	3-2
3.1.2.1 Data for Tritium Breeding	3-2
3.1.2.2 Neutron Emission Data	3-5
3.1.2.3 Radiation Damage Data	3-6
3.1.3 Photonics Data	3-6
3.1.4 Nuclear Data Libraries	3-7
3.1.5 Accuracy of Nuclear Data	3-12
3.2 Status of Neutron/Photon Transport Methods	3-14
3.2.1 Introduction	3-14
3.2.2 Transport Theory	3-15
3.2.3 Monte Carlo Method	3-18
3.3 Validation of Data and Methods Against Experimental Benchmarks	3-19
3.3.1 Introduction	3-19
3.3.2 Review of Some Earlier Integral Experiments	3-20
3.3.3 Validation of Data	3-21
3.3.4 Validation of Methods	3-29
3.3.5 Future Trends	3-34
3.4 Application to Fusion Blankets	3-38
3.4.1 Introduction	3-38
3.4.2 Relevant Nuclear Reactions	3-38
3.4.3 Overall Accuracy	3-40
3.4.4 Tritium Production	3-42
3.4.5 Heat Production	3-44
3.4.6 Shielding	3-44
3.4.7 Activation	3-46
3.4.8 Radiation Damage	3-46
3.4.9 Developments in Neutronics	3-46
3.5 Summary	3-47

TABLE OF CONTENTS (continued)

	<u>Page</u>
4. LIQUID METAL BREEDERS	4-1
4.1 Introduction	4-1
4.2 Engineering Considerations for Liquid Metal Breeder Systems	4-2
4.2.1 General Design Requirements for a Blanket	4-2
4.2.2 Thermal and Hydraulic Considerations	4-5
4.2.3 MHD Pumping Resistance	4-9
4.2.4 Maintenance	4-13
4.2.5 Safety	4-14
4.3 Materials Compatibility and Corrosion	4-20
4.3.1 The State of the Literature to Date	4-20
4.3.2 Solubility of Metals and Non-Metals in Liquid Li and Li-Pb Solutions	4-26
4.3.2.1 Liquid Lithium	4-26
4.3.2.2 Liquid Lithium-Lead and Lead	4-29
4.3.3 Behaviour of Austenitic Alloys in Liquid Li and Li-Pb	4-29
4.3.3.1 General Corrosion Behaviour in Li	4-29
4.3.3.2 Selective Dissolution and Intergranular Attack in Li	4-31
4.3.3.3 Effect of Li on Mechanical Properties	4-32
4.3.3.4 Effects of Li Flow Velocity on Corrosion	4-33
4.3.3.5 Overall Corrosion Behaviour in Li-Pb	4-34
4.3.4 Behaviour of Ferritic Alloys in Liquid Li and Li-Pb	4-35
4.3.4.1 General Corrosion Behaviour in Li and Li-Pb	4-35
4.3.4.2 Intergranular Attack and Mechanical Properties in Li and Li-Pb	4-36
4.3.5 Behaviour of Refractories and Other Materials in Liquid Li	4-38
4.3.6 Mass Transfer Considerations	4-41
4.3.7 Some Gettering and Impurity Considerations	4-44
4.3.8 Conclusions on Corrosion	4-45

TABLE OF CONTENTS (continued)

	<u>Page</u>
4.4 Tritium Handling and Extraction with Liquid Metal Blankets	4-46
4.4.1 Tritium Solubility in Liquid Metals	4-48
4.4.2 Tritium Recovery from Liquid Lithium and Li₁₇-Pb83	4-50
4.4.2.1 Molten Salt Extraction	4-50
4.4.2.2 Solid Getters	4-51
4.4.2.3 Cold-Trapping	4-52
4.4.2.4 Permeation	4-53
4.4.2.5 Inert Gas Sparging	4-54
4.4.2.6 Direct Pumping	4-54
4.5 Summary	
5. SOLID BREEDERS	5-1
5.1 Introduction	5-1
5.2 Fabrication and Characterization	5-2
5.2.1 Lithium Ceramic Preparation for FUBR-1A	5-3
5.2.1.1 Powder Preparation	5-3
5.2.1.2 Pellet Formation	5-7
5.2.2 Lithium Ceramic Fabrication for TRIO-01	5-8
5.2.3 Mass Production of Li₂O Pellets	5-8
5.2.3.1 Japan	5-8
5.2.3.2 France	5-8
5.2.3.3 USA	5-9
5.2.4 Characterization	5-9
5.3 Physical and Chemical Properties	5-11
5.3.1 Thermal Properties	5-18
5.3.2 Thermal Stability	5-20
5.3.3 Operating Temperature Limits	5-23
5.3.4 Compatibility with Structural Materials	5-24
5.4 In-Reactor Behaviour	5-28
5.4.1 Fundamental Studies	5-29
5.4.2 Mechanical Behaviour of Irradiated Capsule Specimens	5-30

TABLE OF CONTENTS (continued)

	<u>Page</u>
5.5 Tritium Recovery from Solid Breeders	5-34
5.5.1 Tritium Release	5-34
5.5.1.1 Bulk Diffusion	5-34
5.5.1.2 Gas Phase Transport	5-38
5.5.1.3 Solubility	5-38
5.5.2 Tritium Inventory Considerations	5-42
5.5.3 Tritium Extraction	5-42
5.5.3.1 Thermal Extraction Studies	5-42
5.5.3.2 In Situ Tritium Recovery	5-43
5.6 Blanket Technology	5-45
5.6.1 Introduction	5-45
5.6.2 Coolants and Structural Materials	5-46
5.6.3 Blanket Configurations	5-47
5.6.3.1 Water-Cooled Blanket Configurations	5-49
5.6.3.2 Helium-Cooled Blanket Configurations	5-52
5.6.3.3 Neutron Multipliers	5-52
5.6.4 Breeder Temperature Control	5-55
5.6.5 Breeder Ceramic Size Considerations	5-56
5.7 Summary	5-58
6. RESEARCH AND DEVELOPMENT IN BREEDER BLANKETS	6-1
6.1 Introduction	6-1
6.2 US Program	6-1
6.2.1 Blanket Comparison and Selection Study	6-1
6.2.2 US R&D Program	6-7
6.3 EEC Program	6-11
6.4 Japanese Program	6-14
6.5 International Collaboration in Blanket R&D	6-17
6.5.1 IEA	6-17
6.5.2 IAEA	6-19
6.5.3 Bilateral Agreements	6-23

TABLE OF CONTENTS (continued)

	<u>Page</u>
6.6 Canadian Capabilities for Breeder Blanket R&D	6-24
6.6.1 Liquid Metal Breeders	6-25
6.6.2 Solid Breeders	6-26
6.7 Summary	6-28
7. CONCLUSIONS AND RECOMMENDATIONS	7-1
7.1 Conclusions	7-1
7.2 Recommendation	7-2
8. REFERENCES	8-1
APPENDICES	A-1
Appendix A.1: Tritium Production in Fission Reactors	A-1
Appendix A.2: Spallation Breeding	A-1
Appendix A.3: D-D Reactor Breeders	A-2
References to Appendices	A-3

LIST OF TABLES

- 1-1 Fusion Reaction Properties
- 2-1 Liquid Metal Breeders - Critical Issues
- 2-2 Solid Breeder Materials (SBMs) - Critical Issues
- 2-3 Thermal Properties of Candidate Structural Materials
- 2-4 TBRs for Four Blanket Designs
- 2-5 Parameters for Some Commercial Tokamak Designs
- 2-6 Summary of STARFIRE Blanket Design Parameters
- 2-7 Parameters for Some Near-Term Tokamak Designs
- 2-8 Design Parameters for Mirror Reactors
- 2-9 MARS Blanket Parameters
- 3-1 Types of Nuclear Data Required
- 3-2 Nuclear Data of Importance to Neutronics Calculations in Blanket
- 3-3 Evaluated Nuclear Data Libraries
- 3-4 Contents of ENDF/B Library
- 3-5 Required Data Accuracies
- 3-6 Some Earlier Integral Experiments
- 3-7 Ratios of Calculated to Measured Flux Integrals
- 3-8 Comparison of ANISN, DOT-II and MORSE Calculations of Total Tritium Production Normalized to One Source Neutron
- 3-9 Comparison of TFTR and RTNS-II Neutron Parameters
- 3-10 Predictions Required from Neutronics Calculations
- 3-11 Nuclear Performance Characteristics
- 3-12 Estimated Tritium Breeding Ratio Likely to be Achievable in Fusion Power Reactors
- 4-1 A Summary of Corrosion Test Conditions and Results for Liquid Lithium and Lithium-Lead Alloys
- 4-2 Typical Compositions of Alloys Mentioned in Section 4.3
- 4-3 Solubility of Various Elements in Liquid Lithium
- 4-4 Limiting Temperature Criteria ($^{\circ}$ C) for Liquid Metal Corrosion
- 5-1 Data on Breeding Materials: Physics-Chemical Properties, Neutronic Properties, Tritium Breeding and Extraction, Irradiation, Activation Products
- 5-2 Thermal Expansion Coefficient of Lithium Ceramics
- 5-3 Recommended Temperature Limits for Candidate Solid Breeder Materials. Effects of radiation on these limits is not known and not reflected in this table.
- 5-4 References and Test Conditions for Compatibility Studies Between Lithium Ceramics and Cladding and Structural Materials.
- 5-5 Post-Irradiation Examination of Lithium Ceramics Irradiated in ORR for Six Months
- 5-6 Diffusion Coefficient of Tritium in Solid Breeder Materials at 560 $^{\circ}$ C

LIST OF TABLES (continued)

- 6-1 BCSS Preliminary Rankings for Tokamak Blanket Concepts as of 83 December:
Liquid Metal and Molten Salt Breeders**
- 6-2 BCSS Preliminary Rankings for Tokamak Blanket Concepts as of 83 December:
Solid Breeders**
- 6-3 EEC Blanket R&D Program Components for Current 5-Year Plan**
- 6-4 Solid Breeder Material Sources - Primary Materials (Powders) from [317]**
- 6-5 Solid Breeder Material Sources - Formed Materials from [317]**
- 6-6 Solid Breeder Materials in R&D Programs from [317]**

LIST OF FIGURES

- 2-1 Breeder blanket types.
- 2-2 Relationship between helium production and dpa for some stainless steels
- 2-3 Required TBR versus doubling time.
- 2-4 The STARFIRE tokamak.
- 2-5 Details of the STARFIRE blanket.
- 2-6 STARFIRE blanket schematic.
- 2-7 DEMO blanket schematic.
- 2-8 The MARS facility.
- 2-9 MARS central cell cross-section.
- 2-10 MARS blanket details.
- 2-11 MARS solid blanket concept.
- 2-12 MARS solid blanket model.
- 2-13 MARS high temperature blanket.
- 3-1 Lithium experiment at JAERI.
- 3-2 The LBM assembly.
- 4-1 Liquid breeder blanket section showing the gradation in the number of coolant tubes contained with the five rows of breeder tubes.
- 4-2 Example of cold trap plugging by corrosion deposits (primarily Fe) in a lead-bismuth thermal connection loop in operation at CRNL in 1966.
- 4-3 The effect of tritium concentration in liquid metal on the tritium pressure over the metal.
- 4-4 The effect of temperature, tritium pressure, and structural material on the tritium flux (mass flow rate per unit area) times the wall thickness.
- 5-1 Li₂O powder preparation process developed by ANL.
- 5-2 Two methods of powder fabrication of LiAlO₂ developed by ANL.
- 5-3 Organometallic process used to prepare Li₄SiO₄ and Li₂ZrO₃ powders by McDonnell Douglas.
- 5-4 Specific heat capacities of lithium ceramic breeders.
- 5-5 Thermal conductivity of lithium ceramic breeders.
- 5-6 Partial pressure of lithium over various lithium aluminum oxides and Li₂O.
- 5-7 Schematic of tritium recovery from solid breeders.
- 5-8 Diffusion coefficient of tritium in Li₂O as a function of temperature.
- 5-9 Tritium solubility in Li₂O as a function of temperature and partial pressure of T₂O (x = H, D, T)
- 5-10 Power adsorption distributions for a (30% lithium-6 enriched) INTOR design.
- 5-11 Blanket designs for water-cooled solid breeders.
- 5-12 A lobular blanket design for helium-cooled solid breeders, showing breeder location, coolant flow, and first wall arrangements.
- 6-1 Schematic of US solid breeder program.
- 6-2 Schematic of Japanese solid breeder program.

O. EXECUTIVE SUMMARY

The purpose of this study is to provide an integrated critical assessment of the current status of fusion breeder blanket technology, including the international programs in the area, in order to identify potential opportunities for Canadian initiatives, and to make recommendations for specialized research in this area to be supported by the Canadian Fusion Fuels Technology Project.

A deuterium-tritium fusion energy economy must be based on tritium generated in the fusion reactors themselves by means of a tritium breeding blanket. Tritium derived from other sources, such as CANDU reactors, will be useful in the initial R&D and start-up stages of the first fusion reactors; however, it is clear that these external sources in themselves will be inadequate to sustain any significant fusion energy capability. Thus, the successful development of effective breeder blankets is crucial to the success of fusion.

The basic concept of all breeder blankets envisaged for deuterium-tritium fusion include the conversion of lithium to tritium by means of fusion reaction neutrons. The lithium may be present as a liquid metal, or eutectic alloy, or in solid form such as a lithium-bearing ceramic. The breeder blanket consists of this breeding material in an assembly fabricated of specified structural materials, a coolant, possibly a neutron multiplier, a neutron reflector if required, and a tritium recovery system. An effective means of extracting tritium from the blanket is essential to the fuel cycle and to prevent an excessive build-up of tritium in the reactor, i.e. to minimize tritium inventory. Furthermore, the blanket will also be required to remove heat to generate the electrical output of the reactor. Therefore, the design of the blanket has a direct impact on the efficiency of the reactor and, in this manner, on its overall economics.

No fusion reactor has yet operated and no breeder blanket has been built. However, a variety of blanket design studies have been done for near-term reactor concepts, i.e. those intended to demonstrate fusion feasibility, and for longer-term commercial types. They are useful in defining the scale and

requirements of blankets and as these studies are refined over time, they reflect the current state of blanket technology. In this way, they define critical issues for blankets and hence, directions for future R&D. Lacking the data required for a definitive choice, no single blanket concept can now be singled out as potentially the most successful; indeed, it is not even possible to choose between liquid metal and solid breeders at this time.

The process of designing a blanket involves deciding between a variety of factors on the basis of materials properties and compatibilities, neutronic performance, mechanical strength, heat transport, etc., within the ranges allowed by the particular fusion reactor for which the blanket is intended. These factors are strongly interrelated but require input from widely different disciplines. In particular a good knowledge of fusion structural materials is needed for the intelligent choice of a breeder blanket.

Neutronics calculations are essential to test the validity of a blanket design since the tritium breeding ratio (the amount of tritium bred/the amount consumed by the reactor) must exceed unity by some reasonable margin. Also, the nuclear heat deposited in the blanket must be favourable for energy production. Therefore, every blanket concept must satisfy these tests of its neutronic performance. The data base and numerical methods for these calculations are fairly well established but improvements are certainly possible. Canada has good neutronics capability through its fission program which can be used in the fusion blanket field.

Liquid metal breeders appear to generate adequate tritium. There are, however, serious concerns over their safety with respect to liquid metal spills, the corrosion of blanket structures by liquid metals, and the interaction of the flowing breeder material with the magnetic fields of the fusion reactor. The situation on tritium extraction is that liquid lithium may pose difficulties in tritium removal and the other leading candidate, a lithium lead alloy, may present problems in tritium containment. R&D on liquid metals generally requires large loops for development work, although specialized generic work on specific topics may be possible. Since these facilities are

not available in Canada and the resources of our fusion program are not sufficient to construct such a facility, the conclusion is that our contributions to liquid metal breeders must be limited.

The solid breeder option has come to the fore in the past few years mainly because of the perceived safety concerns with liquid metals. The basic problem with solid breeders is that it is not certain whether a sufficient tritium breeding ratio could be achieved in a practical system and if so, whether the tritium could be extracted in a reliable manner. These questions depend on detailed investigations of the behaviour of lithium-bearing ceramics under irradiation and in particular, how the evolution of tritium is affected by radiation damage. This involves not only in-reactor tests of these materials but also their understanding at the atomic level. To perform these experiments, well-characterized samples of lithium-bearing ceramics must be fabricated. If solid breeders progress to the blanket stage, one must be able to reproducibly fabricate large quantities of them with well-defined specifications. Canada is well placed to contribute to this field with experience in ceramics from the fission fuels program, expertise in tritium handling and a strong tradition in fundamental studies of nuclear materials. Programs on solid breeders are now underway in the US and Japan and just beginning in Europe and the prospects for Canadian collaboration with these larger programs are excellent, being facilitated by a number of multilateral and bilateral agreements. Therefore, this report recommends a solid breeder program for Canada.

1. INTRODUCTION

1.1 The Scope and Conduct of the Study

This study was initiated by the Canadian Fusion Fuels Technology Project (CFFTP) and done by the Chalk River Nuclear Laboratories (CRNL) of Atomic Energy of Canada Limited Research Company (AECL-RC). The study commenced in 1983 January and was completed in 1984 January; its total cost was 271 k\$, of which 215 k\$ was contributed by CFFTP and 56 k\$ by AECL-RC.

1.1.1 Scope of the Study

The objectives of the study were to:

- survey the current status of research and development in the breeder blanket field;
- report on the existing international programs on solid and liquid metal breeders;
- and hence, to produce a program plan for a Canadian breeder blanket project.

These objectives were pursued against the background of the circumstances of the Canadian fusion program. Firstly, the relatively small budget of the Canadian program means that activities should be integrated and focused with well-defined areas of concentration. No attempt to cover a large portion of the fusion technology area is feasible and selectivity is essential. Furthermore, these R&D areas must be built on the basis of existing expertise and must utilize facilities now largely in place; there is a very limited capability for entry into completely new fields. Finally, it is clear that international collaboration is very important to ensure that the R&D components of the program are meaningful in the wider context of the world fusion community.

These considerations have influenced the emphasis of the study in that there is no attempt to undertake a selection between breeder blanket options or development paths. Such choices are the prerogatives of much larger fusion programs. For similar reasons, the emphasis is not on systems development or the analysis of breeder design concepts. Rather, such work in other programs is used to guide the identification of R&D areas where Canadian expertise can make a recognizable contribution to the world fusion effort. Therefore, the reader should be aware that this study contains a bias towards the Canadian context.

One practical outcome of this reasoning has been in the coverage given to the various breeder blanket topics in this report. Those that are judged to be more promising for Canadian participation have been discussed in more detail. Specific exclusions that have been made are: (a) only tritium breeding blankets are covered, with no consideration of fissile fuel or hybrid breeders; (b) only the main line concepts for magnetic confinement fusion, i.e. tokamaks and mirrors, are included; and (c) no attempt has been made to make economic arguments about breeder blankets, since it is judged that this would be premature.

1.1.2 Conduct of the Study

The study was a three-phase project commencing in 1983 January and ending in 1984 January. The phases of the project are described in the following sections.

1.1.2.1 Phase I

This phase consisted of the familiarization of the study group with the dimensions of the breeder blanket problem. It involved the initial literature search, including the collection of data and documents required for the implementation of Phase II. Identification of international programs relevant to the study, significant conferences occurring during the study period and program meetings of interest to blanket technology were used to refine the

travel component of the Phase II budget. The product of Phase I was a plan for the remainder of the study and a detailed outline of the final report, which were submitted to CFFTP in 1983 March, marking the end of Phase I.

1.1.2.2 Phase II

This phase, the main work of the study, began in 1983 May and ended in 1983 December. It consisted of the study as based on the outline developed in Phase I. During Phase II the study team made the following visits to laboratories involved in blanket research:

- Hanford Engineering Development Laboratory, US, to discuss the liquid lithium program there (two visits);
- SCK/CEN laboratories in Mol, Belgium, to look at their liquid metal work;
- EG&G, US, to discuss liquid metal safety;
- Argonne National Laboratory, US, to discuss their work on breeder blankets;
- Los Alamos National Laboratory, US, to visit the Tritium System Test Assembly;
- CEA (Saclay), France, to discuss their solid breeder program.

In addition, the following conferences were attended:

- the 5th Topical Meeting on the Technology of Fusion Energy, 1983 April 26-28, Knoxville, TN, US (four team members);
- the 3rd Topical Meeting on Fusion Reactor Materials, 1983 September 18-22, Albuquerque, NM, US (three team members).

And, the team participated in workshops on:

- Thermohydraulics of Liquid Metals, Von Karman Institute for Fluid Dynamics, Brussels, Belgium, 1983 May 30 - June 3;
- Fusion Blanket Technology, Erice, Italy, 1983 June 6-10;
- the Blanket Comparison and Selection Study (BCSS), 1983 September 13-14, Argonne, IL, US (two team members);
- the IEA Solid Breeder Workshop, 1983 September 22-23, Albuquerque, NM, US (four team members).

These visits, conferences and workshops, together with an extensive literature study, formed the major work of Phase II. At the end of Phase II, a program review was done consisting of a presentation to CFFTP on the progress of the study and its preliminary conclusions. This occurred on 1983 December 1.

1.1.2.3 Phase III

Phase III consisted of producing the final study reports in the format required by CFFTP. Two reports were produced: (a) Part I, which was the technical review suitable for general distribution; and (b) Part II, a document that outlines a Canadian breeder program, with time and cost estimates. This phase ended in 1984 January and marked the end of the study phase of the project.

1.2 The Thermonuclear Fuel Cycle

In thermonuclear fusion reactions two light nuclei undergoing a relatively violent collision come sufficiently close that their component nucleons interact with one another and regroup to form two or more product nuclei whose total binding energy is significantly greater than that of the colliding pair. The energy represented by this overall change in binding appears as kinetic

energy of motion of the reaction products. Some properties of the more favourable fusion reactions are listed in Table 1-1.

The reaction property that plays the dominant role in the selection of a thermonuclear reaction for any near-term application is the ease with which the reaction can be made to go, i.e. the plasma conditions required to realize a significant thermonuclear reaction rate. This temperature is determined by the velocity dependence of the fusion reaction cross-section. As seen from Table 1-1, the fusion reactions involving hydrogenic partners, D-T and D-D, exhibit the lowest threshold temperatures, with the D-T reaction showing an especially favourable value of only 4 keV (~ 50 million $^{\circ}\text{C}$).

In addition to having the lowest temperature threshold, the D-T reaction provides a large energy yield per fusion event. These properties make D-T thermonuclear fusion easiest to achieve from the plasma physics standpoint, and as a consequence, the main effort of the international fusion community is concentrated on this option.

1.3 The Necessity for Breeding

As we have seen, the nuclear physics properties of the D-T reaction render it particularly attractive for use in thermonuclear fusion reactors. Selection of this reaction does, however, introduce a fueling problem not shared by the other reactions listed in Table 1-1. Deuterium is a naturally occurring stable isotope of hydrogen that can be extracted in essentially limitless quantity and at acceptable cost from water using well developed techniques. Tritium, on the other hand, is a radioactive isotope of relatively short half-life (12.3 years) and is present in nature in extremely small quantities. The three factors responsible for its presence are nuclear weapons tests, fission reactor operations, and cosmic ray interactions in the earth's atmosphere. The tritium needed to fuel any fusion device must be bred, i.e. manufactured, and this study is directed toward some of the technological and engineering problems associated with this breeding.

Table 1-1 Fusion Reaction Properties

Reaction	Energy Release per Fusion (MeV)	Thermonuclear Reaction Temperature Threshold (keV)
D + T → n + ^4He	17.6	4
D + D → n + ^3He	3.2	50
D + D → p + T	4.0	50
D + ^3He → p + ^4He	18.3	100
p + ^6Li → ^3He + ^4He	4.0	900
D + ^6Li → p + ^7Li	5.0	> 900
D + ^6Li → p + T + ^4He	2.6	> 900
D + ^6Li → ^4He + ^4He	22.0	> 900
p + ^7Li → ^4He + ^4He	17.5	> 900
p + ^{11}B → ^4He + ^4He + ^4He	8.7	300

Tritium can be produced by both charged particle and neutron-induced nuclear reactions. The use of accelerator-based charged particle reactions in which an accelerated beam is incident on target material of solid or gaseous form proves to be uneconomic for the same reason that accelerator-based fusion of solid or gaseous targets is uneconomic: the majority of the accelerator particles incident on the target dissipate their kinetic energy through inelastic collisions with the electrons in the target rather than inducing the desired nuclear reaction. The result is that the average energy required to produce a triton in this way is orders of magnitude greater than the energy that can be ultimately removed by burning the tritium thus produced in a fusion reactor.

Neutron-induced reactions can produce tritium with very high particle efficiency. The favoured reactions are the following:



The problem is to find mechanisms which produce the needed neutrons at an acceptable cost in energy (and in dollars) and in sufficient quantity. For first generation D-T fusion power reactors the only practical source for the major portion of these neutrons will be the D-T reaction itself. The reaction vessel will be surrounded by a Li-bearing structure which will serve the two functions of converting the 14.1 MeV of kinetic energy carried by each neutron to thermal energy and of producing tritium to sustain the needed fuel supply through the two reactions listed above. While one can confidently predict breeding ratios (tritium atoms produced per tritium atom burned) greater than unity for neutronically favoured materials and geometries it is less clear that such ratios will be achieved in practical circumstances. This study reviews the current state of knowledge on a range of subjects influencing the choice of breeder materials including neutronics, materials properties and tritium recovery.

Neutrons from other sources must be used to provide the tritium needed for the initial phases of the fusion development programs and to provide the needed inventory for the first tritium breeding fusion reactors built. In the event that the effective breeding ratio (tritium atoms recovered from the blanket per DT fusion reaction) falls below unity, there will be a further need for such tritium. Fission reactors are seen as the near-term source of the extra breeding neutrons. Indeed some tritium is already produced as a by-product of the operation of water-moderated and -cooled reactors, in particular of heavy water reactors. The yield of tritium from Pickering-type CANDU reactors is ~250 g/a/GWe. The cumulative tritium supply from this source for the overall nuclear power operations of Ontario Hydro is estimated to approach 50 kg by the year 2000. To put this production in perspective one should recognize that the actual tritium burned in a 1000 MWe DT fusion power station in one year will be ~150 kg.

Tritium production in CANDU reactors can be increased in a modest way through the introduction of suitable Li-bearing materials. This question is addressed in Appendix A. Thermal reactors could be designed for the specific task of breeding tritium; indeed such reactors exist in other countries. It must be noted, however, that in qualitative terms, each fission event in such a reactor provides approximately 200 MeV of energy and one neutron that can be used for tritium breeding. When the tritium atom is burned in the D-T fusion reactor, only ~20 MeV of energy is released. An energy economy which looked to fission reactors for the total fuel requirement of D-T fusion would necessarily be dominated by the fission power component. Furthermore, utilization of the neutrons to generate fissile fuel for fission reactors would lead to an ultimate energy return of >>200 MeV/neutron.

An accelerator-based fissile fuel breeder has been the subject of R&D at AECL for a number of years. In this proposed device high energy protons are incident on a liquid metal target of a high Z material such as lead, and copious quantities of neutrons are produced by spallation reactions. The tritium breeding capabilities of this device are considered briefly in Appendix A.2. It is noted here that the electrical energy input per neutron

produced is ~ 60 MeV, and the power station thermal requirement, ~ 180 MeV. As with fission, economic and power considerations would limit the tritium supply from this type of source to at most a few percent of the DT power station fueling requirements.

Thermonuclear fusion of D-D is a potential source of neutrons for tritium breeding. Some aspects of a D-D breeding scenario are reviewed in Appendix A.3. Implementation of any D-D breeding scheme demands solutions to several of the plasma physics and engineering problems which force the fusion community to focus its sights on D-T reactors. For this reason, it is unlikely that dedicated D-D tritium breeders will play a role in a first generation D-T reactor economy.

In conclusion, it should be noted that D-D breeding of tritium may well play an "indirect" role in solving any minor shortfall in D-T breeding ratio. This can be achieved by requiring that the D-D reaction make a small but significant contribution to the D-T reactor power [1,2]. To achieve this the reactor will have to meet more stringent reactor requirements in terms of magnetic field and plasma temperatures, but nevertheless less stringent requirements than those to be met in a pure D-D fusion power reactor.

2. BREEDER BLANKETS

2.1 Overview of Breeder Blankets

This chapter is intended to give a broad overview of the fusion breeder blanket problem, to survey the types of blankets, to indicate the choices that have been made to arrive at the various blanket concepts, and hence, to relate the more detailed discussions in the remainder of the report in a unified perspective. These topics will be illustrated by discussions of some of the major reactor design studies done to date in order to set the blanket problem in its overall fusion context. At the outset it is important to realize that no present plasma machine has a breeder blanket and no existing device has achieved D-T fusion conditions, although this is expected in the next few years. Therefore, at this stage blanket designs are still concepts which are being continually refined in an idea phase. There are many recent reviews of breeder blankets[3-8] and what follows will be based on them.

As stated in the previous chapter, the purposes of a breeder blanket are to remove the heat produced in the blanket by the fusion reaction neutrons and to breed the tritium required to sustain it. For the latter objective the only feasible tritium breeding reactions are equations (1) and (2) of Chapter 1. Hence, a breeder blanket must contain lithium in some form. Furthermore, this lithium-bearing material must be contained in a structure and there must be a heat transport fluid which could be the breeding material itself. These are the indispensable components of a blanket. In addition, there may be a neutron multiplier, a neutron reflector, perhaps a neutron moderator and a tritium recovery system. The result is a complex assembly of interdependent components with a wide spectrum of possibilities in the choice of these components. Figure 2-1 shows in a simplified manner the broad categories of blankets and some of the choices which must be made in selecting a blanket configuration. (The selection of a structural material is reserved for Section 2.2.1.) The first major division refers to the form in which the lithium-bearing breeding material is present, i.e. in liquid metal or solid form.

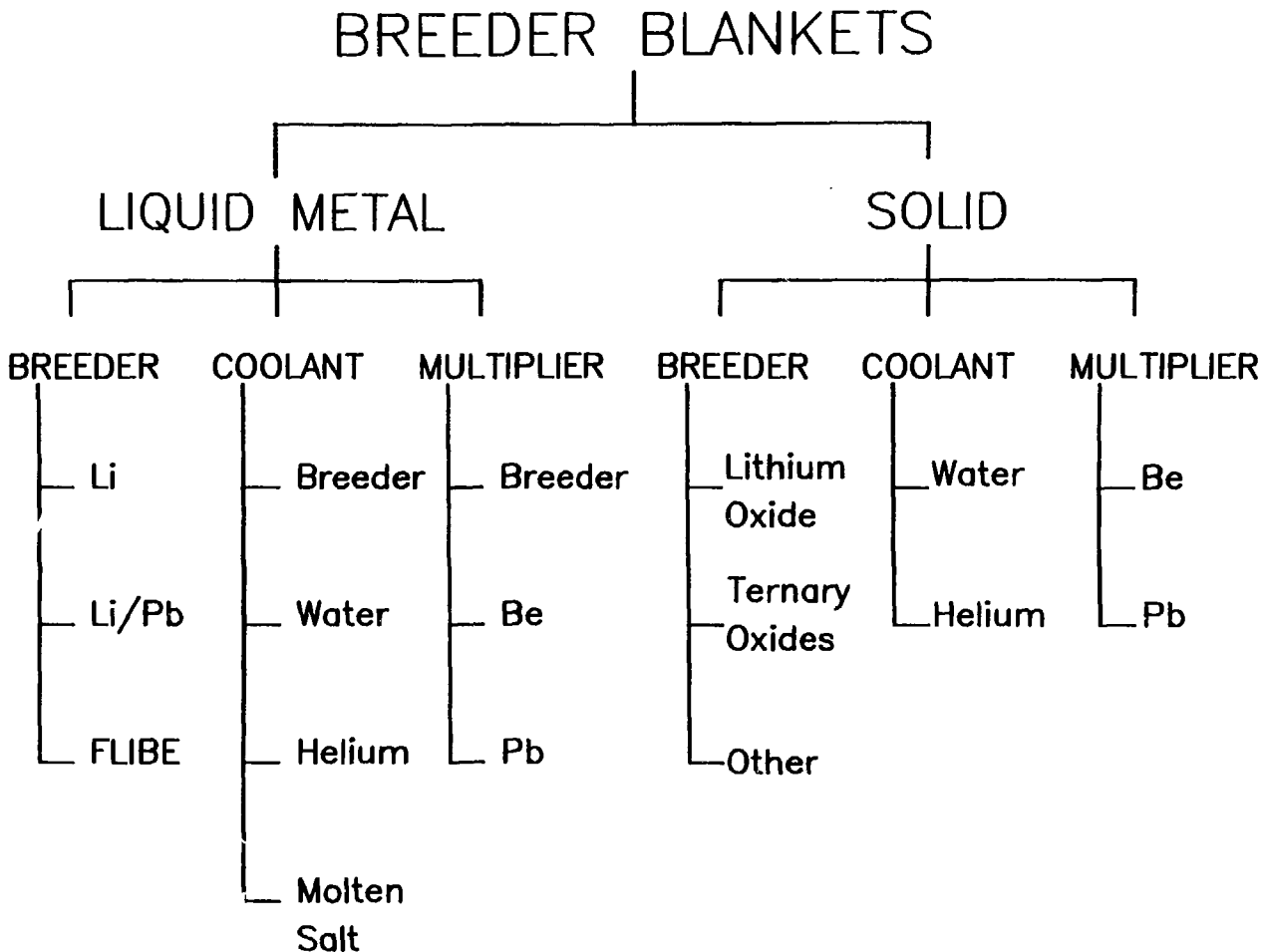


Figure 2-1 Breeder blanket types.

2.1.1 Liquid Metal Breeders

The main liquid metal candidates are liquid lithium and the eutectic alloy $^{17}\text{Li}-83\text{Pb}$. (This denotes an alloy containing 17 atomic % Li and 83 atomic % Pb and strictly speaking, the notation $\text{Li}_{17}\text{Pb}_{83}$ is not correct, although it is widely used: a more accurate abbreviation is $^{17}\text{Li}-83\text{Pb}$.) FLIBE, a molten salt consisting of $(\text{LiF})_2\text{BeF}_2$, although certainly not a metal, is included in this category to illustrate some of the more peripheral possibilities; this material has been rejected because of its low breeding potential. Li-Pb-Bi, lithium-lead-bismuth eutectic is another non-mainstream choice generally rejected because of the production of ^{210}Po from Bi under irradiation. The liquid metal breeders, as distinct from the solid breeder compounds, present the possibility of self-cooling, i.e. the breeding material can also be the heat transport fluid. Other coolant possibilities are water, helium and molten salts such as HTS (Heat Transfer Salt - Section 5.6.2). In the case of $^{17}\text{Li}-83\text{Pb}$ the $\text{Pb}(n,2n)$ and $\text{Pb}(n,3n)$ reactions allow the breeder to be used as its own neutron multiplier. More conventional neutron multipliers such as Pb or Be could be used in conjunction with liquid lithium if it were considered necessary.

Liquid metals are attractive because of the apparent simplicity of the blanket systems they offer and, indeed, in the early days of fusion when all attention was focused on plasma physics, it was simply assumed that the breeder blanket would be liquid lithium. However, in the past decade increasing emphasis has been placed on the technology and engineering of fusion reactors, with the result that serious concerns have emerged about liquid metal breeders.

Table 2-1 lists these critical issues and the report sections in which they are discussed in detail. The major issue concerns the safety problems inherent in using liquid metals and the danger of fire with these materials resulting in tritium release. The crux of this concern is largely judgemental in that arguments can be made from the LMFBR experience that liquid metals could be safely used but on the other hand, there is strong pressure from the fusion community to avoid any perceived safety issue with fusion. At the moment no definitive resolution of this concern is possible.

Table 2-1 Liquid Metal Breeders - Critical Issues

	Issue	Section
1. Safety	- lithium or $^{17}\text{Li}-\text{Pb}$ fires with consequent tritium release; water cooling dangerous	4.2.5
2. Corrosion	- degradation of blanket structure by flowing liquid metals and resulting plugging and activity transport	4.3
3. MHD Effects	- interaction of flowing liquid metals with reactor magnetic fields may lead to high pumping powers and poor heat transport	4.2.3
4. Tritium Control	- high solubility of tritium in lithium requires an effective large-scale extraction method; very low solubility in $^{17}\text{Li}-\text{Pb}$ causes concerns about tritium permeation	4.4

Some other problem areas for liquid metals are now under active investigation. Corrosion and compatibility with structural materials are important concerns. Not only is degradation of the structure possible, but also the blocking of flow channels by corrosion products and the radiological problems from the transport of these products throughout the cooling circuits. The MHD (magnetohydrodynamics) problem refers to the difficulties of pumping liquid metals through the high magnetic fields characteristic of fusion reactors. One important consequence of this is that the MHD effects make the moving metal tend to a laminar flow regime which is poor for heat transfer since stagnant regions may develop in that regime. Tritium extraction from liquid metals presents opposite situations for liquid lithium and 17Li-83Pb. Tritium is highly soluble in liquid lithium and thus there may be a problem in removing it completely and reliably. In 17Li-83Pb, tritium has a very low solubility, and tritium permeation and possible escape are major concerns. The discussion of these and other issues forms Chapter 4 of this report.

2.1.2 Solid Breeders

The search for alternatives to the liquid metals has lead in the last few years to the consideration of solid breeder materials. Referring again to Figure 2-1, the major compounds considered are Li₂O and the ternary oxides: LiAlO₂, Li₂SiO₃, Li₄SiO₄, Li₂TiO₃, Li₂ZrO₃, and Li₈ZrO₆. Other compounds such as the intermetallic alloys, Li₇Pb₂ and LiAl have been considered, but they suffer from high reactivity with water and air - precisely the problems one is trying to avoid by using solid breeders. The oxides are ceramics and being relatively inert, permit safe water cooling. Helium cooling is also possible but, of course, there can be no self-cooling. As we shall see below, a neutron multiplier is required for the ternary oxides (perhaps excepting Li₈ZrO₆) and possibly for Li₂O. Because of this close association, our discussion of neutron multipliers appears in this report in the chapter on solid breeders (Section 5.6.3.3).

The critical issues for solid breeders are given in Table 2-2, again keyed to the content of the rest of this report. The foremost among them is the

Table 2-2 Solid Breeder Materials (SBMs) - Critical Issues

	Issue	Section
1. Breeding Ratio	- the tritium breeding capability of some SBMs is in question; neutron multipliers are needed for most SBMs	3.4.4 5.6.3.3
2. Tritium Recovery	- adequate tritium recovery depends on keeping the breeder temperature within narrow limits; sweep gas extraction needed; radiation effects on SBMs are important	5.5 5.4
3. Integrity	- cracking under thermal stress depends on performance of SBMs; thermal decomposition	5.3.1 5.3.2 5.4.2
4. Heat Transport	- large numbers of thin-walled tubes necessary; BOT and BIT systems; low thermal conductivity of SBMs	5.6 5.3.3
5. Corrosion	- Li ₂ O may form LiOH (LiOT) with corrosion then a problem	5.3.4

difficulty with the tritium breeding ratio due to the low lithium density of these materials and the necessity for neutron multipliers. Tritium recovery in the solid breeders must be accomplished by means of a sparging or sweep gas stream of helium which picks up the tritium evolved by the blanket and takes it to an extraction facility external to the reactor. In order to ensure a steady production of tritium in this manner, it is essential to keep the tritium freely moving throughout the breeder material. This, in turn, implies that the breeder must be kept above the temperature at which bulk diffusion is initiated and below the temperature at which the porosity in the sintered breeding ceramics starts to close up. Since the ceramics in question have relatively low thermal conductivities, these temperature limits (see Table 5-4 for values) cause heat transfer problems. In particular, it is necessary to use a large number (thousands) of closely spaced thin-walled coolant tubes in these blankets to stay within the required limits. This necessitates a complex design with many welds, and leads to blanket reliability concerns. Another problem for tritium recovery involves the effects of radiation on the breeder material. Radiation damage produces defects which can trap the tritium and inhibit bulk diffusion, and radiation-induced sintering may retard flow through the porosity. An effect of the low thermal conductivities of the lithium ceramics is to cause cracking of monolithic blocks of the material, which can lead to heat transport problems. Finally it should be noted that Li_2O in contact with water vapour produces lithium hydroxide, leading to a corrosion problem. Chapter 5 covers these matters in detail.

2.2 Factors in the Design of a Breeder Blanket

The previous section has given an outline of the general aspects of breeder blankets; in this section the selection criteria for blanket concepts will be discussed in more detail. The first step in the design process is to decide whether a solid or liquid metal breeding system is to be used. This is a somewhat arbitrary choice, as we have seen, and it is often made for non-technical reasons. There appears to have been some tradition in recent years of liquid metal breeders for mirror machines and solid breeders for tokamaks; however, numerous counter examples to this "rule" can be produced and, in fact,

some large design studies have included both types as possibilities. Having made this basic decision, a materials selection process is initiated to choose the breeder, structural materials, coolant, neutron multiplier, etc. The next step is to derive a design concept based on these materials and then to do neutronics calculations to optimize the dimensions and configuration. Parallel mechanical stress and thermohydraulic computations set limits on the blanket parameters and proceed in an iterative manner with the neutronics. This procedure can be very simple, consisting of a materials selection with some one-dimensional neutronics work, or very elaborate, as can be seen from some of the larger design studies that we shall encounter later in this chapter.

2.2.1 Materials Selection - Structural Materials

As pointed out in Section 2.1, extensive discussion of breeder materials will be given in Chapters 4 (Liquid Metals) and 5 (Solid Breeders) and neutron multipliers will be discussed in Section 5.6.3.3. It remains therefore to discuss structural materials and how they impact on the choice of a blanket design. What follows is largely based on a recent review by Gold et al.[9].

Since no existing facility is capable of simulating the harsh radiation environment of a fusion reactor, there is no direct knowledge of materials behaviour under these conditions. Thus, much of the materials content for breeder blanket designs is based on an extrapolation from what is currently known. Hence, these designs cannot claim a very high degree of confidence in their arguments about materials choices. For current reactor designs the fusion neutron flux on the first wall is likely to be in the range of 3 to 5 MW/m² (see Tables 2-5, 2-7 and 2-8), where 1 MW/m² \approx 5 \times 10¹⁷ neutrons/m²/s. Hence, the total lifetime accumulated neutron fluences may exceed 40 MWy/m² (\sim 6 \times 10²⁶ neutrons/m²), depending on reactor availability and projected lifetime. Such a fluence implies radiation damage of about 500 dpa (displacements per atom) in austenitic stainless steels for which 1 MWy/m² corresponds to about 13 dpa. In addition to this formidable radiation damage dose, the helium atom concentrations produced simultaneously by transmutation

will reach very high levels. Again for austenitic stainless steel a dose of 15 dpa means that about 200 appm* of He is generated, and so for 500 dpa the total He generation would be approximately 6700 appm. (Hydrogen is also produced in comparable amounts but is not considered a significant problem, since hydrogen readily diffuses out of metals.) Such large He concentrations cause substantial swelling, resulting in severe degradation of mechanical properties. Furthermore, it is known that the defects and the He atoms will interact in a synergistic manner by mechanisms such as He trapping at vacancies[10] and other temperature-dependent processes[11].

Irradiation tests in current fission reactors can produce either of these effects, i.e. high dpa or high He production but not, in general, the two together. Figure 2-2, from [9] and [12], shows this for some steels as irradiated in the Oak Ridge Research (ORR) reactor, the High Flux Isotope Reactor (HFIR) and the Experimental Breeder Reactor II (EBR-II). HFIR, which has a thermal neutron flux, produces much higher He levels for equivalent dpa than the fast reactor EBR-II. Conversely EBR-II is able to achieve a high dpa but with low He generation. The ORR, a mixed spectrum reactor, comes closer to fusion conditions. However, a limitation on all of these reactors, representative of others available throughout the world, is the small fluences that can be achieved compared with those required to simulate fusion reactor conditions. For example, it would take about 15 years to reach 10 MWy/m^2 [13]. Figure 2-2 also shows a "trick" which is possible with high Ni alloys. Using a two-step reaction $^{58}\text{Ni}(n,\gamma)^{59}\text{Ni}$ and $^{59}\text{Ni}(n,\alpha)^{56}\text{Fe}$, He can be generated at the levels typical of fusion reactors. The problem with this is that high-Ni steel alloys are not attractive for fusion applications because of radiation-induced embrittlement [16].

Existing neutron generators such as RTNS-II are severely limited in fluence, capable of achieving only a few dpa in irradiations within practical times[13]. Ion beam techniques, employing accelerated light or heavy ions, are of interest in studying basic mechanisms, but they are limited to depths

* appm = atomic parts per million

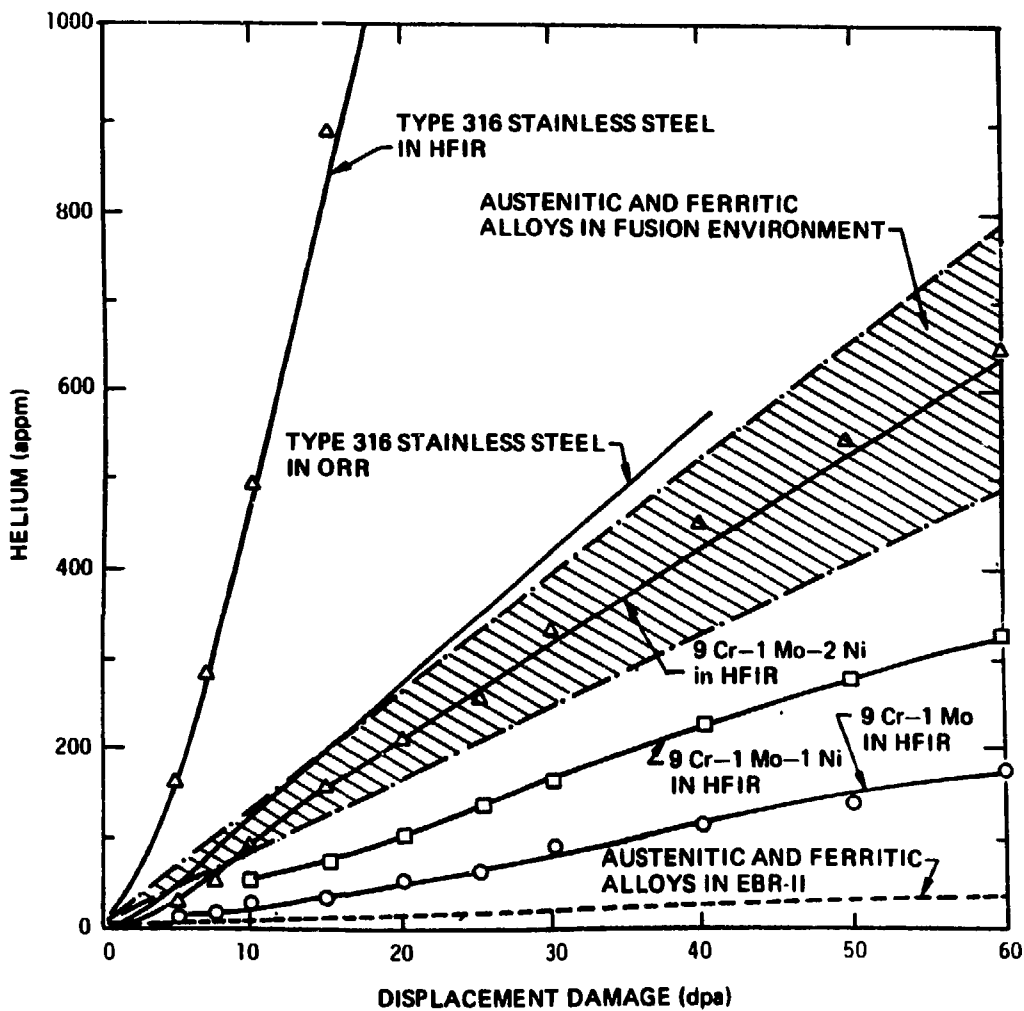


Figure 2-2 Relationship between helium production and dpa for some stainless steels (from [9] and [12]).

of the order of at most a few microns into the material. These considerations have been discussed in more detail by an expert panel convened by the International Energy Agency (IEA)[14] to assess the materials testing needs for fusion and in particular, to recommend on the feasibility of the Fusion Materials Irradiation Test facility (FMIT) planned for the Hanford Engineering Development Laboratory (HEDL) in the United States. FMIT consists of an accelerator of advanced design which produces a 100 mA deuteron beam at 35 MeV which impacts on a flowing lithium target system, resulting in a high energy neutron flux[14,15]. The average flux is 10^{19} neutrons/m²/s in the volume of 10 cm³ immediately behind the target, and 2×10^{18} in a larger (500 cm³) volume farther from the target. The neutron energy spectrum from the D-Li reaction used in FMIT is somewhat different from that of the fusion D-T spectrum, but it was judged by the IEA panel to be sufficiently close for fusion simulation purposes. A further concern with the FMIT experimental program is the necessity of testing miniaturized materials specimens due to the small irradiation volume; this, the panel concluded, could probably be overcome by careful specimen design. Notwithstanding these limitations, it is clear that no facility other than FMIT or some similar device would permit realistic testing of fusion materials up to their lifetime fluence ranges on a convenient time scale. R&D and detailed design on FMIT have been done to a level of 80 M\$ US up to this time, including testing of the Experimental Lithium System (ELS), the world's largest liquid Li loop, to be discussed in Section 4.2. Negotiations are now underway to obtain additional funding (of the order of 140 M\$ US) from the IEA countries to complete FMIT. If this funding were to become available in 1984, FMIT would be in full operation by 1990, with fusion materials testing data coming in the early 1990s. Lacking the necessary data from an FMIT-type device, all materials arguments used for blanket designs must be based to some extent on guesses with regard to their properties under irradiation. This point is sometimes mentioned but seldom emphasized in blanket design studies.

Most near-term fusion devices, and indeed current large machines, use 316 stainless steel as their structural material because of its convenient fabrication properties, relatively low cost, availability and the familiarity

gained from its nuclear applications. However, swelling is one of many problems that make SS 316 an unlikely candidate for fusion reactor structures. Therefore an extensive R&D program has been underway for some years to come up with better candidate materials. In the US, this effort has been organized by the Department of Energy (DoE) into a path structure for R&D[9]. These paths are:

- Path A. austenitic stainless steels
- Path B. high strength Fe-Ni-Cr alloys
- Path C. reactive and refractory metal alloys
- Path D. innovative materials and concepts
- Path E. ferritic/martensitic steels

Of these the most promising materials, based on what is known to date, are prime candidate alloy (PCA) of Path A, the vanadium alloys of Path C and the ferritic steels of Path E.

Representative of the latter two are VCrTi alloys and the Sandvik HT-9 ferritic steel. Typical nominal compositions are (see Table 4-2):

PCA: Fe-14Cr-16Ni-2Mo-2Mn-0.3Ti-0.5Si-0.06C
HT-9: Fe-12Cr-1Mo-0.5W-0.3V-0.2C
VCrTi: V-15Cr-5Ti

PCA in this context can be regarded as an improved version of SS 316 tailored by titanium addition to better resist swelling; a cold-worked (20%) PCA is understood. The data for PCA under irradiation, although not to full fusion conditions, is the most extensive. Some data for HT-9 exists and there is very little for the vanadium alloys. For the latter alloys even unirradiated properties are scarce. We will now briefly review the important points on which current choices for breeder structures are based.

A figure of merit[9] for the resistance of a material to the stresses caused by loads at high temperature can be developed from the thermal expansion

coefficient α , the Young's modulus E , the thermal conductivity k and the Poisson's ratio ν :

$$\sigma_T = \frac{\alpha E}{k(1 - \nu)} \quad (1)$$

The results for the three materials of interest are shown in Table 2-3. A lower σ_T indicates better resistance to thermal stresses and hence, HT-9 is a factor of 2 better in this respect than PCA, and VCrTi is superior to PCA by a factor of 4. This relatively poor response of PCA to thermal stresses is a major concern. Notable also is the higher melting point of VCrTi, which indicates its possible superiority for high temperature operation.

HT-9 has a relatively high ductile-to-brittle transition temperature (DBTT) in the room temperature range, whereas the other two candidate alloys have DBTTs well below room temperature. This means that HT-9 components could fail if the structure were allowed to cool to the DBTT while still under load. Furthermore, irradiation, temper embrittlement and aging at temperatures in the 400° to 600°C range can push the DBTT upwards[9], perhaps even into the design coolant temperature range for the blanket. Further data on the DBTT behaviour of ferritic steels under irradiation is essential before they could be used for practical blanket structures.

The upper operating temperatures for structural materials are dictated largely by helium embrittlement, with accompanying large losses in ductility. For PCA, the results to date show acceptable engineering properties for temperatures lower than about 500°C - thus setting a coolant upper temperature limit. A more limited data base for HT-9 indicates that a similar maximum, i.e. 500°C, would probably be appropriate. For vanadium alloys, it is estimated that He embrittlement is likely to be small for temperatures up to 750°C[8].

Swelling, due to radiation damage and helium production, is a critical issue in limiting the lifetime of structural materials. HT-9 and VCrTi are much

Table 2-3 Thermal Properties of Candidate Structural Materials from [9] and [8]

	PCA	HT-9	VCrTi
Melting Point, °C	1400	1420	1890
Poisson's Ratio ν	0.27	0.27	0.36
σ_T , MPa.m/w ²	0.22	0.11	0.055
Temperature for σ_T, °C	400	400	500

more resistant to swelling than PCA and indeed the VCrTi alloys were developed for the US LMFBR program specifically for this property. In the interim report of the Blanket Comparison and Selection Study (BCSS)[8], estimates have been made of the radiation damage level which would induce a 5% swelling of the candidate materials. For PCA, 100 dpa at 500°C and 150 dpa at 400°C are the estimates, with 200 dpa for HT-9 and > 200 dpa for VCrTi; thus, the latter alloys are a factor of 2 better than PCA in this respect. However, the numbers quoted above are based on extrapolations from SS 316 results for PCA, on theoretical models for HT-9 and on a very slim data base for VCrTi.

Very little is known about the irradiation-induced creep of any of the three alloys. It is probable that ferritic steels (e.g. HT-9) will exhibit less creep than austenitic steels (e.g. PCA) on theoretical grounds and one can also argue for the same conclusion on thermal properties. There is no information about the creep of VCrTi.

Although the fabrication and welding characteristics of SS 316, and by analogy PCA, are well established and convenient, this is not the case for the other two candidates. The ferritic steels such as HT-9 require pre-heating and post-weld heat treatment (PWHT) to ensure that cracking does not occur in the weld or surrounding heat-affected area and to recover the fracture toughness lost during welding. This could be very difficult in the remote maintenance environment of a fusion reactor. Refractory metals such as the vanadium alloys are costly and relatively difficult to fabricate; welding has to be done in an inert atmosphere, since vanadium alloys are susceptible to deterioration by oxidation.

Other material-specific factors which should be considered in choosing a blanket structure are the ferromagnetic properties of HT-9 in a magnetic confinement fusion reactor, the higher tritium permeation rate of vanadium alloys and their lower activation and parasitic neutron capture rates. Coolant choice also impacts on the selection. For example, vanadium alloys are undesirable for water-cooled systems because of the oxidation problem mentioned above. Corrosion of the structural material, a key issue for liquid metal breeders, is discussed in detail in Section 4.3.

2.2.2 Neutronics Evaluation of Blankets

The next step in blanket concept design is to evaluate the neutronics characteristics and optimize the chosen configuration for tritium breeding ratio (TBR). The details of these calculations are given in Chapter 3, and the intention of this section is to give an initial impression of these procedures.

The two lithium breeding reactions (equations (1) and (2), Section 1.3) have essentially different characteristics; the $^6\text{Li}(n,\alpha)\text{T}$ reaction is a "thermal" * neutron process, whereas the $^7\text{Li}(n,n'\alpha)\text{T}$ is a "fast" reaction with significant cross-section for 5 to 15 MeV neutrons[5]. Therefore, for the ^6Li reaction to proceed, the 14 MeV fusion neutrons must be slowed down by collisions with the nuclei in the blanket assembly. This slowing-down will take place simultaneously with parasitic capture in the blanket structural elements, neutron losses from the assembly, ^7Li reactions and other processes discussed in Chapter 3.

The significance of this reaction classification can be shown by Table 2-4, which is adapted from the work of Jung and Abdou[5,17]. The table shows calculations made for the STARFIRE/DEMO (Sections 2.3.2 and 2.3.3) three-dimensional toroidal geometry using the MORSE Monte Carlo code (Section 3.2.3) and data from the ENDF/B-IV library (Section 3.1.2). A decrease of 15% in the ^7Li cross-section over previously published data was used (Section 3.1.2). Here, and typically in similar calculations, the blanket assembly is represented by the compositional percentages of its component materials included in such structures as the first wall and its "armour" (against plasma attack), and the blanket itself. The results are presented for four breeding concepts: a lithium self-cooled blanket with water-cooled first wall, a water-cooled $^{17}\text{Li}-83\text{Pb}$ blanket, a Li_2O blanket and a LiAlO_2 blanket, both of the latter

* "Thermal" is not used to mean thermal in the fission reactor sense, but rather, to indicate lower energy neutrons, < 5 MeV in the context of blankets.

Table 2-4 TBRs for Four Blanket Designs (from [5] and [17])

	Liquid Li	17Li-83Pb	Li ₂ O	LiAlO ₂
Armour (1 cm)	100% HT-9	100% HT-9	100% PCA	100% PCA
First Wall (1 cm)				
- coolant	35% H ₂ O	35% H ₂ O	35% H ₂ O	35% H ₂ O
- structure	65% HT-9	65% HT-9	65% PCA	65% PCA
Blanket Region (68 cm)				
- coolant	-	5% H ₂ O	5% H ₂ O	5% H ₂ O
- structure	10% HT-9	10% HT-9	5% PCA	5% PCA
- breeder	90% Li	85% 17Li-83Pb	90% Li ₂ O	90% LiAlO ₂
Breeder Material				
- ⁶ Li enrichment	none	90%	none	60%
- density	TD*	TD	70% TD	70% TD
Breeding Ratio (Calculated)				
- from ⁶ Li	0.89	1.48	0.90	0.85
- from ⁷ Li	0.36	0.002	0.29	0.03
- total TBR	1.25	1.48	1.19	0.88

* TD = theoretical (usual) density

without neutron multipliers. The lower densities for the solid breeder materials are to allow for the porosity needed for tritium recovery.

Since Li is not a very efficient neutron moderator, the fusion neutrons can penetrate relatively deeply into the liquid-lithium blanket without large energy losses. As can be seen from the table, the ^7Li reaction is an important contribution (~ 29%) to the breeding ratio of this blanket and hence, it can be classified as a "fast" system. Similarly, the Li_2O blanket is also fast, with a slightly smaller ^7Li contribution (~ 24%) that is due mainly to increased moderation by the coolant. On the other hand, the $^{17}\text{Li}-^{83}\text{Pb}$ blanket produces essentially all its tritium from the ^6Li reaction, with the $\text{Pb}(n,2n)$ and $\text{Pb}(n,3n)$ reactions yielding effective neutron multiplication. This is a "thermal" blanket. The LiAlO_2 blanket gains only 3% of its breeding from the fast reaction and is also "thermal". It is notable that this latter concept gives a TBR of only 0.88 which shows, as mentioned in Section 2.1, that a neutron multiplier is essential for the ternary lithium oxides (excluding perhaps Li_2ZrO_6) to achieve adequate breeding.

This simple-minded approach, i.e. the fast-thermal categorization, is useful in considering the question of whether or not to enrich the lithium in the ^6Li isotope. According to Abdou[5] the natural abundance (92.5% ^7Li , 7.5% ^6Li) is about the optimum combination for liquid lithium and Li_2O , i.e. for fast systems. Furthermore, if a neutron multiplier were to be added to these blankets, they would then become "thermal". This would result only in a relatively small increase in the TBR[5] because of compensating losses in ^7Li breeding. For the "thermal" systems, ^7Li serves no useful function and ^6Li enrichment is desirable to increase the TBR. This is particularly true for $^{17}\text{Li}-^{83}\text{Pb}$, which contains only a modest amount of lithium to begin with; this system cannot succeed without ^6Li enrichment. Similarly, enrichment is worthwhile for ternary oxide systems because of their marginal breeding performance.

The ordering of the TBRs given in Table 2-4 also reflects the situation generally found in other similar calculations. In essence, $^{17}\text{Li}-^{83}\text{Pb}$ is virtually certain to achieve a good breeding ratio, with liquid lithium somewhat

behind but also a good prospect. Of the solid breeders, Li_2O has the best performance because of its higher Li atom density, but the ternary oxides (with the possible exception of Li_2ZrO_3) have a high risk of failing to achieve adequate breeding without a neutron multiplier.

2.2.3 Tritium Breeding Ratios

As has been shown in the last section, neutronics calculations are used to calculate the TBRs for blanket concepts. In this section, the relationship between the TBR and the tritium inventory will be discussed in somewhat more detail.

Following the notation of Jung and Abdou[17], the TBR, T_o , can be defined as:

$$T_o = N^+ / N^- \quad (1)$$

where N^+ is the production rate of tritium in the blanket and N^- is the rate of consumption in the plasma. Clearly T_o must be greater than unity to allow for the decay of tritium between its production time and usage time - defining T as the half-life of tritium. Furthermore, if one is to have a fusion power economy, T_o must provide for the startup tritium inventories of succeeding reactors. Thus, a margin in the TBR, A , must be included to allow for these effects. An additional margin, B , must also be put in to reflect uncertainties in reactor design, nuclear data cross-sections and blanket design effects. An example of the latter would be the penetrations through the blanket for plasma heating and diagnostic equipment which, by occupying spaces where breeding material could be put, degrade the blanket's potential TBR. Jung and Abdou[17] have estimated B to be in the order of 5 to 6%, on the basis of their experience of past designs. In order to estimate A , Jung has derived a detailed model for T_o :

$$T_o = 1 + (I_o / TN^-) F (td/T) = 1 + A \quad (2)$$

Here I_0 is the startup tritium inventory and t_d is the doubling time. F is a calculated function of the doubling time. The total tritium inventory at a given point in time at equilibrium can be expressed as:

$$I = I_B + I_F + I_S \quad (3)$$

where I_B is the total inventory in the blanket, I_F is the quantity of tritium in the fuel and exhaust systems and I_S the amount in storage. The quantity I_B depends strongly upon the type of breeder material used; for solid breeders it might be large, e.g. 10 kg or more, but for a $^{17}\text{Li}-^{83}\text{Pb}$ system it could be quite low, e.g. < 1 kg, due to the low solubility of tritium. I_F depends on the fractional burnup of the tritium in the plasma (f_b) and therefore the reactor performance. I_S is really a safety factor to guard against disruptions in tritium recovery and is also related to the required startup inventory. $I_{S,\min}$ is defined as the minimum on hand for such disruptions.

Figure 2-3 shows the result of one set of calculations [5] using these equations with N^- , consumption, = 0.5 kg/d, $I_{S,\min} = 0$ and $I_S = 0$, and burnup between 0.01 and 0.1. The B margin has not been included in the TBR; thus, for practical applications the TBRs would have to be increased by ~5 to 6%. It is clear from the figure that to achieve shorter doubling times requires higher TBRs, as one would expect. And for a given doubling time, a higher TBR gives rise to a larger inventory. This latter result should be viewed against the fact that generally the safety risk of fusion power is directly related to the magnitude of the tritium inventory in the reactors. Without going into further detail here, this relationship between the TBR and the tritium inventory is crucial for the viability of fusion energy, its public acceptability and ultimately its economics.

On an engineering level, similar calculations done in an earlier Argonne Blanket Study[18] have shown that it is unattractive to use a batch system for tritium recovery because of the large tritium inventory in the processing system. (A further negative factor is the substantial volumes of structural

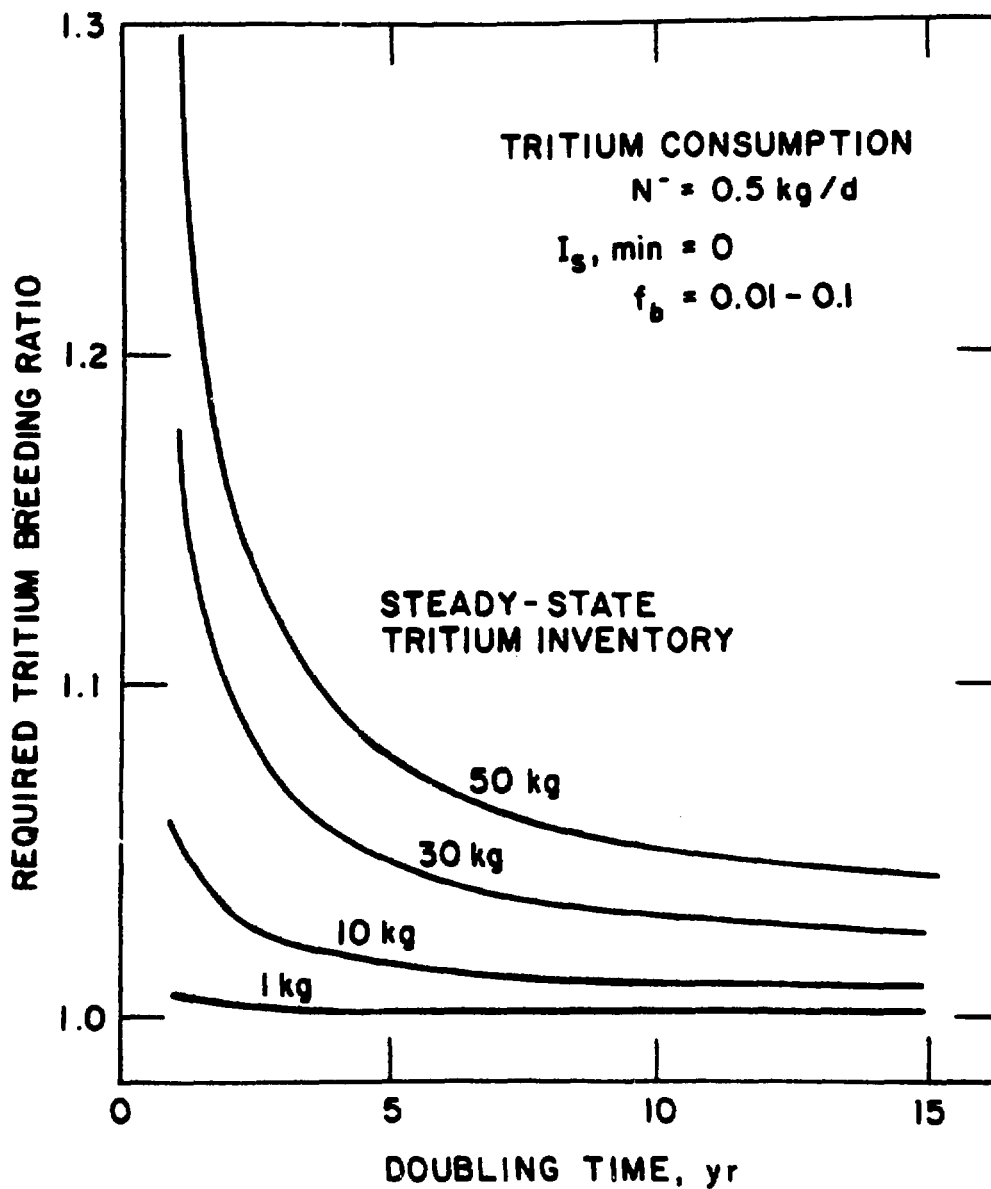


Figure 2-3 Required TBR versus doubling time (from [17]).

materials involved in such a system.) Therefore, on-line tritium recovery is considered essential for blanket designs.

Other calculations, with more emphasis on the various engineering components of the tritium systems, have been done by Carré et al.[19]. They have confirmed that the required TBR and initial inventory are strongly dependent on the total equilibrium inventory. They also showed that the distribution of this inventory among the various components of the system, e.g. blanket, fueling, storage as above, and the residence times of the tritium in these systems substantially influences the doubling time.

2.3 Examples of Blanket Design Concepts

Thus far, the principal processes in blanket design have been discussed, i.e. materials selection and neutronics evaluation. However, the practical design of a blanket must recognize several other factors. Heat transport, mechanical design, maintainability, safety, etc. are all important considerations. As in any engineering design, numerous trade-offs must be made between all of these elements in iterating toward a final concept. Some of these interactions between factors have already emerged in Sections 2.1 and 2.2. Rather than attempt to bring out additional ones by further discussions structured by topic, e.g. heat transport, etc., it is probably more useful to point them out by referring to specific designs. In order to do this it is first necessary to survey the field of fusion reactor concepts.

2.3.1 Fusion Reactor Concepts

Fusion is remarkable for the number of reactor studies that have been done; a veritable alphabet soup of abbreviations for reactor concepts exists that is intimidating and bewildering on first exposure. There is no possibility of reviewing this welter of material and hence, to simplify the task, the discussion will be confined to the most important recent blanket designs for tokamaks and mirror machines. Blanket development is an evolving activity and the outcome of older work has been incorporated in the newer designs. While

blanket designs have been proposed for other fusion systems such as inertial confinement, stellarators, compact toroids, etc., these have been much less detailed than those for the mainstream fusion machines.

The timing of the introduction of fusion power should be recognized to clarify the hierarchy of blanket designs. At present the emphasis in fusion is on demonstrating scientific feasibility in the large tokamak experiments JET (EEC), TFTR (US), JT-60 (Japan) and T-15 (USSR). The first two machines are now operating* and the second two are expected to be operational within the next two years. A large mirror experiment, MFTF-B (US), with the same purpose is also under construction. The next step in the progress of fusion will be to demonstrate the engineering feasibility of fusion technology - the largest single "new" component in that stage will be the breeder blanket. INTOR (Section 2.3.6) and related machines are typical of this group of intermediate devices. The next step before commercialization is often called DEMO, meaning a prototype to demonstrate commercial fusion power - DEMO also now refers to a specific reactor concept of this type (Section 2.3.3). The final stage is commercial fusion operation as represented by the STARFIRE (Section 2.3.2) tokamak and the MARS (Section 2.3.4) mirror reactor. This is the order in broad outline, but it should be pointed out that the intermediate stage is still somewhat murky, especially in the US program.

What follows, then, will concentrate on the three broad lines of development in blanket technology today: (a) the STARFIRE study, (b) the MARS study, and (c) the INTOR activity.

2.3.2 STARFIRE

The STARFIRE study[20] is the most elaborate and detailed commercial tokamak reactor design concept developed to date. It is also representative of a major centre of blanket design activity at Argonne National Laboratory, which has

* However, no feasibility demonstration with D-T fuel has yet been attempted in JET or TFTR.

also produced a blanket study[19], the DEMO design[23] and is the lead agency for the current BCSS[8]. This line of development continues to exert a very significant influence on the contemporary view of breeder blankets.

The STARFIRE study was intended to develop a viable fusion reactor design that could be used by a utility for electrical generation. The main parameters are given in Table 2-5, with two other concepts for comparison. The net electrical power is 1200 MW from 4000 MW of thermal power resulting from a fusion power of 3490 MW with energy multiplication in the blanket. It is a continuous-burn steady-state tokamak, as distinct from a pulsed operation. The scale of this reactor is notable, with a 7.0 m major radius and 1.94 m minor radius - commercial fusion reactors will be very large devices.

Figure 2-4 gives an exploded view of STARFIRE. Without going into the plasma physics, which is beyond the scope of this study, it is sufficient to point out that the D-shaped plasma is created in the hollow torus vacuum chamber and is confined by the arrangement of magnetic field coils shown in the figure - EF (equilibrium field) and TF (toroidal field) coils. The torus structure is composed of 12 TF coils with two first-wall/blanket sectors associated with each for a total of 24. The first-wall is defined as the first surface that the plasma "sees" - it is subject to plasma attack with consequent erosion and degradation[25]. In STARFIRE the first-wall is integral with the blanket structure in order to avoid undue complexity of design; this is now the case with most other recent blanket designs and is one example of the effect of the STARFIRE study on this field. Because of the degradation of the first-wall it is estimated that the lifetime of the first-wall/blanket sectors will be six years. Therefore, STARFIRE has been designed for easy disassembly, as shown in Figure 2-4. Two other features are included in the sectors in this design: an RF (radio frequency) heating duct through which energy is delivered to raise the plasma temperature for ignition and a limiter whose purpose is to control the edge of the plasma and remove impurities. Neither of these is part of the blanket per se and both are examples of the penetrations discussed in Section 2.2.3 that reduce the TBR by displacing breeding material. Some of the coolant pipes, shown in the figure, have pressurized water circulated through them to remove the heat generated in the blanket; another set of piping, not shown, removes the tritium generated by means of sweeping low pressure helium.

Table 2-5 Parameters for Some Commercial Tokamak Designs (after [4])

	NUWMAK US 1979 [21]	STARFIRE US 1980 [20]	SPTR-P Japan 1981 [22]
Major Radius (m)	5.1	7.0	6.8
Minor Radius (m)	1.13	1.94	2.0
Thermal Fusion Power (MW)	2100	4000	3700
Neutron Wall Loading (MW/m²)	4.0	3.6	3.3
Plasma Current (MA)	7.2	10.1	16.4
Average β (%)	6.5	6.7	7.0
Burn Pulse Length (s)	225	continuous	continuous
Toroidal Flux Density (T)	12	11	12
Structural Material	Ti-Al-V	PCA	PCA
Coolant	H ₂ O	H ₂ O	H ₂ O
Breeder Material	Li ₆₂ Pb ₃₈	LiAlO ₂	Li ₂ O

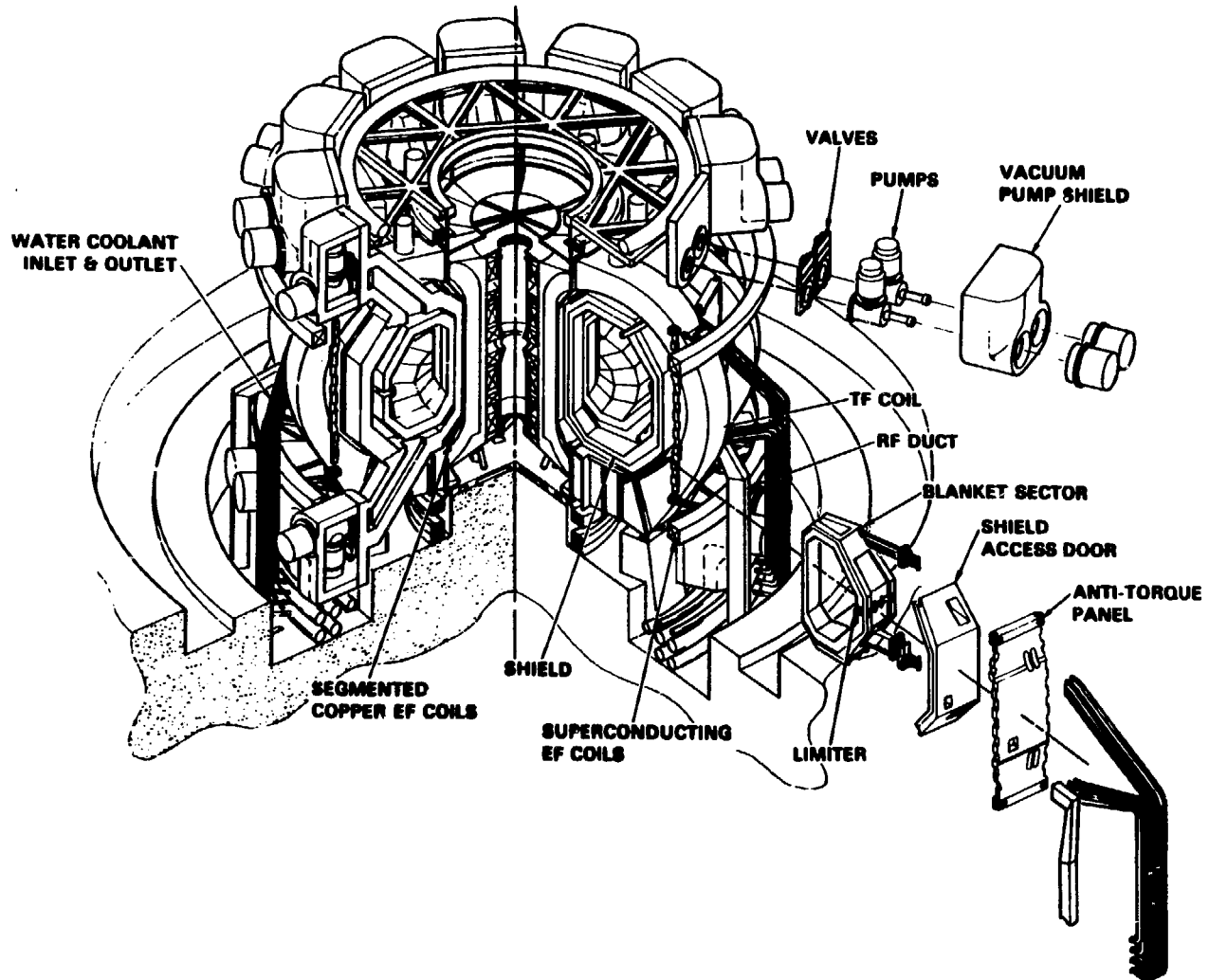


Figure 2-4 The STARFIRE tokamak (from [20]).

A complete specification of the STARFIRE blanket design is given in Table 2-6 and schematic diagrams are shown in Figures 2-5 and 2-6. The breeder material, LiAlO_2 , is packed in the form of pellets around a large number (60 000 tubes with 120 000 welds) of thin-walled coolant tubes circulating water. There are two independent cooling loops for safety; the first-wall, because of its high heat load, has a separate cooling system. The first-wall is essentially a beryllium-coated corrugated panel - the choice of beryllium was made because its low Z is desirable for plasma impurity reasons[25] and for its neutronics properties. For the main neutron multiplier two options were examined, Be and Zr_5Pb_3 - the latter because of the perceived danger of a Be shortage (see Section 5.6.3). Of these two, the Be was clearly superior. The second wall separates the neutron multiplier from the actual breeder zone. Cooling of this wall is again separate, since the thermal conductivity of the LiAlO_2 is relatively low. Note that the coolant tube density is much higher nearer the second wall and the tubes become further apart as one goes to the outside of the blanket. The reason for this is that the nuclear heating falls off roughly exponentially with distance from the plasma (see also Figure 5-10). This is a common feature of all blanket designs for both liquid and solid breeders.

The breeder material is packed at an effective density of 60% to allow for removal of the tritium (see Figure 2-6). It is interesting to note the mass of the breeder material required for STARFIRE, $\sim 600 \text{ Mg}$, showing that large-scale production of well-characterized, formed lithium ceramics will be required to implement solid breeder blankets. After the breeding zone a graphite neutron reflector is used to improve the overall neutronic performance of the blanket.

Many other issues were also covered in the STARFIRE study before arriving at the final design. For coolant selection helium was considered, and was rejected because of the large structural requirements related to the volume of helium flow required for heat transport, which reduced the TBR. Shielding problems, leakage of helium into the plasma and misgivings about using a structural material under irradiation with helium were other factors in the decision. Thus, water was selected as the coolant. Interestingly, D_2O was also considered, and was shown to have neutronic advantages. The D_2O is

Table 2-6 Summary of STARFIRE Blanket Design Parameters (after [20])**First-Wall**

Form	Be-coated panel
Structural material	Austenitic stainless steel
Outer wall structural thickness, mm	1.5
Maximum structural temperature, °C	~423
Coating/cladding	Beryllium
Coating/cladding thickness, mm	1.0
Coolant	Pressurized water, H ₂ O
Coolant outlet temperature, °C	320
Coolant inlet temperature, °C	280
Coolant nominal pressure, MPa	15.2
Coolant velocity, m/s	6.1

Neutron multiplier

Material Options	Be	Zr ₅ Pb ₃
Maximum Temperature, °C	490	840
Thickness, m	0.05	0.05
Theoretical density, g/cm ³	1.8	8.9
Effective density, %	70	100
Total mass, kg	51,800	356,000

Breeding Region

Structural material	PCA
Maximum structural temperature, °C	425
Breeder material	α -LiAlO ₂ (natural Li with Be) (60% ⁶ Li with Zr ₅ Pb ₃)
Theoretical density, g/cm ³	3.4
Effective density, %	60
Grain size, 10 ⁻⁶ m	0.1
Maximum/minimum temperature, °C	850/500
Region thickness, m	0.46
Total mass of α -LiAlO ₂ , kg	606,500
Total volume of α -LiAlO ₂ , m ³	178.1
Coolant	Pressurized water, H ₂ O
Coolant outlet temperature, °C	320
Coolant inlet temperature, °C	280
Coolant nominal pressure, MPa	15.2
Tritium processing fluid	He (0.05 MPa)

Reflector

Material	Graphite
Thickness, m	0.15
Maximum temperature, °C	~800
Structure	Austenitic stainless steel (low Mo)
Structure temperature, °C	300-400

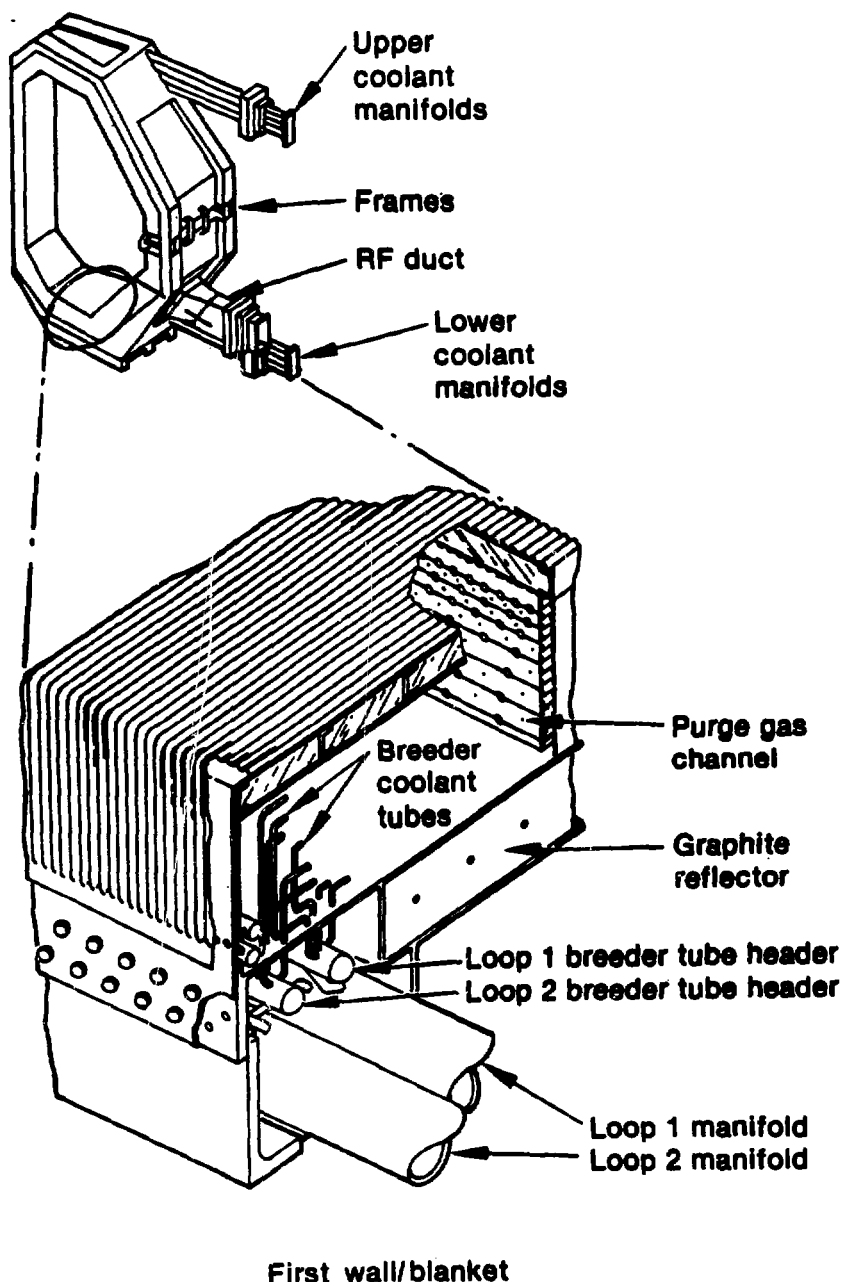
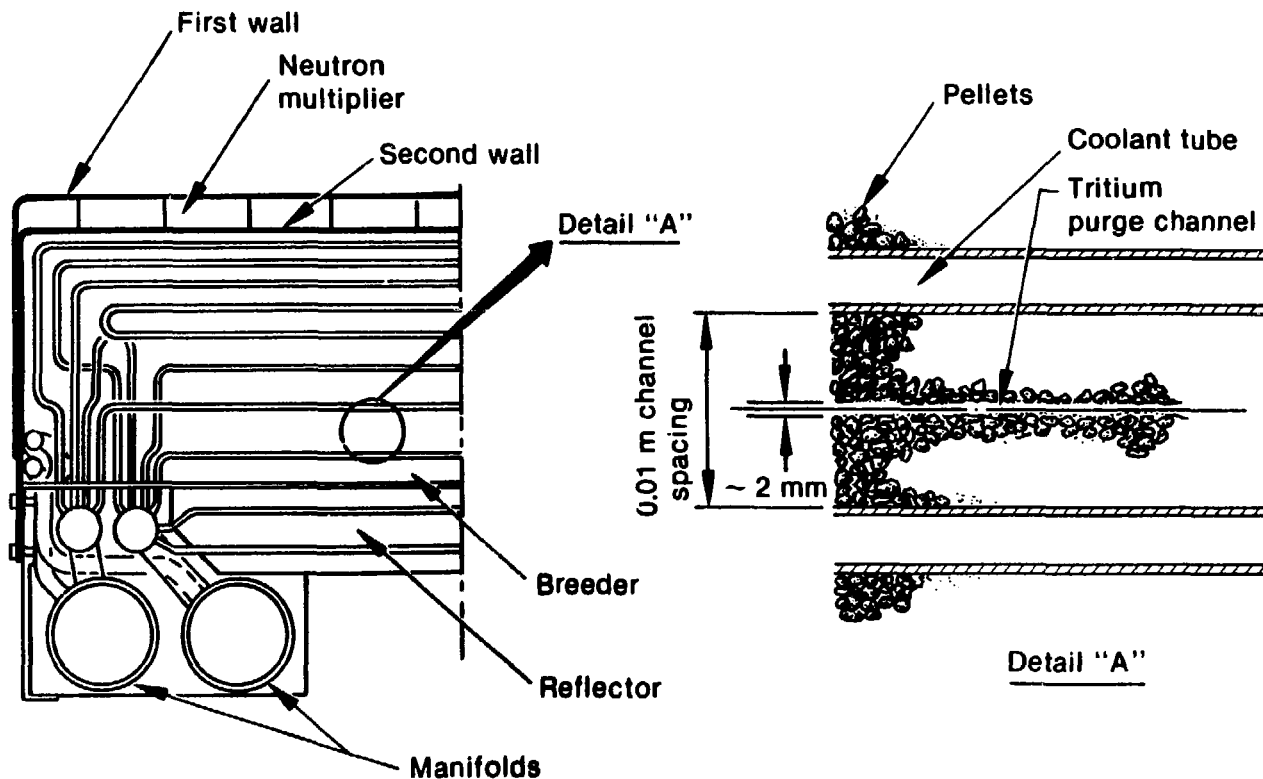


Figure 2-5 Details of the STARFIRE blanket (from [20]).



2-30

Figure 2-6 STARFIRE blanket schematic - (from [20]).

somewhat less effective in slowing down the neutrons than H₂O and therefore, because neutron multiplication works better for higher energy neutrons, a more favourable situation is obtained. Also the isotopic separation of any tritium that found its way into the coolant by permeation would be easier for D₂O than H₂O. However, D₂O was rejected on the basis of cost.

2.3.3 DEMO

The DEMO[23,24] design is an outgrowth of the STARFIRE study made by essentially the same group and therefore, this is the natural place to present it, even though it is an intermediate design. The main DEMO parameters are given in Table 2-7. Its net electric power is 330 MW, having roughly a quarter of the power of STARFIRE. Its dimensions are similar to those of INTOR, but it has increased plasma parameters and higher wall loading, in addition to a continuous operation mode.

DEMO has had some simplifications made to it relative to the STARFIRE design other than just down-sizing it. The number of TF coils has been reduced from 12 to 8 and there is only one first-wall/blanket sector associated with each TF coil for a total of 8. The result of this is to reduce the number of parts by a factor of two, compared with STARFIRE, and the number of connections by a factor of four, leading to easier maintenance and higher reliability, which in turn would impact favourably on the availability and hence the economics of DEMO. The cost of DEMO is estimated to be 2.35 G\$ US.

Two blanket options are proposed for DEMO. The first (see Fig. 2-7) is a Li₂O blanket with pressurized water coolant. Generally speaking, the design is similar to the STARFIRE blanket and also uses a PCA structure. However, other than the same Be coating on the first wall (a very minor effect), there is no neutron multiplier, resulting in a calculated TBR of 1.05. The pressurized water circulates at somewhat lower temperatures (260 to 300°C) and pressure (11.0 MPa) than in STARFIRE, since the reduced wall loading of 2.1 MW/m² requires less stringent heat transport requirements. The Li₂O is 70% dense and no ⁶Li enrichment is used, since this is a fast blanket (Section 2.2.2).

Table 2-7 Parameters for Some Near-Term Tokamak Designs (after [4])

	FER Japan 1981 [36]	INTOR IAEA 1982 [34]	DEMO US 1982 [23]
Major Radius (m)	5.5	5.1	5.2
Plasma Radius (m)	1.1	1.3	1.3
Thermal Fusion Power (MW)	440	620	1069
Neutron Wall Load (MW/m²)	1.0	1.3	2.1
Plasma Current (MA)	5.3	6.4	8.7
Average β (%)	4.0	5.6	7.5
Burn Pulse Length (s)	100	200	continuous
Toroidal Flux Density (T)	12	11	10
Structural Material	SS	SS	PCA/HT-9 or V
Coolant	H ₂ O	H ₂ O	H ₂ O/liquid Na
Breeder Material	Li ₂ O	Li ₂ SiO ₃	Li ₂ O/17Li-83Pb
Tritium Breeding Ratio	1.05	0.65	1.05

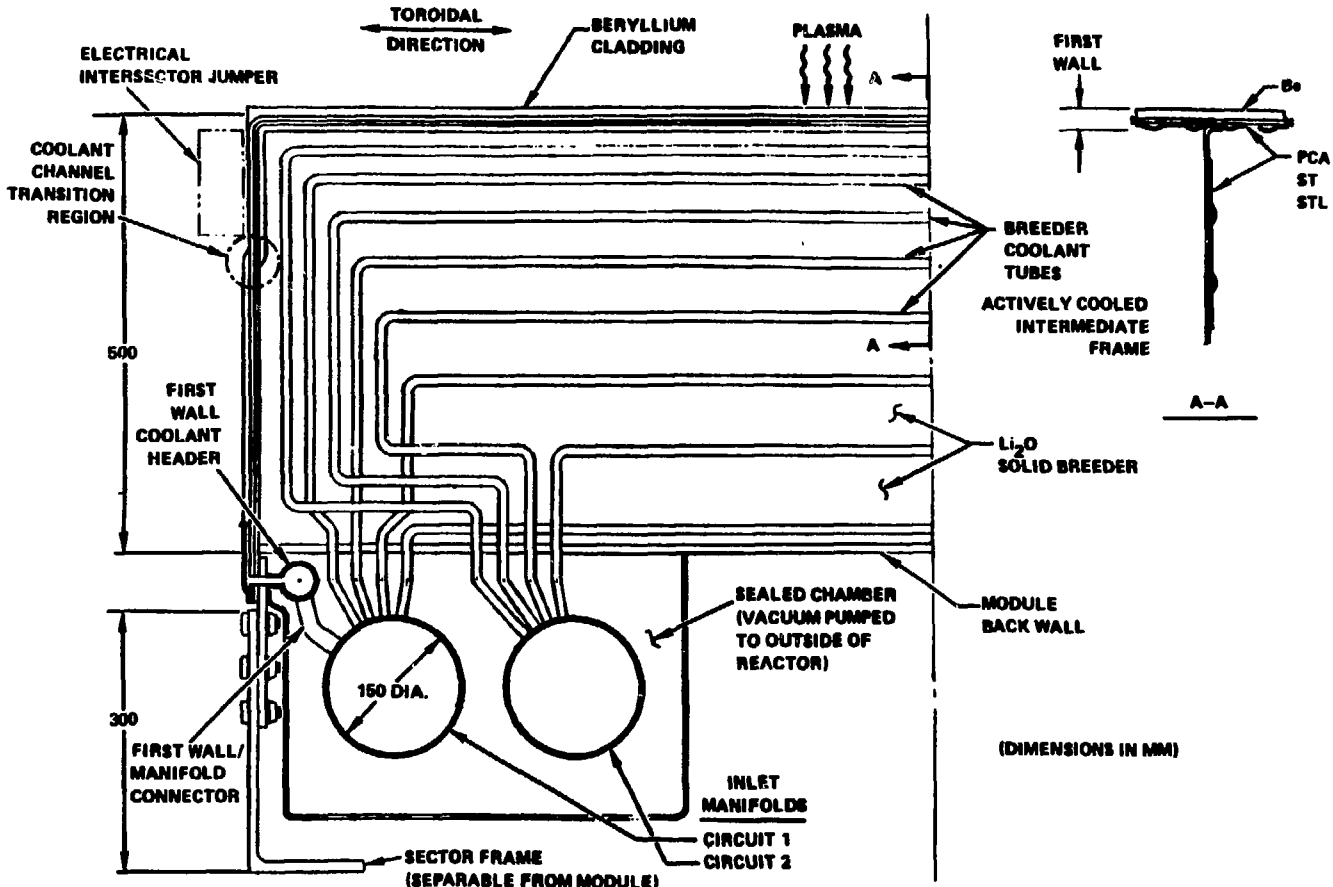


Figure 2-7 DEMO blanket schematic (from [24]).

Considerable attention was given to Li_2O cracking and thermal contact between the coolant tubes and the breeder material - more discussion of this issue is given in Section 5.6. The tritium recovery system is essentially the same as for the STARFIRE design.

The second blanket option uses $^{17}\text{Li}-83\text{Pb}$ separately cooled by sodium in an HT-9 or vanadium alloy structure. The sodium is preferred over water or helium because of its good heat transfer properties, its low reactivity with $^{17}\text{Li}-83\text{Pb}$ and its potential as a tritium recovery fluid. Separate cooling was chosen because of the weight of $^{17}\text{Li}-83\text{Pb}$ and associated large pumping power requirements and the corrosion problems of flowing $^{17}\text{Li}-83\text{Pb}$. As expected from the calculations discussed in Section 2.2.2, the breeder was enriched to 70% in ^{6}Li in this purely thermal blanket. The liquid-metal blanket design looks very similar to the one shown for the solid breeder concept in Figure 2-7. The coolant tubes are less dense because of the superior thermohydraulic properties of sodium, and frame stiffeners have been added because of the weight of the $^{17}\text{Li}-83\text{Pb}$. This seems to be a rather eccentric design, from the safety point of view, and sodium cooling has been rejected in the BCSS[8] for this reason.

2.3.4 MARS

The Mirror Advanced Reactor Study (MARS)[29,30] was intended to design a 1200 MWe commercial tandem mirror reactor comparable to STARFIRE. It represents the second main school of blanket development by Lawrence Livermore National Laboratory and the University of Wisconsin. The MARS blanket is an optimized version of the WITAMIR[28] due to that university. The main parameters of these machines are shown in Table 2-8 and an overview of the MARS facility is shown in Figure 2-8.

MARS, like STARFIRE, is a very large machine, with a cylindrical central cell 130 m in length and 0.49 m in radius. Since it is a linear device rather than a torus, as is the case for a tokamak, a method of preventing plasma from escaping from the end of the reactor is required. This consists of electrostatic plugs with confining potentials. While the central cell is ignited,

Table 2-8 Design Parameters for Mirror Reactors (after [4])

	Near-Term		Commercial	
	TASKA US/FRG 1981 [26]	FPD US 1983 [27]	WITAMIR US 1980 [28]	MARS US 1982 [29]
Central Cell Length (m)	21	75	165	130
Fusion Power, Thermal (MW)	80	1750	3000	2570
Neutron Wall Load (MW/m ²)	1.5	3.6	2.3	4.3
Magnetic Flux Density (T)	6	3.5	6	4.7
Structural Material	HT-9	HT-9	HT-9	HT-9
Coolant	17Li-83Pb	17Li-83Pb	17Li-83Pb	17Li-83Pb
Breeder Material	17Li-83Pb	17Li-83Pb	17Li-83Pb	17Li-83Pb

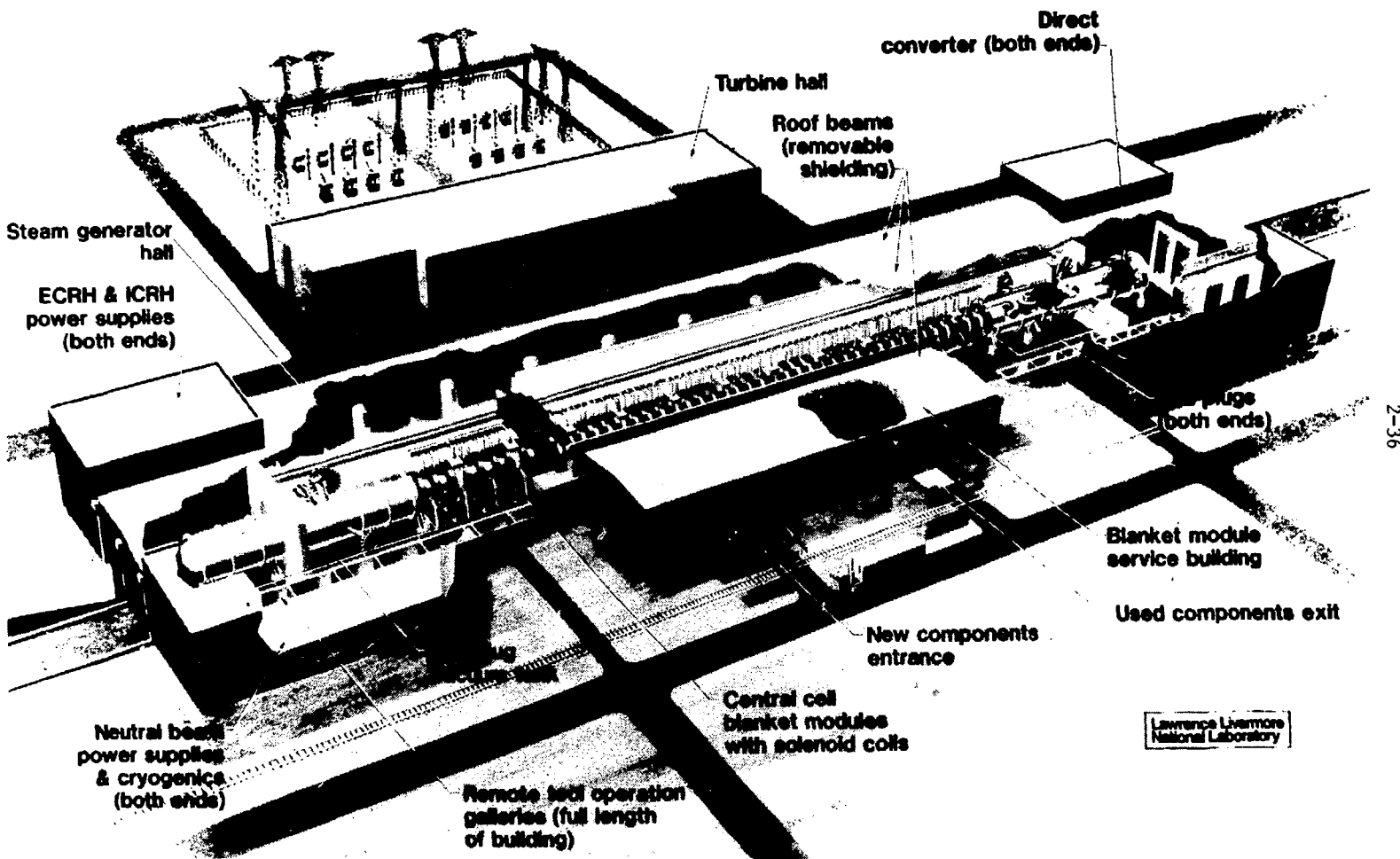


Figure 2-8 The MARS facility (from [30]).

i.e. heated by the fusion alpha particles, the end plugs require continuous heating power of 100 MW. However, about 50% of the injected plug power and alpha particle heating power can be extracted from end plugs by direct conversion schemes (i.e. from charged particles directly rather than by a thermal cycle). This end plugging problem is the crux of the mirror device; if it can be solved, then mirrors will have many advantages compared with tokamaks. For example, since a large fraction of the cost will be in the end plugs, one can scale up a mirror reactor by adding to the central cell, thus achieving a much better economy of scale than is possible with tokamaks. Mirrors are also inherently easier to maintain and probably easier to construct, since the central cell segments are duplicates. The higher β of mirrors, which derives from their simple solenoid-like central cell, is also very attractive. (β refers to the ratio of the kinetic pressure of the plasma to the pressure of the confining magnetic field - a high β is desirable in magnetic confinement fusion.)

The MARS blanket concept is shown in Figures 2-9 and 2-10, and its design parameters are given in Table 2-9. Here $^{17}\text{Li}-\text{83Pb}$ is the breeder and coolant material in a configuration similar to the WITAMIR design[28]. The $^{17}\text{Li}-\text{83Pb}$ flows vertically through tubes and channels made of HT-9, which also form the device's first wall. The central cell is divided into 73 replaceable modules, as shown in Figure 2-10, which weigh only 2.7 Mg without the $^{17}\text{Li}-\text{83Pb}$, making handling and maintenance easier. It is envisioned that each such module would have to be replaced every two or three full power years (FPY), and that it would require about 11 days to replace one. Energy multiplication in the blanket is 1.39 and the TBR is 1.13 in the optimum configuration derived from neutronics calculations. Another important feature is the very low tritium inventory, $< 5 \text{ g}$ at 10^{-4} torr partial pressure, which is a consequence of the low solubility of tritium in $^{17}\text{Li}-\text{83Pb}$. This also implies that the tritium could be extracted just by vacuum pumping (see also Section 4.4). This design requires heat exchangers between the $^{17}\text{Li}-\text{83Pb}$ loop and a steam cycle; the designers of MARS claim that double-walled heat exchangers, under development for the LMFBR program in the US with double-walled tubes, should provide effective tritium containment and safe operation. They have calculated a

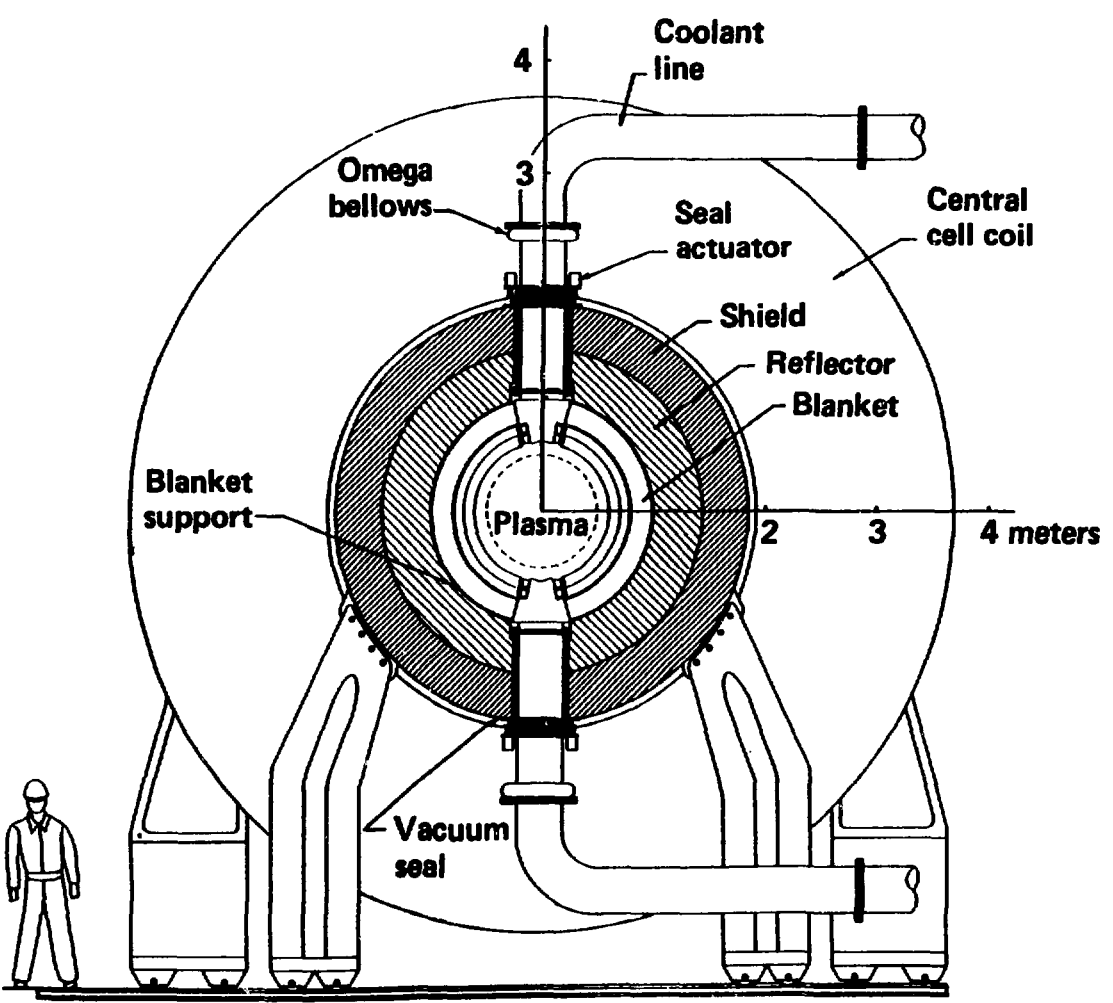


Figure 2-9 MARS central cell cross-section (from [30]).

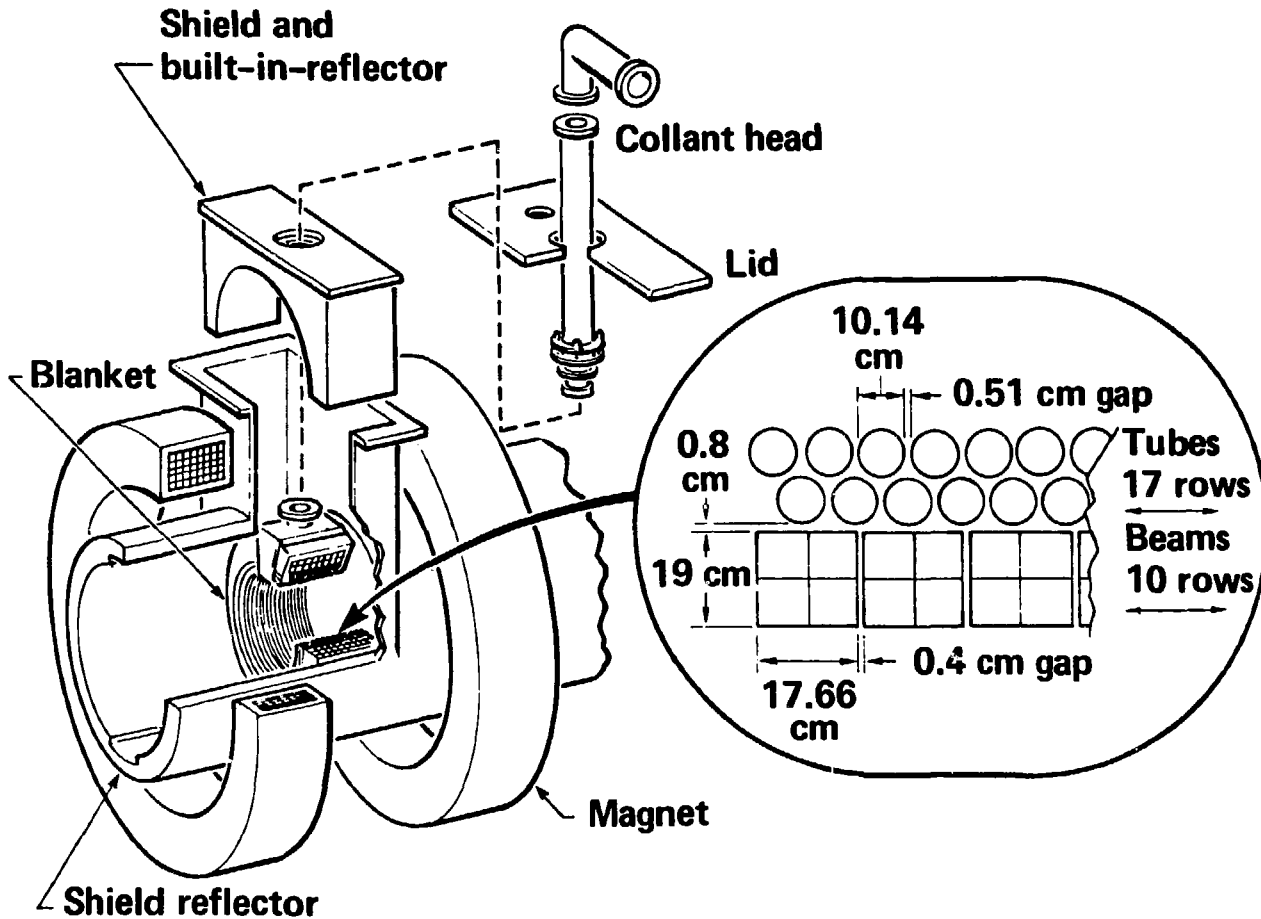


Figure 2-10 MARS blanket details (from [30]).

Table 2-9 MARS Blanket Parameters (from [30])

Blanket thermal power, MW	2070
Reflector thermal power, MW	790
Dia./thickness of blanket tubes, cm	10/0.23
Max. ^{17}Li -83Pb coolant velocity, m/s	0.17
Max. MHD pressure drop, MPa	1.57
^{17}Li -83Pb pumping power, MWe	40
Min./max. structure temp., °C	350/550
Max. dpa rate, FPY ⁻¹	71
Max. appm He production/FPY	560
Max. corrosion rate, cm/FPY	0.0002
Steam temperature, °C	480
Steam pressure, mPa	16
Net efficiency (inc. pumping), %	37
Net central cell power, MWe	1110

tritium loss of ~ 10 Ci/d to the steam side of the cycle. MARS represents the largest design study yet undertaken for a liquid metal breeder system and is thus an important benchmark for such configurations. Overall, the blanket design is simple compared with that required for the STARFIRE blanket.

It was mentioned in Section 2.2 that mirror device designs showed a preference for liquid metal blankets. The reason for this is that the plasma particle and radiative heating at the first wall is typically much less for mirrors than for tokamaks. For example, the surface heat at the wall of STARFIRE is 0.92 MW/m^2 , whereas that for MARS is 0.1 MW/m^2 . This means that the heat transfer requirements at the first wall are less difficult to satisfy even when a degree of laminar flow is present from MHD effects.

Having expressed this bias toward liquid metal blankets for mirror machines, it should be pointed out that a solid breeder concept has been proposed for MARS[31]. Figures 2-11 and 2-12 show schematics of this design, which has Li₂O pellets contained in vanadium tubes cooled by helium. The primary structure of the rest of the blanket is HT-9, and tritium recovery is by means of the helium coolant gas. As Figure 2-12 shows, the Li₂O-bearing tubes have the smallest diameters near the plasma and larger diameters towards the outside, to account for the heat distribution and to keep Li₂O within its operating temperature limits. Neutronics calculations (one-dimensional) showed that a TBR of 1.32 could be achieved without a neutron multiplier; replacement of some of the Li₂O by Be made a dramatic improvement but a neutron multiplier was not included for Be resource reasons. However, it was noted that the energy multiplication factor in the blanket was only 1.1 to 1.15 without a neutron multiplier - for the 17Li-83Pb MARS blanket it is 1.39. A high pumping power is required for the helium circulation; this is 265 MW, $\sim 8.6\%$ of the blanket thermal energy, or at $\sim 40\%$ efficiency about 106 MWe. In contrast, in spite of its high weight the 17Li-83Pb MARS self-cooled blanket uses only 40 MWe (Table 2-9), because of its low velocity. Another concern for helium-cooled systems concerns the structural material compatibility problem. In this design the vanadium alloy tubes will require special coatings to prevent oxidation due to T₂O and in general, against attack by gaseous impurities in the helium. Also, tritium

* 10 Ci = 3.7×10^{11} Bq

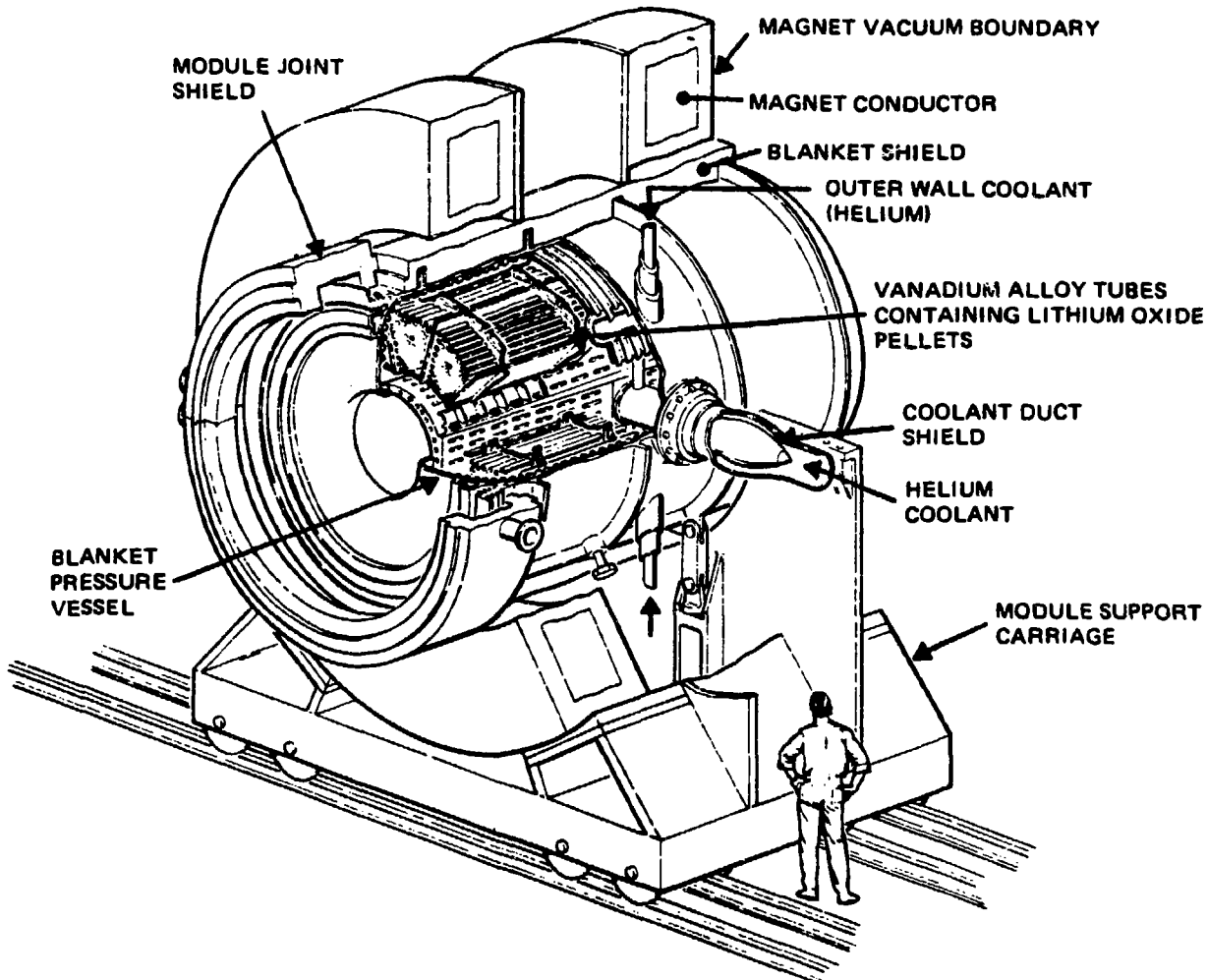


Figure 2-11 MARS solid blanket concept (from [37]).

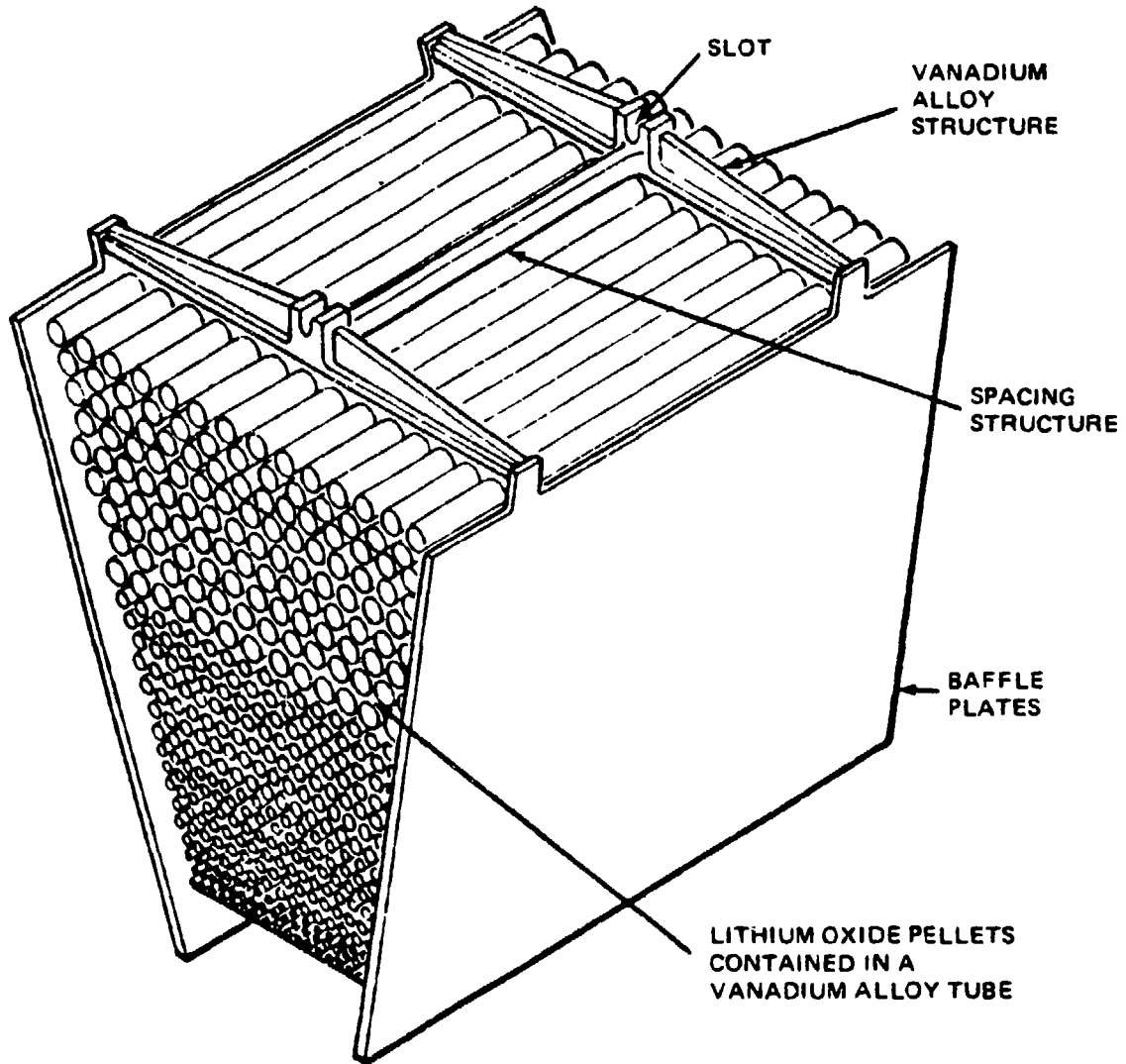


Figure 2-12 MARS solid blanket model (from [31]).

permeation barriers in the helium-steam cycle interface must be very effective to prevent tritium loss and biological contamination.

Before leaving the topic of MARS blankets, it is interesting to note that a combined solid-liquid metal breeder blanket design[32] has also been put forward - this is a rarity and indeed, as far as we can determine, probably unique. The system is shown in Figure 2-13. It consists of a 17Li-83Pb self-cooled low temperature zone (outlet 482°C) with an HT-9 structure, and a high temperature zone (outlet 900°C) made up of a bed of SiC pebbles in SiC baskets containing 2% LiAlO₂ enriched to 90% in ⁶Li that is helium-cooled. In this configuration the 17Li-83Pb serves primarily as a neutron multiplier for the solid breeder and is depleted in ⁶Li to 1%. Therefore, the total design is referred to as the "MARS High Temperature Blanket". The key idea in the whole concept is that the small amount of LiAlO₂ dispersed in the SiC allows operation in excess of the normal upper temperature limit for LiAlO₂ - surprisingly this gives an adequate TBR of 1.13 at startup, declining to 1.03 after four years of full power operation. At startup, a TBR of 1.056 arises from the LiAlO₂ and only 0.070 from the 17Li-83Pb. The advantage of this interesting design is that it delivers 46% of the blanket energy at high temperature and is therefore more thermally efficient (~ 44%) for power generation and also produces process heat suitable for synthetic fuel production.

2.3.5 FPD

The FPD (Fusion Power Demonstration)[27] is intended to fulfill the role of a DEMO for mirror machines, i.e. the next step after MFTF-B on the path to MARS - and in fact, this study is an outgrowth of the MARS study. The main parameters of FPD in its demonstration version have been given in Table 2-8. Because of the ease of scale-up characteristic of mirror machines, the central cell will be essentially the same as MARS, but with total length of 75 m instead of 130 m. It is estimated that tritium consumption would only be in the order of 22 kg/a at full availability. Thus, for 10% availability it would be feasible to buy the tritium but an availability of 50% would imply the necessity of breeding tritium. The modular central cell design would then offer the

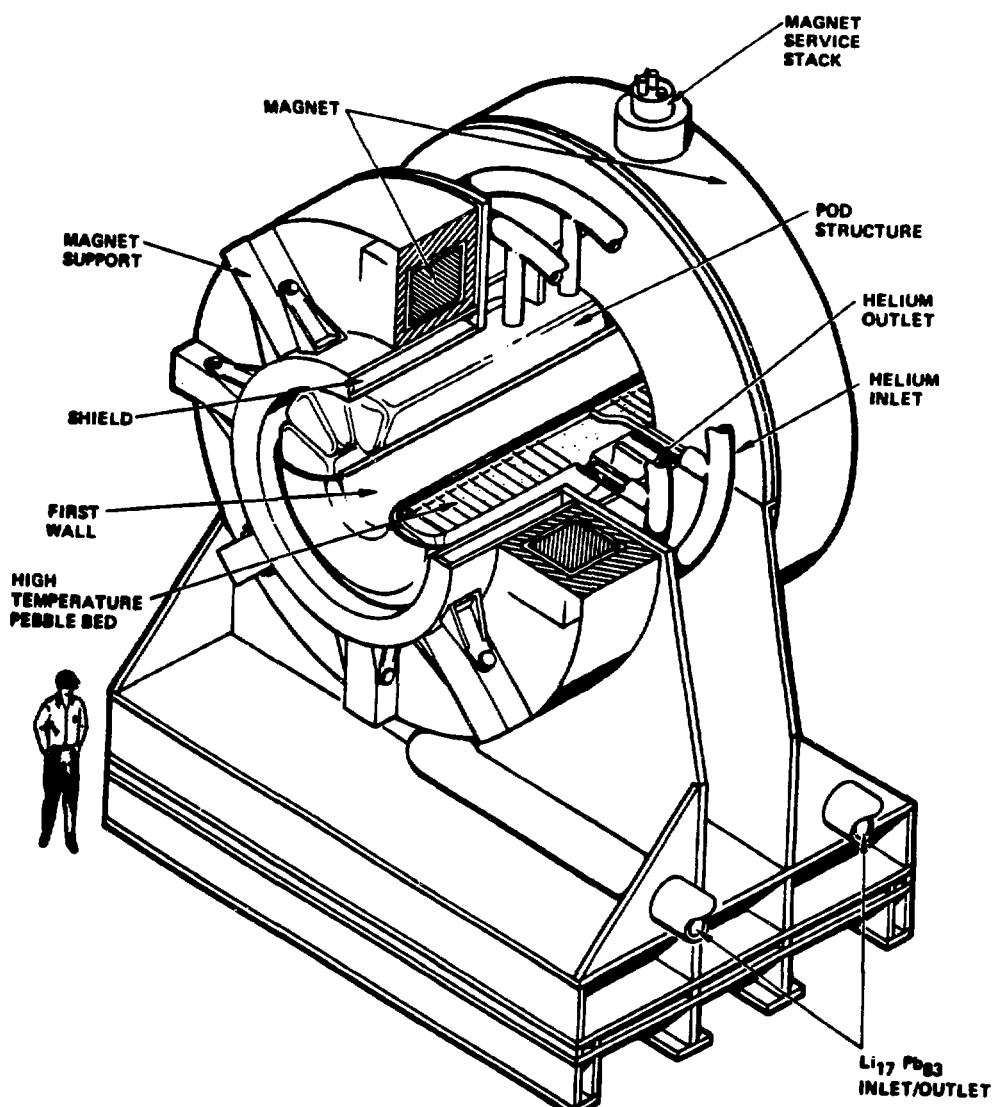


Figure 2-13 MARS high temperature blanket (from [32]).

possibility of testing several different blanket designs in the modules. At this time the FPD study is still in its initial scoping stage.

2.3.6 INTOR

The INTOR activity[33,34] is an international study, sponsored by the IAEA (International Atomic Energy Agency) of the next stage in fusion development after the current large machines. This has been an ongoing study over the past five years on an evolving design concept and hence, it represents with STARFIRE and MARS a third main line of blanket development. While it is very doubtful that the original intention of constructing a US-USSR-EEC-Japan next-step tokamak will ever come to pass for political reasons, the study is very useful for the exchange of ideas on current developments in fusion technology and in some ways can be regarded as a continuous seminar on fusion reactor design. It is probably for this reason that INTOR participation goes on in spite of little hope of meeting the stated objective.

INTOR has had a great effect on the next-step designs of the participants in the study. The US FED (Fusion Engineering Device)[35] and its FED/INTOR version, the Japanese FER[36] from INTOR-J[37], the EEC NET (Next European Torus), and the USSR T-20[38] have all been greatly influenced by INTOR and in most cases the teams for these national designs participate directly in INTOR (see also [39]). The reference INTOR blanket concept[33] was water-cooled Li_2SiO_3 with Li_4SiO_4 as a backup material, and with alternate Li_2O and 17Li-83Pb concepts also for backup. For the Li_2SiO_3 reference concept two designs were evolved, one a breeder outside the coolant tubes with graphite moderator, the other with the breeder material inside tubes concentric with the coolant tubes and moderated by the H_2O coolant. Both designs have a lead neutron multiplier, and D_2O cooling of this multiplier and the first wall is present in design 2. The Li_2SiO_3 is enriched to 30% in ^{6}Li and is packed at 70% density. Tritium is removed by a helium purge gas stream. Since the INTOR blanket is intended to cover only the outboard and upper regions of the machine, an effective TBR of only 0.60 with a local TBR = 1.0 is possible; the designs above are calculated to give an effective TBR of 0.65. This would require a purchase of

0.5 G\$ of tritium over the machine's lifetime which is not a very attractive prospect for most national groups. Furthermore, INTOR has moderate cooling requirements; its blanket would operate at 50°C inlet and 100°C outlet temperatures.

The trend in the development of the national next-step machines has been toward full blanket coverage and operating conditions more realistic in terms of power generation. More discussion of the INTOR design itself is therefore not very useful and the following section will give one example of these national machines - FER.

2.3.7 FER

The Fusion Experiments Reactor (FER) study to design Japan's next-step tokamak after JT-60 is being done at Japan Atomic Energy Research Institute (JAERI)[36]. The mission of this device is to demonstrate the engineering feasibility of fusion with tritium breeding an important goal. Its main parameters are given in Table 2-7. The design is based on INTOR-J[37] (Japan's contribution to INTOR) and FER is essentially an INTOR-class machine with slightly less ambitious plasma performance requirements.

The FER blanket design consists of Li_2O with water coolant and He as a tritium recovery gas; SS 316 is used as the structural material and is considered adequate due to FER's relatively low wall loading. Even so, it is anticipated that the first-wall/blanket will have to be replaced at least once during FER's lifetime of 5×10^5 100 s burns - equivalent to a total of 3 MWy/m^2 . The design TBR of 1.05 is marginal without a neutron multiplier, as extensive one-dimensional neutronics calculations have shown. A 5 cm Pb multiplier between the plasma and the Li_2O combined with ^{6}Li enrichment was shown to increase the TBR by about 15%. Additional improvement resulted from mixing Be pellets with ^{6}Li enriched Li_2O pellets.

As we have seen (Section 2.1.2), a major concern with solid breeding materials is preventing them from experiencing temperatures outside their operating

range. For Li₂O (see Table 5-3), this range is 410 to 800°C. In a pulsed operation mode the plasma is ignited and burned and then the plasma is extinguished for a dwell time before being reignited; the ratio of the burn time to the total burn plus dwell time is the duty factor for the machine. The FER team has done extensive thermohydraulic analysis on the breeder material temperature as a function of duty factor; some results for the minimum and maximum breeder temperature are:

Burn Time (s)	Dwell (s)	Duty Factor	Breeder Max. T (°C)	Breeder Min. T (°C)
100	100	0.50	741	490
200	100	0.67	918	592
300	100	0.75	992	635
100	50	0.67	863	652

These results show that in the FER design the Li₂O would stay within the desired lower temperature limits during pulsed operation. However, the upper limit of 800°C would be exceeded, requiring further design work in this area.

2.4 Summary

No definitive choice can be made between the many breeder blanket concepts proposed to date. The two main classes of breeders, liquid metals and lithium-bearing ceramics, both have unresolved critical issues associated with them. Many fusion reactor studies have indicated the operating parameters required of a real breeder blanket and together with the critical issues, shape the direction of R&D in this area.

3. NEUTRONICS ASPECTS OF BREEDER BLANKETS

3.1 Status of Neutronics/Photonics Data

3.1.1 Introduction

The status of neutronics/photonics data and how well they meet the needs of fusion have been reviewed regularly in the past few years. For example, at the IAEA Advisory Group Meeting on Nuclear Data for Fusion Reactor Technology held in 1978 December, nuclear data requirements for studies of fusion reactor design were presented and discussed in detail[40-42]. More recently, fusion nuclear data needs have been reviewed by Bhat[43] and other workers in this field[44]. It is not the intention of this section to repeat the details of the data requirement list for fusion breeder blankets but to highlight some of the nuclear data development in recent years and to discuss the changes and modifications that have occurred in the data needs.

As we have seen in Section 1.2, the first generation of magnetic fusion reactors will operate on the deuterium-tritium (D-T) cycle. It has also been shown in Section 2.2.2 that neutronic analyses play a key role in the blanket design and significantly influence the overall economics and safety of commercial fusion systems. In the broadest sense, neutronic analyses cover the problems of neutron/photon transport and the computation of the energy spectrum and various reaction rates. In the current stage of development, a wide range of materials are being considered as possible breeder, coolant, and structural materials for different blanket concepts. It is, therefore, essential to have a broad and extensive neutronics/photonics data base to cover a wide variety of materials for neutronic calculations.

Apart from predicting neutron and photon transport, one needs to calculate a number of important nuclear response parameters in the blanket. These are listed as follows:

- tritium breeding ratio (TBR) in the blanket and tritium production distribution;

- nuclear heating;
- radiation damage indicators, e.g. atomic displacements (dpa), gas production and transmutation;
- induced activation and related parameters such as the decay heat and biological dose; and
- neutron and gamma ray shielding attenuation characteristics.

To evaluate these parameters, different types of neutronics and photonics data are needed. The types of data for each application are shown in Table 3-1. The two broad classes of neutronics and photonics data are discussed separately.

3.1.2 Neutronics Data

The types of neutronic data that are important for neutron transport calculations in the blanket are the total, elastic, inelastic, capture and neutron emission cross-sections. Other data requirements are cross-sections for individual neutron reactions and secondary neutron energy and angular distributions. In fusion applications, the high energy reactions, such as (n,α) , $(n,n'\alpha)$ and (n,p) tend to be of great importance, but there is at present little or no information for several important blanket materials[45-46]. Available data in the 7 to 15 MeV energy range are less adequate than those below 7 MeV. Table 3-2 gives an example of the range of data of relevance to calculations of the basic neutronics of the blanket, including neutron flux, spectra and tritium production distribution. The ${}^6\text{Li}(n,\alpha)\text{T}$ and ${}^7\text{Li}(n,n'\alpha)\text{T}$ reactions are of particular importance to breeding and will be discussed first.

3.1.2.1 Data for Tritium Breeding

Neutronic interactions with ${}^6\text{Li}$ and ${}^7\text{Li}$ are important in every fusion blanket design for breeding tritium. While the ${}^6\text{Li}(n,\alpha)\text{T}$ cross section is considered to be reasonably well known, serious questions have been raised about the

Table 3-1 Types of Nuclear Data Required

Data Type	Tritium Breeding	Nuclear Heating	Radiation			Radiation Shielding
			Damage Indicators	Induced Activation		
Total	x	x	x			x
Elastic	x	x	x			x
Inelastic	x	x	x			x
Neutron emission (σ_{en}, $d\sigma/d\Omega$, $P(E')$)	x	x	x			x
(n,2n); (n,3n)	x	x		x		x
(n,α); (n,n'α)		x	x		x	
(n,p); (n,n'p)		x	x		x	
(n,d); (n,n'd)		x	x		x	
(n,t); (n,n't)	x	x	x		x	
(n,γ); (n,n'γ); (n,xγ)		x		x		x
Gamma Production (σ_p, $d\sigma/d\Omega$, $P(E_n \rightarrow E)$)		x				x

Table 3-2 Nuclear Data of Importance to Neutronics Calculations in Blanket

Component	Candidate Materials	Reactions	Remarks
Structure	Refractory materials/alloys Nb, V, Mo, Ti. Stainless Steel, Fe, Ni, Cr.	Neutron absorbing reactions, elastic and inelastic scattering, $(n,2n)$	Secondary neutron spectra and angular dependence
Breeder	^6Li , ^7Li Li ceramic compounds (Li_2O , ternary oxides) Li alloys (Li-Pb, LiAl) Molten salts (FLIBE)	$^6\text{Li}(n,\alpha)\text{T}$ $^7\text{Li}(n,n'\alpha)\text{T}$ absorption, $(n,2n)$ and elastic and inelastic scattering	Secondary neutron spectra and angular dependence
Neutron Multipliers	Be, Pb	$(n,2n)$, inelastic and elastic scattering, neutron absorption	Secondary neutron spectra and angular dependence
Moderators and Reflectors	C, Steel		
Coolants	H_2O , He, Na, HTS		

accuracy of the ${}^7\text{Li}(\text{n},\text{n}'\alpha)\text{T}$ reaction cross section that is currently in the ENDF/B-V data file. The over-prediction of tritium production in integral experiments[47-48] suggested that the ${}^7\text{Li}(\text{n},\text{n}'\alpha)\text{T}$ reaction cross section might be from 10-35% too high near 14 MeV (also see Section 3.3). The new differential data from Swinhoe[49] indicate that the ENDF/B data should be lowered from 15% to 25%. It is apparent that recent experimental results are all consistent with a lowering of the ENDF/B-V tritium production cross section of ${}^7\text{Li}$, but there is still disagreement on the magnitude of the corrections. New evaluations for ${}^6\text{Li}$ and ${}^7\text{Li}$ that consider both old and new experimental data are currently in progress at Los Alamos National Laboratory (LANL).

Recent developments concerning the tritium breeding materials and neutron multipliers in solid breeder blankets are important. Calculations of Section 2.2.2 showed that the tritium breeding ratio with all ternary lithium oxides (with the possible exception of Li_8ZrO_6) is less than one and, therefore, the use of a neutron multiplier such as beryllium, lead or Zr_5Pb_3 is necessary. Tritium breeding capability is thus emerging as a potential feasibility problem for solid breeder blankets. This suggests not only a need for a complete base of nuclear data but it indicates the accuracy required. The magnitude of $(\text{n},2\text{n})$ and parasitic absorption cross-sections as well as the energy distribution of secondary neutrons from all the neutron-producing reactions must be known to a higher degree of accuracy for all the solid breeders and neutron multipliers mentioned above. The neutron slowing down and absorption properties in the structural material and coolant are also critical in the solid breeder systems. The main requirements at present are thus to improve the accuracy of the basic nuclear data for materials in the solid breeder blanket.

3.1.2.2 Neutron Emission Data

The need for more accurate emission data for secondary neutrons has become increasingly evident with improvements in method and codes for neutron transport, heating and radiation damage calculations. Neutron emission spectral data is needed as a function of secondary angle and energy for

selected incident neutron energies in the 9 to 14 MeV range for materials, such as ^7Li , C, ^{11}B , Fe and other structural materials. Experimental facilities have been developed at LANL and at the Triangle Universities Nuclear Laboratory (TUNL) for measuring neutron emission spectra induced by neutrons in the MeV energy region. Thus far, measurements have been made for 6, 10 and 14 MeV incident neutrons at LANL[50,51] for ^6Li , ^7Li , ^9Be , ^{10}B and ^{11}B and at several energies between 8 and 14 MeV at TUNL for Fe, Cu, Ni and Pb. Similarly, neutron spectrum measurements have been made at the Oak Ridge Electron Linac Accelerator (ORELA)[52] for ^7Li , Al, Ti, Cu and Nb. Some of these data have been incorporated into an evaluation that differs significantly from the existing ENDF/B-V data file.

3.1.2.3 Radiation Damage Data

The radiation damage problem is of vital importance for fusion blanket studies. Both displacement effects and nuclear transmutations are expected to contribute to the total radiation damage, the latter phenomenon leading to the formation of hydrogen and helium gases (Section 2.2.1). For displacement calculations, differential angular cross-sections for elastic and inelastic scattering are needed. These needs can be met by existing data and theoretical calculations. For calculations of radiation damage due to nuclear transmutations, the cross section of many reactions, especially those contributing to hydrogen and helium formation are needed. The data base has been very weak. In particular, hydrogen and helium production data for ^7Li , C, Ni, Si, Cu, ^{11}B between 9 and 15 MeV are needed. Recently, there have been some data measurements for a variety of structural materials at 15 MeV[53]. Currently a special gas production file is being set up for the ENDF/B-V data file. However, more experimental data are needed at energies between 9 and 14 MeV for various blanket structural materials.

3.1.3 Photonics Data

Photonics data can be classified into two areas: (a) gamma-ray production and (b) gamma-ray interactions.

Gamma-ray production data is very crucial to nuclear heating and radiation shielding applications. The status of nuclear data in this area has improved over the past several years. Some of the experimental work done at ORNL has been summarized by Dickens and co-workers[54]. These cross-sections have been measured for $0.3 < E_{\gamma} < 10.5$ MeV and $0.1 < E_n < 20.0$ MeV for 22 elements. Data at lower gamma-ray energies may be important for heat deposition calculations. Measurements at lower energies would also be helpful in many cases. For the past few years, there have been significant improvements in the ENDF/B data file, but there is at present still no reliable gamma production data for important materials such as ^{11}B and tungsten.

In general, two types of information are required: (a) the total gamma production cross-section as a function of the incident neutron energy, and (b) the energy distribution of emitted gammas as a function of the incident neutron energy. The angular distribution of emitted gammas is also needed, but at a lower priority. An extensive set of measurements of gamma-ray emission spectra using the ORELA white neutron source has been carried out at ORNL[52]. These results generally span the incident neutron energy range from 1 to 20 MeV and have been performed for most of the common materials. In addition, a series of gamma-ray spectrum measurements for monoenergetic 14 MeV neutrons has been carried out at LANL[55] for a variety of materials. These measurements have been very useful for gamma-ray production evaluations.

Nuclear data for gamma-ray interaction is generally the best known of all types of data. Only modest revisions are required in this area.

3.1.4 Nuclear Data Libraries

The present nuclear data, both experimental and evaluated, constitute an extensive data base for the development of fusion energy. Experimental data are compiled routinely, exchanged through international agreements and available from established centers such as the National Data Center at the Brookhaven National Laboratory. Neutronics codes for carrying out both scoping surveys and detailed design calculation for fusion blanket in general

require the neutronics data in a different appropriate format from the basic nuclear data libraries, e.g. cross section in a groupwise structure. Evaluated data libraries such as ENDF/B[56] and ENDL[57] are extensively and widely used. Table 3-3 lists all the evaluated nuclear data libraries to date. In general, they extend from about 1.0×10^{-5} eV to 15 or 20 MeV and consist of neutron and gamma-ray production data. The evaluations are based on available experimental data supplemented by nuclear model calculations where such data do not exist.

It has been observed that the types of data available in a nuclear data library have to be updated and modified frequently to keep pace with an increasing number of applications. As an example, the growth of the ENDF/B library is shown in Table 3-4. Starting from about 1970, after the release of the Version II library, greater emphasis was placed on the energy region around 14 MeV in the ENDF/B evaluation. This was followed by format modifications to include new data for fusion applications and a conscious planned attempt to satisfy their needs in the subsequent versions of the library. This accounts for the inclusion of gas production, activation and decay data in ENDF/B-V.

The National Magnetic Fusion Energy Computer Center network (NMFECC) and the Radiation Shielding Information Center serve as distribution points in the fusion community for processed data libraries. For example, on the NMFECC network, the ENDF/B-V evaluated library is available as processed data in the DLC series[58,59] and other special series. The GAMMON activation library[60], specially designed for fusion reactor applications, is also operational at the NMFECC. It contains multigroup cross sections - 100 energy groups for 420 neutron-induced reactions and multigroup gamma-ray spectra - 25 energy groups for 107 unique daughter products.

The multigroup coupled neutron and gamma-ray cross-section libraries, the DLC-37 and DLC-41 series have been widely used for fusion reactor blanket and shield design calculations. The DLC-37 library, which was created in 1975 primarily for the fusion experimental power reactor (EPR) design, has a 100-group neutron and 21-group gamma-ray structure. The first group of this

Table 3-3 Evaluated Nuclear Data Libraries

Library	Country	Description
ENDF/B	USA	General cross-section data set
ENDL	USA	Fast reaction cross-section data set
JENDL	Japan	General cross-section data set
KEDAK	Fed. Rep. of Germany	Fast reaction cross-section data set
SOKRATOR	USSR	General cross-section data set
UKNDL	United Kingdom	General cross-section data set
Los Alamos Library	USA	Neutron multigroup data $E_n \leq 60$ MeV
Oak Ridge Library	USA	Neutron-photon multigroup data $E_n \leq 60$ MeV

Table 3-4 Contents of ENDF/B Library

Data Type	ENDF/B-I 1967	ENDF/B-II 1970	ENDF/B-III 1972	ENDF/B-IV 1974	ENDF/B-V 1979
General purpose	48	52	69	90	117
Lumped fission products	9	9	9	9 ^a	9 ^a
Thermal scattering data	7	7	7	7 ^a	7 ^a
Fission products		55	55	825	825
Photon production			11	42	53
Photon interaction			yes	yes	yes
Standards			7	7	7
Dosimetry				36	36
Decay data				825	932
Data covariance				3	65
Actinides					40
Gas production					22
Activation					84

^a Available in ENDF/B-III format only.

library extends from 13.499 MeV to 14.918 MeV, which sufficiently brackets the D-T fusion neutron spectrum. The first 10 groups cover the energy range above 5.5 MeV, adequately treating the important energy range that produces tritium via the $^7\text{Li}(n,n'\alpha)\text{T}$ reaction. The 100th group is the thermal neutron group, whose energy ranges from 0.022 eV to 0.414 eV. The DLC-41 (VITAMIN-C) released in 1977 is a general purpose fusion library which consists of a 171-group neutron and 36-group gamma-ray structure. The upper energy of the neutron group structure (17.333 MeV) is well above that of the DLC-37 library. These changes make the DLC-41 library applicable to selected problems in fusion neutronics. For instance, the DLC-41 library can be used to study the effect of D-T fusion neutron energy spectrum on tritium breeding, which the DLC-37 cannot because there is only one neutron group in the DLC-37 library for these neutrons.

Very often the multigroup cross-section nuclear data libraries are collapsed into a fewer-group structure than the original 171-neutron/36-gamma-ray group structure of the DLC-41 library, before being used in neutronics calculations. The purpose of this further collapse is to reduce computational time and data storage. For conceptual blanket design calculations, a 25-group neutron and a 21-group gamma-ray structure of the DLC-41 library is often used.

Computation codes in general require the neutronics and photonics data in different specified format from basic data libraries. A number of processing codes, including MINX, SUPERTOG, AMPX, NJOY[61-64] have been developed to service the needs for neutron and photon transport and calculations of reaction rates, such as activation, transmutation, radiation damage and nuclear heating. Existing processing codes are generally adequate for producing multigroup cross-sections, kerma factors (Section 3.4.5), photon production matrices and radiation damage functions. Processing individual portions of these data independently often produces inconsistencies (for example, between kerma factors and photon-production matrices), resulting in non-conservation of energy. This may not be due to any deficiency in the individual processing codes, but rather to data evaluation inconsistencies[65]. Nevertheless, most processing codes should prove accurate enough for foreseeable future requirements, especially as compared with data uncertainties.

3.1.5 Accuracy of Nuclear Data

Another area of concern is the required accuracy in the nuclear data. This is a difficult area and is part of the more general question of the required accuracy in predicting nuclear performance characteristics. Table 3-5 lists some target accuracies in predicting the important nuclear design parameters in the blanket and the shield. The target accuracy for calculating nuclear responses in the shield can be much less than those in the blanket. Generally, very good accuracies are required in the blanket, where primary energy conversion and tritium production occur. For example, the accuracy goal for predicting the tritium breeding ratio is 2%. Thus, the accuracy of nuclear data should be such that the contribution of nuclear data uncertainties to the error in tritium breeding ratio estimates is ~ 1% or less. From previous studies, it has been observed that an accuracy of ~ 5 to 10% in data for neutron transport may be sufficient. Exceptions can be noted for several key blanket materials such as beryllium and lead, where accuracies of ~ 3% are required.

Two key questions on data accuracy may arise. One is how much of the tolerance in design calculation accuracy can be permitted for nuclear data.

The second is how much inaccuracy in estimating a nuclear performance results from an error in a particular part of nuclear data in a specific energy range for a given material. Sensitivity analysis is often resorted to for defining such nuclear data accuracy needs. Sensitivity analysis can be used to examine the effects of uncertainties in nuclear data, as well as variations in materials and geometry on the calculated design parameters of interest. The quantitative methodology of sensitivity analysis has been developed based on simple perturbation theory. In the past years, there has been very significant progress in developing theoretical formalisms for sensitivity analysis[66]. A number of sensitivity studies for fusion applications have also been performed[67,68].

Computer codes such as SENSIT[69] and SWANLAKE[70] have been highly developed to provide sensitivities of integral design parameters to cross-section data

Table 3-5 Required Data Accuracies

Location/Response	Desired Accuracy
<u>First Wall/Blanket</u>	
Nuclear heating	total 2%, spatial distribution 10%,
Tritium production	breeding ratio 2%, local 10%
Atomic displacements	10%
Helium production	10%
Transmutations	20%
Induced activation	50%
<u>Bulk Shield</u>	
Nuclear heating	gross 20%, local 30%
He and H production	factor of 2
Activation	factor of 2
Tritium production	factor of 3

and material arrangements. The principal objective in cross-section sensitivity analysis is to provide guidance to improve nuclear data. From the resulting uncertainties in nucleonic parameters one has an integral view of the combined effect of all cross-section errors. Similarly, the sensitivity codes can easily be used to determine the effects of design changes on various nuclear responses. The latest generation of the sensitivity code, SENSIT, is currently operational on the NMFECC network. The code is specially tailored for fusion reactor sensitivity and uncertainty analysis, both for cross-section errors and design perturbations. Included in the cross-section category is the capability to compute sensitivities and uncertainties caused by secondary-neutron energy and angular distribution errors.

At this stage of development, a principal difficulty with the sensitivity studies is that the information they yield on data accuracy is highly system-dependent. For instance, ${}^6\text{Li}$ and ${}^7\text{Li}$ are both critical to tritium breeding but the importance of ${}^7\text{Li}(\text{n},\text{n}'\alpha)\text{T}$ cross-section accuracy depends critically on the blanket system considered. In a thermal neutron system, the ${}^7\text{Li}$ contribution is almost negligible (Section 2.2.2). However, for systems such as those with natural lithium and Li_2O , the ${}^7\text{Li}(\text{n},\text{n}'\alpha)\text{T}$ contribution can be more than one third of the breeding ratio and therefore the required accuracy of this cross section may be as high as 3% in these systems. Furthermore, another difficulty with sensitivity studies is that they require as part of the input information uncertainties in the cross sections and the correlations between the various cross-section errors. These data may not be available for many materials.

3.2 Status of Neutron/Photon Transport Methods

3.2.1 Introduction

In the discussion that follows "gamma rays" can be considered to be interchangeable with the word "neutrons" since the same equations are applicable to both. A complete description of the neutron population must specify simultaneously the distribution in space, energy, time and direction of motion; the

two approaches currently used for this purpose being transport theory and/or the Monte Carlo method. Transport theory is based on neutron conservation equations which in principle could give exact results assuming the availability of perfect nuclear data and an exact geometrical representation. However, in practice it is generally too complicated to solve the equations exactly and various assumptions and approximations are used. In the Monte Carlo method the life history of each neutron is followed, the distance between collisions, the type of reaction at a collision, the change in direction, and the change in energy being regulated by probabilities (cross sections) and random numbers. Advantages of the Monte Carlo method are the avoidance of assumptions of the physical model and fewer restrictions in the geometrical representation. The disadvantage is that the end result is an estimate subject to sampling errors and to obtain a sufficiently good statistical accuracy many thousand neutron histories have to be followed.

These methods were developed for fission reactor calculations. In the fusion blanket application greater emphasis is placed on the $n-\gamma$ coupling interaction.

Both methods require extensive nuclear cross section data as functions of energy and scattering angle.

3.2.2 Transport Theory

A general introductory description of transport theory is given in Weinberg and Wigner[71] and is summarized here. In transport theory, the fundamental variable is the angular flux:

$$\phi(\underline{r}, E, \underline{\Omega}, t) d\underline{r} d\underline{\Omega} dE \quad (1)$$

and the equation that describes the time variation of the neutron population, called "Boltzmann's Transport Equation", is derived by considering the neutron balance for the set of neutrons located in the volume element dV about \underline{r} , having energy E and velocity vectors that lie in the solid angle $d\underline{\Omega}$ about

direction $\underline{\Omega}$ at time t . The neutron density $1/v \phi(\underline{r}, E, \underline{\Omega}, t)$ in a volume element dV and phase space $d\underline{\Omega} dE$ can change in time due to five effects:

- neutrons which stream through the volume element without collision (leakage);
- neutrons which are removed by being scattered into a new direction $\underline{\Omega}'$ and/or a new energy E' ;
- neutrons which are removed by absorption collisions;
- presence of sources;
- introduction of neutrons due to collisions from direction $\underline{\Omega}'$ to $\underline{\Omega}$ or from energy E' to E or by delayed events from t' to t .

In a standard notation the Boltzmann transport equation describing this neutron balance is given below with the above five effects in corresponding order on the right hand side.

$$\frac{1}{v} \frac{\delta \phi}{\delta t} = - \underline{\Omega} \cdot \nabla \phi - \Sigma_g \phi - \Sigma_a \phi + S(\underline{r}, E, \underline{\Omega}, t) + \int dE' \iint d\underline{\Omega}' d\underline{\Omega} \int dt' \phi' (E' \underline{\Omega}' t' - E \underline{\Omega} t) \quad (2)$$

The main application of this equation is the determination of the steady state solution in which case the time dependency is ignored. It is also usual to simplify the problem by splitting the energy range into a number (G) of intervals called groups which eliminates the energy variable but results in a set of G linked equations. In this case it is also necessary to define group average cross sections which impose a fixed flux shape condition within the group.

The set of G linked equations is not solvable analytically in practical heterogeneous geometries, and numerical methods are used. Thus although in principle the method is exact, uncertainties are introduced due to approximations in the numerical method, approximations in the geometrical representation, uncertainties in the group averaging and uncertainties in the absolute values of the nuclear data.

Two numerical approximations which are used to make the problem more manageable are the P_L and S_N approximations, for more detail see Dolan[72]. In the P_L approximation the angular dependence of the scattering cross-section is expressed in terms of Legendre polynomials

$$\Sigma_S(\underline{r}, \mu_0, E' \rightarrow E) = \sum_{\ell=0}^L \Sigma_\ell(\underline{r}, E' \rightarrow E) P_\ell(\mu_0) \quad (3)$$

where μ_0 is the cosine of the angle between Ω and Ω' . In the expansion $L=\infty$, but acceptable accuracy is usually obtained with $L \leq 5$.

In the S_N or discrete ordinates method the phase space $(\underline{r}, \underline{\Omega}, E)$ is separated into intervals \underline{r} , $\Delta \underline{\Omega}$, ΔE and the term "S_N approximation" means that N angular intervals $\Delta \underline{\Omega}$ are used. The Boltzmann equations for each incremental phase space zone produce a set of linear algebraic equations in which all parameters except the flux are known. The derivatives of ϕ may be replaced by the finite difference approximation and the resulting equations are solved iteratively.

If the angular dependence is dropped ($L=0$, $N=1$) we get multigroup diffusion theory which, although used extensively in fission reactor core calculations, is not sufficiently accurate to model fusion blanket concepts.

In practice the solution of the transport equation is usually restricted to one- or two-dimensional problems, and although it may be adapted to three dimensions the computer time becomes prohibitive and Monte Carlo methods are preferred.

Typical transport theory codes used in fusion reactor studies are:

- ANISN[73], which solves the one-dimensional multigroup coupled neutron-gamma time independent Boltzmann transport equation by the discrete ordinates method;
- TDA[74], a Time-dependent version of ANISN;
- DOT[75], a Two-dimensional discrete ordinates transport code.

3.2.3 Monte Carlo Method

A brief description of the Monte Carlo Method is given by Henry[76] and its application to blanket and shield design is discussed by Dolan[72]. For completeness the general principles of the method are included here.

The Monte Carlo method is a procedure in which a large number of neutron case histories are simulated by a computer and is mostly used for the analysis of geometrically complex assemblies for which numerical techniques are extremely time-consuming.

An individual neutron case history is a sequence of events starting with the initial source neutron and ending when the neutron is lost to the system either by absorption or leakage. To make efficient use of computer time, each individual neutron is tracked until its weight becomes less than some value and in practice a neutron is "lost" by leakage only. The particular events that make up an individual case history are determined from the laws of probability that govern the event under consideration (i.e. the appropriate cross section) through application of a table of random numbers. Events treated in this way are: the type of interaction, the products of the interaction (and their eventual histories) and the distance between interactions.

In general, Monte Carlo codes use the multigroup approximation to treat the energy variable except for the LASL Monte Carlo code MCNP[77], which uses a continuous energy approach with a pointwise cross-section data library.

The disadvantage of the Monte Carlo approach is that the end result is an estimate subject to sampling errors, and to obtain sufficiently high statistical accuracy many thousand neutron histories have to be followed. To improve the statistical accuracy for a given number of neutron histories, several variance-reducing techniques have been developed, for example: variable weighting, biasing to increase the importance of particles going in a desired direction, correlation techniques for differential effects, Russian Roulette and splitting.

Typical Monte Carlo codes used in fusion blanket studies are MORSE [78], MCNP [77], continuous energy and TARTNP [79].

3.3 Validation of Data and Methods Against Experimental Benchmarks

3.3.1 Introduction

In the development of fission reactor neutronics, benchmark experiments using subcritical and critical assemblies have been extremely useful in checking both nuclear data and calculation methods. It is expected that similar benchmark experiments on integral assemblies are likely to be equally valuable for fusion systems. In particular, validation of neutron spectra, tritium breeding and other reaction rate calculations will play an essential role in fusion breeder blanket development. Neutronic benchmark experiments can be classified in three basic categories, according to the nature of the information that is to be extracted. There are experiments to:

- validate and improve the basic nuclear data and, to a lesser extent, calculational methods;
- test the feasibility of generic design; and
- verify the performance of detailed designs.

Fundamental experiments in the first category should be "clean" so as to allow the highest confidence in interpreting subsequent analysis in terms of basic

cross sections. Data would be collected from homogeneous material or mixtures in very simple spherical, cylindrical or slab assemblies. Information developed would be made available to cross-section evaluators for use in identifying nuclear data deficiencies and in improving nuclear cross-section data sets. These experiments could also provide well documented benchmarks for code evaluation.

Feasibility experiments in the second category are "simple" design-oriented ones that incorporate some degree of geometrical or compositional complexities to test generic engineering design approaches. Each experiment may be designed to simulate a particular blanket design or feature to generate a more representative blanket neutron spectrum. However, the configuration in this type of experiment is still kept "simple" enough to allow for neutronic calculation to be performed relatively easily and accurately. The emphasis is to determine the real design parameters such as tritium breeding, heating, dose and damage rates. These experiments are also to provide directly usable design information such as thick shield attenuation factors and provide tests of the codes used in engineering designs.

Experiments in the third category are engineering mock-ups for final design verification. The experiments are designed to incorporate all the essential features of a proposed real blanket and would be performed just before the design was to be finalized. Because of the complexities involved, it would be rather difficult to identify the actual cause of any poor performance and to resolve any discrepancies between calculations and measurements. Very few such experiments would normally be performed because they are usually expensive.

3.3.2 Review of Some Earlier Integral Experiments

In the past, a number of 14 MeV source neutron experiments have been performed and analyses carried out on lithium metal as spheres and cylinders and a wide variety of other materials, including lithium deuteride, lithium fluoride, graphite and iron. Leonard[80] and Maynard[81] have given a comprehensive review of these experiments. Table 3-6 lists a number of fusion blanket

integral experiments[47,82-93] performed over the period from 1954 to 1976. All these experiments employed D-T sources, both steady state and pulsed, at the centre of simple homogeneous spherical or cylindrical assemblies. Attempts were made to keep the geometry simple. Thus, the experiments tend to fall in the first category of benchmark experiments, which are reasonably easy to calculate and test data in a general way.

The quantities measured include tritium production, foil activation rates, fission rates and leakage spectra. Analyses were performed with a variety of basic cross-section data sets (ENDF/B-III, -IV, ENDL) and both Monte Carlo (TART, MORSE) and deterministic (ANISN, DTK, DOT-I, TWOTRAN, DTF-IV) codes. Experimental accuracies were reported to range from 5 to 10%. Comparison of experimental results with calculations revealed many discrepancies, sometimes over 50%.

In an earlier era, it was almost impossible to discuss results between different institutions, as they used different data bases and calculational procedures. An inspection of Table 3-6 shows that the situation has almost reached the opposite extreme. The limited independence in the calculation method data sets used leads to some concern that all the tests will miss important errors completely. For example, two reports gave no analysis, five used S_N calculations implemented with the ANISN computer code for calculations. One employed DTF-IV and one DTK, which are hardly independent codes. Two experiments were analysed with the TART program (an analogue Monte Carlo), which represents an independent calculational method. The data sets also tend to be the same: generally only ENDF/B-III and -IV were used. The only exception being the LLL analyses that employed ENDL as well as ENDF/B. The data difference between sets and the relative agreements with experiments were used to gain insight into the data adjustment. However, none of the other studies included an uncertainty analysis to assess possible data adjustment.

3.3.3 Validation of Data

A number of recent lithium integral experiments have indicated that serious errors may well exist in the ENDF/B and UKNDL files for the reaction

Table 3-6 Some Earlier Integral Experiments

Experiment Number	Year [Ref.]	Experimental Facility and Laboratory	Measurements	Data and Calculational Basis	Experimental Error: Experiment-Calculation Discrepancies
1	1954 [47,82]	30 cm sphere of natural LiD at LANL	Reaction rates for $^7\text{Li}(n,t)$ and natural Li(n,t) as a function of detector position	ENDF/B-III, IV; NJOY; DTF-IV; ALVIN	Experimental 5% Volume integrated results \leq 12% Spatial discrepancies \leq 20%
2	1961 [83,84]	Natural uranium metal pile 106.6 cm high and up to 99 cm in diameter at ANRE	Reaction rates as a function of position for $^{63}\text{Cu}(n,2n)$, $^{235}\text{U}(n,f)$, $^{238}\text{U}(n,f)$, $^{238}\text{U}(n,\gamma)$, $^{239}\text{Pu}(n,f)$	ENDF/B-IV, ENDL, CLYDE, TART	Experimental 3-6% except for $^{238}\text{U}(n,3n)$ reaction rate. Discrepancies 5-40%
3	1964 [85]	Metallic natural lithium cylinder 101.6 cm high and 99 cm in diameter	Flux spectra and neutron leakage. Reaction rates: $^7\text{Li}(n,t)$; $^6\text{Li}(n,t)$; $\text{Au}(n,\gamma)$; $\text{Au}(n,2n)$; $^{238}\text{U}(n,\gamma)$; $^{31}\text{P}(n,p)$; $^{22}\text{Al}(n,p)$; $^{27}\text{Al}(n,\alpha)$; $^{107}\text{Ag}(n,2n)$; $^{63}\text{Cu}(n,2n)$. Fission rates: $^{235}\text{U}(n,f)$; $^{237}\text{Np}(n,f)$; $^{232}\text{Th}(n,f)$; $^{236}\text{U}(n,f)$		Experimental: total tritium production $<$ 5%. Spatial scatter in excess of 10%.
4	1974 [86]	Metallic natural lithium cylinder 120 cm high, 120 cm OD, 20 cm void at the axis at IFR Jilich	Li(n,t) as a function of position by radiochemical methods and by solid state track recorders, fast flux by thorium fusion fragment track recorders.	ENDF/B-I,-III; SUPERGIC; ANISN, DOT II, MORSE	Not given quantitatively, but figures indicate large experimental errors and discrepancies with calculations

Table 3-6 Some Earlier Integral Experiments (cont'd)

Experiment Number	Year [Ref.]	Experimental Facility and Laboratory	Measurements	Data and Calculational Basis	Experimental Error: Experiment-Calculation Discrepancies
5	1974 [87]	Large graphite stack at BNL	As a function of position, reaction rates for $^{197}\text{Au}(n,\gamma)$; $^{197}\text{Au}(n,2n)$; $^{55}\text{Mn}(n,\gamma)$; $^{63}\text{Cu}(n,\gamma)$; $^{65}\text{Cu}(n,2n)$; $^{58}\text{Ni}(n,p)$; $^{58}\text{Ni}(n,2n)$; $^{27}\text{Al}(n,p)$; $^{27}\text{Al}(n,\alpha)$; $^{24}\text{Mg}(n,p)$; $^{48}\text{Tl}(n,p)$	ENDF/B-III, ETOG, ANISN, TWOIRAN	
6	1974 [88]	100 cm lithium metal sphere with 0.6 cm stainless steel shell at IFNR at Karlsruhe	Flux spectra at 10 and 32 cm by time-of-flight, 10 m flight path; ^6Li glass detector, 10 keV to 1 MeV; NE-213 detector, 250 keV to 14 MeV	ENDF/B-III, DTK(SN)	10% mean error, spectral error 0.5-10% Discrepancies around 30%
7	1975 [89]	Pseudo-spherical metallic Li with and without graphite reflector. Inner cavity 10 cm, Li to 34.1 cm, graphite to 55.3 cm at JAERI	A function of position, fission rates in ^{235}U , ^{237}Np , ^{238}U and ^{232}Th	ENDF/B-III, SUPERTOG, ANISN	Experimental ratio 6-7% Discrepancies 10-50%

Table 3-6 Some Earlier Integral Experiments (cont'd)

Experiment Number	Year [Ref.]	Experimental Facility and Laboratory	Measurements	Data and Calculational Basis	Experimental Error: Experiment-Calculation Discrepancies
8	1975 [90]	76 cm diameter iron sphere at U. of Illinois	NE-213 neutron spectrometry	ENDF/B-III,-IV; DNA; CLD-2D; ANISN	
9	1975 [91]	244 cm cube of graphite at U. of Texas	NE-213 proton recoil spectrometry	ENDF/B-IV, SUPERG-III, DLC-2D; ANISN	Discrepancies as large as 73%
10	1976 [92,93]	Spheres of carbon, oxygen, aluminum, titanium and iron. 1-5 mean free paths in radius at LLL	Time-of-flight NE-213 detector measurement of leakage spectra at two angles. Flight paths of 766 and 975 cm	ENDF/B-III,-IV; ENDF; TART	Experimental error +7% Discrepancies generally 10-20% but as high as 50%

$^7\text{Li}(\text{n},\text{n}'\alpha)\text{T}$, which will contribute significantly to the prediction of the tritium breeding ratio in the fusion blanket. Particular attention is drawn to this by the Karlsruhe measurements[48,94] of tritium breeding and scalar and angular fluxes in a 50 cm radius sphere of lithium metal with natural isotopic composition contained in ~6 mm thick stainless steel shell. Time-of-flight measurement of the directional neutron spectra at various locations in the sphere were made. Scalar neutron spectra were also measured with small proton recoil proportional counters in the energy range 50 keV to 1.5 MeV. Calculations of neutron spectra were performed with 1-D S_N code DTK[95] with ENDF/B-III data for the lithium and KEDAK-II[96] data for iron. Directional neutron spectra were calculated for several radial and angular locations in the sphere and compared with the experiment. It was observed that the calculations significantly overpredict the number of neutrons in the 3-11 MeV range, probably due to the fact that the non-elastic scattering is treated inadequately with respect to angular and energy distribution of the outgoing neutrons. This experiment also overpredicts the measured tritium production using ENDF/B-III data by about 35%. About half of the discrepancy was attributed to the excess neutron flux between 3 to 11 MeV and the remainder to the $^7\text{Li}(\text{n},\text{n}'\alpha)\text{T}$ neutron cross-section, which should be lowered by 15-20%.

An earlier experiment by Muir and Wyman[47] at Los Alamos using a 30 cm radius sphere of LiD also indicates up to 18% overprediction of measured tritium production rates. A detailed analysis of this experiment[97] indicates that a reduction of the ENDF/B $^7\text{Li}(\text{n},\text{n}'\alpha)\text{T}$ reaction cross section of up to 13% in the range 7.5 to 15 MeV will give improved agreement with the measured tritium production rates.

More recent integral measurements by Hemmendinger and co-workers [98] also indicated that about a 15% reduction of the $^7\text{Li}(\text{n},\text{n}'\alpha)\text{T}$ reaction cross-section is required at 14 MeV. Tritium production measurements were performed in a 60 cm sphere of ^6LiD irradiated by a central source of 14 MeV neutrons. The spatial distribution of tritium production has been determined by measuring the tritium radioactivity in test samples of ^6LiH and ^7LiH inside small quartz ampules embedded in the sphere. The tritium was extracted by thermal

decomposition of the samples, followed by gas proportional counting of the evolved tritium. The experiment was analysed with the 3-D Monte Carlo code MCN[99]. The data base consisted of the ENDF/B-III evaluation of the lithium isotopes and a 1967 UK-LANL evaluation for the deuterium cross-section. Comparison between experiment and calculation for the ^6Li samples showed reasonable agreement within the measurement uncertainties. This experiment provided benchmark measurements for checking calculations of neutron transport and tritium production that used the $^6\text{Li}(\text{n},\alpha)\text{T}$ cross-section data. However, for ^7Li samples, the calculated values are systematically higher than experimental values. It is thus concluded that a 15% reduction in the $^7\text{Li}(\text{n},\text{n}'\alpha)\text{T}$ cross-section data would result in good agreement.

So far, no unambiguous picture has yet emerged from integral experiments other than a strong indication that a reduction of 15% near 14 MeV in the existing ENDF/B-V evaluation of the $^7\text{Li}(\text{n},\text{n}'\alpha)\text{T}$ reaction cross section is required.

There are other integral experimental results that test microscopic nuclear data. These are the Pulsed Sphere Integral experiments[92,93,100] at Livermore that have been carried out for a number of years, for a simple geometry and composition designed to provide a stringent test of input nuclear data cross sections. The calculations of neutron and photon transport in the materials being used in fusion reactor blankets have been performed using nuclear data libraries with Monte Carlo and discrete ordinate transport codes. The accuracy of these calculations can be verified by finding out how well the neutronics/photonics libraries reproduce integral measurements of the neutron and photon leakage spectra from the material of interest under bombardment by 14 MeV neutrons.

The nominal 14 MeV neutrons are produced from the $\text{T}(\text{d},\text{n})^4\text{He}$ reaction; the 400-keV deuterons being produced by the Livermore Insulated-Core-Transformer (ICT) Accelerator. The pulsed and bunched deuteron beam impinges upon a tritium-titanium target mounted at the end of a low mass assembly and centred in solid spheres of the material to be studied, of typical thicknesses ranging from one to five mean free paths. The neutron production was monitored by counting the associated recoiled alpha particles with a thin lithium drifted

silicon solid-state detector set at 174° with respect to the deuteron beam line. The neutron and gamma spectra are measured using the sphere transmission and time-of-flight techniques for typical flight paths between 7 and 10 m. The high energy neutron and gamma spectra are detected using NE 213 liquid scintillators, positioned at 30° and 120° with respect to the deuteron line.

Earlier measurements of the integral neutron spectra from carbon, oxygen, aluminum, titanium and iron have been obtained by Hansen[93] using the pulsed sphere. Experimental results are compared with the predictions of the Monte Carlo neutron transport code TART using both the ENDF/B-III and -IV neutron libraries. Use of the ENDF/B-IV cross section results in larger calculated integral neutron spectra and closer agreement with the measurements. Discrepancies of 10 to 20% still exist for the thick samples. Overall, the ENDF/B-IV library reproduces the measurements quite well and represents a clear improvement over the III version, where discrepancies of as much as a factor of 2 exist between the measurements and calculations.

Similar experiments, measuring the neutron and gamma ray leakage spectra, have been undertaken for pulsed spheres of various fissionable and fertile materials, such as ^{233}Th , ^{235}U , ^{238}U and ^{235}Pu . Recently, neutron spectra measurements have been repeated for Be, ^6Li , ^7Li and teflon with better resolution[101]. Measurements for other materials of interest to the fusion community have also been made. Measurements made on spheres of Cu, Nb, Th, and ^{238}U were compared with calculations utilizing ENDF/B-IV and -V data in [102]. The results are summarized in Table 3-7, which lists the ratios of the calculated to measured flux integrals in three energy groups. For Cu, both evaluations provide the same flux ratios with a discrepancy of nearly 50% in the region between 5 and 10 MeV. It may be attributed to an underestimation of inelastic scattering that proceeds via pre-equilibrium processes. For Nb, it is seen from Table 3-7 that the calculation seriously underestimates measurement below 10 MeV. A calculation carried out with the ENDL-evaluated Nb showed better agreement. The ENDL evaluation has increased pre-equilibrium (n, n') emission, as well as a higher ($n, 2n$) cross-section. It can also be seen from Table 3-7 that the large discrepancy between 5 and 10 MeV for

Table 3-7 Ratios of Calculated to Measured Flux Integrals

Material	mfp	E (MeV)	R _{IV} (+7%)(a)	R _V (+7%)
Cu	1.0	0.8-5.0	0.898	0.895
		5.0-10.0	0.610	0.537
		10.0-15.0	0.988	0.964
Nb	0.9	0.8-5.0	0.763	(b)
		5.0-10.0	0.581	(b)
		10.0-15.0	0.987	(b)
²³² Th	1.0	0.8-5.0	1.057	1.048
		5.0-10.0	0.513	1.000
		10.0-15.0	0.974	1.008
²³⁸ U	1.0	0.8-5.0	0.888	0.984
		5.0-10.0	0.780	0.610
		10.0-15.0	0.964	0.967

(a) Ratios of calculated to measured integrals. Uncertainty due to measurement.

(b) Same cross-sections in ENDF/B-IV, -V libraries.

^{232}Th is removed in Version V due to the improvement of the total elastic, inelastic and $(n,2n)$ reaction cross sections for ^{232}Th in this energy range.

3.3.4 Validation of Methods

Measurement of blanket parameters, such as tritium production and other reaction rates, can be used for testing calculation methods. The following experimental results on measuring tritium production and other reaction rates are considered to be very useful in validating transport methods and codes commonly used in the fusion community (see Section 3.2).

The experimental assembly used by Herzing[103] to measure tritium production rate consisted of a hollow cylinder of lithium metal, 120 cm OD, 20 cm ID and 120 cm in length. The D-T source was centred inside the cylinder with 20 h of run time required to generate adequate tritium for measurement. Radial channels located at various distances along the cylindrical axis allow the insertion of lithium carbonate test samples. The tritium production was measured by three methods:

- liquid scintillation;
- internal gas counting of the tritium β -activity; and,
- recording of the α -particles associated with the tritium producing reactions by solid state track detectors.

The total experimental uncertainty for tritium breeding was less than 6%. Analyses were performed with discrete ordinates and Monte Carlo methods using ENDF/B-III cross-section data. The calculated results of tritium production by different codes of ANISN, DOT-II and MORSE are shown in Table 3-8. With DOT-II using the P_3-S_{12} approximation, good agreement was obtained between the two calculations of DOT-II and MORSE. The agreement between liquid scintillation measurements and the Monte Carlo calculation results for the spatial distribution of tritium production rates is as good as can be expected, taking into account the uncertainty of the nuclear data used for the calculations. Details of experimental data comparison with calculation are given in [103].

Table 3-8 Comparison of ANISN, DOT-II and MORSE Calculations of Total Tritium Production Normalized to One Source Neutron

Reaction Type	ANISN	DOT-II	MORSE
$^6\text{Li}(n,\alpha)\text{T}$	0.169	0.164	$0.165 \pm 4.95 \times 10^{-3}$
$^7\text{Li}(n,n'\alpha)\text{T}$	0.680	0.642	$0.645 \pm 1.94 \times 10^{-2}$
Total breeding rate	0.849	0.806	$0.810 \pm 2.43 \times 10^{-2}$
$^7\text{Li}(n,2n)$	0.028	0.024	$0.026 \pm 7.32 \times 10^{-4}$
Parasitic absorption	0.088	0.083	$0.084 \pm 2.52 \times 10^{-3}$
Total leakage	radial 50%	90%	89%

In Japan, neutronic benchmark experiments have been performed by Iguchi[104] on the lithium fluoride (LiF) slab assembly (50 cm x 50 cm x 17 cm) with a simulated plane neutron source at the Controlled Thermonuclear Blanket Engineering Research facility of the University of Tokyo. Two kinds of neutron sources have been used; one is extracted from the Fast Column of the Fast Neutron Source Reactor YAYO I, another is a 14 MeV (D-T) neutron source from a Cockcroft-Walton accelerator. Measurements have been made on the emerging neutron spectrum using the time-of-flight technique and NE 213 organic liquid scintillators. The results were compared with ANISN P5-S32 transport calculations using the ENDF/B-IV cross-section library. Discrepancies existed for the angular neutron spectrum at both 0° and 30° as measured from the LiF slab to the 14 MeV neutron source. It might be due to the inadequate treatment of the angular distribution of inelastic scattering in the ANISN code. Similar effects have been observed in other lithium metal experiments. However, the discrepancies for the LiF experiment were not so large as the lithium metal ones. Measurement of the tritium production rate and nuclear heating rate through the LiF slab have been made and compared with ANISN results. It was concluded that the accuracy of the current neutronic design code ANISN plus data base is accurate to within 20 to 30% for integral quantities such as the tritium production rate and the heating rate in the LiF assembly.

In another series of experiments, the absolute fission rate distribution in four types of spherical blanket assemblies have been measured by Seki and co-workers[105-107] at JAERI, using micro fission chambers of ^{235}U , ^{237}Np , ^{238}U and ^{232}Th . The four types of spheres were of lithium metal, lithium with a graphite reflector, and lithium-uranium assemblies with and without a graphite reflector, i.e. Li, Li-C, U-Li and U-Li-C. The results of measurement were compared with ANISN calculations using 100 group cross sections derived from the ENDF/B-IV data file. It was shown that the ratios between calculated and experimental values of ^{232}Th , ^{238}U and ^{237}Np fission rates decrease with distance from the assembly centre where D-T neutrons are generated. An overestimation of about 50% was observed in the calculated ^{235}U fission rate for the graphite reflector region (Fig. 3-1). The results of the analysis indicate that the method of calculation currently employed in fusion

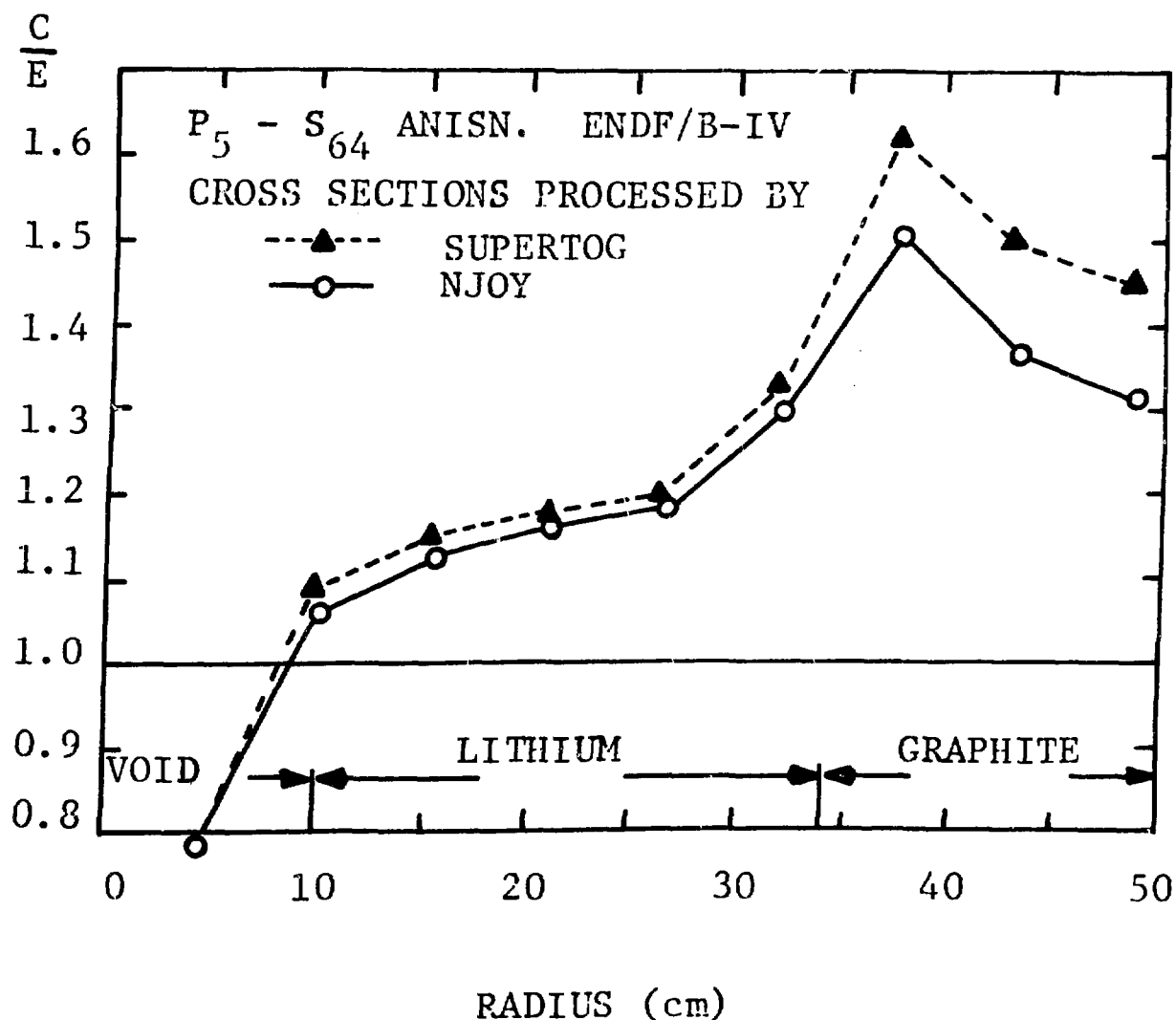


Fig. 3-1 Lithium Experiment at JAERI: Spherical Assembly with Reflector.
 ^{235}U Fission Rate Measurements: C/E = calculated/experimental.

reactor neutronics overestimates the reflection of neutrons and underestimates the penetration of fast neutrons in a reflector such as graphite. It was also observed that the discrepancies between calculation and experiment were mainly due to the inability of the code to take into account the angular distribution of the secondary neutrons resulting from non-elastic reactions in the calculation.

Another series of experiments that are useful in validating calculation methods are the clean benchmark experiments performed in the Li₂O assemblies at the Fusion Neutronics Source (FNS) facility at JAERI. The continuous 14 MeV neutron source strength is 5×10^{12} neutrons/s. Nakamura[108] recently reported that three sets of clean benchmark experiments had been completed and more benchmark experiments were scheduled.

These three sets of experiments are as follows.

1. Reaction rate measurements in a reflected spherical Li₂O assembly

Fission rate and tritium production rate distributions were measured in an approximately spherical Li₂O assembly of 45 cm diameter with a 24 cm thick graphite reflector. The 14 MeV neutron source was placed at the centre of the assembly. The tritium production distribution was measured by a liquid scintillation method using Li₂CO₃ pellets and the self-irradiation method of LiF thermoluminescent dosimetry (TLD). The neutron flux spectral change in the system was determined by measuring the fission rates at various locations using a set of microfission chambers of ²³²Th, ²³⁸U, ²³⁷Np and ²³⁵U. The experiment was analysed by ANISN with a P₅-S₁₆ approximation.

2. TOF experiment for the Li₂O slab assembly

Angular dependent fast neutron spectra leaking from Li₂O slabs of different thickness were measured to provide benchmark data on the treatment of angular dependence of secondary neutrons from the inelastic scattering reactions in the transport calculation. The experimental

assemblies were approximately cylindrical slabs 63 cm in diameter and 5, 20, and 40 cm thick. The neutrons emitted were measured by the time-of-flight method using a NE 213 detector. The angles of observation were selected out of the symmetrical S₁₆ angular quadrature set. Codes used for comparison purposes include transport codes of (1-D) ANISN, (2-D) DOT-3.5, BERMUDA-2DN[109] and the (3-D) Monte Carlo MORSE-DDX.

3. Reaction rate measurement in the Li₂O slab assembly

In the third experiment, a 40-cm thick Li₂O cylindrical slab was irradiated and the tritium production rate distribution was measured by the liquid scintillation method using Li₂CO₃ and Li₂O pellet samples and the TLD technique. Foils of Al, Ni, Nb, Zr and Au were placed inside and on the surface of the Li₂O assembly. Reaction rate distribution measurements such as the (n,2n), (n, α) and (n, γ) reactions were carried out by the usual foil activation technique to obtain benchmark data to test 2-D transport code calculations.

At this stage, it is still too early to draw definite conclusions on the neutronics behaviour of the Li₂O breeder and on the calculational methods. Experiments on a thicker slab (60 cm) are in progress. Further benchmark experiments are planned to study the neutronics behaviour in design-oriented blankets, which incorporate the effect of the first walls, neutron multipliers and coolant channels.

3.3.5 Future Trends

In the near future, it will be feasible to conduct fusion blanket integral neutronics experiments under conditions close to those expected in current blanket designs at the Tokamak Fusion Test Reactor (TFTR)[110] and the Rotating Target Neutron Source (RTNS-II) Accelerator facility[111]. A comparison of TFTR and RTNS-II operating parameters is presented in Table 3.9. RTNS-II became operational in 1979 and the TFTR is scheduled to begin D-T operation during 1985.

Table 3-9 Comparison of TFTR and RTNS-II Neutron Parameters

	TFTR	RTNS-II
Neutron yield	3.6×10^{18} n/pulse	4×10^{13} n/s
Pulse length	0.5 s	continuous
Flux incident on test blanket module	6.26×10^{12} n/cm ² ·s	3.2×10^{10} n/cm ² ·s*

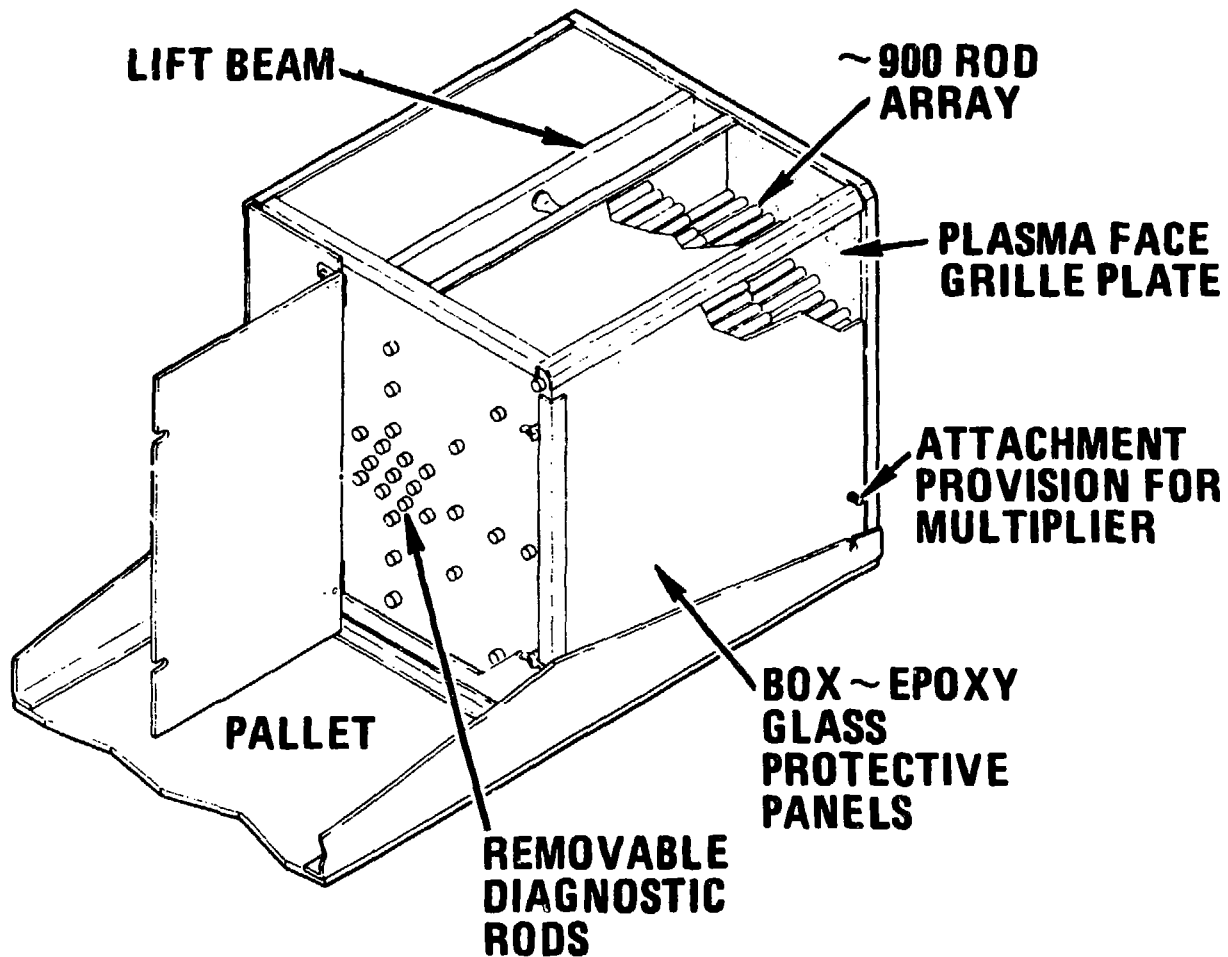
* At module centre, with module 10 cm from the source.

A program to place a Lithium Breeding Module (LBM)[112] on the Tokamak Fusion Test Reactor (TFTR) at Princeton in 1985 is being supported by the Electric Power Research Institute. The LBM is shown in Fig. 3-2. It will use 30 000 pellets of Li₂O, and while mainly used to perform neutronics experiments, should give other engineering data as well. The TFTR Lithium Module program is a first-of-a-kind neutronics experiment involving a representative fusion reactor blanket module with a distributed neutron source from the plasma of the TFTR at the Princeton Plasma Physics Laboratory. The main objectives of the LBM program are to:

- test the capabilities of the neutron transport codes when applied to fusion test reactor conditions, and
- obtain tritium breeding performance data on a typical design concept of a fusion breeder blanket.

The Rotating Target Neutron Source facility (RTNS-II) at Lawrence Livermore Laboratory was built to provide high intensities of 14 MeV neutrons for determining the effects of fusion neutrons on materials of interest to the fusion energy program. The facility contains two identical accelerator based neutron sources using a deuteron beam striking a water-cooled rotating titanium-tritide target (at 4000-5000 rpm) to produce high energy neutrons. The facility has been conducting irradiations on a regular scheduled basis since 1979. The irradiations done at RTNS-II can be roughly divided into two categories with respect to fluence, the higher being 10^{17} - 10^{18} n/cm² and the lower $\leq 10^{15}$ n/cm².

The above experimental programs at the TFTR and RTNS-II facility would provide reaction rate data of direct importance to blanket design in environments of neutron spectra close to those expected in actual blankets. Standard foil dosimetry and other techniques can be employed to obtain reaction rate data for the most important reactions that affect blanket performance for both the TFTR and RTNS-II driven prototype blanket configurations. These measurements would certainly provide a basis for experimental benchmarks against which nuclear data and calculational codes utilized in blanket design can be validated.



3-37

Fig. 3-2 The LBM Assembly from [112]

3.4 Application to Fusion Blankets

3.4.1 Introduction

Not only are the functions of the blanket in a fusion reactor to convert the energy of fusion neutrons into useful heat and to breed tritium, but also at the same time adequate shielding must be provided to protect vital components from excessive radiation damage and to reduce occupational exposures to acceptable limits.

The neutronic calculations cover these aspects with the main goals listed in Table 3-10, taken from Dolan[72].

3.4.2 Relevant Nuclear Reactions

The nuclear reactions of interest in fusion reactor blankets, introduced in Section 1.3, are discussed below in more detail[113].

The only neutron-induced reactions which offer any promise for tritium breeding are $^6\text{Li}(\text{n},\alpha)\text{T}$ and $^7\text{Li}(\text{n},\alpha\text{n}')\text{T}$. The ^6Li reaction has a $1/v$ cross-section dependence below ~ 0.3 MeV and in a practical blanket has to compete with parasitic absorptions in structural and other materials. The ^7Li reaction has a threshold at ~ 2.8 MeV, and therefore must compete with neutron down-scattering processes; note also that this reaction produces one additional neutron which is available for further breeding. In some cases there is an incentive to increase the ^6Li content relative to natural lithium (92.5% ^7Li , 7.5% ^6Li) in order to improve the tritium breeding performance (see Section 2.2.2).

Neutron scattering reactions are important from the viewpoint of energy degradation, particularly elastic scattering in light elements over the whole energy range and inelastic scattering of fast neutrons in heavy elements. Inelastic scattering events also provide a significant source of secondary gamma rays.

Table 3-10 Predictions Required from Neutronics Calculations

1. Tritium Breeding Ratio TBR = number of tritium atoms produced per tritium atom destroyed.
2. Blanket Energy Gain M = total energy deposited in blanket divided by neutron kinetic energy.
3. Nuclear Heating = power deposited per unit volume at each point in the first wall, blanket, shield, and coils.
4. Radiation attenuation of neutrons and gamma rays.
5. Radiation streaming through ducts and interfaces.
6. Structural activation by neutron absorption.
7. Radiation Damage to Materials: number of displacements per atom per year (dpa/year), and hydrogen and helium gas production rates via (n,p) and (n,α) reactions.
8. Corrosive element production by nuclear reactions.

The high initial kinetic energy of the DT fusion neutron leads to $(n,2n)$ and $(n,3n)$ reactions in structural materials or multiplier materials such as lead or beryllium which may be included in the blanket for this purpose. The (n,xn) reactions are also important downscatter processes so that an increase in the neutron density due to the use of a neutron multiplier is always associated with a decrease in $^7\text{Li}(n,\alpha n')\text{T}$ reactions.

Parasitic absorption reactions such as the (n,γ) capture reaction are important in the neutron balance and as a source of secondary gamma rays. The less frequent (n,α) and (n,p) reactions do not significantly affect the neutron balance but are important from the viewpoint of radiation damage due to helium and hydrogen gas production. Radiation damage is also caused by atomic displacements produced primarily in the down-scattering reactions.

All reactions result in heat production via the slowing down of the reaction products. Nuclear heat is also deposited by the attenuation of secondary gamma rays, the major sources being inelastic scattering and radiative capture.

In fusion blanket neutronic studies it is essential to include gamma ray effects since gamma heating typically accounts for 20% or more of the total nuclear heating and for this reason and also for shielding studies coupled neutron-gamma codes are required. The usual approach is to do parametric scoping studies using 1D transport codes such as ANISN followed by detailed 3D Monte Carlo calculations for specific designs.

3.4.3 Overall Accuracy

There are inherent errors in all calculational methods and three areas of uncertainty applicable in fusion blanket neutronics studies are discussed below.

(A) Numerical Techniques

- (i) Convergence error: can in principle be made as small as desired by using as many iterations as necessary. However, there is always a practical limit on computer time.
- (ii) Round-off error: is usually negligible on modern computers.
- (iii) Truncation error: arises from using a finite number of increments to approximate a continuous variable i.e. P_ℓ order, S_n order, mesh spacing and number of energy groups.

Reducing the calculational error related to the numerical techniques discussed above to < 2% appears to be a very difficult goal[5].

(B) Concept Definition

An exact geometrical description is impractical because of limitations in current computer codes due to both storage requirements and computer running time. As a result the errors introduced due to the approximate geometrical representation which has to be assumed are probably the greatest source of uncertainty in predicted neutronic results. The difference between a 2D and 3D calculation of the tritium breeding ratio can easily be > 15%[114].

(C) Nuclear Data

Uncertainties in nuclear cross sections introduce errors in the calculated tritium breeding ratio which are system-dependent but probably < 6% in the worst case. For cross-section sensitivity studies see, for example, [5].

If the combined effect of the three areas of uncertainty discussed above is 15%, then the calculated tritium breeding ratio must be almost 1.2 in order to assure an actual tritium breeding ratio (TBR) greater than 1.0. Thus it is very desirable to reduce this calculational uncertainty.

3.4.4 Tritium Production

The spatial variation in the tritium production rate through the blanket is obtained from the sum over the energy groups of the product of the calculated group fluxes and the corresponding macroscopic group cross sections for the $^6\text{Li}(n,\alpha)\text{T}$ and the $^7\text{Li}(n,\alpha n')\text{T}$ reactions. Parametric or general assessment studies usually rely on one- or two-dimensional transport code calculations of the neutron flux. As a design becomes better defined, more realistic geometrical modelling is required, it being particularly important to model the effects of ports and duct penetrations through the blanket, especially for blankets with marginal breeding potential.

To ensure that the actual TBR has a value of > 1.0 , the accuracy required from the calculation depends on the calculated value. For example, if the calculated TBR is 1.15, then a 10% uncertainty in the calculation would be adequate, however, if the calculated value is 1.05, then the required calculational accuracy to give an acceptable margin would be 2% or better. In both cases the better the calculational accuracy the more flexibility is available to the designer because the allowable margins can be reduced.

The nuclear performance of eleven different breeding materials has been investigated by Daenner[127]. Common assumptions for all calculations were (1) natural isotopic composition of lithium, (2) 316 SS as the first wall and structural material, (3) a 10% structural material volume fraction in the breeding zone, and (4) a 1 cm thick first wall. The breeding zone was assumed to be backed by a 100 cm thick shield composed of 35% stainless steel, 35% lead, and 30% boron carbide. No additional materials such as moderators, reflectors, or neutron multipliers were considered.

The most important performance characteristics are summarized in Table 3-11. As far as tritium breeding as the most crucial requirement for a power reactor blanket is concerned, five out of the eleven substances ($^{17}\text{Li}-^{83}\text{Pb}$, LiAl , LiAlO_2 , Li_2SiO_3 , Li_2ZrO_3) show inadequate results in that the breeding ratio, TBR, stays below unity in a 100 cm thick breeding zone. Two materials (FLIBE, Li_4SiO_4) exhibit values slightly above unity and seem, therefore, applicable

Table 3-11 Nuclear Performance Characteristics, after[127]
(Assuming no ^6Li enrichment, and no neutron multipliers or coolant present)

Material	TBR (TBR=1.22)	d_{BZ}	M	M_{BZ}	d_{SH}	d_{tot}
met. Li	1.37	64	1.27	1.16	96	160
$^{17}\text{Li}-83\text{Pb}$	0.97		1.32			
LiPb	1.36	57	1.26	1.18	77	134
$\text{Li}_{17}\text{Pb}_2$	1.46	47	1.26	1.13	87	134
FLIBE	1.08		1.31			
LiAl	0.98		1.28			
LiAlO ₂	0.86		1.26			
Li ₂ O	1.29	38	1.27	1.22	81	119
Li ₂ SiO ₃	0.91		1.21			
Li ₄ SiO ₄	1.02		1.23			
Li ₂ ZrO ₅	0.97		1.33			

d_{BZ} cm = blanket thickness to give TBR = 1.20

M = Blanket energy multiplication factor

M_{BZ} = Blanket Energy Multiplication Factor with blanket thickness d_{BZ}

d_{SH} cm = shielding thickness

d_{tot} cm = shielding + blanket thickness to give TBR = 1.20

only in reactors with high blanket coverage. The remaining four substances (Li , LiPb , Li_7Pb_2 , Li_2O) are the only ones which guarantee breeding ratios of $\text{TBR} > 1.2$.

If the radial extension of the breeding zone is restricted such that just $\text{TBR} = 1.2$ is obtained, Li_2O will be the material which allows for the most compact breeding zone with a thickness, d_{BZ} , of about 40 cm. Metallic lithium needs about 65 cm to fulfil the same requirement and the two lithium-lead alloys lie in between.

An energy multiplication factor of $M > 1.0$ is assured in all cases. It is again Li_2O which exhibits with $M_{BZ} = 1.22$ the highest value if the breeding zone thickness is restricted such as to reach just $\text{TBR} = 1.2$. The necessary shield thickness d_{SH} has been derived from the specific flux attenuation coefficients and a typical fluence limitation for the superconducting magnet. The last column lists the total thickness d_{tot} for the entire nuclear system and shows again the superiority of Li_2O .

If ${}^6\text{Li}$ enrichment and neutron multipliers are included, the estimated tritium breeding ratios likely to be achievable in fusion power reactors are shown in Table 3-12 for various breeding materials[5]; see also Section 6.2.1.

3.4.5 Heat Production

Nuclear energy deposition through the blanket and shield is calculated from the flux distribution using tabulated KERMA ("Kinetic Energy Released in Materials") factors from, for example, the DLC-60 MACLIB-IV-82, 171 neutron groups and 36 gamma ray groups library.

3.4.6 Shielding

Two dimensional transport codes are adequate for solving most blanket-shielding problems provided there are no large streaming effects through ducts or ports. When streaming effects are present 3-D Monte Carlo calculations are employed. Although for the most part the available methods are adequate,

Table 3-12 Estimated Tritium Breeding Ratio Likely to be Achievable in Fusion Power Reactors from [5]

Breeding Material	Breeding Ratio	Comment
Liquid Lithium*	1.15	Low Risk
$^{17}\text{Li}-83\text{Pb}^{***}$	1.3	Attractive
Solid Breeders		
Li_2O^*	1.1	Medium Risk
$\text{Li}_2\text{O } (+\text{Be})$	1.3	Attractive
LiAlO_2^{**}	0.8	Impossible
$\text{LiAlO}_2 \text{ } (+\text{Zr}_5\text{Pb}_3)^{**}$	1.04	Rejected
$\text{LiAlO}_2 \text{ } (+\text{Be})^{**}$	1.08	High Risk

* Natural lithium enrichment

** 60% ^6Li enrichment

*** 90% ^6Li enrichment

improvements in accuracy would allow the designer to reduce uncertainty factors in the shield thickness with a resulting saving in capital cost.

3.4.7 Activation

Neutron induced activation is determined using the calculated neutron flux distribution and neutron activation and decay codes such as DKR[115] or RACC[116], which rely on activation data libraries, such as the LASL GAMMON Library[60]. If necessary, long term radioactive levels in fusion reactor structures could be reduced by isotopic tailoring of structural materials as discussed by Youssef and Conn[117], and Conn[118].

3.4.8 Radiation Damage

Calculational methods are available for estimating radiation damage effects in structural materials. For example, the RECOIL program[119] computes gas production and nuclear displacements for an input neutron spectrum up to 20 MeV using a heavy charged particle recoil data base. All neutron reactions of significance, i.e. elastic, inelastic, $(n,2n)$, $(n,3n)$, (n,p) , (n,α) and (n,γ) , which have cross sections available on the ENDF/B data files, have been processed and placed in the data base for most of the elements of interest to the radiation damage community.

3.4.9 Developments in Neutronics

No fundamental nucleonic issues are seen as insurmountable barriers to the development of commercial fusion power[44]. The current one- and two-dimensional transport codes, with occasional recourse to 3-D Monte Carlo calculations, are adequate for parametric surveys and general assessment purposes. However, tritium breeding is a major feasibility question, and more sophisticated analysis is required to establish the TBR as the designs become better defined.

Due to the competition between the different requirements posed to the breeding blanket, the margin that is left in the TBR to cover the inaccuracy

in the prediction of the TBR, and to cover unforeseen design problems, has the tendency to become smaller. Therefore it becomes more and more necessary to accurately calculate the effective tritium breeding ratio[120]. To achieve this goal the ability to handle complex geometries in an efficient calculational scheme is required.

Although 3-D transport codes are available, for example the THREETRAN code[121], and are continually under development[122,123], the computing time required to handle a complex practical blanket design is prohibitive and two other approaches currently in use are outlined below.

One approach is to couple a three-dimensional Monte Carlo calculation with a two-dimensional discrete ordinates calculation in which the Monte Carlo calculation provides the internal and external boundary surface sources for a subsequent discrete-ordinates calculation. As an example of this technique, Urban and co-workers[124] have used it to investigate the shielding for the Engineering Test Facility Neutral Beam Injector Duct, and Engholm [125] refers to a special version of MCNP[77] named MCNPS which has been developed for this purpose.

Filippone and co-workers[126] describe a "streaming ray" method which economizes on computing time and computer storage requirements for particle streaming and deep penetration problems. This approach was used in a new 2-D transport code, developed at ECN for neutronics calculation on JET and will be further developed for application to NET[120].

3.5 Summary

In Section 3.1, a brief review of the current status of neutronics/photonics data for fusion applications was presented. In recent years, progress is evident in several important areas and significant advances have clearly been made. Despite some disagreement among $^7\text{Li}(\text{n},\text{n}'\alpha)\text{T}$ cross-section measurements, and existing gaps in some of the required data between 7 and 14 MeV, the present data base is in general adequate for the present and near term future requirements in scoping and survey type of blanket calculations. However,

further refinement and improvement of nuclear data are needed for more detailed realistic blanket design calculations.

There will certainly continue to be a great number of nuclear data needs for fusion. For instance, new requirements for evaluated primary-knock-on atom spectra, updating activation files, more data for neutron energies beyond 14 MeV for fuel material irradiation test facilities, etc., will arise. The data needs will change with time as blanket design concepts change. New types of data will be needed as new materials will be suggested and greater accuracy may be required. A steady improvement in the neutronics and photonics data is definitely essential to satisfy the changing needs of future realistic blanket designs.

A review of integral fusion blanket neutronic experiments was given in Section 3.3. These experiments include the Livermore pulsed sphere leakage spectrum measurements, JAERI reaction rate measurements, tritium production and spectra measurements in various homogeneous spherical and cylindrical assemblies. These integral experiments have been valuable in identifying cross-section deficiencies and in demonstrating the importance of pre-equilibrium neutron emission to the transport of 14 MeV neutrons. It is expected that such "clean" experiments with homogeneous spheres and cylinders will be continuing on a long-term basis, since these experiments provide useful basic information with respect to cross-section data improvement and code development. In the near future, the second category of integral experiments is to be emphasized. These would be "simple" experiments but would incorporate geometrical and computational complexities to test a genuine engineering design approach. Measurement would include real design parameters, such as nuclear heating, spectra, tritium production and activation dosimetry. It is expected that the experimental programs at the TFTR and RTNS-II facility and the Fusion Neutronics Source Facility at JAERI will provide useful data of direct importance to realistic blanket design in the years to come.

Neutronics calculational capability is not at present a key issue in the development of commercial fusion power. As shown in Sections 3.2 and 3.4, current codes are adequate for parametric studies and general assessment purposes.

However, as the designs become better defined, improvements in computing efficiency and geometrical modelling ability are necessary. One aspect which has yet to be addressed in fusion blanket neutronics is the accurate modelling of the geometrical heterogeneity which occurs in a practical engineered design. A solution to this problem poses a considerable challenge in the long term development of fusion blanket neutronics.

4. LIQUID METAL BREEDERS

4.1 Introduction

Liquid metals were the earliest materials considered for breeders in D-T fusion reactors. Lithium metal and lithium alloys, such as $^{17}\text{Li}-83\text{Pb}$, give very good tritium breeding (Section 2.2.2) and for the latter the lead enhances the TBR by acting as a neutron multiplier. Liquid metals also offer the option of circulating the liquid metal as both breeder and coolant. This is attractive, allowing continuous extraction of tritium and direct removal of heat, resulting in enhanced thermodynamic efficiency and lower temperatures in the blanket structures. In Section 2.3 some reference designs were discussed for liquid metal breeders, for instance MARS (Section 2.3.4) and DEMO (Section 2.3.3). In this chapter some of the critical issues (Section 2.1.1 and Table 2-1) relating to the practical application of liquid metals as breeders are discussed. These may be grouped within the general areas of engineering and safety, materials compatibility and tritium extraction.

Liquid metals have excellent heat transfer properties but they also generate high pressure gradients, and therefore structural stresses, when pumped across strong magnetic fields. This has made it necessary to consider the use of electrically insulated pipe walls or cooling by non-conductive fluids, such as helium or water. It is also important to contain liquid lithium within the blanket structure because of its vigorous reaction with air, water and oxygen-containing materials such as concrete. Liquid $^{17}\text{Li}-83\text{Pb}$ is not as reactive, but its high density poses pumping and engineering difficulties.

Engineering designs must also take into account the corrosive effects of lithium, and especially lithium-lead alloys, on most structural materials. It is predicted that both ferritic and austenitic alloys could be made compatible over the expected lifetime of a breeder structure, provided that external contaminants such as nitrogen, oxygen and carbon are minimized, for example by maintaining an argon atmosphere over the lithium. It has been shown, however, that vanadium alloys are likely to be a better material for containing liquid lithium and particularly lithium-lead alloys.

Lithium has the highest solubility for tritium of all candidate breeder materials, resulting in some difficulty in removing the bred tritium. Tritium solubility in $^{17}\text{Li}-\text{Pb}$ is much reduced from that of liquid lithium and hence tritium inventory will be reduced and its recovery will be easier. However, tritium permeation will be a concern. Solubility and diffusion data for tritium in liquid metals are required to optimize tritium breeding and recovery. A number of methods for recovering tritium from Li and $^{17}\text{Li}-\text{Pb}$ have been developed but so far none has been demonstrated on an engineering scale.

4.2 Engineering Considerations for Liquid Metal Breeder Systems

4.2.1 General Design Requirements for a Blanket

The blanket forms part of the first wall/blanket/shield system surrounding the hot plasma, and performs three main functions in a D-T reactor. By capturing and thermalizing the 14 MeV fusion neutrons, it partially shields the outer structure, produces tritium and provides a medium for the transfer of heat[128,129]. The liquid metal may be circulated as the primary coolant, allowing direct extraction of the energy, or it may be retained in the blanket and cooled by some other fluid circulated through tubes or ducts in the blanket[5]. To ensure a net breeding ratio > 1.0 it may be necessary, depending on the structural details and blanket neutronics, for the lithium to include a neutron-multiplying element such as bismuth or lead as an alloying material. Bismuth is unattractive because of neutron-induced polonium production, making lead the only good candidate. The prime liquid metal breeders are liquid Li and $^{17}\text{Li}-\text{Pb}$. Once a design envelope has been achieved that satisfies the tritium breeding requirement, the heat transfer and shielding functions can be optimized with respect to safety, operation and economics. At the present time it is not clear whether an acceptable design can be found because basic information on materials, and experience in designing, building and operating such complex systems, is lacking[4].

For engineering purposes, Li has the advantage of a low melting point, low density and high heat capacity. Its strong chemical reactivity with water

would likely rule out water as a coolant. $^{17}\text{Li}-\text{83Pb}$ is less reactive with water, but its high melting point (235°C) would be an operational disadvantage, and its high density would create large structural stresses from flows around bends, flow transients and static pressures[130,131].

Various conceptual designs have been proposed for liquid metal blankets (Section 2.3) which represent a number of solutions to the engineering problems presented, i.e. vacuum integrity of the first wall, breeder containment, breeding and heat removal. In MARS (Section 2.3.4), the liquid metal is contained in tubes assembled into modular segments which could be easily removed for maintenance, and isolated in the event of a leak. For self-cooled blankets, the shape of the tubes and liquid metal flow paths in the magnetic field region must be carefully designed to minimize the MHD pressure drop. In tokamaks, the toroidal field is the dominant component since it is usually much larger than the poloidal field. For non-metallic coolants (helium, organic or water) there is no MHD pressure drop, but since their heat transfer characteristics are inferior to those of liquid metals, larger heat transfer structures must be designed. This not only increases the complexity of the design but also degrades its neutronic performance [132].

A major engineering consideration for all fusion power reactors will be pumps, since any heat removal system for a blanket will require substantial pumping capacity. This is a particular problem for self-cooled liquid metal designs where it is anticipated some pump development will be required. For helium or water cooling the designer will have reasonable flexibility in the design of the heat removal circuit and relatively orthodox pumps or gas circulators are likely to be available and satisfactory.

Historically, developmental liquid metal systems have used electro-magnetic (EM) pumps. They have substantial advantages over mechanical pumps; namely, there are no moving parts and no moving seals or glands and small EM pumps are commercially available. Early EM pumps had poor efficiency ($\approx 10\%$) and while this was acceptable on small systems, it was inappropriate for the pumps required for second generation sodium-cooled fast reactors (LMFBRs). As a

result, centrifugal pumps with gas seals were developed[133]. The hydraulic characteristics of self-cooled liquid metal blankets will likely be large volumetric flow and low pressure drop (provided MHD effects can be limited). This may not be well suited to centrifugal pumps so axial flow pumps may be needed. There appears to be no incentive yet to develop large rotary pumps for liquid blanket systems. Improved EM pumps will probably meet the requirements. The development work at HEDL in connection with the ELS (Experimental Lithium System) for FMIT (Section 4.2.5) and elsewhere has produced significant increases in both EM pump size and efficiency. Pumps for 31.5 L/s (500 USGPM) and 23% efficiency are operating[134]. A pump of 915 L/s (14 500 USGPM) and 43% efficiency has been reported[135].

MHD effects (Section 4.2.3) arising from pumping liquid metals in the high magnetic fields of a tokamak require ingenuity in limiting the pressure losses. One requirement may be a suitable insulator between the liquid metal and its containment ~ developing such insulators is not a trivial problem. Also, blanket geometries in some machine types themselves create MHD problems; e.g. the pressure permitted to pump the liquid metal may well be limited by the design of the pressure containment which may have a poor shape for a pressure shell. Various types of flow patterns have been considered to solve this problem in tokamaks[8].

The engineering design problems of external loop components such as instrumentation, heat exchangers and steam generators have not been specifically considered as part of this study. To some extent, these problems can be solved by methods which are "conventional" or at least in place, based on experience with liquid sodium. This appears to apply especially in the areas of instrumentation and loop chemistry [136]. Other problems may be specific to fusion applications. For example, the prevention of tritium escape into the secondary coolant circuit for $^{17}\text{Li}-^{83}\text{Pb}$ designs may require the use of double-walled heat exchangers and/or specially designed tritium permeation barriers, see MARS (Section 2.3.4). There is, of course, no experience with large-scale heat exchangers or steam generators, which will represent a considerable scale-up from current experience; for example, in the ELS-FMIT facility,

organics will be used to cool lithium using a tube-in-shell heat exchanger; however, the temperature (250°C) and size ($\approx 3 \text{ MW}$) are modest.

4.2.2 Thermal and Hydraulic Considerations

Methods of heat transfer and hydraulic analysis for liquid metal systems are well established[137,138]. The main departure from conventional methods of analysis is caused by the thermal conductivity of liquid metals, which for both sodium and lithium is about 100 times that of water, with correspondingly smaller Prandtl numbers. Therefore the viscosity is a less relevant parameter, and the thermal diffusivity is significant in scaling heat transfer processes. Even in turbulent flow, the molecular conductivity is of the same order as the eddy conductivity, so that the thermal boundary layer extends to the turbulent core of the flow. As a result, the conventional correlations for heat transfer coefficients are invalid, and must be replaced by correlations specific to liquid metals. Complicating factors include possible thermal contact resistance between solid surfaces and liquid metals caused by a thin layer of oxide or other corrosion at the wall, non-wetting of the wall by the liquid metal, and axial conduction in the fluid.

Mean power densities in fusion blankets will be in the neighborhood of 10 MW/m^3 . This is about an order of magnitude lower than the power density in fission reactors, e.g. in CANDU fuel and coolant it is typically 200 MW/m^3 . The relatively low power density results from the large size required for the blanket, which must surround a plasma region some metres across, and have thickness typically of 0.5 to 1.0 m to stop the 14 MeV neutrons. Thus liquid metal blankets will generally contain large masses of liquid metal, flowing at low coolant velocities by comparison with fission reactors. There is some loss of thermal efficiency as a result, but this is offset by operating at higher temperatures, and by the superior heat transfer properties of liquid metals. Another complicating factor is the radial distribution of blanket power, which is the largest near the first wall and decreases exponentially outwards (see Fig. 5-10), and which requires the designer to distribute coolant flows to limit temperatures and heat fluxes[139]. One such solution

for this problem is shown in Fig. 4-1 from [140] in which the coolant tubes are arranged to be denser nearer the plasma.

The heat balance equation for the blanket coolant is

$$P = M \cdot \Delta T \cdot C_p$$

where P is the blanket power, and M , ΔT and C_p are respectively the mass flow rate, temperature rise and heat capacity of the coolant. If the blanket is self-cooled, these values apply to the blanket as well. In the trade-off between M and ΔT , economics generally favours large ΔT , since this increases thermal efficiency and reduces the cost of pumps, pumping power, heat exchangers and steam generators. The limitations on ΔT are determined by permissible inlet and outlet temperatures. Coolant inlet temperatures must be kept at a safe margin above liquid metal melting temperatures. Since the melting points of Li and 17Li-83Pb are respectively 180°C and 235°C, inlet temperatures in the range 250°C to 300°C may be expected. Coolant outlet temperatures are determined by temperature limitations on structural materials. For stainless steels, this is currently in the neighborhood of 500°C[140]. In a self-cooled blanket, where the energy is deposited in, and extracted from, the same medium, there will be little difference between the temperatures of breeder and structural materials. For a separately-cooled blanket, a film temperature drop of about 50°C will separate blanket and coolant[141]. From the above discussion, coolant temperature differences around 150 to 250°C may be expected, and this range has been the basis for most of the proposed designs[142]. Temperature-induced stresses at the above temperatures do not appear to cause any problems that cannot be solved with careful design and choice of materials; see e.g. [143] and Section 2.2.1.

For a self-cooled blanket, lithium has the most attractive properties, combining high heat capacity with low density. At fusion blanket temperatures (500°C) these values for Li are 4.2×10^3 J/kg K and 0.48×10^3 kg/m³, respectively, comparable to the values for water at 100°C. By contrast, for the alloy 17Li-83Pb, these values are 0.17×10^3 J/kg K and 9.4×10^3 kg/m³. Other alloys containing large amounts of lead have similar values. The viscosity of

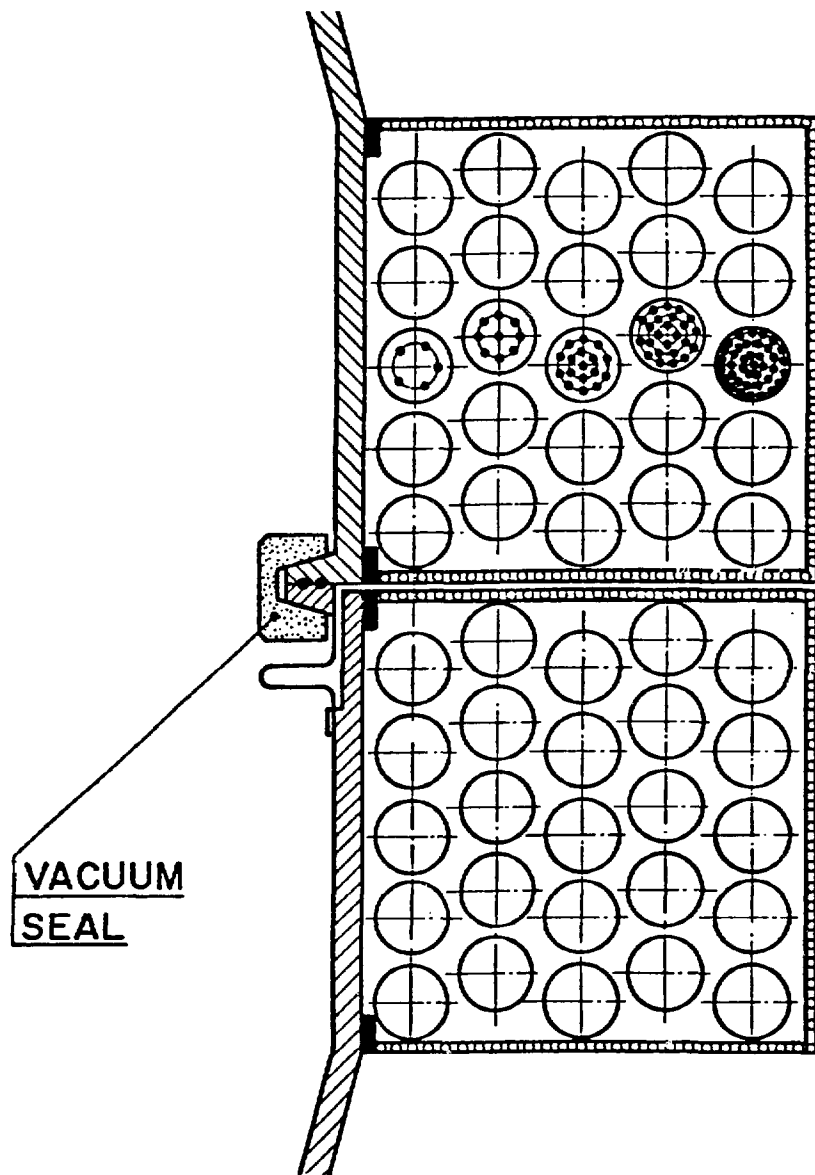


Fig. 4-1 Liquid breeder blanket section showing the gradation in the number of coolant tubes contained within the five rows of breeder tubes. The plasma is at the right and two blanket modules are depicted (after F. Carré[140]).

of lead and lead alloys is about ten times the viscosity of Li at 500°C or water at 100°C, although the Reynolds numbers of the flows are generally so large that the viscosity is not critical in determining hydraulic behaviour in the absence of magnetic fields. The mass flows required for a number of reactor designs using liquid 17Li-83Pb as a self-cooled blanket have been calculated[144]. For a reactor the size of STARFIRE (Section 2.3.2), with a blanket power of 3800 MW, the required mass flow would be 113 000 kg/s, assuming a temperature rise in the blanket of 200°C. If liquid Li were used instead, the flow rate would be 4600 kg/s. Because the specific heats of lead and lithium are roughly in the same ratio as their densities, the volume flow rates are comparable, $\approx 10 \text{ m}^3/\text{s}$ in this example. Due to the high density ratio, the circulating kinetic energy of a lead alloy blanket would be perhaps an order of magnitude larger than the circulating kinetic energy of a lithium blanket of the same volume, and the spin-up and coast-down times for the system would be correspondingly longer. The mechanical stresses resulting from gravity loads, flow transients and flows around bends would also be larger for 17Li-83Pb.

4.2.3 MHD Pumping Resistance

Liquid metals are electrically neutral due to their high electrical conductivity, so that their motion in a magnetic field can be described by the MHD approximation to Maxwell's equations and the fluid equations which govern plasmas. In this approximation[145,146] it is assumed that the displacement current $\partial\bar{D}/\partial t$ in Maxwell's equations as well as currents due to the convective movement of charge by the fluid, are insignificant compared with the conduction current, and that the electrostatic body force due to the electric field \bar{E} can be neglected in the equations of motion. The magnetic field \bar{B} interacts with the velocity field \bar{V} through the transport equation,

$$\partial\bar{B}/\partial t = \nabla \times (\bar{V} \times \bar{B}) + (\sigma\mu)^{-1} \nabla^2 \bar{B}$$

For liquid Li, the electrical conductivity σ is $\approx 2.5 \times 10^6 \text{ mhos/m}$ at fusion blanket temperatures[147] and for 17Li-83Pb it is $\approx 1.1 \times 10^6 \text{ mhos/m}$ [144]. The magnetic permeability μ is $\approx 10^{-6} \text{ H/m}$ for all liquid metals, so that the

"magnetic diffusivity" $(\sigma\mu)^{-1}$ is $< 1.0 \text{ m}^2/\text{s}$ for these liquids. If L is a typical length scale in the flow, then the magnetic Reynolds number,

$$Re_m = LV\sigma\mu$$

determines the behaviour of the magnetic field, just as the hydraulic flow regime is determined by the ordinary viscous Reynolds number. For small Re_m the magnetic field equation reduces to a diffusion equation, in which case the magnetic field lines penetrate the fluid by diffusion, and the induced magnetic field becomes small compared to the external field, their ratio being of order Re_m . For large Re_m , the diffusion term is unimportant, and the external magnetic field is convected with, or "frozen into" the fluid. It has been shown, however[148], that even for Re_m of order unity, which is the situation for liquid metals in a fusion blanket, the induced field will be small, provided the walls confining the flow have moderate electrical conductivity, the significance of which is discussed below. By analogy with ordinary viscous flow, the "magnetic boundary layer thickness" is of order $(Re_m)^{-1/2}$.

The ratio of magnetic to viscous forces in the fluid is measured by the Hartmann number,

$$H = BL (\sigma/\eta)^{1/2}$$

where η is the ordinary viscosity of the fluid. Since $\eta \approx 3 \times 10^{-4} \text{ kg/m}\cdot\text{s}$ for liquid Li at fusion blanket temperatures (about 10 times larger for $^{17}\text{Li}-^{83}\text{Pb}$), a magnetic field of a few tesla will give a large value of H , of the order of several thousand or more. The effect of large H is to suppress flow instabilities caused by viscosity and to increase the critical Reynolds number, in some cases up to order 10^6 , at which the transition to turbulence occurs.

A magnetic field superimposed on a flowing liquid metal interacts with the flow to generate resistance (i.e. pressure drop) in three ways.

- (i) Eddy currents are induced in the fluid, flattening the velocity profile and decreasing the boundary layer thickness. This increases the viscous drag at the channel walls but creates no electromagnetic body force.
- (ii) If the channel walls are electrically conducting they provide a return path for eddy currents generated in the fluid. This is analogous to connecting a generator to a resistive load, which increases the torque required to drive the generator. The result is a significant increase in flow resistance.
- (iii) Where the liquid enters or leaves a magnetic field, the field gradient there generates eddy currents which increase flow resistance.

Since the magnet coils in a fusion reactor would have to be outside the region of high neutron flux, they would also have to enclose the Li blanket region. Thus the liquid metal would have to be pumped in and out of the magnetic field to get from the blanket to pumps, heat exchangers, etc. Depending on the path used, MHD pressure drops would result. Thus the pumping power required may be unacceptably high, up to several percent of the net electrical output of the reactor. However, an even more severe limitation in a fusion environment may be the mechanical stresses which result from these high gradients and pressures. Increasing the pipe or duct wall thickness in this case increases the wall conductance and therefore the MHD pressure drop, so that the wall stress remains constant to first order. This is one of the fundamental problems that MHD resistance poses for liquid metal flows, and points out the need for a non-conducting wall material, or a non-conducting coolant.

In [148], some of the experimental and theoretical results on liquid metal flows in magnetic fields were reviewed, and presented as formulas suitable for calculating the MHD pressure drop in a practical design. These included the effects of magnetic fields parallel and perpendicular to the flow, as well as a number of channel configurations, with and without conducting walls. Because of the turbulence suppression at large H , laminar flow was assumed. A hypothetical example of a fusion reactor blanket in a mirror magnetic field

with a maximum value of 10 tesla was used to illustrate the calculations. The most significant result was that the pressure drop was very sensitive to the wall conductivity, and to the choice of path through the magnetic field. Even slight misalignment between pipes and magnetic field direction, resulting from practical necessity, could increase the pressure drop an order of magnitude. Similarly, abrupt pipe bends gave large flow resistance. For this design example, the overall pressure drop could be made to vary by six orders of magnitude, from < 0.1 psi to $> 10^5$ psi. Although the latter figure seems prohibitively large, the authors conclude that MHD pressure losses could be kept acceptably small in practice, with careful design. It is pointed out that a solution of the pipe wall conductance problem using ceramic pipe or pipe liners would considerably reduce the MHD pressure drops, but would possibly create further materials problems, since ceramic materials tend to crack in tension.

A review article[149] deals with the state of the art (in 1975) of MHD flows, in particular with what the author calls "magnetohydraulics". The article cites 200 references, a large fraction of which were published between 1950 and 1970. Many of these references contain basic experimental results on flows (using mainly sodium and mercury) in magnetic fields, and provide data on MHD pressure drops in a variety of pipe cross-section configurations, changes of cross-section, entry and exit losses, and the effects of pipe wall conductivity and magnetic turbulence suppression. Some heat transfer studies are also cited. Thus there is considerable generic data available for at least the first stages of the hydraulic design of a liquid metal fusion blanket. However, recent publications[150,151] point out some discrepancies between theory and observation, especially for flows in conducting pipe, that require interpretation and resolution, and suggest the need for further work in this area.

MHD pressure drops were calculated for a theoretical multipass blanket configuration surrounding three different conceptual reactors, [144]. The blanket material considered was 17Li-83Pb. It was concluded that pressure drops and pumping power could be limited to acceptable values, provided the pipe walls were electrically insulated from the blanket material. Such insulation might

be achieved by the use of a ceramic coating on the pipe walls; however, it was pointed out that porosity and cracks in the ceramic would have to be closely controlled to limit eddy-current drag due to trapped metal. The use of 17Li-83Pb or other alloys containing large amounts of lead would lead to increased mass flow rates, although volume flow rates are comparable to those for a lithium metal blanket. For the reactor examples quoted in [144], the mass flow rates for the liquid blanket materials ranged from 40 to 113 tonnes per second.

4.2.4 Maintenance

Maintenance and component reliability will be a significantly greater challenge for fusion reactors than for fission reactors, due to their increased structural complexity and the need to maintain or replace major components. Because of the large capital costs involved, maintenance and reliability will be deciding factors in the economic viability of fusion reactors and it will be necessary to achieve high component reliability and plant availability.

The principal hazards will be high radiation fields, resulting from activation by high fast neutron fluxes as well as contamination from tritium, particulate matter and corrosion products (i.e. "crud"). Radiation fields in the neighbourhood of 10^6 R/h can be expected due to neutron activation of structural components[152]. Present experience with fission reactors has provided a broad base, but additional specialized techniques will have to be developed, especially in the areas of vacuum technology and cryogenics. The main objectives are the reduction of radiation exposure to personnel and reduction of down time.

Several studies have been done on this problem; one [153] concluded that these objectives will be reached by increased emphasis on remote viewing and handling and decreased use of contact, or "hands-on" maintenance. This result is typical of the fusion situation and, as is well known, significant development programs in remote viewing and handling technology are underway in all fusion programs including Canada's.

Effective maintenance will require modular construction and high component accessibility[154]. Examples of such modular construction for liquid metal breeder blankets are shown in Figs. 2-9 to 2-11 referring to the MARS design. Since most of the high maintenance items are within the vacuum envelope, access ports will have to be provided[155], even though this results in some loss in design optimality[156,157].

4.2.5 Safety

Safety is a crucial concern for liquid metals as breeders. However, it is an extremely difficult issue to resolve since there is a large subjective element in the arguments put forth on all sides of the issue. There are three basic areas of argument: (i) the experience gained with the nuclear applications of liquid metals from the use of liquid sodium in LMFBRs; (ii) the current operating experience with liquid lithium loops; and (iii) safety studies relevant to liquid metal breeders. These arguments are as follows.

(i) There has been extensive experience with LMFBRs worldwide, including such reactors as Phénix in France, which has operated successfully for some 10 years. However, the important differences between liquid Na in LMFBRs and liquid Li in future fusion blankets are: (a) the chemical reactivity of Li is greater than that of Na, making it more difficult to control; and, (b) the liquid Li would contain a large quantity of tritium, resulting in a much greater radiological hazard in the event of a leak. Therefore, arguments for liquid metal breeders based solely on the LMFBR experience are not in themselves sufficient to predict the safe operation of blankets based on that concept.

(ii) The operating experience with current liquid lithium loops is an important part of the safety picture. The study team visited the ELS loop at HEDL[158] and the Mol loops at SCK/CEN, Belgium[159] and hence, it is relevant to describe these facilities and their operations in some detail.

The ELS at HEDL, with a total inventory of 3800 L (\approx 1,000 US gallons), is the world's largest liquid lithium loop. Although it is intended not as a

facility for fusion blanket studies but for the development of the FMIT target, and the operating temperature is limited to about 250°C, it provides valuable information on handling large quantities of liquid Li. The ELS is operated by two professional and three technical staff. Annual operating budget is one million dollars. The loop is mostly 0.1 m (4") stainless steel pipe. Main flow is 32 L/s (\approx 500 USGPM). A chemistry side-stream of 0.03 L/s (\approx 5 USGPM) has its own pump and so can be isolated from the main loop. Since there are no hot or cold legs in the main loop, there is no need for a large heat exchanger, and temperature is maintained by balancing trace heat, pump heat, and heat losses. Pressure is regulated by a surge tank, and is controlled at zero (actually $\approx 1.33 \times 10^{-4}$ Pa or 10^{-6} torr) at the FMIT target section. Cold traps and hot traps (gettering on titanium sponge) are provided in the chemistry loop. A dump tank with argon cover gas is used for make-up. Preheating, using shaped and wrap-around calrod type electrical elements, requires about 1½ days from a cold start. Filling and drawing a vacuum at the target section each require about two hours. Operation is unattended during offshifts and weekends, which demonstrates that the operation is fairly routine. The loop is computer controlled with CRT display. If it is necessary to open the loop during maintenance, an argon purge reduces air contamination of the exposed lithium, and pipe ends are sealed with plastic sheeting. Lithium vapour exposure produces more severe irritation and discomfort than sodium; in experiments with lithium leaks it was noted that low concentrations of the aerosol irritated the respiratory system and required the use of respirators.

Carbon microspheres and graphite flakes ("Graphex") were found to be effective against small-scale fires. The ELS is in metal containment, above a metal tray. The tray is protected by a working floor grill and sealed with a brass or lead foil. Lithium leaks rapidly corrode the foil and are collected in the tray which is substantially sealed and can be flooded with argon for fire control. By emphasizing tightness in the design, the hazard of lithium fires in ELS has been considerably reduced. The ELS experience has given the designers and operators confidence that with careful procedures and the right operating environment, liquid Li can be handled in large quantities without undue hazard.

Further information on liquid lithium loop operation was gained during a visit to the SCK/CEN Laboratories in Mol, Belgium. Their liquid metal facilities include 40 L and 140 L lithium loops and a $^{17}\text{Li}-\text{83Pb}$ loop scheduled to start up this year. These are much smaller loops than ELS. The two lithium loops are designed as a figure-of-eight with a counter-flow heat exchanger between the hot and cold legs. Static pressure levels are fairly low, not more than 0.2 or 0.3 MPa (2 or 3 atmospheres). The mechanical part of the loop design, pipe sizing, pressure drop calculations, etc., is fairly conventional. The main piping in these loops is, respectively, 19 mm and 25 mm ($\frac{1}{2}$ inch and 1 inch) type 316 stainless steel. For loops of this size, EM pumps are satisfactory, and AC conduction-type pumps (approximately 15% efficient), obtained from Novatome (France), are used. These pumps are air-cooled by natural convection, require about 5 kW of power, and deliver from $2 \text{ m}^3/\text{h}$ to $8 \text{ m}^3/\text{h}$, depending on type, at $\Delta p = 0.1 \text{ MPa}$ ($\approx 1 \text{ atm}$). Stainless steel bellows valves are used. Even with these, there is a tendency for the seats to leak after a period of service and back-up valves are frequently installed in tandem. Level indicators are installed above the bellows to act as leak detectors. Satisfactory operation is obtained provided the temperature is kept below 650°C . Flow and temperature instrumentation seems generally satisfactory, with the exception of some plugging by corrosion products.

The loops are filled by placing pieces of solid Li in a purification tank, evacuating the air from the tank and heating it electrically to the melting point. Initially the dump tank was used for this operation, but a preconditioning period for fresh Li, to exclude non-metallic impurities, was found necessary. When the required purity is reached in the purification tank, the Li is transferred to the (evacuated) dump tank, the argon cover gas is used to force it into the rest of the loop, and flow is established. The start-up operation requires an 8-hour shift to complete. Dumping the loop into the dump tank by gravity requires approximately 15 minutes, and may be done, if judged necessary by the operator, in the event of fire or major leak. The test section can also be isolated during an emergency. The loops are operated on a continuous shift basis with an operator in attendance. A total of 40 000 hours operation has been obtained with the Li loops since 1976. The maximum temperature in the forced convection loops is approximately 400°C , and

this will not be increased to the target value of 550°C until the impurities can be better measured and controlled. The maximum temperature reached in the purification stand and in the sodium loops was approximately 800°C.

Maintenance in Li loops has required some different techniques from those used in Na loops. To change a section of pipe, e.g., containing an instrument or valve, it was possible in Na loops to isolate the section by freezing, and to expose the Na to the air at the cut ends. For Li, the preferred method is to drain the loop to minimize nitrogen contamination of the lithium, before cutting. To ensure a good weld, all residual lithium must be removed from the weld area. This can be done by wiping with a cloth wetted in water (alcohol in the case of sodium). Although various mechanical joints have been used, none have so far been leak-free at high temperatures, and all-welded construction is now recommended.

There have been two accidental lithium fires resulting from leaks, and both have been contained with a small amount of damage. There have been, as well, a number of test fires. Lithium burns at a very high temperature ($\approx 1000^\circ\text{C}$) and the fire can escalate rapidly if sufficient lithium is present. Therefore, fire suppression measures have concentrated on early containment. Conventional foam-type fire extinguishers, useful for sodium fires, have not been effective. Sand is not used because of a reaction between lithium and silica. The most effective fire-retardant found so far has been an expensive form of powdered graphite ("Graphex"). This is a very light powder and is most effective if it suppresses the fire in its early stages, before enough buoyancy-induced turbulence is generated to disperse the powder. To suppress air circulation and control fires, the loop rooms are compartmented by trays, which are loaded with "Graphex" in plastic bags. The intention is that a leak of liquid Li will melt the plastic and allow the powder to smother any fire in its early stages. Although Li and Na fires burn rapidly, no explosions have been observed.

Thus the operating experience with liquid Li loops currently in place has been very encouraging for liquid metal breeder blankets and it is assumed that similar work with less reactive 17Li-83Pb will also be favourable from the

safety point of view. Nevertheless, it must be emphasized that these installations are at best (ELS) at least an order of magnitude smaller than what would be required for a breeder blanket and no tritium is present in them to complicate the safety problem. Therefore, it involves a very large extrapolation to argue for the acceptability of liquid metal breeders on the basis of current loops.

(iii) In the fission reactor field, numerous studies have analyzed the hazards resulting from malfunctions or accidents within the reactor system. The same approach can be used for fusion reactors but suffers from the same limitations, i.e. the necessity of covering all possible events and the assignment of realistic probability distributions for their occurrence. Furthermore, the test data on which such studies are based is very small for fusion compared to fission.

EG&G, Idaho Falls, the lead laboratory in the USDOE's fusion safety program since 1978, has carried out a number of such studies[160]. In addition to system studies[161,162], they have sponsored work relating to liquid metal breeders, specifically liquid lithium, which because of its large chemical energy represents a new and less predictable hazard, although previous experience with liquid Na provides some guidance. Liquid Li sprays and spills (up to 100 kg quantities) have been tested[163]. A result which is significant for the spread of tritium and other contaminants as well as safety generally, is that while Li burns rapidly in air at high temperatures, combustion in a confined space seems to be reasonably containable, due to the reaction with atmospheric nitrogen. Safety procedures involving containment by argon flooding or smothering by carbon microspheres or graphite flakes have been developed by those laboratories with experience in liquid Li operations. A key feature of liquid Li safety therefore appears to be secondary confinement. Prevention of contact with concrete, where the reaction liberates water which further reacts with the Li, is important. The use of sand as a fire suppressant is not recommended because of the reaction with silica. The consensus of these studies and of those with experience in liquid Li operations is that safety considerations require special care and new

techniques, but for the scale of operations experienced thus far, these are not beyond what is possible with present engineering expertise.

None of the above arguments, either singly or together, are conclusive on the safety of liquid metals as fusion breeders, and confusion frequently arises in discussions of this issue from the emphasis given to one or the other of them by opponents or proponents of the various breeder concepts. Unfortunately, it has also been our observation during this study that a high degree of subjectivity prevails concerning the safety of liquid metal breeders - much of this revolves around the perceived necessity to make fusion a "safe" energy concept, i.e. one without an ostensible serious accident scenario. There is no doubt that the possibility of a serious accident would always be present if liquid metal breeders were to be used in fusion reactors; the safety issue in fusion would then become similar to that of fission reactors where arguments about the adequacy of the safety precautions taken and the probability of accident events dominate the discussion. For some segments of the fusion community, especially in those countries having difficulties with criticism of fission reactor safety, there is a reluctance to enter into the same situation with fusion reactors. And hence, in these quarters there is an incentive to avoid liquid metal breeders and, of course, fission-fusion hybrid systems for similar reasons. However unsatisfactory these non-technical arguments may be in a scientific report, there seems to be little doubt that at present they form part of the basis for discussions on whether or not to use liquid metal breeders in fusion reactors and hence, they must be recognized.

From a technical standpoint, what is required to resolve the safety issue is more experience on liquid metal systems nearer fusion reactor conditions and on the same scale. This would involve the construction of one or more very large liquid metal facilities in order to give a demonstration of safe and reliable operation under normal conditions and also to gain experience under simulated accident conditions. Such a major commitment to liquid metal systems is unlikely to occur until the situation with regard to the breeding capability of solid breeder materials is clarified. If the result is negative, then the fusion community will have no recourse but to build these large liquid metal experiments.

4.3 Materials Compatibility and Corrosion

4.3.1 The State of the Literature to Date

Probably the major concern, after safety, with the use of liquid lithium and lithium alloys as breeder blanket/coolant materials is corrosion of the containment structure. Compared with data for liquid sodium/structural materials compatibility, there is relatively little information available so far on corrosion by liquid lithium and lithium-lead. There is a broad but thin scatter of information covering most of the anticipated liquid metal breeder blanket concepts, and consisting of corrosion data for a range of alloys, temperatures and impurity concentrations. In some cases corrosion data have been given[164-183] and this information is summarized in Table 4-1. In Table 4-2 are the compositions of the alloys tested. In other cases the results are more descriptive than quantitative, or not amenable to tabular presentation, and this information will be summarized in the text. These other references are concerned with the effects of lithium and lithium-lead on mechanical properties of structural materials[184-192], with the purity of liquid breeder blankets and effects of liquid breeder blanket impurities and/or additions on the corrosion/mechanical properties of structural materials[193-201], with the general area of intergranular attack or grain boundary effects of liquid lithium and lithium-lead[178-183,202-205] and with the general properties of liquid Li/Li-Pb[206-208]. To a large extent there are significant overlaps between these effects and references, because, of course, intergranular attack and localized corrosion will affect the mechanical strength of an alloy. Many of these references also include discussions on selective dissolution or leaching by the liquid metal, and these will be discussed in later sections.

This review of materials compatibility with liquid lithium and lithium-lead is restricted to those candidate structural materials that have actually been tested; a number of other alloys have been proposed for various fusion applications, and some of these may contact a liquid breeder blanket. These alloys are discussed, with respect to their uses in fusion engineering, in a number of review articles which include breeder blanket materials compatibility.

Table 4-1 A Summary of Corrosion Test Conditions and Results for Liquid Lithium and Lithium-Lead Alloys

TEST MATERIAL(S)	TEST CONDITION	INITIAL IMPURITIES	TEMP	TEST DURATION	CORROSION RESULTS AND COMMENTS*	REF
304 304L 316 2 Cr-1Mo 9Cr-1Mo	Pumped Li loop (fabricated from 304)	0.027 wt% Na; 70-100 ppm N ₂ ; < 110 ppm O ₂	538°C hot leg; ΔT = 152°C	948 h	austenitics 37-29 μm/a; ferritics 12-7 μm/a, depending on position in loop and steel heat treatment	[164] [175]
304 304L 304 with 308 welds titanium zirconium yttrium 321 seam-welded bellows	various pumped Li loops (304 tubing, 316 connectors)	<400 ppm N ₂ <150 ppm Lithium nitride	230-270°C up to 6500 h		austenitics and welds, 0.2 μm/a; Ti 0.04 μm/a; Zr 0.25 μm/a; Y became embrittled (YH ₂). Erosion at 24 m/s of 304/304L was effectively < 0.5 μm/a.	[165]
304L	static Li in a 304L crucible	420-8750 ppm N ₂	575-960°C	168 h	A mechanistic model proposed. Parabolic time dependence for weight loss and grain boundary penetration kinetics (see text); corrosion rates varied from 5-50 × 10 ⁻⁶ g/mm ² (in 168 h), depending on N concentration.	[166]
316	static Li in a 316 crucible	carbon and nitrogen impurities added	600°C	336-672 h	In Li containing unit nitrogen activity, surface Cr depletion and intergranular penetration to 200 μm occurred. In unit carbon activity Li, Cr-rich carbides precipitated at surface and intergranular penetration to 400-600 μm was observed.	[168]

* penetrations calculated on basis of uniform metal removal.

Table 4-1 A Summary of Corrosion Test Conditions and Results for Liquid Lithium and Lithium-Lead Alloys (continued)

<u>TEST MATERIAL(S)</u>	<u>TEST CONDITION</u>	<u>INITIAL IMPURITIES</u>	<u>TEMP</u>	<u>TEST DURATION</u>	<u>CORROSION RESULTS AND COMMENTS</u>	<u>REF</u>
304 316 Nitronic 30, 33,40 Carpenter 18/18 tubing) + WR 1,4922 Ti-6V-4Al V-20Ti	forced and natural convection Li loops (316 + WR 1,4922)	50-1600 ppm N ₂	400-700°C (mostly 402°C)	11-833 h (350°C in cold trap)	austenitic steels 6-120 µm/a, depending on temperature and exposure time; ferritic (WR 1,4992) 83-88 µm/a; nitronic alloys 97-112 µm/a; Ti-6V-4Al 2.3 µm/a; V-20Ti 1-2.6 µm/a.	[169]
2 Cr-1Mo HT9	Li in capsules		400-600°C	500-3000 h	Decarburization of 2 Cr-1Mo; not of HT9 Corrosion rates from 0.55-2.55 g/m ² after 3000 h at 400-600°C, respectively.	[171]
Nb TZM Nb 304 316 Ni Hastelloy N	Natural convection Li loop (304)	0.1,0.5 and 1wt% N ₂ ; 0.006, 0.01 and 0.02 wt% O ₂	600°C (250-275°C in cold trap)	1000 h	TZM and Nb showed almost 0, up to 2 µm/a in contaminated Li; Nb was resistant at low impurity levels, corrosion of 15 µm/a in contaminated Li; austenitic steels resistant at low impurity levels, increasing to 26 µm/a in contaminated Li; Hastelloy N corrosion rates > 366 µm/a in pure Li, dissolved if impurities present. Ni dissolved completely in all cases.	[172]
Incoloy 800 316 2 Cr-1Mo	Pumped Li loop (316)	60-250 ppm N ₂	560-580°C, 458°C cold leg	1000 h	Incoloy 800 insensitive to variations in N; 316 corrosion proportional to N content; 2 Cr-1Mo suffered only decarburization; corrosion rates ranged from 5×10^{-3} g/cm ² to 10^{-5} g/cm ² at 460°C for Incoloy 800 to 2 Cr-1Mo, and 4×10^{-2} g/cm ² to 10^{-4} g/cm ² at 560°C.	[173]
304 304L 316 316L	Pumped Li loop		400°C, ΔT=45°C	up to 7275 h	austenitic steel corrosion rates from 10 µm/a (low impurity levels) to 70 µm/a (more impurity, higher Li velocity). Carbon steel corroded at rates approximately 30% higher.	[174]

Table 4-1 A Summary of Corrosion Test Conditions and Results for Liquid Lithium and Lithium-Lead Alloys (continued)

TEST MATERIAL(S)	TEST CONDITION	INITIAL IMPURITIES	TEMP	TEST DURATION	CORROSION RESULTS AND COMMENTS	REF
304L 321 2 Cr-1Mo	Li thermal convection loops (constructed of materials at left)	46-142 ppm O ₂ 15-48 ppm N ₂	600°C (ΔT=200°C)	3000-10000 h	Ferritic steel, 2.3 μm/a (600°C) -net wt. gain in cold leg; austenitic steels 14 μm/a (600°C) -net wt. gain in cold leg; more localized attack noted on austenitic steels, compared with 2 Cr-Mo alloy.	[176]
316L	Static Li-99.3 w/o Pb (304L)	10 ppm N ₂ ; 20 ppm Fe	400-600°C	750-6130 h	no corrosion after 6000 h at 400°C; although embrittlement may occur; no corrosion data for higher T: considerable Ni leaking and embrittlement noted.	[177]
2 Cr-1Mo	Static Li-17.6 w/o Pb in 2 Cr-1Mo crucible	45-65 ppm N ₂	400-625°C	up to 500 h	intergranular penetration of 400-1200 μm as T varied and as sample heat treatment changed.	[178]
2 Cr-1Mo	Various Li-Pb alloys in static tests	<100 ppm N ₂	300-600°C	up to 1000 h	500°C, 1000 h exposure to Li-99.3 w/o Pb caused no intergranular penetration; in Li-53 w/o Pb intergranular penetration of 400-700 μm had occurred after 25-120 h.	[179]
EM12 Chromasco 3	Thermal convection loop containing liquid Pb (fabricated from EM12 and chromasco 3)		550°C ΔT 80°C	3000 h	After 3000 h a wt. loss corresponding to 30 μm for EM12, and 90 μm for chromasco 3 was noted.	[180]
304L	Static Li (304L crucible)	1.17 - 1.72 w/o N ₂	600-1000°C	up to 200 h	Grain boundary penetration ranged from approximately 3000 μm in 35-65 h at T=727-800°C, 2000 μm in 200 h at 650°C to 1000 μm in 150 h at 600°C.	[181, 182]

Table 4-1 A Summary of Corrosion Test Conditions and Results for Liquid Lithium and Lithium-Lead Alloys (continued)

<u>TEST MATERIAL(S)</u>	<u>TEST CONDITION</u>	<u>INITIAL IMPURITIES</u>	<u>TEMP</u>	<u>TEST DURATION</u>	<u>CORROSION RESULTS AND COMMENTS</u>	<u>REF</u>
AMCR ICL 016 NMF3 Nitronic 32 Carpenter 18/18+ (Cr-Mn, low Ni steels)	Static Li in capsule tests	20 ppm N ₂	600°C	up to 600 h	After sufficient time (750 h for Nitronic 32 up to 6000 h for ICL 016) a Mn-depleted surface layer and grain boundary penetration noted. Below that time only the Mn-depleted layer was seen. Order of resistance to grain boundary penetration was ICL 016 > AMCR > NMF3 > 18/18 plus > Nitronic 32.	[183]

Table 4-2 Typical Compositions of Alloys Mentioned in Section 4.3

discussions, see references[4,9,209-210] and Section 2.2.1. A number of papers that give overviews specific to liquid lithium breeder blankets are also available: references[3,8,130,211-213] are good examples.

Clearly, a large number of alloys have been evaluated for compatibility with liquid lithium or lithium-lead, but for most of these only one or two measurements have been made. Reasonably extensive data are available for the ELS-FMIT (Section 4.2.5) facility[165], but much of this is for 270°C, a lower temperature than that suggested (400-600°C) for fusion reactors. However, the available data can be grouped in terms of a general alloy classification, i.e. austenitic steels, ferritic steels, other alloys (of Mo,Ti,V) and individual elemental metals. The discussion to follow will consider just the solubility of various elements in lithium and lead, and then the behaviour of austenitic steels, ferritic steels, and other alloys, in that order, in liquid lithium and lithium-lead. Finally, a discussion of mass transfer and gettering will be given.

4.3.2 Solubility of Metals and Non-Metals in Liquid Li and Li-Pb Solutions

4.3.2.1 Liquid Lithium

It has been known for some time[206] that nickel is very soluble in liquid lithium, particularly in comparison to metals such as Fe, Cr, Ti, Ta, Mo, Nb and V. These solubilities are affected by the presence of nitrogen, carbon and oxygen in the lithium[168,172,197-199,207] or by the oxygen and carbon content of the metal itself[172,198,199]. Although similarities between liquid lithium and liquid sodium, for which extensive data are available[214,215] do occur, there are enough differences that predictions for lithium based on sodium experience are not useful[207]. Thus no attempt is made here to predict solubilities of metals in lithium, particularly with respect to impurity content, based on observations for sodium. Table 4-3 summarizes some of the available data for solubility of various elements in lithium. Clearly the nitrogen content of the lithium strongly affects the solubility of metals in that solvent. Nitrogen is highly soluble in lithium

Table 4-3 Solubility of Various Elements in Liquid Lithium

<u>ELEMENT</u>	<u>SOLUBILITY*</u> (appm)	<u>REFERENCE</u>
Ni	396 at 800°C and 146 ppm N	[207]
	3,522 at 800°C and 220 ppm N	[207]
	~600 at 800°C and 50-100 ppm N	[206]
Fe	7 at 800°C and 90 ppm N	[207]
	~7 at 800°C and 50-100 ppm N	[206]
Cr	~8 at 800°C and 50-100 ppm N	[206]
	7 at 800°C and 150 ppm N	[207]
	18 at 800°C and 790 ppm N	[207]
Ti	1 at 800°C and 55 ppm N	[207]
	~1 at 800°C and 50-100 ppm N	[206]
Mo	~0.8 at 800°C and 50-100 ppm N	[206]
Nb	2 at 800°C	[207]
	1 at 800°C and 38 ppm N	[207]
	12 at 800°C and 70 ppm N	[207]
	34 at 800°C and 260 ppm N	[207]
N	~80,000 at 500°C	[198]
H	~10,000 at 500°C	[198]
C	~13,000 at 500°C	[198]
O	~1,100 at 500°C	[198]
Si	21,880 at 450°C	[207]

* the original data are referenced in the reference given;
some of these numbers are approximate, based on graphical
data presented in the quoted reference.

to form a mixture of lithium and lithium nitride, thus requiring strict precautions against nitrogen ingress in liquid lithium systems. This fact alone appears to be responsible for the large variation in corrosion data for liquid lithium. It has been reported[201] that the solubility of Si in lithium is similar in magnitude to that of N, and Si in lithium reacts readily with both nitrogen and nickel.

It is important to recognize that the equilibrium between a metal and liquid lithium, represented by the distribution coefficients[198,199], may change the initial impurity element concentration of the liquid lithium. Further, metals in contact with the liquid lithium may absorb impurities from the liquid, which can have significant consequences for subsequent mechanical properties[216]. Conversely, loss of impurity elements from the metal or alloy to the liquid lithium can result in a reduction in mechanical strength and/or grain boundary penetration, as will be described in Sections 4.3.3.3 and 4.3.4.2. Oxygen is readily scavenged by lithium from Nb and Zr and their alloys, for instance, often leading to grain boundary penetration[198]. Compound formation, such as that observed when Cr comes into contact with nitrogen-contaminated lithium[197], can result in both corrosion and mass transport problems in dynamic systems. Consequently removal of impurities from liquid lithium is required to maintain the highest purity commensurate with adequate structural materials integrity and mass transport considerations.

It has been shown that liquid lithium can, with care, be handled routinely at temperatures of 270°C[165]. To some extent this is because of equipment designed to maintain low impurity levels of non-metallics like nitrogen, but to a larger extent is the result of the lower solubility of both non-metallics and metallics in liquid lithium at 270°C compared to that at 500°C or higher. From a solubility point of view, the lower the liquid lithium temperature the less the corrosion of the structural materials that contact it.

4.3.2.2 Lithium-Lead and Lead

Very little information appears to be available on solubility of metals and non-metals in lithium-lead solutions. It has been estimated that the solubility of Ni in Li-Pb is about 100 times that in Li, based on data for Pb[217]. In lead the solubility of Ni at 635°C was estimated to be ~ 28 000 appm and that of Fe at 600°C ~ 8 appm[130]. A study on the solubility of Ni and Cr in molten lead[218] gave the solubility of Ni as 0.53 a/o (5300 appm), where a/o means atomic percent, at 372°C and 18.63 a/o at 1200°C. The solubility of Cr was given as 0.63 a/o at 1210°C. Molybdenum and tungsten were essentially insoluble in lead up to 1200°C. The lithium activity in 17Li-83Pb, the most commonly used lithium lead alloy, is very low at < 500°C[8] and hence, it may be assumed that the solution behaviour of metals and non-metals in lithium-lead will be very similar to that in lead. Based on this, the high solubility of Ni in lead at temperatures above 500°C probably eliminates nickel and nickel alloys from consideration as structural materials with lithium-lead solutions. However, considerably more data need to be generated before an unequivocal statement can be made.

4.3.3 Behaviour of Austenitic Alloys in Liquid Li and Li-Pb

4.3.3.1 General Corrosion Behaviour in Li

At this stage the assessment of corrosion data is still largely a qualitative exercise. Even for the austenitic alloys, for which the largest data base exists, there is insufficient detail in the corrosion data (for instance see Table 4-1) to make reasonably accurate predictions of structural materials lifetimes in flowing lithium. Most of the available data are for types 304/304L and 316/316L stainless steel. An associated concern, corrosion product mass transport, involves loop design, pumping requirements and system maintenance. Radioactivity transport may also be involved. Most of the data quoted in Table 4-1 gives corrosion rates as a loss of material per unit area of surface over a given time period. This averages out much deeper, and shallower, intergranular penetration and ignores selective leaching of alloying elements. However, weight loss data are a useful guide to general corrosion resistance.

Austenitic steels, most commonly types 304, 304L and 316, seem to be resistant to corrosion by lithium up to 400°C at low nitrogen impurity levels. At 500°C and up in pumped systems the corrosion of these steels is strongly dependent on the nitrogen impurity content of the lithium, ranging from 50–100 µm/a with nitrogen contents of a few tens to several hundreds of ppm at around 500°C. As temperatures increase the corrosion rates increase, particularly in flowing systems where a greater ΔT is correlated with an increased corrosion rate[212,8]. There appears to be little difference between corrosion rates for types 304 and 316 stainless steels, taking into account the variability of the data accumulated so far, but the higher Ni-containing alloy PCA (see Table 4-2) shows corrosion rates about 1.5 times that of 304/316[8]. In static or thermal convection tests the corrosion rates are somewhat lower, probably because no cold trapping of corrosion products takes place in these systems to maintain a high solubility for alloying elements such as Ni. It appears that the corrosion rates for austenitic stainless steels approach steady state values after an initial high corrosion rate period, of up to 3000 h. Based on data summarized so far[8] the weight loss, W (mg/m^2), dependence on time, t , in a circulating system is approximately $W = kt^{0.7}$, assuming no unusual impurity, flow or ΔT effects.

Increasing the nickel content of the austenitic alloys, for instance to include Incoloy 800, resulted in increased corrosion, as would be anticipated from considerations of solubility of Ni in lithium. In addition to the loss of Ni from the alloy, results suggest that the presence of nickel in the liquid lithium leads to higher chromium dissolution rates[193,219,220]. The presence of nitrogen exacerbates this effect in stainless steels[219] although it was shown recently for Incoloy 800 that the corrosion behaviour was independent of the lithium nitrogen content up to 250 ppm nitrogen[173], as opposed to types 304 and 316 stainless steels. A brief summary of corrosion data for nickel alloys in liquid lithium is that it is unacceptably high. It has been reported that aluminum additions of 5 w/o (where w/o means weight percent) to the lithium reduce corrosion rates for the austenitic alloys by a factor of five at 500–700°C under static conditions[193]. Thus it may be possible to use the austenitic alloys, even those nickel-based, if the liquid lithium is inhibited or the metal surface aluminized[212]. At high

temperatures ($> 800^{\circ}\text{C}$) very high rates of mass transfer took place and although such effects are much smaller at temperatures around 500°C , there is still the possibility of increased plugging of loops by aluminides.

4.3.3.2 Selective Dissolution and Intergranular Attack by Li

Exposure of austenitic alloys to lithium results in near-surface depletion of nickel and the presence of a porous ferrite layer 10 to 20 μm thick. Near surface microstructural changes were also noted[164,169,170,174,176] in which the initial equiaxed grain structure changed to a fine-grained ferritic structure with evidence of grain boundary grooving, particularly deeper into the base metal. Although one of the properties of this porous ferrite layer is that it is non-protective to further lithium attack, the mechanism of formation of this layer has implications for the mechanical integrity of the alloy. The ferrite layer is thought to form by selective nickel dissolution resulting in destabilized austenite, which converts to ferrite[176]. Interstitial formation and grain boundary precipitation are also important, and the type of impurity in the liquid lithium is important in defining the type of liquid lithium attack to be expected. For instance, it has been shown[168] that carbon impurities in the lithium form $M_{23}C_6$ (where M stands for iron, nickel or chromium) chromium-rich carbides as corrosion products which can co-exist with the surface austenite and ferrite and also precipitate in the sub-surface grain boundaries. On the other hand, nitrogen impurities form nitrides of the type Li_9CrN_5 , which diffuse out to the surface, resulting in chromium depletion of the steel. In both cases, i.e. the presence of nitrogen and carbon impurities, embrittlement to a depth of 400 μm (672 h, 600°C) had occurred.

Intergranular attack and selective dissolution is likely to be a more serious limitation to the use of austenitic alloys in liquid lithium than general corrosion. The degree of attack is, like the depth and porosity of the overlying ferrite layer, a function of temperature. It has been suggested that an initiation time correlated with formation of a Li-metal-N corrosion product[181,182] is followed by grain boundary attack showing parabolic time dependence. The rate of grain boundary penetration was controlled by the

diffusion of lithium through the corrosion product found in the attacked grain boundaries. Additions of nitrogen to the steel resulted in an increase in grain boundary penetration rate[181,182]. Low Ni Cr-Mn austenitic steels studied in low nitrogen lithium required longer initiation times than type 304 stainless steel before grain boundary penetration occurred[183,201], but variations in alloy nitrogen content appeared to be responsible for variations in initiation time. Substitution of Mn for Ni appeared to have no effect on overall corrosion behaviour. Cr-rich M₂₃C₆ carbides were also noted along the grain boundaries, the surrounding matrix being highly Fe-rich[201]. It has been suggested that carbide precipitation is necessary for the penetration of grain boundaries by lithium to take place[181,182,201,204], but it is probable that other factors are also necessary, since it has also been noted recently[205] that type 316 and a duplex Cr-Mn stainless steel were not penetrated by pure Li at 600°C, in agreement with previous results showing that types 316 and 316L stainless steels offer better corrosion resistance to liquid lithium than type 304 stainless steel[203].

4.3.3.3 Effect of Li on Mechanical Properties

Subjecting a structural material to stress in an environment that can cause both corrosion and grain boundary attack could result in rapid mechanical failure. At temperatures below 500°C it was found that type 304 stainless steel and type 308 weld metal had a higher rate of fatigue crack growth in lithium than in argon[165]. Similar results were obtained over the temperature range 200-700°C[191]. It was suggested that in this case the presence of lithium limits plastic flow at the crack tip and thus promotes localized fracture, enhancing the rate of fatigue crack growth. At 482°C the fatigue crack growth behaviour of type 304 stainless steel was found to be strongly influenced by the lithium nitrogen content[185,186], and at strain ranges > 1% the fatigue life in lithium was greater by a factor of two than in air. Fracture has been observed to occur intergranularly in type 304 stainless steel. Comparisons with time to failure in air might be misleading unless it is remembered that oxidation of the surfaces of a propagating crack may cause strain accumulation and/or interfere with slip band movement and hence decrease the crack initiation period, shortening total fatigue life in air[221].

In liquid lithium no oxidation can occur, and, for instance, type 316 stainless steel in lithium at 482°C had a fatigue life 3 to 8 times longer than that in air[184]. However, samples pre-exposed to lithium suffered a decrease in fatigue life, which may be related to the presence of a weak surface layer (ferrite) which may facilitate crack initiation. However, crack growth rates are a strong function of cyclic loading frequency and lithium temperature[191], and considerably more data are required before design of safe lithium containment structures can be made.

Information on tensile testing of austenitic steels in liquid lithium, similarly to fatigue testing, is subject to a scarcity of data. To date the data show that the tensile and creep properties of types 304 and 316 stainless steels are unaffected by a static or flowing lithium environment up to 500°C[173,184,186]. Above that temperature degradation occurs[173]. Tensile properties of the Cr-Mn austenitic steel AMCR in lithium with hydrogen additions to 40 ppm were relatively unaffected[192]. Pre-exposure of austenitic alloys to static lithium appeared to have no effect on subsequent tensile properties at 500°C whereas pre-exposure to flowing lithium resulted in a significant decrease in tensile strength[186]. The effects of impurities, temperature and time on the mechanical properties of austenitic steels in flowing lithium have yet to be determined. Overall, the results obtained so far are encouraging and suggest that mechanical properties of austenitic alloys in lithium may not be a limiting factor. Inconsistencies in the effects of nitrogen impurities between austenitic and ferritic alloys[191], when compared to general corrosion behaviour, and the effect of long-term lithium exposure need to be established.

4.3.3.4 Effects of Li Flow Velocity on Corrosion

Examination of the data in references quoted in Table 4-1 suggest that corrosion rates increase with lithium flow rate. There has been no attempt to interpret these data further because of the wide range of experimental conditions used, particularly with respect to nitrogen impurity levels. An exception is the study of erosion in lithium reported in HEDL-TME 82-42[165]. This study, using rotating discs in static lithium and a pumped Li loop, both

at 270°C, showed weight losses less than 0.5 µm/a for types 304 and 304L stainless steel up to flow velocities of 24 m/s over a 4000 h time period. The weight loss was linear, but no erosion corrosion effects were noted. It would appear that erosion corrosion in lithium is probably not significant at low temperatures in clean (70 ppm N) lithium, but experiments involving higher temperatures, a temperature gradient and effects of impurities need to be carried out before any conclusions are drawn.

4.3.3.5 Overall Corrosion Behaviour in Li-Pb

Relatively few corrosion experiments have been carried out in Li-Pb. Some data are available for lead alone, which is expected to have corrosive properties similar to that of most Li-Pb alloys being considered. Note that 17Li-83Pb is 99.3 w/o Pb. Experiments in static Li show that austenitic alloys corrode in 500°C 17Li-83Pb at substantially higher rates than those measured in pure Li, which were essentially negligible[212], and a recent estimate[188] suggests the increase in rate is more than an order of magnitude. Another estimate for the corrosion rate of type 316 stainless steel in liquid lead suggests that the rate is more than 100 times that in Li. This increase in corrosion rate has been attributed to the very high solubility of nickel in lead. In general, corrosion rates in lead appear to be related to the solubility of a metal or alloy in lead[223]. It has been reported, however, that Inconel 600 was not appreciably attacked by lead up to 600°C, although severely attacked at 675°C[224]. In both lead and lithium-lead a ferrite layer is formed on the steel surface. This layer is weak and spalls off readily, and on PCA was removed during cleaning of corrosion specimens[8], rendering accurate comparison of corrosion rates between lithium and lithium-lead very difficult. Corrosion rates increase with flow rate and the temperature dependence of the rate was found to be the same as that for lithium. Corrosion tests for 6000 h in the range 450°C to 600°C showed strong Ni depletion of type 316L stainless steel[177], resulting in structural changes and penetration of the matrix by Pb and Li. Below 400°C no corrosion was observed after 6000 h exposure. Tensile tests at 350°C, below the 316L yield stress, resulted in many Pb- and Li-filled surface cracks after 500 to 1000 h. It was not possible to decide whether liquid metal embrittlement had occurred[177]. Steels tested in tension in the

presence of liquid lead at temperatures above 400°C became embrittled[222]. The use of neutron multipliers other than lead, for instance bismuth, is not recommended from a materials compatibility point of view, since bismuth is more corrosive to steels than lead[212,215].

4.3.4 Behaviour of Ferritic Alloys in Liquid Li and Li-Pb

4.3.4.1 General Corrosion Behaviour in Li and Li-Pb

As was noted for austenitic alloys, there are insufficient data to other than qualitatively assess the corrosion behaviour of ferritic alloys in lithium. The most commonly tested ferritic alloy is 2½Cr-1Mo. Some work has been carried out on Sandvik HT9, a higher chromium variant of 2½Cr-1Mo. Whereas dissolution rates for austenitic alloys reached steady state after some initial high-dissolution period, those for ferritic alloys were linear with time. Carbon steel had a corrosion rate about twice that of austenitic alloys[174], but the principal effect of lithium on 2½Cr-1Mo steel at 600°C was decarburization, which can lead to changes in tensile properties. Decarburization did not occur on HT9. The degree of decarburization appears to be dependent on the initial microstructure of the steel; a steel containing relatively unstable carbides is attacked by lithium, whereas a normalized and tempered alloy resisted decarburization[178]. At 500°C and below ferritic and austenitic steels have similar corrosion rates, less than 15 µm/a. In a circulating loop corrosion of ferritic steels at temperatures greater than 500°C appears to be a factor of two or more less than that of austenitic alloys[164,173,176], although other studies suggest that the rates are similar[169]. Because of various discrepancies between the experiments it is not possible to quantify this difference. However, it is likely that the corrosion rates of ferritic steels in static lithium are no higher than those for austenitic steels, and very recent results at 482°C in a pumped loop suggest they are up to a factor of 10 lower[188]. Ferritic steels do not develop the porous ferrite surface layer that results from nickel depletion of austenitic steels[164,173,188] and this may account for the better corrosion resistance reported here, although in thermal convection loops HT9 and type

316 stainless had similar corrosion rates[8]. As with austenitic alloys, the ferritic alloys showed a decrease in corrosion rate as lithium nitrogen content decreased in pumped loops, but relatively little effect of nitrogen was noted in static or thermal convection systems[173].

In lithium-lead solutions, ferritic steels corrode at rates higher than in lithium, but again ferritic steels are more resistant than austenitic alloys. HT9 and 2½Cr-1Mo appeared to suffer little or no internal attack if the initial bainitic (an iron-carbon phase) microstructure was tempered to convert ε-carbide to more stable carbides such as Cr₂₃C₆. Alloying with Nb also resulted in increased resistance[178]. In liquid lead two ferritic steels, EM12 and Chromasco 3, suffered weight losses corresponding to 30 and 90 µm in 3000 h at 550°C. It was postulated that a Cr-rich protective oxide forms which reduces subsequent corrosion. Overall, there is virtually no information relating to material loss from ferritic steels in lithium-lead. This is largely because the ferritic alloys are quite resistant to selective dissolution effects that occur on austenitic alloys and hence do not suffer large dissolution losses. The corrosion rate is controlled by mass transfer of iron unless intergranular attack occurs.

4.3.4.2 Intergranular Attack and Mechanical Properties in Li and Li-Pb

As just noted the corrosion susceptibility of ferritic alloys in lithium and lithium-lead solutions is controlled more by intergranular penetration than selective dissolution of the alloy, in contrast to the situation for austenitic alloys where both mechanisms contribute. As mentioned above, the main effect of lithium on 2½Cr-1Mo is to attack the prior austenite grain boundaries in an untempered, and largely bainitic, microstructure. This finding is significant in that it relates to the heat-affected zone of a welded ferritic structure, and such welds require a proper post-weld heat treatment (Section 2.2.1). Consequently it has been shown[178,179] that tempering treatments can dramatically reduce intergranular attack at 500°C in lithium, even if the as-welded microstructure was not heat treated. In lithium-lead no intergranular attack occurred up to 1000 h. Carbon steel, type 410 stainless steel and 2½Cr-1Mo all corroded at 250-400 µm/a at 600°C,

about 50% less than for austenitic alloys. It was discovered that the initial rate of penetration of 2½Cr-1Mo steel by lithium-lead solutions decreased with increase of the lead content, whereas secondary attack (lithium dissolution of cementite - another iron-carbon phase) was independent of lead content. Corrosion rates for HT9 were generally lower than 2½Cr-1Mo, in agreement with the effects expected by increasing Cr content[171].

Surface-related mechanical properties, such as embrittlement and grain boundary attack, carburization, oxidation and selective dissolution can all affect ductility and crack propagation in metals. It is also likely that long term exposure to liquid metals will change the bulk properties of the metal, but no data for this exist so far. Ferritic steels susceptible to decarburization and/or lithium penetration of grain boundaries show a decrease in tensile properties after exposure to lithium, for example Armco iron and 2½Cr-1Mo in 500 to 600°C lithium[212]. Creep strength was also reduced; time to failure of Armco iron in 400°C lithium was reduced by five to six times over that in argon. This effect of lithium decreases with increasing temperature. HT9 did not show any significant reduction in (room temperature) tensile properties in lithium, compared to those in argon[171] and corrosion behaviour was found to be independent of applied stress[187]. With 5 w/o aluminum additions to the lithium the strength and ductility of 2½Cr-1Mo steel, after 600°C exposure, were severely reduced. This effect was not observed with austenitic alloys. During this exposure to Li-5w/o Al weight gains for the 2½Cr-1Mo ferritic steel were much higher than for austenitic steels and than weight gains in pure lithium. Loss of ductility did not appear directly related to the brittle surface (8 µm thick) aluminized layer but perhaps was more the result of aluminum at grain boundaries, consistent with the observed intergranular fracture mode and increase of crack penetration with temperature[171]. Redistribution of carbon as carbides could also sensitize the microstructure, perhaps one of the reasons why HT9 is resistant to decarburization and embrittlement under static conditions. Under flow conditions with a temperature gradient chromium depletion would be a concern but decarburization from this steel would probably be less than in 2½Cr-1Mo.

Fatigue properties of ferritic steels in liquid lithium show trends similar to those for the tensile and creep properties. The effect of lithium nitrogen content on tensile properties has not been investigated, but fatigue life of HT9 in flowing lithium was decreased with increasing nitrogen content at 482°C. In fact, the fatigue life at 100 to 200 wppm nitrogen was two to five times that at 1000 to 1500 wppm nitrogen, and high nitrogen-exposed samples failed by intergranular cracking, reminiscent of increased grain boundary attack experienced in nitrogen-contaminated lithium. At higher nitrogen concentrations the HT9 and 2½Cr-1Mo fatigue life decreased with a reduction in strain rate in static tests, a phenomenon which was attributed to internal corrosive attack along grain boundaries or through the martensitic structure. This type of corrosive attack was postulated to be more important at low strain rates, where most of the fatigue life is spent in crack initiation with subsequent rapid failure[185,187]. The initial fracture mode was intergranular, becoming transgranular after about 150 µm of penetration.

The addition of lead would likely result in a severe loss of ductility for ferritic alloys. Armco iron and several ferritic alloys, tested at 200 to 400°C in lead, suffered embrittlement and loss of tensile strength as the temperature increased[212]. There is essentially no information available for ferritic alloys in lithium-lead solutions that would allow mechanical properties to be incorporated into design decisions. So far the only statement that could be made even for pure lithium would be somewhat negative unless nitrogen concentrations could be kept very low. In lithium-lead the acceptable nitrogen level, if any, is not known. It has been shown that the corrosion rate in lead for 2½Cr-1Mo (up to 500°C) can be reduced by adding trace amounts of Zr and Mg to the lead[223].

4.3.5 Behaviour of Refractories and Other Materials in Liquid Li

In general the refractory metals show good corrosion resistance to liquid lithium, as will be discussed below, but these materials are often very expensive and/or difficult to fabricate, and hence do not figure prominently in corrosion testing programs. One exception is the vanadium alloys, which have recently received attention because of their corrosion resistance and

good performance in high flux high energy neutron fields (Section 2.2.1). A drawback with vanadium alloys, besides expense, is their susceptibility to degradation at high temperatures under oxidizing conditions such as in steam, air or commercially-pure helium. Vanadium also reacts with the nitrogen present in lithium or air. However the beneficial properties mentioned above, in conjunction with good mechanical strength at high temperature, low impact on tritium breeding and low long term activation, make vanadium alloys a potential candidate for fusion engineering materials. In particular, the V-15Cr-5Ti alloy has been designated as a reference alloy, along with V-20Ti[8,9] - see Section 2.2.1. Vanadium is rapidly attacked by oxygen-contaminated liquid sodium (5-15 ppm O) compared to oxygen-free sodium[198], and citing the previously-mentioned similarity, in terms of corrosion properties, between oxygen-contaminated sodium and nitrogen-contaminated lithium, it would appear essential to fully characterise the behaviour of vanadium alloys in lithium with varying nitrogen content. Because oxygen is probably preferentially leached from vanadium by lithium[199,225], low oxygen vanadium is probably essential.

Both titanium and vanadium possess low solubility in liquid lithium[170,206] and hence the V-Ti alloys would be expected to have good corrosion resistance. This was indeed found to be true for V-20Ti in 50 ppm lithium (slow flow rate) at 400°C, where a rate of 1-3 µm/a was found. No effect of lithium nitrogen impurity content was investigated[169].

As just mentioned titanium possesses good resistance to liquid lithium, developing a hard and non-porous surface layer about 5 µm thick at 700°C. Ti-6V-4Al was found to corrode at a rate of 2.3 µm/a in 400°C (50 ppm N) lithium[169]. In the presence of variable concentrations of nitrogen in the liquid lithium it was found that the weight gain, to form a surface Ti₂N layer, was higher on titanium in the presence of increased nitrogen[173]. Although titanium and its alloys possess good resistance to lithium, good thermal stress properties and low radioactivation characteristics, the limited high temperature potential and susceptibility to hydriding are serious drawbacks. Similar considerations apply to zirconium.

Niobium-base alloys have been of interest because of their good high temperature strength (up to 800°C). However, niobium is expensive and has poor radioactivation characteristics. In liquid lithium at 600°C niobium is known to suffer oxygen leaching and lithium penetration if the niobium oxygen content is greater than about 200 ppm. At bulk oxygen contents less than 100 ppm, niobium appears resistant to pure lithium attack[199,225]. A threshold level of 400 ppm was reported - see also[226]. Zr additions appear to suppress this effect. Niobium, however, seems susceptible to attack in lithium containing 175 ppm N at temperatures above 650°C[170]. The attack was considered consistent with the high distribution coefficient for carbon and nitrogen in Nb-C-Li and Nb-N-Li systems[198,199], and the high solubility of the corrosion products in lithium led to significant weight losses. In a series of experiments with impure lithium (O,N,Ni), Nb was found to form Nb₂N on the surface[172]. This reaction suggests that if niobium were to be considered for the containment of liquid lithium the effects of nitrogen content would have to be evaluated.

Other refractory metals/alloys have been investigated in liquid lithium: these include molybdenum, tantalum and tungsten. Molybdenum has very low solubility in lithium, lower than that of titanium, up to 900°C[206]. Even in heavily contaminated 600°C lithium (1 w/o N, 0.02 w/o O) with a ΔT of about 350°C the corrosion rate was only on the order of 2 μm/a[172]. MoNi₃ was found on the specimen surfaces, the result of reaction with dissolved nickel (from austenitic alloy used to construct loop). Tantalum also does not appear to be significantly attacked by lithium up to 700°C in 50 ppm N lithium[170], but is predicted to have an oxygen redistribution coefficient in lithium similar to that for niobium and vanadium, and hence low-oxygen tantalum would be required[199]. Small additions of hafnium to tantalum appear to suppress this effect[212]. Tungsten also is somewhat resistant to lithium attack up to 700°C[170,212] although indications were that uniform dissolution was taking place.

Overall, the refractory metals generally possess good resistance to liquid lithium, particularly if metal impurity levels (oxygen, nitrogen) are kept low. However, fabrication and supply problems, in addition to other fusion

compatibility questions, probably rule out all but the vanadium alloys for serious consideration. Much more work is needed on vanadium alloys before they can be qualified for lithium service, particularly in the area of impurity requirements and partitioning of non-metallics between the vanadium alloy and liquid lithium. There appears to be no useful information on corrosion of refractory metals in Li-Pb or liquid lead.

4.3.6 Mass Transfer Considerations

All of the liquid metal blanket design models proposed to date require some circulation of the blanket material, if only gentle stirring, to facilitate tritium recovery. In flowing systems, which are necessarily non-isothermal, a temperature gradient exists which implies differences in materials solubility in the liquid metal at different points in the system. To date, most of the serious mass transfer problems in liquid lithium have occurred in the cold section, where plugging by corrosion deposits is common. For instance, Figure 4-2 shows a section from the cold trap of a lead-bismuth loop constructed at Chalk River Nuclear Laboratories in 1966 and since dismantled. Because trapping of impurities is necessary to minimize corrosion and plugging, the solubility limits of many materials in liquid lithium remain unsaturated, maintaining the tendency for corrosion to occur. Mass transfer models include not only solubility in the liquid lithium or lithium-lead, but also diffusion of various species through the metal-liquid metal boundary, diffusion of alloying elements through the metal, and the bulk velocity of the liquid metal[212,8]. Consideration also has to be given to the effects of the ferrite layer formed on austenitic steels, which appears to thicken gradually with time of exposure to liquid lithium, and to changes in alloy structure and composition, i.e. in near-surface regions particularly, with total lithium exposure. Calculations have been made with a model containing liquid boundary layer and solid diffusion mechanisms, which, assuming chromium and nickel dissolution to be constant with time and assumptions about the effect of the ferrite layer, gives predictions in good agreement with experimentally-observed data[8].



Figure 4-2 Example of cold trap plugging by corrosion deposits (primarily Fe) in a lead-bismuth thermal convection loop in operation at CRNL in 1966. Magnification is 16x [227].

The mass transfer rate has been shown to be dependent on the nitrogen concentration of the lithium or lithium-lead. For instance, an increase from 125 to 375 wppm N resulted in a 42% increase in the mass transfer rate of austenitic alloys. Similarly, more mass transfer occurred in air-contaminated lithium than pure lithium[219], where the greater corrosivity of the lithium increased chromium dissolution. Mass transfer effects may complicate other effects such as nitrogen impurity effects, in fact they may act synergistically, so considerable effort is still required to quantify the mass transfer in a given circulating lithium design. Furthermore, differences in mass transfer effects between thermal convection loops and pumped loops may be related to deposition of magnetic corrosion products in magnetic field regions associated with lithium pumping. It has been shown that rate of deposition and composition of deposits in a type 316 stainless steel loop are typically time dependent, the initial pure chromium deposits gradually incorporating iron and nickel[212], in thermal convection systems. In pumped systems chromium is much less prevalent[174,212,8]. Variations in nitrogen content of the lithium may also be a factor here.

Although mass transfer rate is expected to correlate with corrosion rates or dissolution rates, the composition of deposits certainly being linked to selective dissolution processes, there is insufficient evidence to date to determine whether austenitic or ferritic steels are preferable for liquid lithium service. Mass transfer rate appears to be proportional to alloy nickel content[193,194], although saturation effects occur, but in actual practice austenitic and ferritic steels appear to have steady state corrosion rates of less than 15 $\mu\text{m/a}$ at temperatures below 500°C at low flow velocities, suggesting that mass transfer under these conditions is low and similar for each alloy. The formation of corrosion-inhibiting surface layers must play an important role here. In this regard, inhibition of lithium, for instance with aluminum, may be practical. Interactions between various dissolving elements, and including any inhibiting additions, may also have important consequences for mass transfer considerations. For instance Li_3N , formed when nitrogen is present in lithium, reacts to form precipitates with Cr,Fe and compounds such as $\text{Li}_{22}\text{Si}_5$ and Li_2C_2 , which are corrosion products formed by the interaction of silicon or silicides and carbides with liquid lithium[207]. Other

interactions, not yet investigated, are likely between impurities, corrosion products and lithium. Such reactions would complicate mass transfer modelling for design purposes[8] and would require careful attention to methods for removal of the reaction products. This will not be discussed here, and neither will neutron activation and radioactive transport associated with mass transfer, although the latter may well limit the materials choice for a future blanket module. It is assumed, however, that both cold and hot trapping as currently practiced, and any future on-line systems intended to remove one impurity may unintentionally add other impurities into the system and perhaps change the corrosivity of the lithium to the structural material. Such interactions will have to be considered in future corrosion research and development. Some of these concepts will be addressed in Section 4.4 when tritium removal is considered. All of the above general discussion on mass transfer also applies to lithium-lead alloys, with force since, as we have seen, the corrosion and deposition rates are expected to be much higher.

4.3.7 Some Gettering and Impurity Considerations

Since the purpose of the breeder blanket is to generate tritium, some means has to be developed to separate it from the liquid lithium or lithium-lead alloy. One of the more promising approaches is sorption by yttrium. Other practical methods include contacting with molten salts and, for lithium-lead, indirect contact processes such as helium sparging. It is generally conceded that molten salt contacting will introduce unwanted impurities into the lithium, but little research appears to have been carried out on this to date. This brief discussion is designed to illustrate the corrosion considerations involved in gettering and trapping and is not intended as an exhaustive review.

Generally tritium sorption from molten lithium, using a getter, has used yttrium sponge and gettering experiments have been carried out in the range 300 to 400°C[195]. Exposure of yttrium to pumped lithium at 270°C for 3700 h resulted in total conversion to YH_2 and severe embrittlement, leading to fragmentation[165]. Yttrium needs to have a high surface area and porosity to achieve acceptable tritium sorption, and this will tend to increase lithium

impurity levels, since high porosity/high surface area yttrium samples have high impurity content[195]. These impurities (C,H,N,O) did not appear to have an adverse effect on the sorption properties of yttrium, but clearly have important consequences for the corrosivity of lithium.

The mass transfer considerations described in the previous section not only affect cold trap areas but also the hot trap materials. With vanadium alloys in particular care must be exercised to remove carbon and nitrogen from the lithium in order to avoid carburization and nitriding reactions. Carbides and nitrides of titanium and zirconium are thermodynamically stable and hence these metals may be used to remove impurities. Both titanium and zirconium have low corrosion rates in liquid lithium[165,170,173]. Evaluation of these materials as getters showed that the anticipated efficiency is reduced by mass transfer. Surface layers of nickel and iron- or chromium-rich alloys were formed, although the effect was less for titanium than zirconium[196]. The lower nickel mass transfer noted with titanium would be expected to lead to lower corrosion of austenitic alloys in liquid lithium. Capsule tests did, however, show that decarburization of vanadium and molybdenum did not occur[196].

4.3.8 Conclusions on Corrosion

Corrosion data measured to date can be summarized as follows:

- corrosion rates are lower for ferritic alloys than austenitic alloys, but typical rates of 20-50 $\mu\text{m/a}$ are not a structural limitation on blankets;
- corrosion rates are much lower for vanadium alloys but no details are available on effects of oxygen and nitrogen on vanadium at high temperature;
- nitrogen concentrations in lithium have a large effect on corrosion rates of ferritic and austenitic alloys;

- corrosion rates are strongly temperature-dependent, increasing in some cases by a factor of ten for a 100°C increase in lithium temperature;
- corrosion rates are higher for Li-Pb than Li;
- mass transfer effects may be more of a limitation than corrosion (this is because the blanket life is only a few years); deposition in heat exchangers will be a real concern;
- activation of corrosion products may also be a limitation on the material used; vanadium alloys are particularly advantageous in this regard.

Some general conclusions on temperature limitations, based on all the data quoted in this review and using the BCSS criteria[8] are given in Table 4-4.

In conclusion it may be stated that data for three classes of alloy discussed in Section 2.2.1., austenitic, ferritic and vanadium-based, suggest that corrosion rates in liquid lithium or lithium-lead are low enough to permit their use as structural blanket materials. All three types of alloy have their particular strengths, but a vanadium-clad austenitic steel may be the best compromise solution. A lithium-lead loop using this alloy has been constructed at Argonne National Laboratory. Successful use of liquid metals as breeder materials will require careful attention to impurity control and mass transfer/deposition, both of which may act synergistically.

4.4 Tritium Handling and Extraction with Liquid Metal Blankets

Various techniques to recover tritium from liquid lithium and the lithium-lead alloy, 17Li-83Pb, have been proposed and reviewed for many blanket/coolant concepts[8,23,211,228-230]. Important considerations for the evaluation of these techniques include tritium inventory in the blanket, the effectiveness of tritium recovery, and the release of tritium to the environment. Experimental results on the physical and chemical properties of Li and 17Li-83Pb, feasibility studies, and demonstrations of proposed recovery techniques have provided information concerning the use of these materials as breeder blankets.

Table 4-4 Limiting Temperature Criteria (°C) for Liquid Metal Corrosion from [8]

System	Austenitic Steel PCA	Ferritic Steel HT9	Vanadium Alloy V-15Cr-5Ti
Lithium			
Circulating	400*	500	700+
Static	450*	550	700+
17Li-83Pb			
Circulating	350	450	650
Static	400	500	650

* depends on tolerance of initial nickel dissolution rate; limits could be slightly higher if type 316 stainless steel used.

+ based on oxygen and nitrogen pickup from lithium.

4.4.1 Tritium Solubility in Liquid Metals

The physical and chemical properties of lithium are well known and are summarized in [8] - see Table 5-1. Various investigations have also been carried out on the thermochemistry and thermodynamics of dilute solutions of hydrogen isotopes in liquid lithium[231-233]. Lithium has a great affinity for hydrogen isotopes, as indicated by the low partial pressures of hydrogen and lithium hydride compounds over lithium-hydrogen solutions. Ihle[232] has determined the pressures of D₂, LiD and Li₂D to be between 10⁻⁸ and 10⁻⁹ Pa at 500°C and ~ 1 ppm mole fraction deuterium in solution.

There are limited materials properties data available for the eutectic, 17Li-83Pb, some of which are given in Table 5-1. However, recent studies[232,234] have provided some information on the thermochemistry and thermodynamic properties of the alloy. Hydrogen isotope solubility in lithium-lead alloys is much lower than for pure lithium. Ihle[232] makes the comparison between Li and 17Li-83Pb by reporting the D₂ pressure over 17Li-83Pb to be $\sim 2.5 \times 10^7$ times higher than that over Li at the same concentration of deuterium in the liquid. This comparison is also shown in Figure 4-3, taken from reference[8]. Sievert's constant for the solubility of tritium in 17Li-83Pb was determined by Wu and Blair[235] to be $\sim 1.6 \times 10^6 \text{ Pa}^{\frac{1}{2}}$ ($\sim 5 \times 10^3 \text{ atm}^{\frac{1}{2}}$), independent of temperature. Experimental work on hydrogen absorption kinetics and diffusion at various temperatures and pressures, and investigations of surface tension, viscosity and thermodynamic properties are continuing[234,236] in order to characterize the H/17Li-83Pb system.

Safety and economic considerations dictate low maximum allowable tritium concentrations in the blanket, as explained in Section 2.2.3. This concentration depends on the liquid metal, tritium pressure and temperature (Figure 4-3). Because of the low solubility of tritium in 17Li-83Pb, a blanket system of this material will be controlled by the maximum allowable tritium partial pressure, usually taken to be 1.0 Pa[8]. This will result in a small tritium inventory. In contrast, an Li system will be controlled by the maximum allowable tritium inventory; design studies have indicated 0.5 kg of tritium to be a reasonable goal. Reference[8] extrapolates this to 3 appm tritium (using

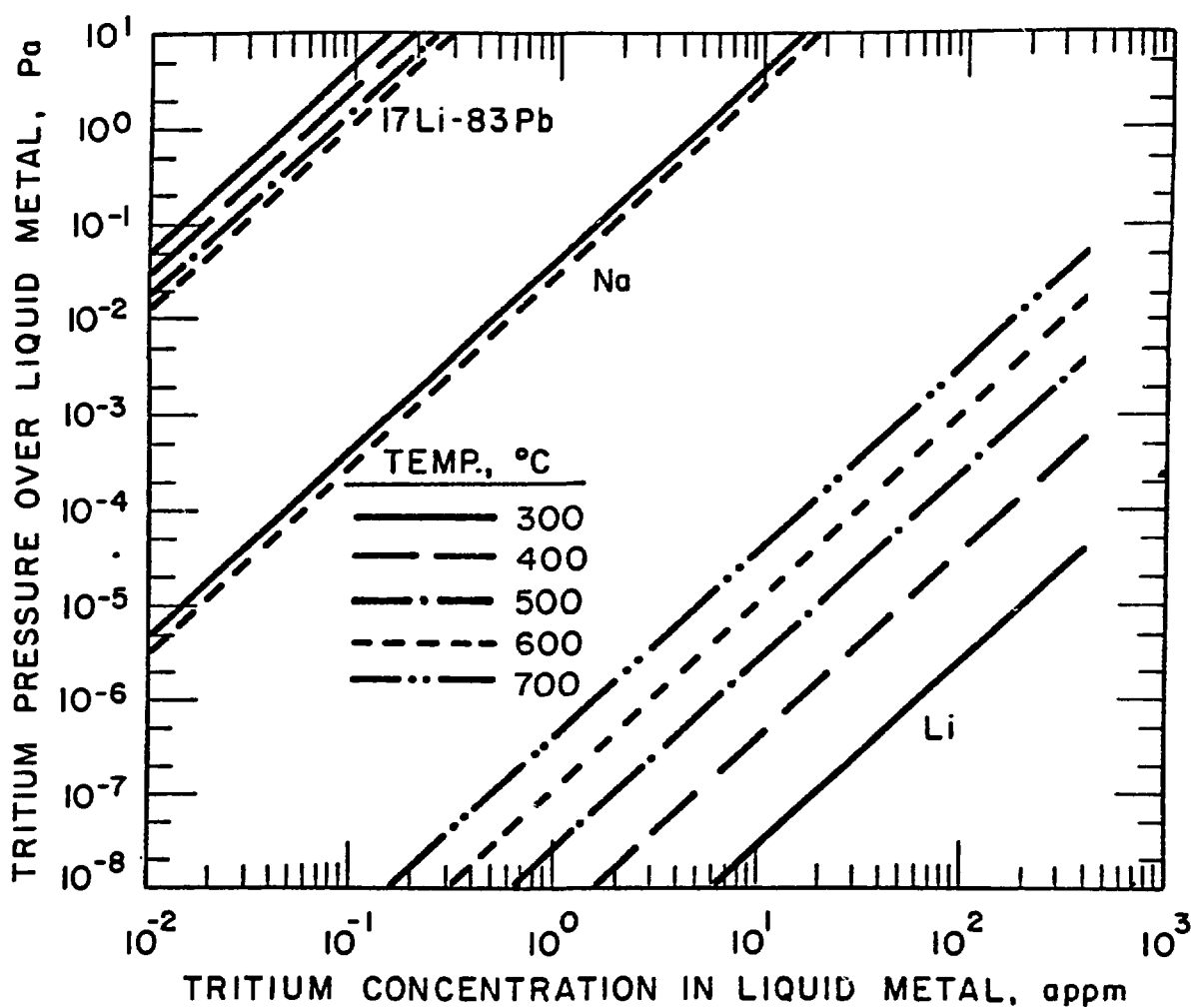


Figure 4-3 The effect of tritium concentration in liquid metal on the tritium pressure over the metal (from [8]).

the STARFIRE design) and a tritium pressure over Li of 10^{-7} Pa at 450°C. The tritium recovery methods developed must be very efficient at removing low concentrations of tritium from a lithium blanket. The low tritium solubility in $^{17}\text{Li}-83\text{Pb}$ may facilitate tritium recovery; however, the processing rates must be adequate to maintain a tritium partial pressure of only 1 Pa above the blanket.

4.4.2 Tritium Recovery from Liquid Lithium and $^{17}\text{Li}-83\text{Pb}$

Comprehensive reviews of tritium recovery from liquid metal breeders have been prepared by many authors including Buxbaum and Johnson in 1980[230], Blink, Krikorian and Hoffman in 1982[211], and Abdou et al. in the DEMO study [23]. The BCSS Report[8] also reviews the various methods. Readers are referred to these reviews for specific process details of the various design concepts.

4.4.2.1 Molten Salt Extraction

The feasibility of molten salt extraction to remove hydrogen isotopes from liquid lithium has been demonstrated[230,237,238]. In the process, some portion of the Li (specific gravity ~0.5) is circulated out of the breeder to a processing loop where it is mixed with and then separated from a lithium halide molten salt, LiF-LiCl-LiBr (specific gravity ~2.2). The salt-like impurities (e.g. LiT , Li_2C_2 , Li_3N) are extracted from the lithium into the salt phase. The salt is then sent to an electrolyzing unit where impurities are evolved (as T_2 , N_2 , CH_4) by means of a specially designed gas-sparged electrode. The tritium and evolved impurities may be recovered by hot metal getter beds. Preliminary tests indicate that a tritium inventory of less than 1 $\mu\text{g/g}$ (i.e. 1 μg of tritium per gram of liquid lithium) can be maintained in the Li[237]. An advantage of the molten salt extraction process is its ability to remove corrosive impurities (e.g. O, N) from the breeder along with the tritium.

Two concerns (Section 4.3.7) of the process are: 1) possible contamination of the liquid Li with the lithium halide salts, which may increase the corrosivity of Li; and 2) the compatibility of candidate structural materials with Li at the process temperatures (400–500°C).

Molten salt extraction of tritium from $^{17}\text{Li}-^{83}\text{Pb}$ has not been investigated. The presence of Pb would make the system more complex and corrosive. The process would require a molten salt compatible with $^{17}\text{Li}-^{83}\text{Pb}$, the lithium to remain in the alloy phase, and a compatible structural material.

4.4.2.2 Solid Getters

Although lithium has a very high affinity for hydrogen isotopes, one of the techniques considered for removing tritium from Li is to use yttrium, which has a greater affinity for the hydrogen isotopes than Li[239]. Various experimental studies have been carried out on the lithium-yttrium-tritium system[195,240,241]. Talbot et al.[195] have shown that the mass transfer rate will depend on the nature of the yttrium surface. With an yttrium surface area to lithium volume ratio of 0.9 cm^{-1} and at a temperature of 400°C , the concentration of tritium in stagnant lithium was reduced by a factor of 2 in 50 minutes. The mass transfer rate would likely increase with forced convection. A sponge form of the metal with a high surface area is recommended[241] to achieve optimum extraction.

Equilibrium pressure data[230] at 200°C suggest that the minimum achievable atomic tritium concentration in lithium would be less than $0.25 \mu\text{g/g}$ using yttrium as a getter. If operated as high as 450°C , $1 \mu\text{g/g}$ tritium in lithium could be maintained[8]. A practical recovery system described by Buxbaum and Johnson[230], would have three identical getter systems, one in operation, one being regenerated, and one on standby. The mass of yttrium required to extract a daily production of 0.5 kg of tritium is about 15 kg. During regeneration, the yttrium would be heated to 1000°C and the tritium gas released passed through niobium walls to a vacuum jacket where it would be cryopumped away and stored. This process has not yet been demonstrated.

Basic experimental data on thermodynamic and transport properties is still lacking, as is information on the effect of impurities on the long-term gettering capability of yttrium. Oxygen and nitrogen impurities can deactivate the surface, and also result in spalling and a loss of mechanical integrity[242]. And, as has been argued in Section 4.3.7, gettering may

introduce undesirable impurities into the lithium. The mechanical stability of the yttrium under thermal and tritium loading cycles also requires investigation. The final system design must provide effective removal of tritium from lithium during normal operation and from the yttrium during recovery, and function repetitively for a reasonable lifetime.

A ^{17}Li -83Pb-yttrium-tritium system has also been considered. Because of the higher tritium pressure over ^{17}Li -83Pb compared to lithium, it would be easier to recover tritium from the ^{17}Li -83Pb. However, both the BCSS[8] and the DEMO study[23] rejected the concept of direct contact of yttrium with ^{17}Li -83Pb because of formation of the Y-Pb alloy and impurities (O, N) from the recovery system reacting with the liquid metal. The BCSS recommends indirect contact of the ^{17}Li -83Pb with yttrium. Tritium, which has permeated into a secondary volume surrounding the blanket, could then be recovered by an yttrium getter bed.

4.4.2.3 Cold-Trapping

A cold trap is a cool section of a liquid metal loop where metal hydride (or tritide) forms as a solid precipitate in a packed bed[8]. Natesan and Smith[245] first examined the effectiveness of cold trapping secondary metals to remove tritium from liquid Li using thermodynamic calculations. Details of the thermodynamic considerations are given in reference [245]. More recently, both the DEMO study[23] and the BCSS[8] evaluated cold-trapping to remove tritium from liquid Li and ^{17}Li -83Pb. A primary cold trap, which is part of the liquid metal going through the blanket, would not be effective in removing tritium to ~ 0.5 kg (reference [8] calculates an inventory of ~ 100 kg in a STARFIRE reference blanket) in a Li blanket. If secondary cold-trapping were used, where the cold trap is part of a secondary metal loop (e.g. Na) into which tritium permeates, a large inventory in the Li would remain, although it would be reduced from that of a Li primary cold trap[8].

Both techniques would maintain a low tritium inventory in ^{17}Li -83Pb; however, for the primary cold-trapping technique, more information is required on tritide solubility in ^{17}Li -83Pb at the temperatures of interest (508-708 K)[8].

If secondary cold-trapping is used, high permeation and processing rates will be required to maintain 1 Pa tritium above the $^{17}\text{Li}-\text{Pb}$ blanket. An analysis in the DEMO study[23] (Section 2.3.3) of a $^{17}\text{Li}-\text{Pb}$ blanket (6×10^6 kg) and cold-trapping (388 K) of the sodium coolant concludes that the tritium partial pressure in sodium could be maintained at 10^{-3} Pa and in the $^{17}\text{Li}-\text{Pb}$ blanket at 1 Pa with a flow rate of 40 kg/s and vanadium alloy as the structural material.

4.4.2.4 Permeation

Permeation of tritium from the liquid metal blanket through a highly permeable metal or alloy, for example niobium or vanadium, has been evaluated as a potential recovery technique[211,23,8,233]. The blanket may be in stagnant contact with the permeation material or continuously circulated to a processing unit outside the main blanket area. The metal or alloy must have sufficiently high permeability to tritium and mechanical strength that the total required surface area and metal thickness be of reasonable size[23]. The effect of temperature, tritium pressure and structural material on permeation is shown in Figure 4-4 for the candidate structural materials (taken from reference [8]). Corrosion and contamination of the surface by impurities to reduce permeation are also a concern. Vanadium reacts readily with oxygen resulting in a surface oxide and a thousand-fold reduction in permeability[243]. After permeating, the tritium may be collected by solid metal getters, gas purging or cold-trapping of secondary liquid metal.

Because of the much higher equilibrium tritium pressure for liquid $^{17}\text{Li}-\text{Pb}$ than Li, the technique may be more effectively used to recover tritium from the alloy. The driving force for permeation is dependent on the tritium pressure differential between the two sides of the permeation material. The BCSS[8] concluded that direct permeation of tritium from a Li blanket into the plasma vacuum chamber of a STARFIRE design would not maintain the required tritium inventory because of the relatively high pressure, 0.012 Pa, in the vacuum chamber. For $^{17}\text{Li}-\text{Pb}$, vanadium is recommended as the structural material because of low corrosion at operating temperatures (Section 4.3). Because of high tritium permeation through vanadium, the tritium recovery

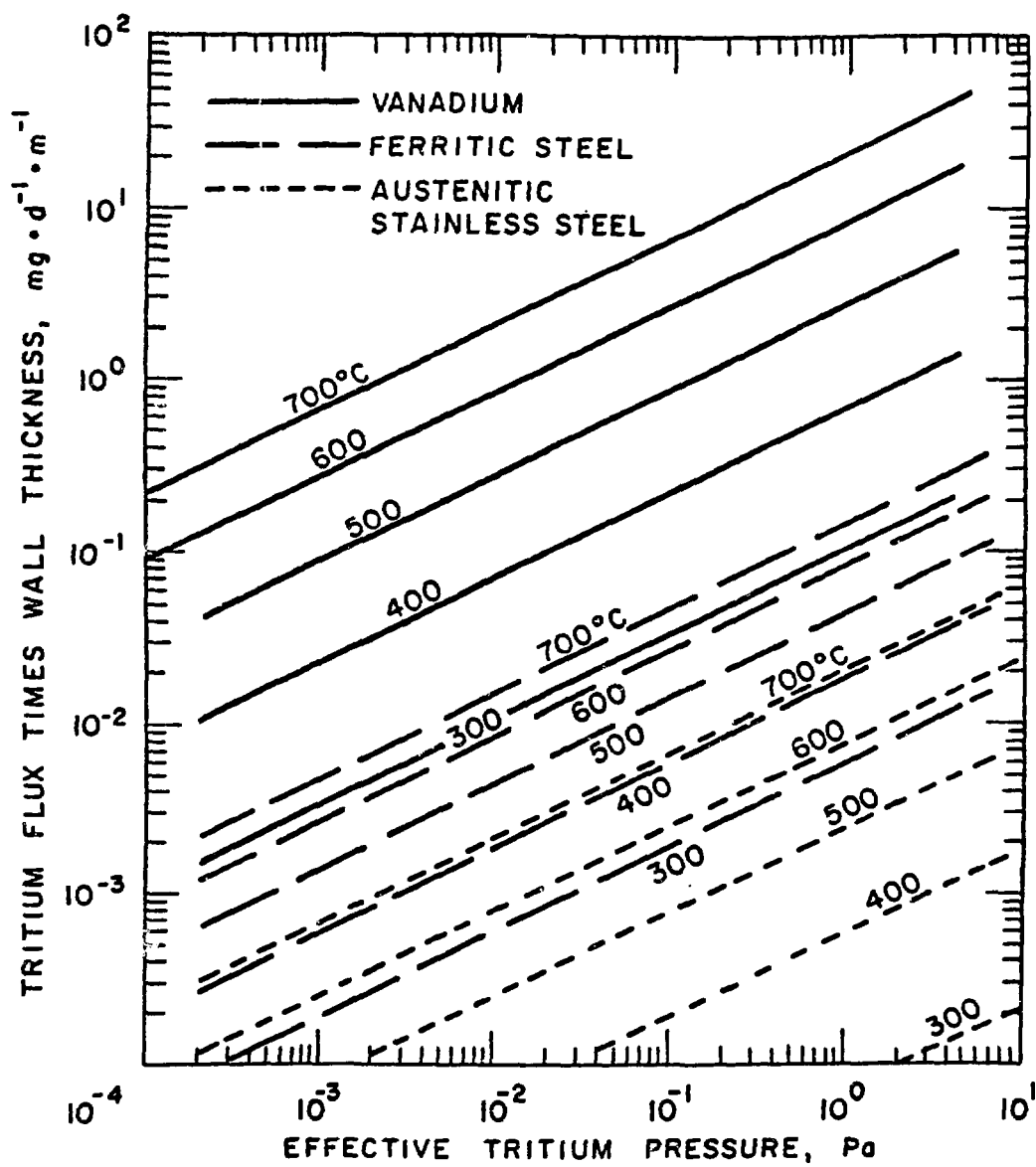


Figure 4-4 The effect of temperature, tritium pressure, and structural material on the tritium flux (mass flow rate per unit area) times the wall thickness (from [8]).

techniques rely on permeation, and are not in direct contact with the $^{17}\text{Li}-83\text{Pb}$ for reasons mentioned previously.

No experimental work has been done on tritium recovery by permeation; however, the technique has been evaluated for reactor designs using hydrogen (tritium) permeation data[8,23]. The permeation material will be required to be compatible with the breeder material and any secondary loop material, and be resistant to surface contamination, which will affect tritium permeation.

4.4.2.5 Inert Gas Sparging

In the proposed scheme of inert gas sparging, a finely dispersed stream of inert gas (helium) bubbles is passed through the liquid metal in a processing unit external to the reactor. This will enhance the mass transfer of tritium compared to direct pumping (Section 4.4.2.6). The tritium may then be recovered from the He stream. Because of the very low tritium partial pressure above liquid lithium, a large volume of sparge gas will be required to process a Li blanket. The tritium partial pressure is much higher for $^{17}\text{Li}-83\text{Pb}$ resulting in more efficient tritium extraction; however, extraction efficiency and processing rates will have to be sufficient to maintain the 1.0 Pa tritium pressure limit[23]. Casini[131] has estimated the required flow rate of helium, containing about 40 $\mu\text{g/g}$ tritium, to be $\sim 7200 \text{ m}^3/\text{d}$ for a $^{17}\text{Li}-83\text{Pb}$ blanket in an INTOR design[34] to achieve a suitable tritium inventory (i.e. $\sim 100 \text{ g}$). The DEMO study[23] estimates a flow rate of 330 kg/s would be required to maintain 1 Pa above the $^{17}\text{Li}-83\text{Pb}$ blanket, assuming > 90% extraction efficiency. No conductance losses were assumed in the calculations.

Few assessments of this option have been made and only preliminary experimental data has been obtained. At JRC-Ispra, a pilot plant facility is being constructed to demonstrate tritium extraction by this method[236]. This recovery method has also been assessed for the MARS design[244].

4.4.2.6 Direct Pumping

This removal scheme has been described by Pierini[236] to extract tritium by pumping on a blanket of liquid $^{17}\text{Li}-83\text{Pb}$. His calculations, using experimental diffusion coefficients and absorption rates, indicate that a tritium inventory of ~ 160 g could be maintained for an INTOR design $^{17}\text{Li}-83\text{Pb}$ blanket, if the liquid alloy is completely agitated. Because of the difficulty in agitating the entire blanket, the liquid would have to be pumped to a separate processing unit. The feasibility of such a scheme is being investigated further at JRC-Ispra.

4.5 Summary

Liquid Li has long been a contender as a circulating blanket material in D-T fusion reactor designs. It has excellent heat transfer properties and permits good thermodynamic efficiency and continuous extraction of tritium. Although there has been successful experience with liquid Li at moderate temperatures in small and medium-sized loops, it is clear that operation of large fusion systems at high temperatures will represent a considerable scale-up from present experience and will require the solution of some difficult materials problems. The most crucial issue for liquid Li is safety, because of its vigorous reactions with many materials. Its high solubility for tritium would cause an additional hazard in the event of a loss of containment. These safety problems with Li have shifted attention to the less reactive alloy $^{17}\text{Li}-83\text{Pb}$ as an alternative blanket/coolant material. Its lower solubility for tritium makes it attractive for both tritium extraction and safety, and its Pb component, which acts as a neutron multiplier, may in fact be necessary to achieve an acceptable TBR. Its disadvantages include corrosiveness on most structural materials, and its high freezing point and density, which would pose engineering problems. All liquid metal coolants will incur substantial MHD pressure losses, and although it may be possible to minimize these by careful design, a program to develop electrically non-conducting pipe will likely be necessary if liquid metals are to be circulated in regions of high magnetic fields.

5. SOLID BREEDERS

5.1 Introduction

Solid lithium compounds are the other main class of tritium breeding materials in addition to the liquid metals discussed in the previous chapter. These compounds include lithium oxide, lithium-lead and lithium-aluminum alloys, and the ternary ceramics, such as the lithium aluminates, silicates, zirconates and titanates. Solid candidate materials are lithium-lead and lithium-aluminum alloys, and the ternary ceramics, such as the lithium aluminates, silicates, zirconates and titanates. The solid lithium-lead and lithium-aluminum alloys have been rejected because of their unacceptably low melting temperatures. New candidates such as octalithium zirconate (Li_8ZrO_6) and lithium-beryllium oxides have been proposed, but still lack a credible data base. Therefore, only Li_2O and the earlier ternary ceramic candidates are reviewed here.

As we have seen in Chapter 2, several reactor studies such as STARFIRE, INTOR and DEMO have utilized solid breeders in their blanket designs. Solid breeders have also received considerable attention recently in comprehensive reviews, including those by Nygren[7], Bull et al.[246], Johnson and Hollenberg[247], Abdou[5], Gold et al.[9], and Johnson et al.[248]; the BCSS is currently addressing the viability of various concepts[8].

Solid breeders do not have the safety and corrosion problems inherent in liquid metal breeders but their use does involve a number of critical issues which are detailed in subsequent sections of this chapter (see also Table 2-2). These are as follows:

- tritium breeding ratio (TBR) - most of the ceramics will require a neutron multiplying material, such as beryllium or lead, to obtain an acceptable TBR. Li_2O and Li_8ZrO_6 are the only candidates which may not require a neutron multiplier - the need for a multiplier adds complexity and uncertainty to the blanket design;
- tritium inventory and recovery from the blanket;

- maintenance of the breeder within specified upper and lower temperature limits;
- radiation damage and in-reactor sintering;
- stability of Li₂O - residual moisture impurities from fabrication, or in the helium purge gas stream can decrease stability and increase vapourization of the Li₂O - this leads to mass transfer of the breeder material and corrosion of the cladding and structural materials.

Although a limited data base exists for the candidate materials, laboratory testing and irradiation experiments are providing information on the use of these materials as tritium breeding blankets.

5.2 Fabrication and Characterization

The last three years has seen a large growth of interest in lithium ceramic fabrication techniques. Purity control and techniques to produce uniform, well-characterized pellets in the large quantities that will be required for fusion reactors are the central issues. Fabrication programs are also being coordinated with irradiation testing to determine microstructures that will optimize in-reactor behaviour. Cold pressing followed by sintering, and hot pressing techniques have been employed successfully to produce pellets. Sol-gel techniques to produce microspheres are also being tested[249]. The most severe preparation problem in a large-scale operation, especially for Li₂O, is controlling the moisture content. In this section, techniques developed for powder and pellet production for the US irradiations, FUBR-1A[250,251] and TRIO-01[252] will be reviewed, followed by the US, French and Japanese efforts to produce large volumes of Li₂O pellets with uniform microstructures. Finally techniques used for pellet characterization will be briefly examined.

5.2.1 Lithium Ceramic Preparation for FUBR-1A

5.2.1.1 Powder Preparation

Argonne National Laboratories (ANL) developed techniques[250] for Li₂O and LiAlO₂ powder preparation, and McDonnell Douglas Astronautics Corporation (MDAC) did the same for Li₄SiO₄ and Li₂ZrO₃[251]. Figures 5-1, 5-2 and 5-3 show flow charts of these powder preparation techniques. The starting material for ANL was lithium carbonate (Li₂CO₃), which is the usual form for purchasing enriched lithium. To prepare Li₂O, the Li₂CO₃ was melted rapidly (~ 2 min) in a covered platinum crucible, and then further rapidly heated (~ 2 min) to 950°C. The Li₂CO₃ thermally decomposed, evolving CO₂ gas which was removed by maintaining a vacuum of less than 100 Pa in the furnace chamber. After 30 min the temperature was raised to 1050°C. The Li₂O yield was about 90% of the theoretical maximum, and less than 10 ppm Pt from the crucible had been incorporated. This high temperature, short duration calcination minimized crucible corrosion and maximized yield and purity.

Two successful methods were employed by ANL for LiAlO₂ preparation, both requiring an intimate mixing of Li₂CO₃ and Al₂O₃ in strict stoichiometric proportions, followed by heating to decompose the mixture to LiAlO₂ and CO₂. Figure 5-2 shows the processes in flow chart form. The first method began with ball milling mixed powders of Al₂O₃ (< 0.02 µm grain size) and Li₂CO₃ in methanol, and was followed by centrifuging and drying. The second technique was to spray dry mixed slurries of Li₂CO₃ and Al₂O₃. Both methods required calcination at 650°C. Inert hardware could be used for the ternary ceramics, for example Al₂O₃ crucibles for LiAlO₂ or SiO₂ for Li₂SiO₃ making calcination easier than with Li₂O which required Pt crucibles. When sintered at 1000-1100°C, γ-phase LiAlO₂ was obtained, free of α phase, with density 60-80% of the theoretical density (T.D.), i.e. 20-30% porosity.

For production of Li₄SiO₄ and Li₂ZrO₃, MDAC found that calcination of Li₂CO₃ in a platinum crucible led either to stoichiometry problems or contamination from the ball grinding media. An alternate organometallic process was developed, leading to the following procedure (see Figure 5-3 for a flow sheet):

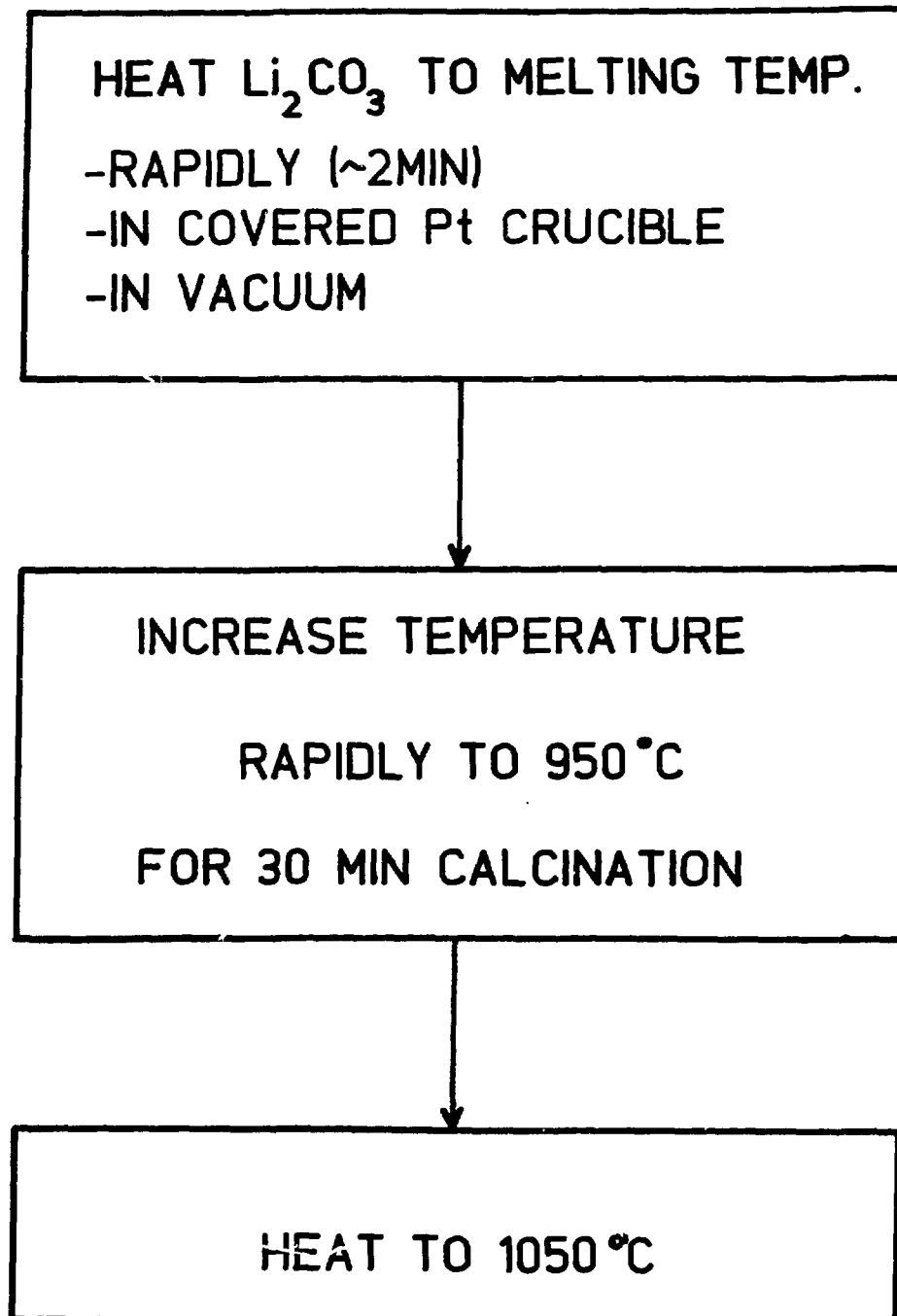


Figure 5-1 Li_2O powder preparation process developed by ANL[250]

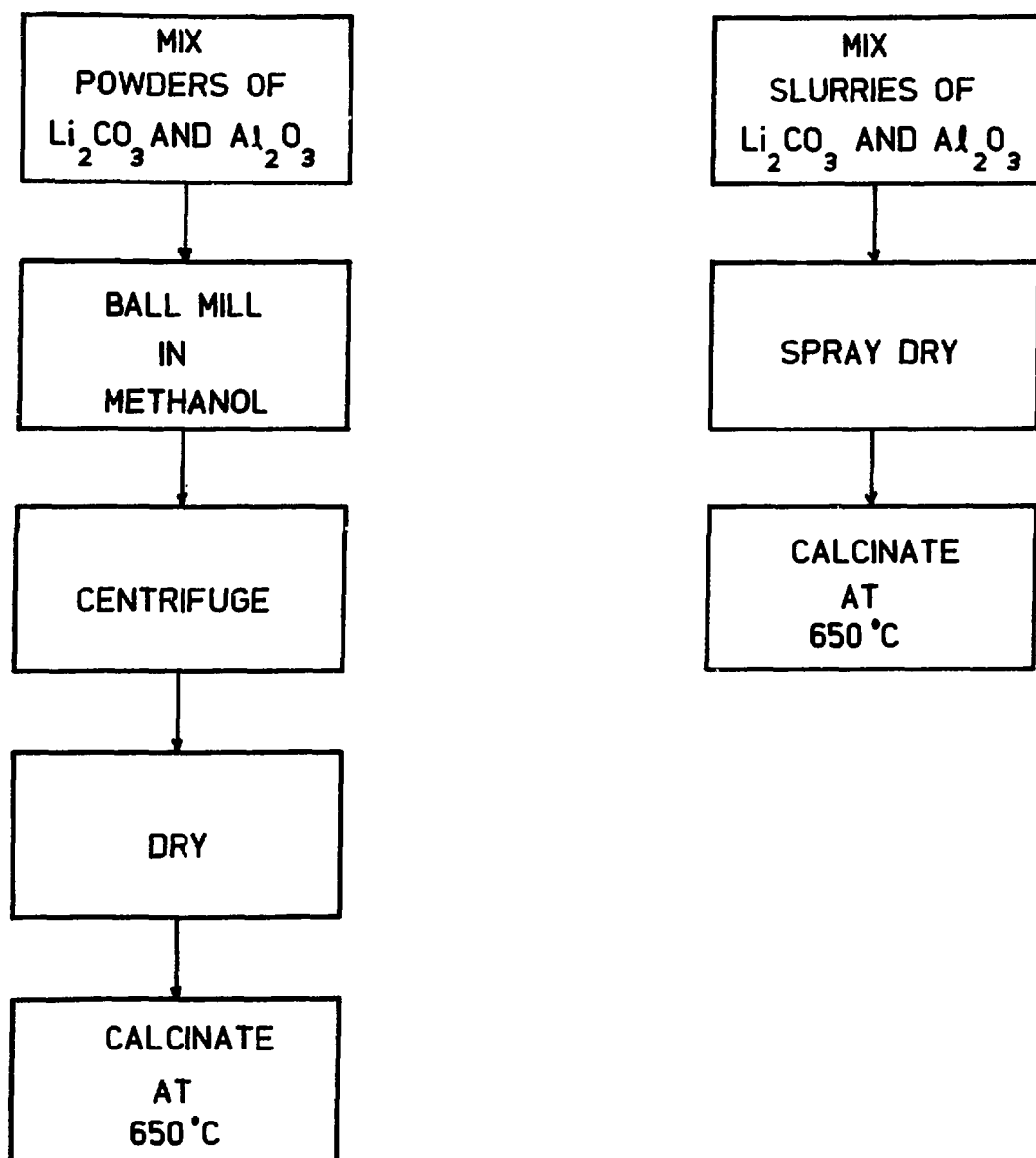


Figure 5-2 Two methods of powder fabrication of LiAlO_2 developed by ANL[250]

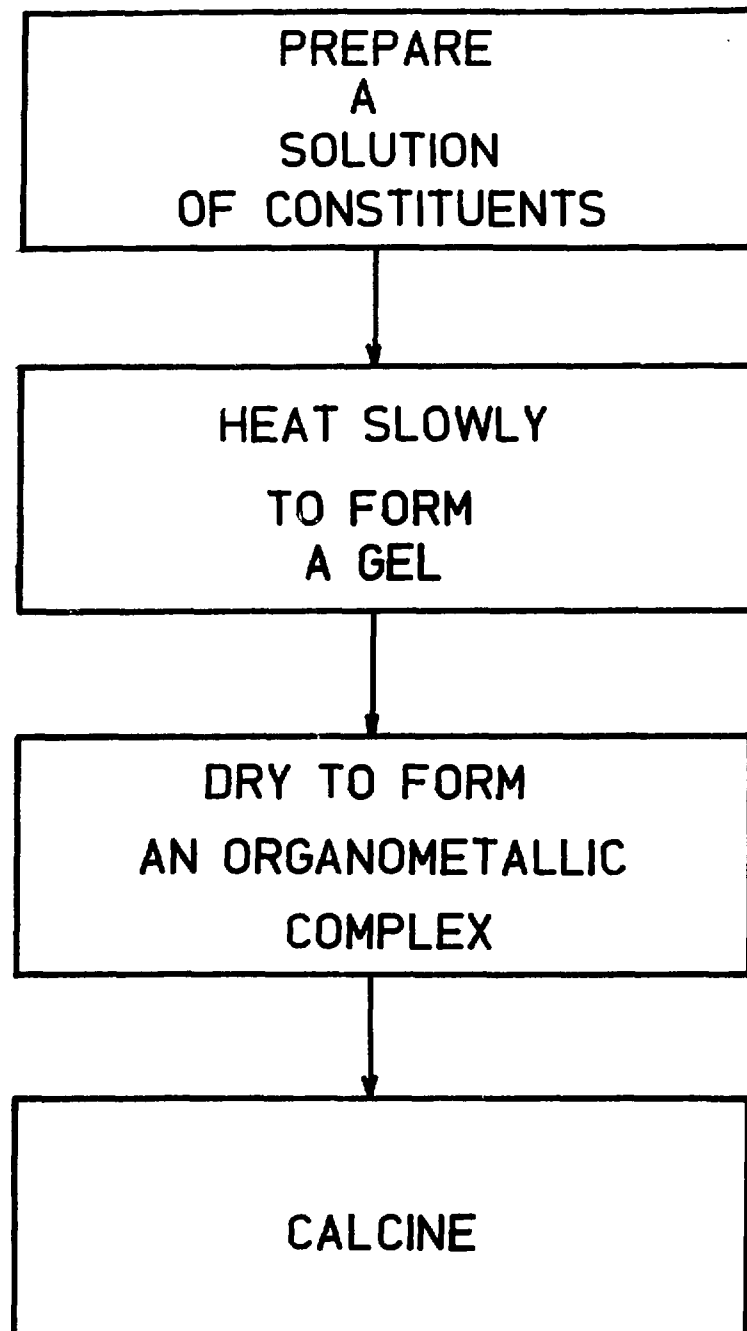


Figure 5-3 Organometallic process used to prepare Li_4SiO_4 and Li_2ZrO_3 powders by McDonnell Douglas[25]. Solution constituents were different for the two powders.

- prepare a solution of the constituents (different solutions of various chemicals were used for the silicate and the zirconate, but the starting form of the lithium was still Li_2CO_3),
- heat slowly to form a gel,
- dry to form an organometallic complex, and
- calcine to form the powder.

After calcining, the powders were cooled under vacuum and stored under inert gas, since both powders are hygroscopic. Sub-micron high purity powders were obtained.

5.2.1.2 Pellet Formation

Hot pressing was used in preference to cold pressing and sintering by Wilson[253] at Hanford Engineering Development Laboratory to obtain smaller grain sizes in the pellets. This occurs because lower operating temperatures can be used in the hot pressing method. The powders of Li_2O , LiAlO_2 , Li_4SiO_4 , and Li_2ZrO_3 were stored in vacuum, handled in inert atmospheres, and vacuum annealed at 750°C to remove volatiles prior to hot pressing.

Additional vacuum annealing procedures were developed for each powder type to remove excess volatiles. Care was required because overheating the powder at this stage resulted in pellets of low strength. Sieving was followed by hot pressing at temperatures between 700°C and 1200°C for times between 35 and 50 minutes. The goals of uniform densities and fine grain sizes ($< 1 \mu\text{m}$) were not completely attained: uniform densities of 85% T.D. were achieved, but average grain sizes for LiAlO_2 , Li_2ZrO_3 , and Li_2O were 1, 2, and $6 \mu\text{m}$, respectively. The Li_4SiO_4 grain size was bimodal ($2 \mu\text{m}$ and $20 \mu\text{m}$ averages). Li_2O , with the highest lithium content of the four materials, was the most difficult to handle to avoid moisture contamination, and a compromise between micro-structural and dimensional thermal stability, grain size, and moisture content had to be accepted.

5.2.2 Lithium Ceramic Fabrication for TRIO-01

ANL[252] fabricated γ -LiAlO₂ pellets for the TRIO-01 experiment with a bimodal pore structure to improve gas release. The ceramic was 60–65% of the theoretical density, composed of an agglomeration of particles of size 50–100 μm . The particles themselves were porous with a grain size of 0.1–0.2 μm , and this accounted for the biomodal pore structure. The pellets were cylindrical, with a length of 8.89 cm, a diameter of 2.54 cm, and a central hole diameter of 1.58 cm.

5.2.3 Mass Production of Li₂O Pellets

5.2.3.1 Japan

Kawasaki Heavy Industries began a program in 1982 to develop mass production techniques to produce sintered Li₂O pebbles, i.e. small spheres[254,255]. To reduce the content of the major impurities, LiOH and Li₂CO₃, the powder was preannealed at 700°C, which is above their decomposition temperatures, in a dynamic vacuum (< 100 Pa). Cold pressing was followed by sintering between 1000 and 1200°C, also in vacuum (< 100 Pa). Reported values for LiOH and Li₂CO₃ content in the pellets is "less than 2%".

5.2.3.2 France

Commissariat à L'Énergie Atomique (CEA) at Saclay, France, has been investigating techniques[249] for the large scale production of lithium aluminates, LiAlO₂ and LiAl₅O₈, along the lines they successfully developed for the production of thousands of tons of alumina with uniform properties for gaseous diffusion uranium enrichment. The techniques they are studying are described briefly below:

- thermal decomposition of aqueous solutions of salts to produce powders, which are then pressed and sintered;

- dry mixing of aluminum and lithium salts followed by one of the two sequences, compression/decomposition/sintering or decomposition/compression/sintering;
- making a paste of aluminum compounds and lithium salts, and then drying, decomposing, and sintering;
- soaking a porous alumina with a lithium salt solution, and then heating to dry the mixture and to induce a phase change to produce an aluminum-lithium ceramic.

Mechanical strength, grain size, and pore size distribution are properties that were measured and controlled. Uniform pore sizes from 0.04 to 40 μm and total porosity from 5 to 50% have been produced. Furthermore, they have produced samples by the third technique above, with a bimodal pore size distribution (total porosity 14%) designed to facilitate tritium removal.

5.2.3.3 USA

A lithium blanket module (LBM) has been designed[110,112,286] for testing in the Tokamak Fusion Test Reactor (TFTR) at Princeton, NJ, beginning in 1985 (see Section 3.3.5). Detailed procedures for cold pressing and vacuum sintering 30 000 Li_2O pellets (2.54 cm diameter by 2.54 cm long, 80% T.D.) have been demonstrated. Parameters studied included pressing pressure, sintering temperature and time, effects of handling sintered pellets in air, and particle size effects on powder flow and pellet densification.

5.2.4 Characterization

Generally, characterization techniques used in the study of lithium ceramic powders and pellets are similar to those used in other areas of ceramics. Phase identification and phase purity tests can be performed with X-rays. Emission spectrophotometry and X-rays are used for measurement of chemical impurities, the former especially for metallic impurities. Powder size distributions are obtained by X-ray monitored sedimentation techniques

(Sedigraph 5000, made by Micromeritics), scanning electron microscopes, or calibrated sieves. Surface area measurements can be made by the BET gas adsorption technique, in particular, by krypton or nitrogen adsorption at -196°C. Total pellet porosity is simply determined by weight and volume measurements to obtain the density. To measure the closed porosity, an immersion density measurement technique was reported by Naruse et al.[255]. The specimens were degassed in vacuum for 1 h and then immersed in liquid paraffin which has a low viscosity. The paraffin penetrated the interconnected open porosity, and a new density measurement yielded the fraction of the porosity which is closed.

Arons et al.[250] at ANL developed a technique to estimate the LiOH content in Li₂O. Ultrapure He was passed over the Li₂O at a set temperature or series of temperatures. The water that vapourized into the helium stream was monitored continuously with an electrolytic type (P₂O₅) hygrometer. The measurements were then integrated to get the total quantity of water evolved and used to estimate the original LiOH content (at room temperature H₂O and Li₂O combine to form LiOH). Pellets of Li₂O prepared, with maximum glove box use, by ANL from enriched Li₂CO₃ (as described in Section 5.2.1.1) contained 0.5 wt% LiOH. Other samples of powders and pellets from various sources contained 1.8 to 6.9 wt% LiOH.

Ortmann and Larsen[287] described accurate chemical analysis techniques for the measurement of LiOH and Li₂CO₃ in lithium oxide. They also used a neutron activation analysis to measure metal ion impurity concentrations. These techniques were used to analyze high purity powders that they prepared by thermal decomposition of lithium peroxide for the accurate determination of Li₂O melting temperature. Their specimens ranged from 99.8 to 100.0% Li₂O. Maximum lithium hydroxide concentration was 0.20%, and maximum carbonate concentration was 0.02%. Sodium and manganese metal impurities were detected, but at levels below 0.002%. These Li₂O powders are purer by more than a factor of 10 than those produced by the techniques described earlier in this section.

5.3 Physical and Chemical Properties

Many of the fundamental physical and chemical properties for several of the lithium ceramics have been measured in recent years, primarily in Japan, US, and West Germany (FRG). Table 5-1, reproduced from P. Bull. et al.[246], summarizes this data, and shows gaps in the knowledge. Particularly scarce are mechanical properties data, for example, yield strengths, and ductile-brittle transition temperatures. Also, the influence of microstructures on these properties is not well understood.

The information in Table 5-1 and in the remainder of this section shows several interesting correlations between the physical properties and the lithium density in these ceramics. The following properties correlate approximately with increasing lithium density:

- susceptibility to moisture, i.e. absorption and reaction with water; this also causes higher corrosion with the cladding and other structural materials (Section 5.3.4);
- tritium breeding ratio.

The following properties correlate with decreasing lithium density:

- melting temperature;
- thermal stability (Section 5.3.2);
- ease in fabrication of pellets with desired small grains (Section 5.2.1.2).

Thus, the high lithium density materials, such as Li_2O , have the best tritium breeding ability, but also are the most susceptible to thermal decomposition, and attack from moisture with its associated corrosion problems. In addition, although no correlations with lithium density are apparent, Li_2O has the best thermal conductivity, but the most problems with irradiation-induced swelling.

Table 5-1 Data on Breeding Materials: Physico-Chemical Properties, Neutronic Properties, Tritium Breeding and Extraction, Irradiation, Activation Products (from [246])

	Li_2O
(01) Density	2.01
(02) Li content ($\text{g}\cdot\text{cm}^{-3}$)	0.93
(03) Melting point ($^{\circ}\text{C}$)	1430 ^c
(04) Thermal conductivity ($\text{W}\cdot\text{m}^{-1}\cdot\text{K}^{-1}$)	≈3
(05) Vapour pressure	Significant vapour pressure above 1200° (sublimed) volatility increases with H_2O content
(06) Air reactivity (high temperature)	Reactive
(07) Water reactivity ΔH ($\text{kJ}\cdot[\text{mol Li}]^{-1}$ at 25°C)	Reactive → LiOH (-64)
(08) Compatibility with structure materials	Corrosion of: 316 SS : 550° Incoloy 800 : 500° Inconel 600 : 600° HT 9 : 600°
(09) H_2 , D_2 , T_2 solubility	Very low
(10) Sievert's constant ($\text{torr}^{1/2}$)	2.7×10^5 at 600°
(11) T_2 diffusion coefficient ($\text{cm}^2\cdot\text{s}^{-1}$)	$\approx 8 \times 10^{-8}$ at 600°
(12) Useful operational interval	$410^{\circ}\text{-}1000^{\circ}$ $460^{\circ}\text{-}910^{\circ}$ $410^{\circ}\text{-}660^{\circ}$ } (1)
(13) Tritium breeding potential	Good with Pb 10 cm: 1.6
(14) Extraction method and Principal species obtained	He sweeping 600° Vacuum 600° T_2O , HTO
(15) Irradiation behaviour	Stoichiometric change after $2 \times 10^{25} \text{n}\cdot\text{m}^{-2}$ at 750° first sintering at 850° closed pores
(16) Activation products (s: second, min: minute, h: hour, d: day, b: barn)	$\text{O}(\text{n},\text{p})$ 7 s $\text{O}(\text{n},2\text{n})$ 2 min

(1) ANL estimations, (2) INTOR Phase-2 estimations.

Table 5-1 Data on Breeding Materials: Physico-Chemical Properties, Neutronic Properties, Tritium Breeding and Extraction, Irradiation, Activation Products (from [246]) (continued)

LiAlO_2	Li_5AlO_4	LiAl_5O_8
(01) α : 3.4 γ : 2.6	α : 2.25 β : 2.22	3.6
(02) α : 0.36 γ : 0.27	β : 0.6!	0.09
(03) 1610°	1047°	1950°
(04) γ : $\approx 1.5 - 3$		
(05) Vapour pressure at 1400°C	Vapour pressure at about 1000°C	Negligible vapour pressure up to $1400 - 1700^\circ$
(06) Hygroscopic		
(07) Weak reaction, hot soluble (63)		No reaction, insoluble
(08) Weak corrosion at 600° of: 316 SS HT 9 Inconel Ti 6242		
(09) Low	Low	Low
(10)		
(11) $\approx 3 \times 10^{-9}$ at 600°	$\approx 10^{-8}$ at 600°	
(12) $500^\circ - 1000^\circ$ } (1) $550^\circ - 850^\circ$ } (2) $500^\circ - 850^\circ$ } (2)		
(13) Neutron multiplier required with Pb 10 cm: 1.38	1.193 with Pb 10 cm: 1.43	Low: 0.773 with Pb 10 cm: 1.278
(14) He sweeping 650° T_2O , HTO	600° (easier than Li_2O extraction)	
(15) Stoichiometric change after $2 \times 10^{25} \text{ n} \cdot \text{m}^{-2}$ at $850^\circ - 1000^\circ$, microstructure intact, bad mechanical integrity	Stoichiometric change	Stoichiometric change
(16) O (n,p), 7 s O (n,2n), 2 min ^{27}Al (n,2n) ^{26}Al , 6 s 7.2×10^5 years, 0.02 b (n,p) ^{27}Mg , 9.46 min, 0.08 b (n, α) ^{24}Na , 15 h, 0.124 b	O (n,p), 7 s O (n,2n), 2 min ^{27}Al (n,2n) ^{26}Al , 6 s 7.2×10^5 years, 0.02 b (n,p) ^{27}Mg , 9.46 min, 0.08 b (n, α) ^{24}Na , 15 h, 0.124 b	O (n,p), 7 s O (n,2n), 2 min ^{27}Al (n,2n) ^{26}Al , 6 s 7.2×10^5 years, 0.02 b (n,p) ^{27}Mg , 9.46 min, 0.08 b (n, α) ^{24}Na , 15 h, 0.124 b

Table 5-1 Data on Breeding Materials: Physico-Chemical Properties, Neutronic Properties, Tritium Breeding and Extraction, Irradiation, Activation Products (from [246]) (continued)

	Li_2SiO_3
(01) Density	2.52
(02) Li content ($\text{g}\cdot\text{cm}^{-3}$)	0.36
(03) Melting point ($^{\circ}\text{C}$)	1200 $^{\circ}$
(04) Thermal conductivity ($\text{W}\cdot\text{m}^{-1}\cdot\text{K}^{-1}$)	1.5–3
(05) Vapour pressure	Reduced solidus (1030°) if non-stoichiometric
(06) Air reactivity (high temperature)	Hygroscopic
(07) Water reactivity ΔH ($\text{kJ}\cdot[\text{mol Li}]^{-1}$ at 25°C)	Weak reaction, soluble in hot water
(08) Compatibility with structure materials	Weak corrosion at 600° of: SS 316 HT 9 Ti 6242
(09) H_2 , D_2 , T_2 solubility	Low
(10) Sievert's constant ($\text{torr}^{1/2}$)	$\approx 10^{-9}$ at 600°
(11) T_2 diffusion coefficient ($\text{cm}^2\cdot\text{s}^{-1}$)	$420^{\circ}\text{--}900^{\circ}$ } (1) $470^{\circ}\text{--}610^{\circ}$ } (2) $420^{\circ}\text{--}610^{\circ}$ } (2)
(12) Useful operational interval	
(13) Tritium breeding potential	Neutron multiplier required with Pb 10 cm: 1.42
(14) Extraction method and Principal species obtained	He sweeping (easier than LiAlO_2 extraction) T_2O , HTO
(15) Irradiation behaviour	Stoichiometric change Glass formation
(16) Activation products (s: second, min: minute, h: hour, d: day, b: barn)	$\text{O}(\text{n},\text{p})$, 7 s $\text{O}(\text{n},2\text{n})$, 2 min 92.23% ^{28}Si ($\text{n},2\text{n}$) ^{27}Si , 4 s (n,p) ^{28}Al , 2.24 min (n,α) ^{25}Mg , stable 4.67% ^{29}Si (n,p) ^{29}Al , 6 min 3.10% ^{30}Si (n,α) ^{27}Mg , 9 min

(1) ANL estimations, (2) INTOR Phase-2 estimations.

Table 5-1 Data on Breeding Materials: Physico-Chemical Properties, Neutronic Properties, Tritium Breeding and Extraction, Irradiation, Activation Products (from [246]) (continued)

Li_4SiO_4	Li_2TiO_3	Li_2ZrO_3
(01) 2.28	2.6	4.15
(02) 0.54	0.33	0.33
(03) 1250°	1950°	1615°
(04) 1.5-3	2	≈0.9
(05) Vapour pressure ≈1250°		Low vapour pressure
(06)		
(07)		
(08)	Very weak corrosion at 600° of: HT 9 316 SS + Ni	Very weak corrosion at 600° of: HT 9 316 SS + Ni
(09)		
(10)		
(11) $\approx 10^{-9}$ at 600°		
(12) 420°-640° (2)	410°-820° (2)	500°-860° (2)
(13) Neutron multiplier required with Pb 10 cm: 1.10 with Pb 10 cm: 1.492	1.049 with Pb 10 cm: 1.382	Zr is neutron multiplier 1.085
(14) 550°-750° under vacuum	He sweeping (extraction comparable to Li_2O) HTO, HT	He sweeping (extraction comparable to LiAlO_2) HTO, HT
(15) Stoichiometric change $2 \times 10^{25} \text{ n} \cdot \text{m}^{-2}$ 750° first sintering	Stoichiometric change	Stoichiometric change
(16) O (n,p), 7 s O (n,2n), 2 min 92.23% ^{28}Si (n,2n) ^{27}Si , 4 s (n,p) ^{28}Al , 2.24 min (n,α) ^{25}Mg , stable 4.67% ^{29}Si (n,p) ^{29}Al , 6 min 3.10% ^{30}Si (n,α) ^{27}Mg , 9 min	O (n,p), 7 s O (n,2n), 2 min 8.27% ^{46}Ti (n,p) ^{46}Sc , 84 d β, γ , 1 MeV, 0.24 b (n,2n) ^{45}Ti , 3 h, 0.18 b 7.4% ^{47}Ti (n,p) ^{47}Sc , 3.4 d, 0.18 b 73.7% ^{48}Ti (n,p) ^{48}Sc , 1.8 d, 0.06 h (n,α) ^{45}Ca , 153 d, 0.001 h	O (n,p), 7 s O (n,2n), 2 min 51.5% ^{90}Zr (n,p), 64 h, 0.25 b (n,2n) 80 h, 0.5 b 11.2% ^{91}Zr (n,p), 57 d, 0.08 b 17.1% ^{92}Zr 17.9% ^{94}Zr (n, 2n), 1.5×10^6 years 2.8% ^{96}Zr (n,2n), 64 d, 0.6 b

Table 5-1 Data on Breeding Materials: Physico-Chemical Properties, Neutronic Properties, Tritium Breeding and Extraction, Irradiation, Activation Products (from [246]) (continued)

	Li	$\text{Li}_{17}\text{Pb}_{83}$
(01) Density	0.48 at 500°C	9.4 at 240°C
(02) Li content ($\text{g} \cdot \text{cm}^{-3}$)	0.48	0.064
(03) Melting point (°C)	180°	234.7°
(04) Thermal conductivity ($\text{W} \cdot \text{m}^{-1} \cdot \text{K}^{-1}$)	50	≈16
(05) Vapour pressure	Significant vapour pressure above 600°	
(06) Air reactivity (high temperature)	Very reactive	Weak reaction
(07) Water reactivity ΔH ($\text{kJ} \cdot [\text{mol Li}]^{-1}$ at 25°C)	Very reactive → $\text{LiOH} + \text{H}_2(-245)$	Weak reaction (-198)
(08) Compatibility with structure materials	Corrosion of austenitic > 450°C ferritic > 550°C Ti alloys > 500°C V, Ni alloys 700°C	At 400°C no corrosion of austenitic but <i>fragilization under constraint</i> . 450°C corrosion
(09) H_2 , D_2 , T_2 solubility	Very high	Very low
(10) Sievert's constant ($\text{torr}^{1/2}$)	8 at 500°	3.4×10^5 at 400° - 600°
(11) T_2 diffusion coefficient ($\text{cm}^2 \cdot \text{s}$)		
(12) Useful operational interval	250° - 500° (1)	
(13) Tritium breeding potential	Good	Good
(14) Extraction method and Principal species obtained	1.75 Molten salt or getter or permeation T_2	1.48 Molten salt or getter or cold trap or pumping or inert gas bubbling, T_2
(15) Irradiation behaviour	Good	Good
(16) Activation products (s: second, min: minute, h: hour, d: day, b: barn)	No radioactivity besides that of T_2	1.42% ^{204}Pb ($n,2n$) ^{203}Pb , 2 d, 2 b 24.1% ^{206}Pb ($n,2n$) ^{205}Pb , 1.4 10^7 years, 2 b

(1) ANL estimations, (2) INTOR Phase-2 estimations.

Table 5-1 Data on Breeding Materials: Physico-Chemical Properties, Neutronic Properties, Tritium Breeding and Extraction, Irradiation, Activation Products (from [246]) (continued)

Li_7Pb_2	LiAl	$\text{LiAl alloys - Low Li content}$
(01) 4.59	1.76	≈ 2.7
(02) 0.49	0.36	0.075 for 3 w/o Li
(03) 726°	717°	$\approx 630^\circ$
(04) 17	30	≈ 80 for 1 w/o Li at 177°
(05) Reduced solidus if non-stoichiometric	$560^\circ : \log P_{\text{Li}} = -4.5$	$750^\circ : \text{Li loss by vaporization}$
(06) Very reactive	Reactive	Highly reactive for Li > 10 w/o
(07) Very reactive → $\text{LiOH} + \text{H}_2$ (-200)	Very reactive → $\text{LiOH} + \text{H}_2$ (-200)	Weak reaction for 1 w/o Li
(08)	Weak corrosion of s.a.p. ($\text{Al} + 5\% \text{Al}_2\text{O}_3$)	
(09) Low	Low	Medium
(10) 9.5×10^4 ; 500°	4×10^4 ; 500°	for 1.2 w/o Li $\approx 10^3$; 500°
(11) 5×10^{-7} ; 600°	4×10^{-7} ; 500°	1.5×10^{-6} ; 450°
(12) $320^\circ - 530^\circ$ $370^\circ - 390^\circ$ (1)	$300^\circ - 500^\circ$ (1) $350^\circ - 380^\circ$ (1)	$290^\circ - 330^\circ$
(13) Good 1.72	Neutron multiplier required with Pb 10 cm 1.43	Neutron multiplier required + ${}^6\text{Li}$ enrichment
(14) He or He + H ₂ sweeping, 450–500°	He or He + H ₂ sweeping, 500°, 1 h 750° pumping HT, HTO	for a 1 w/o Li alloy 1 h, 500°, vacuum HT, HTO
T ₁ , HT		
(15) Stoichiometric change Reduced solidus temperature, swelling after $2 \times 10^{25} \text{n} \cdot \text{m}^{-2}$ at 600°–1000° unchanged granules	Stoichiometric change Swelling? Bad mechanics	Stoichiometric change Swelling? Dislocations Bad mechanics
(16) 1.42% ${}^{204}\text{Pb}$ (n,2n) ${}^{203}\text{Pb}$, 2 d, 2 b 24.1% ${}^{206}\text{Pb}$ (n,2n) ${}^{205}\text{Pb}$ 1.4x10 ⁷ years, 2 b	${}^{27}\text{Al}$ (n,2n) ${}^{26}\text{Al}$, 6 s 7.2×10^5 years, 0.02 b (n,p) ${}^{27}\text{Mg}$, 9.46 min, 0.08 b (n, α) ${}^{24}\text{Na}$, 15 h, 0.124 b	${}^{27}\text{Al}$ (n,2n) ${}^{26}\text{Al}$, 6 s 7.2×10^5 years, 0.02 b (n,p) ${}^{27}\text{Mg}$, 9.46 min, 0.08 b (n, α) ${}^{24}\text{Na}$, 15 h, 0.124 b

5.3.1 Thermal Properties

Solid breeder properties such as thermal conductivity and thermal expansion coefficient affect the breeder's in-reactor performance, and strongly influence the design configuration. For a given configuration and nuclear heat deposition, the thermal conductivity determines the temperature gradients, and therefore the maximum temperature, in the solid breeder. However, high temperatures cause sintering and high vapour pressures, and large temperature gradients cause thermal expansion gradients, which produce stresses that can cause fractures. These blanket problems are described in more detail in Section 5.6.5. Both of these thermal properties, furthermore, may depend on the ceramic microstructure.

Hollenberg and Baker[256] measured the specific heats, thermal diffusivities, and thermal expansion coefficients as a function of temperature between 75 and 475°C for the ceramics manufactured for the FUBR-1A experiment (Section 5.2). They also calculated thermal conductivities, K, from the expression:

$$K = \alpha \rho c \quad (1)$$

where α = thermal diffusivity

ρ = measured density

c = specific heat

Figure 5-4 shows the specific heat capacity variation with temperature for LiAlO₂, Li₄SiO₄, Li₂ZrO₃. This data agrees satisfactorily with other measured values[257,258] also included on the figure. At high temperatures, the measured specific heat capacities (including that for Li₂O measured by Tanifugi et al.[259] - also shown in Figure 5-4) are in fair agreement with the rough theoretical prediction:

$$c = 3R/M.W. \quad (2)$$

where R is the gas constant and M.W. is the molecular weight. Thus, there is an inverse correlation between specific heat and molecular weight.

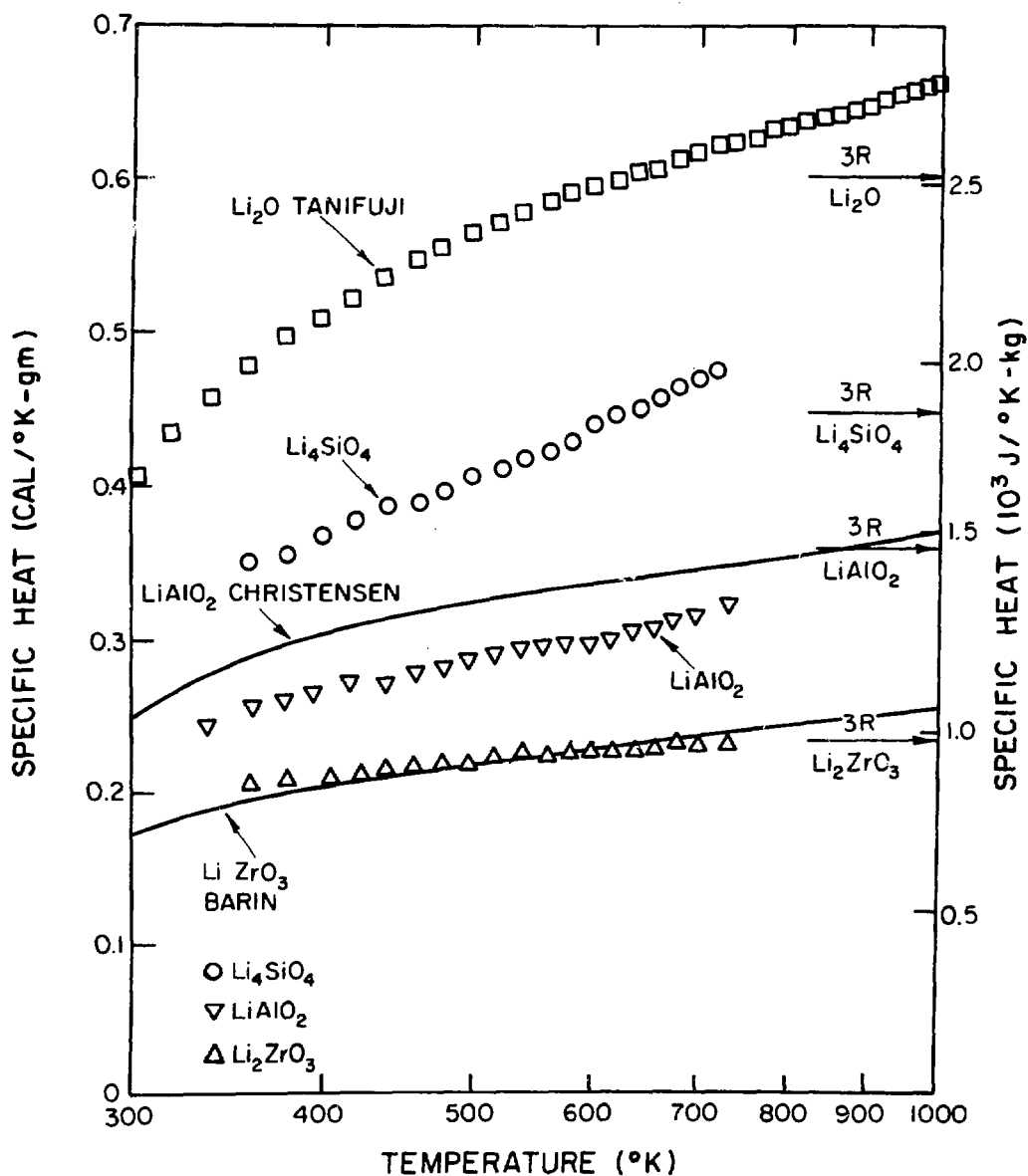


Figure 5-4 Specific heat capacities of lithium ceramic breeders (after Hollenberg and Baker[256]).

The thermal conductivities of these materials are shown in Figure 5-5 to decrease gradually over the measured temperature range. Agreement with previous measurements[260,261] is reasonable. Lithium oxide has the highest value, and therefore should have the lowest temperature gradients in a fusion blanket. Takahashi and Kikuchi[262] also showed that the thermal conductivity decreased with increasing porosity, as predicted by the Maxwell-Eucken relation. Besides equiaxed porosity, however, microcracks caused by stress buildup in the breeder can affect thermal conductivity. Depending on orientation, microcracks generally reduce the thermal conductivity; therefore additional experiments are needed on irradiated and cracked samples, representative of future fusion blankets.

As shown in Table 5-2, the thermal expansion coefficients for Li_2O and Li_4SiO_4 are both high, and increase by about 50% over the temperature range measured (100-800°C). The values for Li_2ZrO_3 and LiAlO_2 are smaller by about a factor of two, and are less temperature dependent. This is in good agreement with the values measured on single crystals and sintered specimens by Kurasawa et al.[263]. The high thermal expansion coefficients of Li_2O and Li_4SiO_4 , and low thermal conductivities of all the materials will have a negative impact on breeder performance. They will tend to cause steep temperature gradients, breeder fragmentation, and difficulty in operating the solid breeder within specified temperature limits (Sections 2.3.7 and 5.6.5).

5.3.2 Thermal Stability

All lithium ceramics exhibit a tendency to thermally decompose and vapourize at high temperatures. As a rough approximation, the higher the lithium density in the ceramic, the greater the tendency to decompose. This correlation holds well for lithium ceramics within a class, such as the aluminates or silicates, but is not strictly valid between classes. Lithium oxide exhibits the greatest tendency to decompose and, for the ceramics that have been tested, it appears to be the only one for which the problem may be significant, e.g.[246]. The new candidate, octalithium zirconate has not been tested, however; based on its high lithium density, stability could be a problem for it also. Moisture in Li_2O , or in the helium purge gas, exacerbates

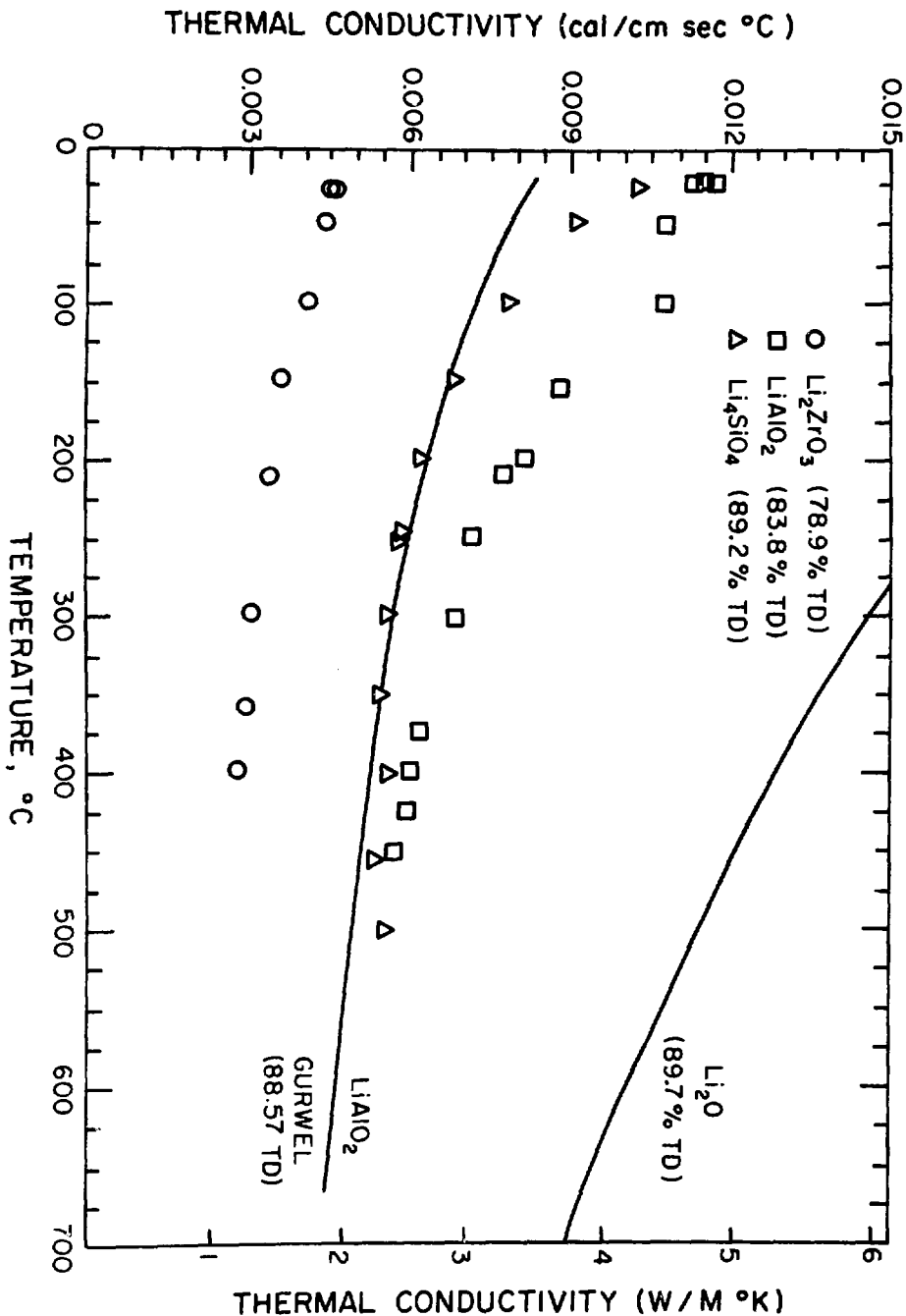


Figure 5-5 Thermal conductivity of lithium ceramic breeders (after Hollenberg and Baker[256])

**Table 5-2 Thermal Expansion Coefficient of Lithium Ceramics
(after Hollenberg and Baker[256])**

Material	Thermal Expansion Coefficient (10^{-6} cm/cm°C)
Li ₂ O	$20.75 + 1.72 \times 10^{-2}T$
Li ₄ SiO ₄	$18.80 + 1.66 \times 10^{-2}T$
Li ₂ ZrO ₃	$9.86 + 2.24 \times 10^{-4}T$
LiAlO ₂	$9.66 + 4.61 \times 10^{-3}T$

the stability problem by reacting with Li_2O to form LiOH which readily vapourizes. This can lead to pore closure, or mass transfer over long distances if carried by the helium purge stream.

Since lithium is the major gaseous species over all the solid breeders, its partial pressure can be used as a measure of the thermal stability. Vapour pressures at equilibrium over Li_2O have been measured[264-268] using effusion Knudsen cells combined with mass spectrometry. The major species identified are Li , O_2 , Li_2O , and small amounts of LiO , Li_2O_2 , Li_3O and Li_2 . Figure 5-6 shows the lithium gas pressure over Li_2O and three aluminates as a function of temperature. The temperature dependence of all the gases over the lithium ceramics is given approximately by $\exp(-Q/RT)$ where $Q = 160 \pm 15 \text{ KJ/mol K}$. The data of Ikeda et al.[267] on the aluminates, Nakagawa et al.[268] on lithium metasilicate and Guggi et al.[269] on Li_2O support this previously unreported correlation.

5.3.3 Operating Temperature Limits

The diffusion rate of tritium out of the ceramic solid increases with temperature, and as a consequence, the tritium inventory decreases. Based on post irradiation anneal experiments to measure tritium release, the BCSS study[8] estimated minimum temperatures to keep the inventory below $0.1 \text{ kgT/GW}_{\text{th}}$. Table 5-3 shows these values. At high temperatures, sintering becomes excessive, and the open porosity network closes, thus isolating the pores and inhibiting tritium permeation. Maximum temperatures established either experimentally from the onset of closed porosity in test specimens, or assuming a value of 0.8 of the melting temperature (K) for this occurrence are also shown in Table 5-3. An exception is the maximum temperature established for Li_2O which is based on limiting the LiOT content in the helium purge stream.

5.3.4 Compatibility with Structural Materials and Water Coolant

Compatibility tests are usually performed by sealing discs of the structural materials between discs of the ceramics in a tubular container and annealing at various temperatures for various lengths of time. Table 5-4 shows the

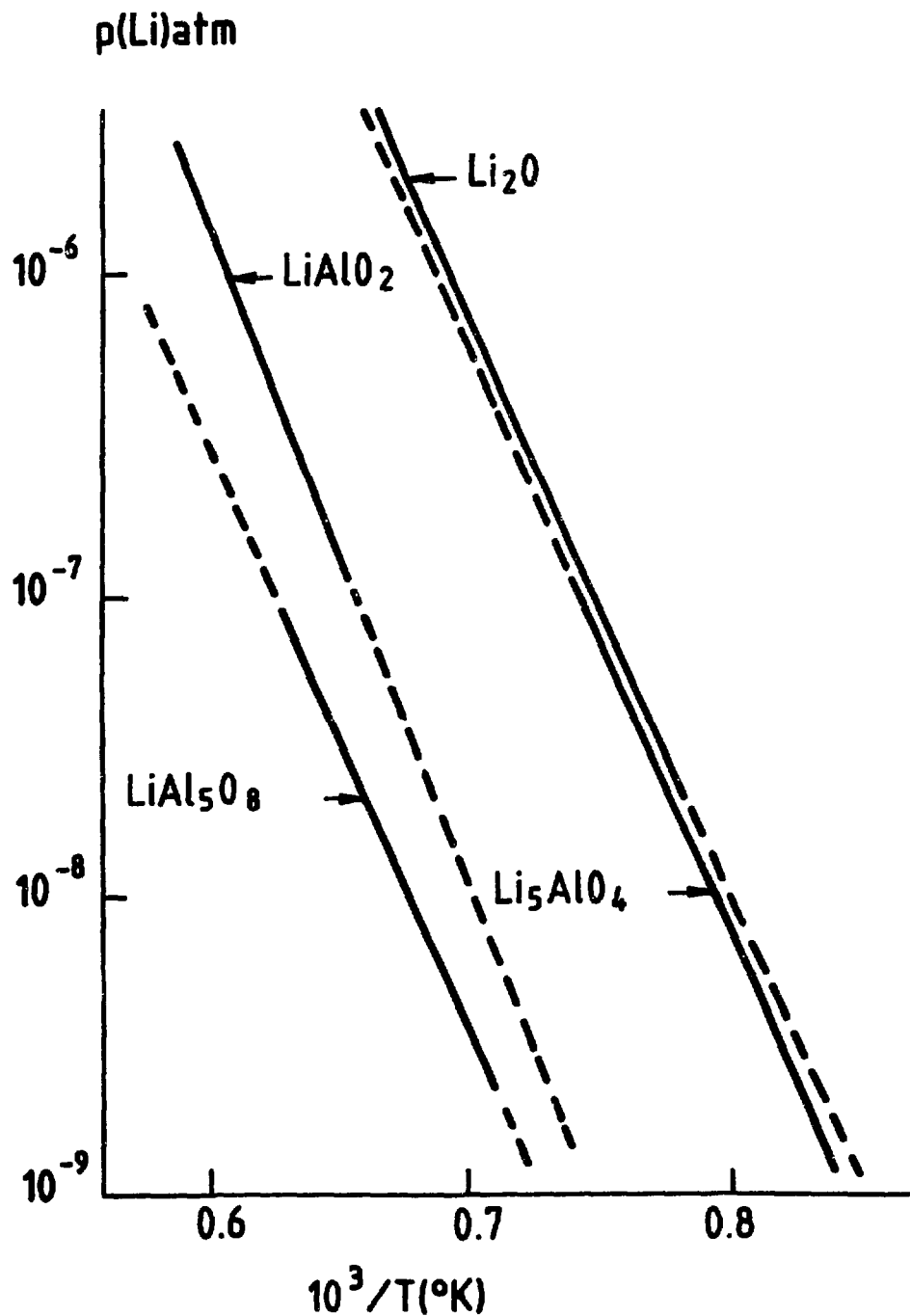


Figure 5-6 Partial pressure of lithium over various lithium aluminum oxides and Li_2O (after Guggi et al.[269]).

Table 5-3 Recommended temperature limits for candidate solid breeder materials. Effects of radiation on these limits is not known and not reflected in this table (after Abdou et al.[8]).

	Li_2O	$\gamma\text{-LiAlO}_2$	Li_5AlO_4	Li_2SiO_3	Li_4SiO_4	Li_2ZrO_3	Li_8ZrO_6	Li_2TiO_3
$T_{\min} (\text{°C})$	410 ^a	300 ^a	350 ^a	410 ^a	320 ^a	400 ^b	350 ^b	400 ^b
$T_{\max} (\text{°C})$	800 ^c	1200 ^d	780 ^e	1000 ^d	950 ^d	1400 ^d	980 ^e	1185 ^e

a Established from diffusion and inventory considerations

b Established assuming similar properties

c Established from chemical considerations, i.e. reaction with moisture to form LiOT

d Established experimentally from the onset of closed porosity

e Estimated assuming $T_{\max} = 0.8 T_m$, K

Table 5-4 References and test conditions for compatibility studies between lithium ceramics and cladding and structural materials. Several different Inconel, Incoloy, and Hastelloy (all nickel alloys) were studied; specifics can be found in the papers referenced.

	Li_2O	LiAlO_2	Li_2SiO_3
SS 316	1,2,3,5,6,7	1,2	1,2
HT-9	1,2,5,7	1,2	1,2
Inconel	1,3,5,6,7	1	1
Incoloy	3,6		
Hastelloy	3,6		
Ni	3,6,7		
Mo	4		
Mo-TZN	4		
Ti-6242	1	1	1

- 1 Finn et al.[270] - 600°C for 1900 h
- 2 Chopra and Smith[275] - 600 to 700°C for 1000 and 2000 h
- 3 Kurasawa et al.[273] - 500 to 700°C
- 4 Takeshita et al.[285] - 800 to 1000°C for 100 h
- 5 Porter et al.[271] - 500 to 600°C; pressurized He;
dry, 1% and 6% LiOH
- 6 Kurasawa et al.[274] - 800 to 1000°C for 100 h
- 7 Chopra et al.[272] - 550°C; flowing He; 1 ppm and 93 ppm
 H_2O

range of temperatures and materials that have been used in these compatibility tests. In the tests by Finn et al.[270], three ceramics and four structural materials were used in the same tube, and cross-contamination may have occurred, especially by lithium oxide which vapourizes most easily. In order to better simulate reactor conditions, Porter et al.[271] pressurized the tubes with helium. Chopra et al.[272] used a flowing helium atmosphere with added moisture and helium impurities to simulate the helium purge gas in a blanket.

The tests show that Li_2O can be aggressive to most structural materials (an exception is pure Ni[273,274]) but that the other ceramics are not. Moisture in either the helium sweep gas or in the lithium oxide strongly influences corrosion[271,272,275], and indications are that elimination of moisture would eliminate corrosion. Moisture reacts with Li_2O to form the corrosive substance LiOH . If the LiOH remains within the solid breeder, no damage occurs, but LiOH vapourizes easily and can be carried by the helium purge gas stream to the cladding or structural materials. Both intergranular attack and the formation of a scale or reaction layer have been observed. In steels, reaction layers of FeLi_5O_4 and FeLiO_2 were identified, along with a Cr rich subscale in HT-9[272]. In nickel alloys, LiCrO_2 was usually observed, and Kurasawa et al.[274] also noted a Cr depleted alloy matrix layer. Stress was not observed to enhance corrosion of SS-316 or HT-9 in contact with Li_2O [271]. The conclusions that Porter[271] reached summarize the available information on Li_2O corrosion and are reproduced below:

- stress, temperature, and $\text{Li}_2\text{O}-\text{LiOH}$ composition conditions covered in this test do not cause significant cladding corrosion over a one-year period;
- stress does not enhance corrosion;
- dry Li_2O does not cause significant corrosion of the austenitic stainless steels tested;
- corrosion which does occur is probably aided by some form of short distance, vapor-phase transport. The resulting corrosion product is of the type MLiO_2 ;

- the two ferritic alloy (HT-9) capsules, which were included only in conditions of highest LiOH content, stress, and time, likewise did not fail at either 500°C or 600°C - the HT-9 samples, however, did show the greatest attack as nearly 10% of the wall depth showed evidence of corrosion after one year at 600°C;
- in-reactor testing has shown that radiation does not enhance the corrosion process - the results do show, however, that care must be taken to provide dry Li₂O as a starting material; the LiOH content is directly responsible for the amount of corrosion which does occur.

Safety studies on the compatibility of solid breeders with water coolant have been carried out by Jeppson et al.[288]. They concluded that the ternary oxides (LiAlO₂, Li₂ZrO₃, Li₂SiO₃, Li₄SiO₄ and Li₂TiO₃) are chemically compatible with water and present no safety problems. Lithium oxide reacted mildly with water to generate small amounts of heat and hydrogen. Their main concern was LiOH production and interaction with structural metals under accident conditions, because hydrogen gas is generated by this interaction.

5.4 In-Reactor Behaviour

Experiments directed toward understanding in-reactor behaviour of lithium ceramics divide into the following categories:

- fundamental studies to examine the physics of radiation damage;
- capsule tests to investigate mechanical behaviour and tritium production;
- tests to measure tritium release in situ;
- large scale "module" tests in fission or fusion reactors.

No module tests have been performed, but material is being fabricated for a test with TFTR commencing in 1985. Tritium release experiments will be described in Section 5.5; the others are described below.

5.4.1 Fundamental Studies

Radiation damage in solid breeders produces the following effects[248]:

- displacement damage - lithium lattice and oxygen lattice vacancies, interstitials, Frenkel pairs, dislocation loops, clusters, etc.;
- reaction products - tritium atoms and helium atoms in the form of interstitials, substitutional defects, and bubbles;
- lithium depletion - lithium burnup produces lithium lattice vacancies and nonstoichiometry;
- microstructural changes - sintering, grain growth, microcracking.

An oxygen lattice vacancy with a trapped electron is a colour center that is called an F^+ -center. These defects have been studied by optical absorption and electron spin resonance[276-279] in Li_2O . Uchida et al.[278] irradiated single crystals and sintered pellets, both with and without cadmium shields to absorb thermal neutrons. In this way fast neutron effects could be distinguished from thermal neutron effects. Noda et al.[276,277] used, in addition, energetic oxygen ions (100 and 112 MeV) to simulate the effects of high energy neutrons. The accelerator-produced oxygen ions produced F^+ -centers at the highest rate - probably several orders of magnitude faster than thermal neutrons. The fast neutron spectrum from the thermal reactor produced F^+ -centers about five times as fast as thermal neutrons. Gamma radiation from ^{60}Co did not produce F^+ -centers in measurable numbers[278]. With oxygen ions and fast neutrons, the damage is caused by direct collisions and associated damage from the primary knock-on atom, but with thermal neutrons the damage is caused by the recoil energy of tritium and helium atoms produced from the $^{6}\text{Li}(\text{n},\alpha)^{3}\text{H}$ reaction. In the fission reactor JRR-4, because of the predominance of thermal neutrons, the majority of the damage in the Li_2O specimens was produced by the ^{6}Li reaction.

These investigators also observed the annealing behaviour of the F⁺-centers in Li₂O. Using 30 min anneals at 15°C intervals, they found that recovery began at about 160°C and was complete at 340°C. In the irradiated sintered pellet specimens, Noda et al.[277], employing electron spin resonance techniques, observed effects attributed to lithium colloids (inclusions) on grain boundaries. These began to recover thermally at 330°C and disappeared above 600°C.

Noda et al.[276] also observed the change in lattice parameter that occurred from irradiation of lithium oxide in thermal neutron reactors and a 14 MeV neutron source (RTNS-II). No lattice parameter change in sintered pellets occurred from a thermal neutron fluence of $1.4 \times 10^{22} \text{ n/m}^2$, but a 0.15% volume expansion was measured from $2 \times 10^{23} \text{ n/m}^2$. The single crystals irradiated with 14 MeV neutrons showed a slight lattice expansion at a fluence of $2.3 \times 10^{20} \text{ n/m}^2$. Curiously, the expansion decreased with increasing fluence to 10^{21} n/m^2 , after which it increased again. (The maximum lattice parameter change was about 0.05%, and the maximum fast neutron fluence was $3 \times 10^{21} \text{ n/m}^2$.) They propose that (at these fluences), irradiation defects, not tritium and helium production, are causing the lattice parameter changes.

In another study, Uchida et al.[280] measured the recoil range of the 2.7 MeV tritons produced from the ⁶Li fission. The recoil tritons that escaped from the surface of a Li₂O single crystal under irradiation were absorbed by an aluminum foil in contact with the crystal. The aluminum was then dissolved, and the tritium collected. They found a mean recoil range of $38.4 \pm 2.3 \mu\text{m}$ which decreased when the reaction density became larger than about $1 \times 10^{24} \text{ reactions/m}^3$. This decrease is not understood at present.

5.4.2 Mechanical Behaviour of Irradiated Capsule Specimens

The major results on the mechanical behaviour of irradiated specimens have come from the study in ORR by Yang et al.[281], the "TULIP" experiment by Porter et al.[271], and the FUBR-1A experiment by Hollenberg[282]. The TULIP and FUBR-1A experiments were done in the fast neutron reactor EBR-II (see Section 2.2.1 for information on remote testing).

Yang et al.[281] irradiated 54 Inconel-clad specimens of Li_2O , LiAlO_2 , Li_4SiO_4 and Li_7Pb_2 in the Oak Ridge Reactor for six months to a fast neutron (> 0.18 MeV) fluence of 1.1 to 2.7×10^{21} n/cm 2 . To reduce self-shielding, depleted lithium (0.05% ^6Li) was used, and the ceramic specimens were small, only 1.5 mm in diameter by 2 to 3 mm long, and 60 to 80% of theoretical density. Irradiation temperatures were 600 to 1000°C. Table 5-5 is a summary of test conditions and results.

Porter et al.[271] irradiated Li_2O specimens, 89% T.D. (93% ^6Li enrichment) in the fast neutron environment of EBR-II to observe the production and retention of helium and tritium, to compare these with calculated predictions, and to observe swelling. Pellet stacks (5 mm diameter by 33 mm long) were irradiated to either 1% or 3% ^6Li burnup at 520 to 550°C surface temperatures. The centerline temperatures were calculated to be about 600 to 650°C. The pellets were not examined for microcracks, but no major fractures occurred, and all remained integral. However, a swelling of 7% by volume occurred between 1 and 3% burnup. Since the volume of helium and tritium in the pellets was the same for the two burnups (as determined by dissolution of the pellets and measurement of the released gases), the swelling was not attributed to helium formation. This is also consistent with Noda's conclusion from lattice parameter measurements, described in Section 5.4.1 above. Formation of open, or interconnected, porosity, as occurs in oxide fission fuels to release fission gases, was believed to be the explanation for the constant amount of helium and tritium in the pellets.

The FUBR-1A tests[282] were designed to test the behaviour of four carefully made, well characterized, fine-grained (~ 1 μm) lithium ceramic pellets, at various temperatures and densities, irradiated to 300 full power days (10^{22} n/cm 2) in EBR-II. Pellet preparation techniques are described in Section 5.2.1 of this report. A homogeneous ^6Li burnup of 3×10^{20} fissions/cm 3 was obtained; Hollenberg[283] commented that this burnup is equivalent to the peak burnup in DEMO after two years, but a factor of 13 lower than STARFIRE after six years. Pellet stacks of Li_2O , Li_4SiO_4 , Li_2ZrO_3 , and LiAlO_2 , 0.95 cm in diameter by 5.7 cm long, 85% T.D. were sheathed in stainless steel with a plenum to accommodate the helium produced in the ceramic, and were irradiated

Table 5-5 Post-Irradiation Examination of Lithium Ceramics Irradiated in ORR for Six Months by Yang et al.[281]

	Density of Sintered Pellet (% T.D.)	Test Temperature (°C)	Cladding Attack (Inconel-600)	Microstructural Changes and Mechanical Integrity
Li_2O	60-70	800	GB attack occurred with all Li_2O specimens. At 1000°C, max. penetration was ~150 μm .	Sintering sufficient to close the pores occurred. No strength reduction was reported.
		600-750	At 750°C, max. penetration was ~75 μm .	Sintering occurred, but pores remained open. No strength reduction reported.
Li_4SiO_4	70-80	750	GB attack occurred with all specimens at all temperatures. At 750°C penetration was ~50 μm .	No grain growth but some pore consolidation.
		800	At 1000°C, penetration was ~125 μm .	Much grain growth. At 1000°C, grain boundary separation caused loss of structural integrity.
LiAlO_2	90-100	750-950	Same results as for 70-80% T.D.	No significant grain growth. Unexplained spherical voids appeared inside grains. Grain boundary separation occurred. Spherical voids appeared.
	60-70	850-1000	No	No sintering. Some strength reduction. Edges and corners crumbled during polishing.

at 500, 700 and 900°C. In addition, LiAlO₂ pellets of 95% T.D. and powder at 60% T.D. were tested at 700 and 900°C.

Initial post irradiation examination of the pellets[283] showed a variation in the mechanical behaviour of the four ceramics. Li₂ZrO₃ pellets were not visibly cracked. LiAlO₂ pellets were cracked except for those tested at the lowest temperature (500°C), and those with 95% T.D. Li₂O and Li₄SiO₄ pellets, with much higher coefficients of thermal expansion, were all cracked. Cracking in Li₂O was the most severe; those tested at 700 and 900°C exhibited fractures approximately perpendicular to the cylindrical axis, separating the pellets into two or more pieces. In addition, radial cracks propagated from the surface toward the center, about 0.3 cm deep. Temperature gradients were initially small (< 50°C), but may have increased during irradiation. Additional stresses occurred in the Li₂O pellets from swelling gradients - no swelling occurred at the midpoints of the pellets, but about 1.7% diametral swelling occurred at the top and bottom. Those tested at the lowest temperature, however, exhibited only ~0.5% swelling, and less than 0.3% swelling occurred for the other ceramics.

No sintering of any of the pellets was observed. Extensive grain growth occurred for Li₂O (from 6 µm to 17 µm at 900°C); in Li₄SiO₄, less grain growth occurred (from 1 µm to 2 µm at 900°C), and no grain growth occurred for LiAlO₂. It has not been demonstrated that grain growth significantly affects either tritium inventory or mechanical properties.

A convenient method to observe changes in mechanical strength of irradiated specimens is to measure the change in microhardness number. If well shaped pits from the indenter can be made in the specimen surface, the microhardness number provides an estimate of the yield strength. Extreme brittleness will be manifested by an inability to form undamaged pits. Nasu et al.[284] measured the microhardness of irradiated Li₂O pellets, and found an increase of 25 to 30% when irradiated to a fluence of 10^{18} n/cm² in the JRR-4 thermal reactor at temperatures below 100°C. Little increase occurred above this fluence. In a series of 15 min anneals at increasing temperatures, abrupt recovery to a value slightly higher than the pre-irradiation value occurred at 350°C; tritium release also commenced at this temperature.

5.5 Tritium Recovery from Solid Breeders

5.5.1 Tritium Release

The most attractive method of removing tritium from a solid breeder blanket is to pass a sweep gas (helium) stream through purge channels in the solid, as shown in Figure 5-7. Factors that affect tritium release include microstructure, operating temperature, and tritium transport and solubility in the solid. The most complete theoretical analysis of tritium release and recovery from a solid breeder blanket was done for the STARFIRE study[20], which considered the following kinetic mechanisms for tritium release: 1) bulk diffusion in the grain, 2) desorption of T_2O at the grain surface, 3) migration through interconnected grain boundary porosity to the particle surface, 4) percolation through the porosity in the packed bed of particles and 5) convective mass transfer out of the blanket in the helium processing stream. Thus, solid state diffusion, desorption rate at the grain surface, and mass transport in the gas phase are important parameters to be considered for determining tritium release from the solid breeder material.

5.5.1.1 Bulk Diffusion

Bulk diffusion is strongly dependent on temperature and the diffusion path length. Minimum operating temperatures have been specified (Table 5-3) to ensure adequate tritium release and maximum temperature limits have been set to minimize thermal sintering and maintain short diffusion path lengths. Radiation damage may enhance sintering, resulting in a lower maximum temperature limit. Tritium inventory (Section 2.2.3) at steady-state, achieved when the rate of diffusion of tritium out of the solid is equal to the tritium generation rate, is dependent on diffusion and is proportional to the square of the grain size, hence the requirement for small grain size ($\sim 1 \mu\text{m}$). Empirical formulas have been developed[298] to predict tritium inventories resulting from diffusion-controlled release (diffusive inventory); however, the uncertainty of diffusivity values for tritium in the breeder materials and the grain size of the solids has resulted in large variations in the predicted inventories for the various candidate materials.

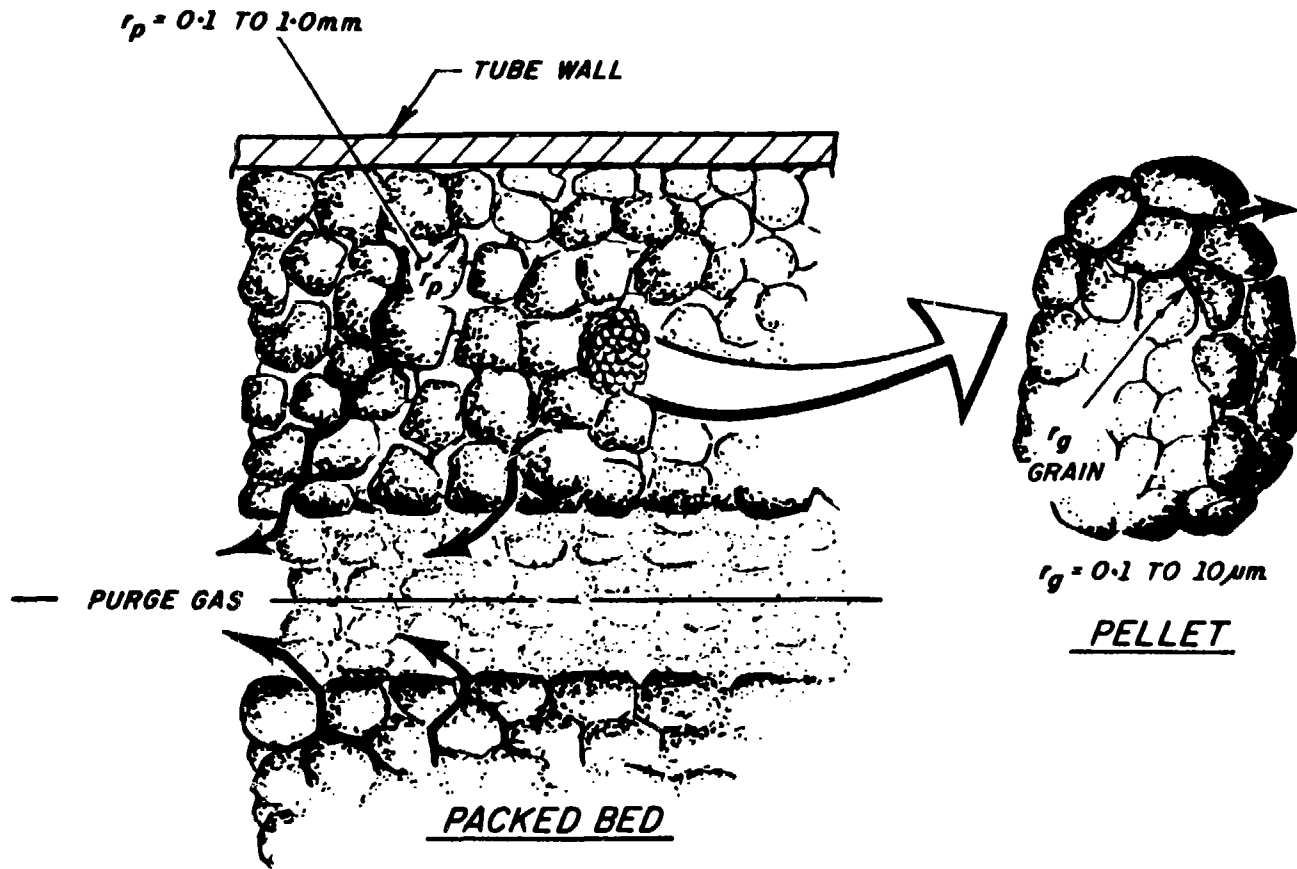


Figure 5-7 Schematic of tritium recovery from solid breeders (from [252])

Tritium diffusion coefficients have been determined for a number of the candidate solid breeders (Li_2O , LiAlO_2 , $\beta\text{-Li}_5\text{AlO}_4$, Li_2SiO_3 , Li_2SiO_4); however, the data are limited and exhibit considerable uncertainty. The most extensive study has been done on Li_2O . Figure 5-8 gives the diffusion coefficient of tritium in Li_2O as a function of temperature, determined by a number of investigators. References [290-296] detail the material characteristics and techniques used to obtain the data. The diffusion rates for tritium are measured by first irradiating the sample and then heating to remove the tritium. The tritium release as a function of time can be used to calculate the diffusivity. The observed differences (Figure 5-8) may be due to the different types of samples used and lack of characterization of the samples. Guggi[290] indicates that the uncertainties may arise from a lack of knowledge of whether diffusion within the solid or chemical reactions at the solid-gas phase boundary control the release of tritium from Li_2O . The experimental studies have not identified the tritium species (i.e. T , T_2 , T_2O) diffusing through the solid.

A model has been developed for tritium transport in Li_2O , consistent with the available qualitative diffusion data obtained by Nasu[296]. A summary of the model description given by Johnson and Hollenberg[297] follows. A Li vacancy (V_{Li}), created by neutron irradiation of ${}^6\text{Li}$, and a tritium atom combine to form a stable defect complex, $\text{V}_{\text{Li}}/\text{T}$. At temperatures $< 400^\circ\text{C}$, the existing data are interpreted to suggest that the $\text{V}_{\text{Li}}/\text{T}$ complex migrates as a unit. Above 400°C , the complex is less stable allowing the T atom to move interstitially within the Li_2O structure. In the temperature region 400 to 500°C , both the $\text{V}_{\text{Li}}/\text{T}$ complex and interstitial tritium should contribute to tritium release from Li_2O and non-Arrhenius behaviour should be observed. This is consistent with Nasu's data which span this temperature range. However, the scatter in the diffusion data is large and more detailed studies are required to affirm this mechanism. Recent data obtained from well-characterized, coarse ($\sim 400 \mu\text{m}$) Li_2O particles by O'Kula and Vogelsang[291] and from single crystals by Guggi[290] indicate diffusion coefficients 2-3 orders of magnitude greater than determined in earlier experiments by various investigators. Further information from well-characterized samples is required to confirm the diffusion coefficient values and a tritium diffusion mechanism in Li_2O .

TEMPERATURE, °C

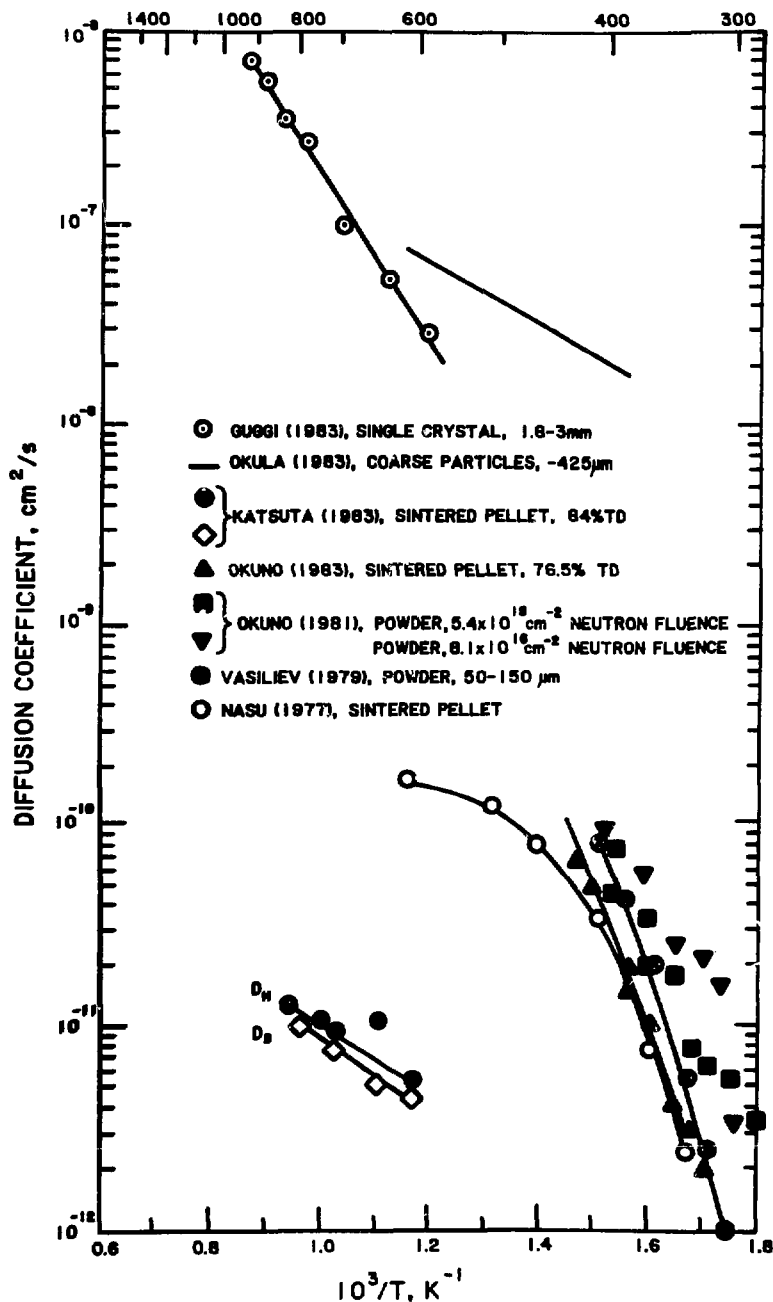


Figure 5-8 Diffusion coefficient of tritium in Li_2O as a function of temperature

No mechanism for tritium transport in the other candidate materials has been proposed. Diffusion data available are taken from reference [8] and summarized in Table 5-6, where the calculated diffusion coefficient is given for various materials at 560°C.

5.5.1.2 Gas Phase Transport

The mechanisms determining release of tritium from the breeder particle surface and transport in the gas phase have received little attention to date. However, understanding these mechanisms is important to determine their effect on tritium recovery and inventory. A "bimodal" microstructure, having a small grain size and a large pore size has been proposed[289] to enhance gas phase transport. A structure of open porosity should optimize tritium migration to the helium sweep stream.

The transport of tritium through the interstitial porosity of the solid has been evaluated by Smith et al.[298] for $T_2O(g)$ transport in Li_2O , using analytical models and the POROUS code developed to model gas release in oxide fission fuels. The variables required for such an evaluation, effective diffusion coefficient, permeability, porosity, and rate of tritium release have not been determined, thus they were varied over a wide range for the model calculations. No significant buildup of T_2O was predicted provided the porosity remained interconnected. A correlation between porosity and tritium release is required to establish criteria on the amount of open porosity required and determine the effects of radiation induced microstructural changes on release[252].

5.5.1.3 Solubility

Tritium release characteristics from the solid ceramics are also affected by thermodynamic considerations. Phase equilibria and tritium solubility are important parameters. Only Li_2O has been investigated in laboratory studies[8]. Measurements of the solubility of water vapour in solid Li_2O indicate a very low moisture solubility, and a strong relationship of the tritium solubility, as $LiOT$ ($2LiOT \rightleftharpoons Li_2O + T_2O(g)$), with the partial pressure of H_2O in the gas

Table 5-6 Diffusion Coefficient of Tritium in Solid Breeder Materials at 560°C (from reference [8])

<u>Material</u>	<u>Reference</u>	<u>Description</u>	<u>D(m²/s) at 560°C</u>
LiAlO_2	Wiswall (1976)	150 - 215 μm	1×10^{-14}
	JAERI (1982)	20 μm	8×10^{-14}
	Vasil'ev (1979)	150 μm	6×10^{-14}
	Guggi (1975)	33 μm	1×10^{-13}
$\beta\text{-Li}_5\text{AlO}_4$	Guggi (1980)	1.5 - 3.75 μm	8×10^{-14}
	Guggi (1976)	10 μm	2×10^{-13} extrapolated to this temp.
$\alpha\text{-Li}_5\text{AlO}_4$	Guggi (1976)	10 μm	4×10^{-14}
Li_2SiO_3	Vasil'ev (1979)	150 μm	1×10^{-13}
	JAERI (1981)	$\sim 20 \mu\text{m}$	
Li_2SiO_4	Vasil'ev (1979)	150 μm	2×10^{-13}
Li_2O	See Figure 5-8		

phase. Figure 5-9 indicates the solubility of LiOT, as a solute in solid solution, increases with temperature at a constant partial pressure of water, contrary to calculations using an ideal solution model with JANAF thermochemical data[297]. The LiOH-Li₂O system is thermodynamically non-ideal. Johnson and Hollenberg[297] report activity coefficients of $\sim 10^3$ at low temperatures (300–600°C), obtained from solubility data and thermochemical calculations on the Li-O-H system. This non-ideality means that the solubility of LiOH is much lower than predicted from ideal solution behaviour. Similar results were obtained in a study by Norman and Hightower[299].

Experimental investigations by Tetenbaum and Johnson, summarized in[297], have determined the partial pressure of water vapour required to precipitate LiOH from Li₂O in the temperature region, 300–620°C. To avoid second phase formation at 425°C, the partial pressure of H₂O must be maintained below 70.9 Pa, at 625°C, 2.4 kPa. The blanket must not operate in the regime where LiOT is the stable phase. However, it must operate at a high enough temperature to recover the tritium, but limit LiOT vapourization. Because of the low solubility of LiOH in Li₂O and the immiscibility of the two phases, at high temperatures (> 700°C) LiOT vapourization could result in significant Li₂O transport.

Hydrogen solubility in Li₂O has also been measured experimentally. Katsuta and coworkers[292] have determined the pressure dependence of the amount of hydrogen dissolved in a Li₂O pellet in the pressure region 7 to 100 kPa and found it to obey Sievert's law. Hydrogen solubility in Li₂O was determined to be $\sim 1.6 \times 10^{-7}$ (H atom/LiO₂ molecule.Pa^{0.5}) at 600°C.

Ihle and Wu[300] have determined the solubility of deuterium in a single crystal of Li₂O at 600°C to be $x_D = 5.6 \times 10^{-5}$ D atom/mol at 133 Pa and 5.0×10^{-6} D atom/mol at 13.3 Pa. Their results indicate that Sievert's law was not obeyed and that the deuterium was in solution as D₂, contrary to the observations of Katsuta[292]. This may result from the different pressure ranges studied or from material differences. Both results indicate the solubility of hydrogen in Li₂O is very low.

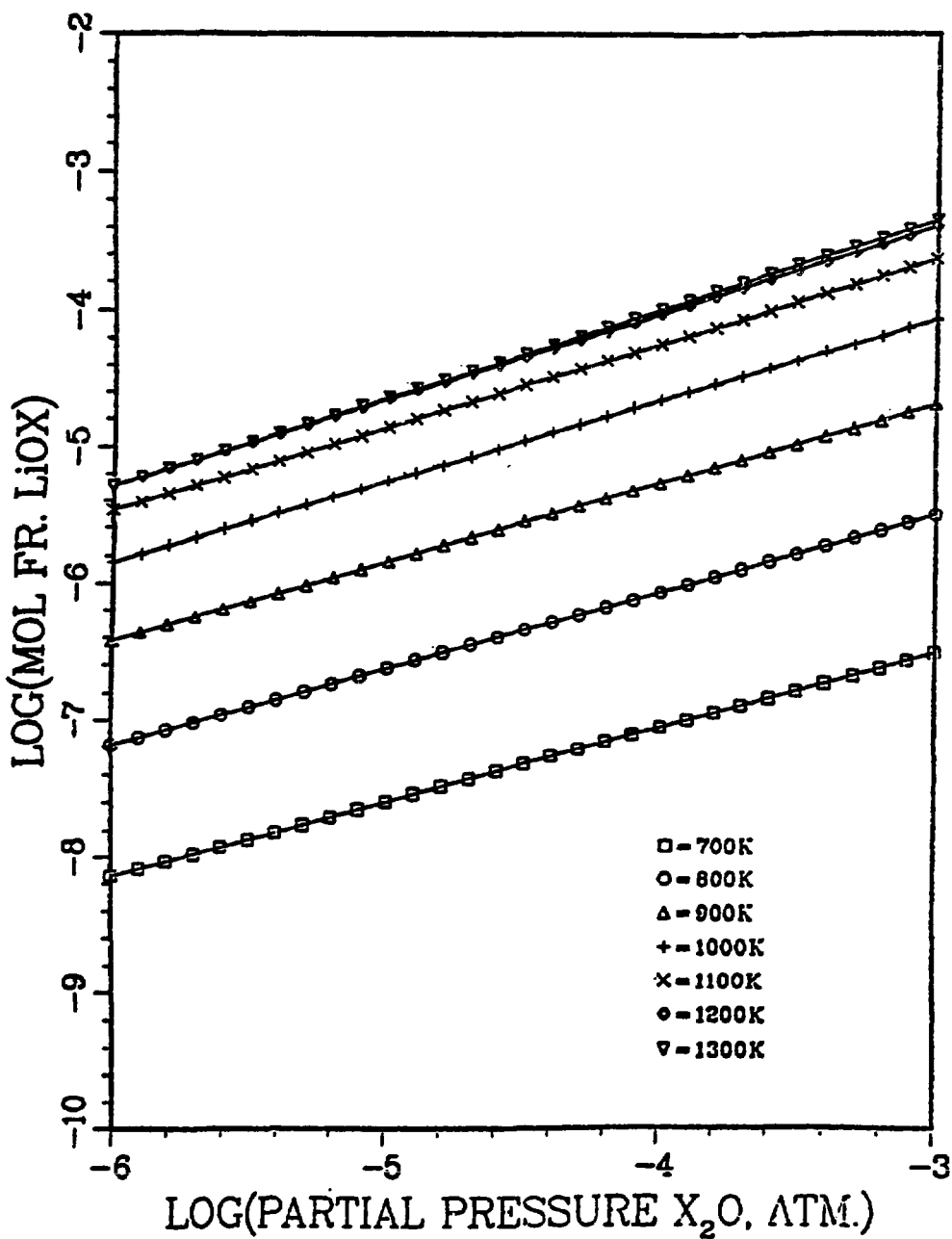


Figure 5-9 Tritium solubility in Li_2O as a function of temperature and partial pressure of T_2O ($X = \text{H, D, T}$) [8].

5.5.2 Tritium Inventory Considerations

The limited experimental data on tritium transport and solubility makes it difficult to predict tritium inventories in an operating solid breeder blanket. A limit of < 10 kg of T/GW_{th} has been set for the initial screening of materials in the BCSS[301]. And, of course, minimizing tritium inventory is important for safety and economic reasons (Section 2.2.3). The effects of radiation, tritium trapping, sintering and pore closure on inventory still need to be examined. Analytical models developed in the STARFIRE study and discussed in[298] estimate a steady state tritium inventory of ~140 g in the $\alpha\text{-LiAlO}_2$ STARFIRE blanket from bulk diffusion considerations only and based on a grain size of < 1 μm , unirradiated hydrogen diffusion data (single crystal), and low fluence, low temperature irradiations. The tritium concentration in the grains (as LiOT) is predicted as a function of the T₂O partial pressure in the gas phase, and this inventory resulting from thermodynamic solubility is estimated as high as 8 kg. The effects of radiation on inventory have also been assessed and increase the total estimated inventory in the STARFIRE blanket to 380 kg (95 kg/GW_{th}). The large predicted range indicates the need for further diffusion and solubility data, and irradiation studies to determine the effect of radiation on the blanket structure and tritium inventory.

5.5.3 Tritium Extraction

5.5.3.1 Thermal Extraction Studies

Preliminary information on tritium recovery from many of the candidate solid breeder materials has been obtained in post-irradiation thermal extraction studies. O'Kula and Sze[302] reviewed the existing data from 1975-1980 and concluded that, because of the variability in the scope and methods of investigation, there were few common bases for comparison of the breeder materials in the tritium release and recovery area. The parameters that have been examined in studies of the various candidate materials include the morphology and particle size, effect of neutron fluence, tritium concentration, anneal temperature, and sweep gas composition and flow rate. Despite the lack of

characterization of the materials and the variability in the tritium release data, the candidate materials indicated satisfactory tritium release kinetics. Vasil'ev et al.[295] reported results on Li₂O, Li₂SiO₃, Li₄SiO₄ and LiAlO₂ powders, which indicated essentially complete recovery in one hour at 450, 700, 700 and 800°C, respectively.

The Japanese program on Li₂O has contributed information on tritium recovery from Li₂O in a number of studies of irradiated single crystals, powders and sintered pellets[293,296,303,255]. The predominant species released was determined to be T₂O(HTO). Isothermal release curves, reported by Okuno and Kudo[293], from a degassed pellet (76.5% theoretical density) indicate > 95% of the tritium was released in approximately 1 h at 670 K; release rates similar to those observed for powders. The data from these extraction studies on Li₂O indicate > 95% of the tritium is released in the condensable form, i.e. as T₂O(HTO).

Tritium will be recovered from the Li₂O blanket module (LBM) of TFTR by post-irradiation thermal extraction[304]. Based on data from experimental extraction studies (e.g. [293,295,303]), the tritium will be thermally driven from the irradiated pellet (650-850°C) into flowing hydrogen. The hydrogen will pass over a CuO bed and the resulting tritiated water collected in a cold trap. Analysis of the sample by liquid scintillation counting will determine tritium release.

5.5.3.2 In Situ Tritium Recovery

In situ tritium recovery has been assessed to be the most feasible method to remove tritium from a solid breeder blanket. Mobile solid blanket concepts and batch-type recovery have been regarded as unacceptable because of questions of breeding capability, design complexity and economics[289]. An experiment (TRIO-01) demonstrating in situ recovery from γ-LiAlO₂ has been carried out by Argonne and Oak Ridge National Laboratories[252,305]. Tritium release and recovery were tested by passing helium sweep gas through the γ-LiAlO₂ capsule, and measuring and collecting the tritium in the sweep stream. The objectives of the TRIO-01 experiment included[252]: 1) determining the

relative importance of factors affecting tritium release-grain size, pore size distribution, temperature, sweep gas flow rate and composition, and radiation damage, 2) demonstrating recovery of tritium from the sweep gas stream, 3) investigating the chemistry of the tritium-containing species (e.g. $T_2O:T_2$ ratio) in the sweep gas. Also investigated were heat transfer, tritium containment, and physical and chemical stability of the material during the short irradiation period (about two calendar months in ORR-A2).

The preliminary results from TRIO[305] indicate that ~ 35 Ci (1.3 TBq) of tritium were collected, and > 99% of the tritium was recovered as $T_2(HT)$. Approximately 5% of the tritium permeated into the annular gas gap. Analysis of the neutron flux and dosimeters located near the capsule indicated that > 99% of the tritium was recovered from the capsule. This will be confirmed by a post-irradiation examination of the capsule. The tritium release rate reached steady state within a few hours at $\sim 600^\circ C$, with a sweep gas composition of He/0.1% H_2 . The addition of H_2 to the purge gas appeared to enhance the tritium release. Quantitative analysis of the data is still required and will include results from in situ recovery and post-irradiation examination.

The effect of experimental variables, such as temperature and the partial pressure of H_2O and H_2 in the sweep gas, on tritium release kinetics observed in the TRIO-01 experiment will add to the understanding of the processes affecting tritium release in solid breeders. Also, the data may allow more quantitative specifications to be developed for temperature, breeder material, tritium partial pressure, pore size and porosity characteristics, and sweep gas configuration and impurities[252].

An in situ tritium recovery demonstration from Li_2O sintered pellets, using a He sweep gas stream, has been performed by researchers at JAERI[306]. The pellets were irradiated in JRR-2 (10^{19} n/cm 2) to 3.1% burnup of 6Li . Preliminary results indicate steady state tritium concentrations were achieved at ~ 550 - $750^\circ C$ after irradiation for ~ 100 h. They determined the ratio of gaseous tritium, HT/HTO , to be 0.1 at steady state in the analysis train. However, the HT fraction appeared to be significantly larger than 10% immediately after the Li_2O pellets, leaving some uncertainties about the tritium species released

under the experimental conditions. Post-irradiation examination of the pellet is also planned and will add to the understanding of tritium recovery from Li₂O.

The results of the recent in situ recovery experiments indicate that the form of the tritium species released from the solid breeder, i.e. as T₂ or T₂O, is an important area which requires further study. While the tritium recovered from LiAlO₂ in the TRIO-01 experiment was largely as HT, the results from the recent JAERI study[306] and earlier post-irradiation studies of Li₂O[293,294,303], indicate the tritium is released from Li₂O in the condensable form (HTO). Many of the early post-irradiation studies of the various candidate materials did not attempt to identify the form of the tritium released. However, identification of the tritium species is important as it will affect tritium release mechanisms and recovery, safety, and design of the fuel cleanup system. Safety is an important issue because of the increased radiotoxicity of T₂O compared to T₂.

5.6 Solid Breeder Blanket Technology

5.6.1 Introduction

As shown in Section 2.3, many conceptual blanket designs exist, in varying states of detail, but no fusion reactor will have a blanket for probably a decade. We can therefore expect considerable evolution as design engineers and materials scientists cooperate to find optimal solutions to the complex problems involved.

Tritium recovery techniques for solid blankets include batch removal and continuous circulation of the breeder out of the reactor. Batch removal is costly because it requires too much reactor down-time[8], and continuous circulation seems to be costly and unreliable. The most common mechanism is in situ recovery by a helium purge gas, which was described in Section 5.5.3.

A major design problem for the solid breeder concepts is the need to maintain breeder temperatures within upper and lower limits. Section 5.6.4 reviews the

proposed solutions. Another major problem is accessibility for maintenance and repair (see Sections 2.3 and 4.2.4). Activation of the structure, and the expense of down-time will limit operator repairs in-reactor, so most designs divide the blanket into 10 to 30 "sectors" which can be individually removed and replaced, permitting out-reactor repair, possibly in hot cells. Designs for fusion reactors are generally for large machines, approximately 3000 MWe, although studies do exist for "compact" machines[307]. The high cost of downtime, therefore, demands a high degree of reliability, and an ease of maintenance. These areas require more research for all blanket concepts.

The Blanket Comparison and Selection Study (BCSS) Interim Report[8] which was produced by a team of investigators led by Argonne National Laboratories is a useful source for critical evaluations of blanket concepts. This section is indebted to that report for its description of the concepts, and assessment of problems. The following text cites it at several places, but has utilized it throughout (see also Section 6.2.1).

5.6.2 Coolants and Structural Materials

Pressurized water and helium are the two candidates most widely considered for use as coolants with solid breeders. Water has a high heat capacity, a high coefficient of heat transfer, good flow properties, and its use in fission reactors has provided considerable experience. For neutronics reasons, both H₂O and D₂O have been considered. Designs with Li₂O typically require inlet and outlet temperatures of about 280 and 320°C at a pressure of 15 MPa. Helium, on the other hand, is inert, and also has a relatively high heat transfer coefficient, and can be operated at a higher temperature than water. However, its low heat capacity means that pumping the helium will be a major power drain (approximately 10% of the electrical power produced for a reactor as described in Section 5.6.3.2). The containment vessels for water and helium will be described in Section 5.6.3.

A molten salt called HTS (Heat Transfer Salt - chemical composition 49% NaNO₂ - 7% NaNO₃ - 44% KNO₃), with good thermal and compatibility properties, is an alternative coolant. It is chemically compatible with the lithium

ceramics, and with Pb, which may be used as a neutron multiplier. Compatibility between HTS and Be has not been investigated, and between HTS and structural materials needs further study, but short-term tests show that chrome steels, such as austenitic and ferritic steels, and Inconel are corrosion-resistant[8]. Another favourable property of HTS is that it deposits an oxide layer on steel which would probably reduce tritium permeation into the coolant. Fortunately also, T_2 converts to T_2O in the presence of this salt. Besides being easily removed by vacuum degassing, T_2O will not pass through heat exchanger walls, thus eliminating the need for intermediate coolant loops and double-walled heat exchangers. The heat transfer coefficient of HTS is only about half of that for water, so that the proportion of coolant in the blanket must be larger. Two-dimensional neutronics calculations for specific blanket designs[8] showed promising tritium breeding. HTS has several disadvantages, the most serious being decomposition from gamma and neutron radiation.

The cladding and structural materials being considered for use with solid breeders are austenitic stainless steels, ferritic steels, and vanadium alloys, which are the same as those proposed for liquid breeders. Since corrosion is less of a problem with the solid breeders, other issues such as radiation damage resistance, thermal stress factor, activation, and neutronic properties will determine the selection. These issues have been discussed in Section 2.2.1.

5.6.3 Solid Breeder Blanket Configurations

The most common configurations for solid breeder, coolant, sweep gas and neutron multipliers considered for fusion reactors are outlined in Sections 5.6.3.1 to 5.6.3.3. Nuclear heat deposition in the blanket for any fusion reactor will be greatest near the first wall (FW) and fall off rapidly with distance from the FW. Figure 5-10 shows the calculated heat deposition distribution for an INTOR design[308] using Li_2SiO_3 solid breeder. The design for cooling must, of course, accommodate this distribution. Usually this is accomplished by varying the density of coolant tubes from a maximum at the FW to a minimum at the blanket outer edge. This is apparent in Figures 2-5 to

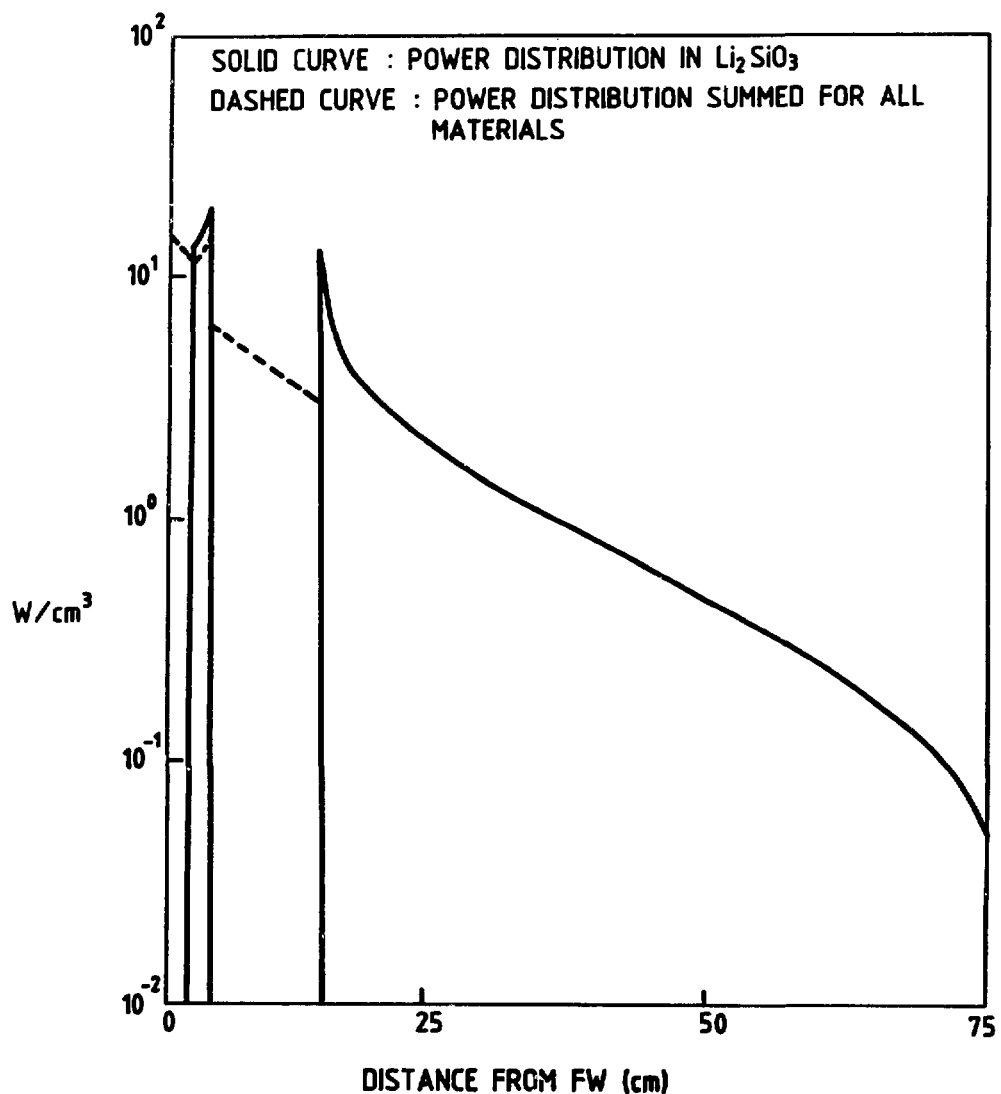


Figure 5-10 Power absorption distributions for a (30% lithium-6 enriched) INTOR design (after [308]).

2-7, for example. In the helium cooled modules, described in Section 5.6.3.2, helium passes through the first wall and then through the blanket, moving progressively towards the outer limits of the blanket. Its lowest temperature, and therefore maximum cooling ability, is next to the FW, where maximum cooling is required.

The ceramic breeder can be either in the form of sintered pellets (as with fission nuclear fuels) or sphere-pac assemblies. Sphere-pac refers to dense packing of two or three sizes of spheres. To maximize density, the diameters of the spheres ought to be a factor of 10 apart. Whether two sizes of spheres will be sufficient or whether three will be required is yet to be determined. Obtaining uniform packing with three sizes would be technically more difficult than with two. Also the hygroscopic nature of the lithium ceramics will add technical problems, especially if very small (approximately 1 μm) spheres are used. Alternate ceramic forms are sheathed "breeder balls"[309] to facilitate batch removal from the reactor for tritium extraction.

5.6.3.1 Water-Cooled Blanket Configurations

Tubes or coolant channels are preferable to pressure vessels or modules because the volume of non-breeding material is less. Figure 5-11 shows three configurations. At the left the coolant pipes surround the breeder. These designs are called breeder-in-tube (BIT). In the centre illustration, the coolant flows through holes or channels in the breeder, and are termed "breeder-outside-tube" (BOT) designs. Designs with the breeder in layers interleaved between layers of coolant channels are called "coolant panel designs" (at the right of Figure 5-11). These concepts are further described below:

1. Breeder-in-Tube

ASME (American Society of Mechanical Engineers) standards for tube thicknesses for the inner and outer coolant tubes result in too much steel and therefore unacceptably low tritium breeding for Li_2O (the "best" solid breeder) with no neutron multiplier. Even with a multiplier, this design will be inferior in breeding ratio, and probably in overall attractiveness[8].

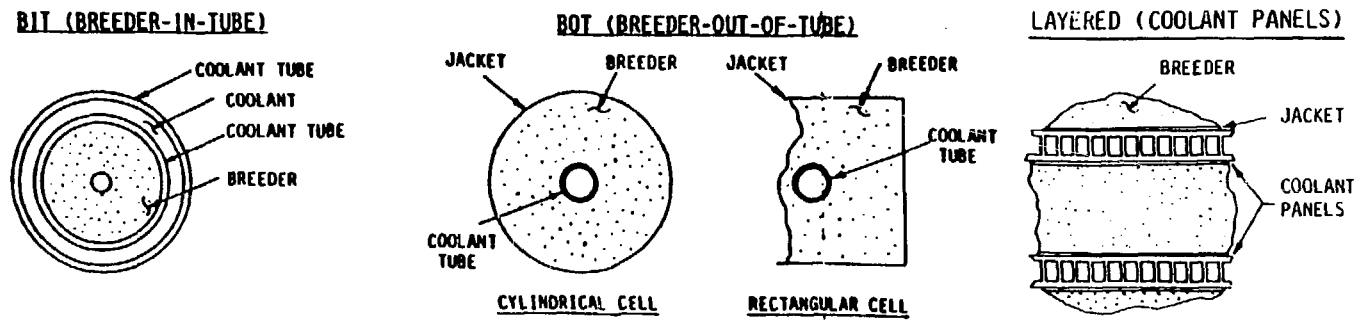


Figure 5-11 Blanket designs for water-cooled solid breeders (from [8]).

2. Breeder-Outside-Tube (BOT)

This design was adopted in the STARFIRE (Section 2.3.2) and DEMO (Section 2.3.3) studies with acceptable tritium breeding characteristics. Care was taken, by sizing and spacing of coolant tubes, and by adjusting coolant flow velocity, to ensure that the breeder temperature remained within the estimated allowable upper and lower temperature limits. This assumed, however, that the thermal conductance at the interface between breeder and coolant tube is accurately known and remains constant throughout the blanket life, or can be controlled during operation. The validity of these assumptions is discussed in Section 5.6.4. Sintered pellets would require containment jackets to prevent redistribution following fragmentation, but sphere-pac fuel might be held in place only by the rigid walls of the blanket. With rigid walls, Li₂O swelling and thermal expansion would tend to maintain compressive contact at the breeder-coolant tube interface, which would assist heat transfer, but stress buildup in the breeder, coolant tubes, and "rigid" walls are factors that need to be carefully considered. Locating the purge gas at this interface would be logical because this is the coolest region of the breeder, and so LiOH(T) vapour transport would be minimized. Also, a temperature jump (70–110°C) that is required between the coolant tube and the minimum breeder temperature (410°C) would occur naturally in this system.

3. Coolant Panel Concept

Breeder layers are interleaved between panels that contain the water coolant. The helium purge gas (not shown in Figure 5-11) flows along the breeder-panel interface through grooves in the sintered breeder or through a metallic felt at the interface. Calculations[8] show that the TBR is equivalent to that for the BOT design. Complex design areas such as structural connections for the coolant panels remain to be worked out. Fabrication might be accommodated more easily with sphere-pac fuel, by simply pouring the spheres into the panel structure, than with pellet fuel.

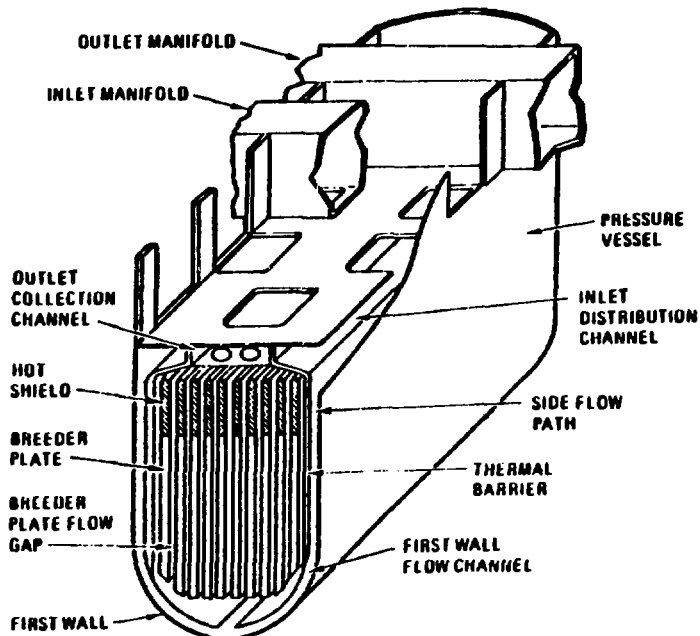
5.6.3.2 Helium-Cooled Blanket Configuration

Blanket designs have utilized pressurized helium coolant in tubes or in modules (vessels). Figure 5-12 shows a recent modular design. The necessity to minimize coolant volume for neutronics (tritium breeding) reasons is less stringent for helium coolant than for water coolant, therefore pressurized modules are acceptable for helium coolant designs, whereas they are not for water-cooled designs. The "lobular" blanket module design shown in Figure 5-12 was designed for a tokamak reactor with 5 MW/m^2 FW neutron loading, by GA Technologies Inc. in connection with the BCSS study[8]. The helium pressure was 5.1 MPa, inlet temperature was 275°C, and outlet temperature was 500°C. Tritium production was acceptable, and the net power conversion efficiency was 36.5%, taking into account the power required to pump the helium coolant. The helium pumping power required was 4% (loop pumping power/reactor thermal power). Because of the severe requirements on the FW, the blanket was designed with a rather short (two-year) FW lifetime. Tritium inventory was estimated to be 1.8 kg/GW_{th} from models as described in Section 5.5.

This modular concept was favoured over the pressurized-tube concept because of the fear of high failure rates that would result from the large number of tubes required ($\sim 10^4$), and the reduced reactor availability that would result. This, however, further emphasizes the risk involved in the Li₂O-water coolant designs in Section 5.6.3.1 that utilized the breeder-outside-tube designs with coolant pressures of 15 MPa.

5.6.3.3 Neutron Multipliers

For acceptable tritium breeding capabilities, neutron multipliers will be required with all solid breeders except possibly Li₂O and Li₂ZrO₃. Neutron multipliers that have been considered include zirconium, lead, and beryllium. Zirconium, however, has been discarded because of its high parasitic absorption. The disadvantage of lead is its low melting point (323°C), which puts severe limitations on the coolant temperature, or requires it to be used in liquid form. This would introduce liquid metal corrosion problems (Section 4.3). However, liquid lead as a multiplier in solid breeder blankets



HELIUM COOLED BLANKET MODULE WITH DETAILS

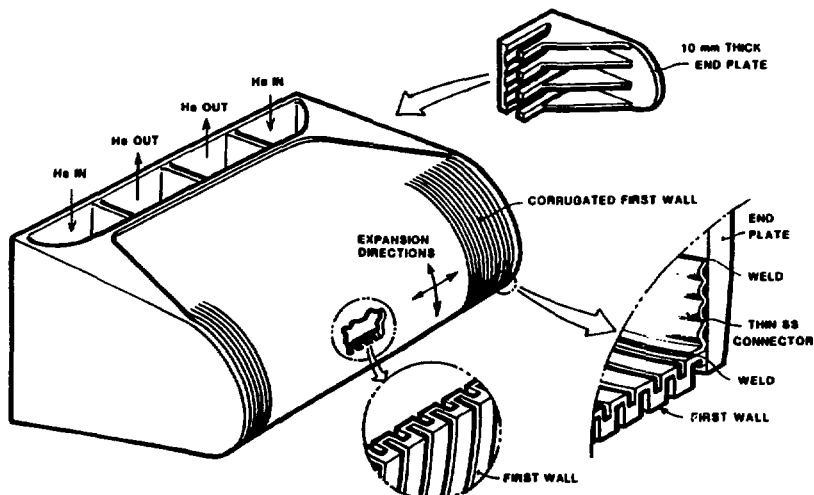


Figure 5-12 A lobular blanket design for helium-cooled solid breeders, showing breeder location, coolant flow, and first wall arrangement (from [8]).

is being investigated by Abdou et al.[8]. For these reasons, beryllium is considered the best candidate - the main concern is its limited supply.

TRW, Inc.[8] investigated the reserves, resources and demand for beryllium in the USA and the world to determine if enough exists to supply a large fusion power industry. They predicted that for thick multipliers (10 cm) with 1% loss of Be during recycling of the blanket, the USA could produce 410 GWe for 60 years. This assumes that the USA can use 15% of the world's Be resources, and apply 50% of that to fusion. Long-term service (1000 GWe for 200 years) would require that the USA use 27% of the world's Be resources. They arrived at the following conclusions:

- it appears reasonable to consider beryllium multipliers for the first and second generations of fusion reactor service, but close attention to beryllium recycle losses will be required;
- without efficient recycle, thick beryllium multipliers should be considered for use in only the first generation of fusion reactors;
- longer use can be obtained through imports; and
- the ultimate fusion-electric blanket cannot use Be.

Factors which influence the multiplier location in the blanket are, among others, optimization of breeding ratio, backscattering properties, and melting temperature of the multiplier. In the simplest designs, a slab 1 to 10 cm thick is located just inside the first wall (Figure 2-6). If the multiplier backscatters neutrons strongly, as does beryllium, a layer of breeder material between the first wall and the multiplier improves the breeding ratio. Be exhibits significant swelling under irradiation and allowance must be made for this in designs, e.g. Be is used at 70% TD in the STARFIRE blanket (Table 2-6). If the multiplier is compatible with the breeder and coolant operating conditions, pellets of breeder and multiplier can be stacked sequentially[310]. This close mixing increases the multiplier's effectiveness for tritium production, and for heat removal if the multiplier has a high thermal

conductivity, as does Be metal. Clearly, the additional structural complexity that neutron multipliers introduce must be weighed against the problems involved in designs that do not require neutron multipliers.

5.6.4 Breeder Temperature Control

To maintain the solid breeder within specified upper and lower temperature limits, the thermal conductance at the interface between breeder and coolant tubes must be known accurately, and held reasonably constant throughout the blanket life. The thermal conductance is controlled by the magnitude of the gap between breeder and coolant tube, the roughness of the surfaces, the thermal conductivity of the gas in the gap, and the surface heat flux. A large temperature jump can exist across a gap filled with helium; for example, for a 0.2 mm gap between Li₂O (15 diameter pellets) and steel, in a region where the nuclear heating is 50 MW/m³, the temperature difference would be about 300°C, assuming no convection occurs, whereas for a 10⁻⁴ mm gap, the temperature difference would be only about 10°C (calculated from equations presented by Abdou et al.[8]). Large temperature jumps are unacceptable because the uncertainty in the ceramic temperature would be too large. Also, processes can occur during reactor operation that affect the boundary locations during blanket operation, and therefore alter the ceramic temperature. These include differential thermal expansion between solid breeder and structural materials; solid breeder cracking and cracked fragment relocation; solid breeder densification due to thermal/radiation-enhanced sintering; solid breeder thermal and radiation-enhanced creep; solid breeder radiation-induced swelling; and time-dependent deformation, i.e. creep and swelling, of the structural materials.

The following solutions for these problems have been proposed.

1. In-reactor control of thermal conductance, for example, by altering the composition of the gap gas. Unfortunately, methods devised so far either do not give enough control or are too complex.
2. Breeder segmentation. Sufficiently small ceramic pellets will not develop enough thermal stress to fracture (Section 5.6.5). Sphere-pac ceramics

would satisfy this, as well as ensuring contact between the breeder and coolant tubes (or panels) at fabrication. Redistribution during operation, to accommodate ceramic swelling or pressure tube creep may ensure continued contact.

3. Using a solid buffer in the gap. A high conductivity solid in the gap would relieve the temperature jump problem and prevent redistribution of the ceramic after fragmentation. The solid would need to be metallurgically bonded to both the breeder and the coolant tube, and these bonds would have to remain intact during blanket operation. Metallic foils could be brazed to the ceramic and coolant tube, or a liquid that cures to a solid could be poured into the gap. However, braze tests conducted at MDAC[8] indicated that cracks in the Li₂O pellets would develop both parallel and near perpendicular to the bonded interface from the temperature changes produced during brazing or reactor startups.
4. Dispersion toughening. In this technique, second-phase particles are used to toughen the ceramic. Although demonstrated in other ceramics, its effectiveness varies, and it has not yet been demonstrated for the lithium ceramics. If BeO inclusions could be used, however, a neutron multiplication benefit would also occur.
5. Elimination of the coolant tubes. For helium-cooled designs, the coolant tubes could be eliminated, and the helium coolant used for tritium collection also (e.g. the British INTOR design[311]). Increased Li₂O mass transfer carried by the large helium flow and greater difficulty in controlling the purity of the pressurized helium coolant as compared with a simple purge gas system, are difficulties with this design type. Ternary ceramics however are more stable and this technique could work for them.

5.6.5 Breeder Ceramic Size Considerations

The requirement that the temperature of solid breeders be within specified limits prohibits the use of pellets with too large a diameter, or layers that

are too thick. Otherwise the breeder material farthest from the coolant would become too hot. Another criterion for limiting dimensions is to prevent thermal-stress-induced fractures from forming. The BCSS interim report[8] derived approximate values from both of these criteria. The results are reproduced below.

For thin plates with a volumetric nuclear heating, Q , cooled by panels along the faces, the maximum thickness, h , permitted by the temperature window criterion is given by:

$$h^2 = \frac{8k}{Q} \Delta T \quad (1)$$

where h = plate thickness

k = solid breeder thermal conductivity (assumed constant)

Q = volumetric nuclear heating, and

ΔT = operating temperature window.

The stresses that the temperature gradient produces in the plate or beam can also be calculated. If it is assumed that plastic flow is negligible at these temperatures, and that fracture will occur when the maximum tensile stress in the breeder exceeds a value, σ_f , the maximum thickness allowable for the plate is:

$$h^2 = \frac{12(1-\nu)k}{\alpha Q} \frac{\sigma_f}{E} \quad (2)$$

where α = thermal expansion coefficient for the breeder

E = Young's modulus, and

ν = Poisson's ratio.

In the high nuclear heating zone near the FW (5 MW/m^2 neutron heating load) Q is about 60 W/cm^3 , and the temperature window criterion gives a maximum layer thickness of 1.5 cm for Li_2O whereas the fracture criterion gives 0.30 cm . At all locations in the blanket, the fracture criterion was the more limiting[8].

For determining dimensions for BOT designs or coolant panel designs, the fracture criterion is too severe, and the temperature window criterion is usually used. Therefore pellet diameter or layer thicknesses for Li₂O can be about 1.5 cm, but fragmentation is expected.

5.7 Summary

Laboratory techniques for producing powder with low impurity content and specific grain size requirements have been developed. The powder is fabricated into pellets by pressing and sintering or by hot pressing, which has proven useful in keeping grain size small. A major problem in production of these ceramics, especially Li₂O, is avoiding moisture contamination during handling procedures. Japan and the US are developing techniques to mass produce Li₂O pellets with uniform microstructures and low moisture content.

Many of the fundamental physical and chemical properties of several of the lithium ceramics have been measured in recent years. Exceptions are the newest breeding candidates such as octalithium zirconate and the lithium-beryllium compounds. Thermal stability of Li₂O, particularly in the presence of moisture, is a serious concern, and work continues on the measurements of vapour pressures, solubility limits, and solution ideality. Estimates of the maximum and minimum operating temperature limits for the ceramics have been established on the basis of tritium diffusion rates, sintering, and stability considerations. Maintaining the breeder within the allowed temperature window is a key blanket design problem.

In-reactor studies of breeder material behaviour is an important area that is beginning to receive considerable attention. These studies investigate tritium release and recovery from both in situ and post-irradiation extractions, physical and mechanical stability, and mechanisms of radiation damage. Tritium release from the solid material is affected by microstructure, temperature, and tritium transport and solubility in the solid. In situ release experiments have been performed in the US (LiAlO₂) and in Japan (Li₂O) with encouraging preliminary results. Tritium inventory in the blanket is an important issue, but limited experimental data make it difficult

to predict inventories; a limit of 10 kg/GWth was chosen for the US Blanket Comparison and Selection Study. Effects of radiation, tritium trapping, and sintering on inventory still need to be examined.

Capsule irradiation tests of ceramic pellets have shown diametral swelling in Li₂O at 700°C and above with negligible swelling occurring in Li₄SiO₄, Li₂ZrO₃, or LiAlO₂. Some cracks were observed in the ceramics tested in the FUBR-1A experiment at HEDL, especially in Li₂O. It is not known if Li₂O swelling is proportional to burnup, or whether the swelling saturates at an acceptable level. In experiments to measure damage mechanisms in Li₂O, fast neutrons were shown to produce color center damage (F⁺-center) much faster than thermal neutrons. Li₂O lattice parameter changes from irradiation by thermal and 14.1 MeV neutrons were also observed, and attributed to irradiation defects rather than tritium or helium production. Further irradiation tests are required to confirm the effects of radiation on tritium release and recovery, and pellet integrity.

6. RESEARCH AND DEVELOPMENT IN BREEDER BLANKETS

6.1 Introduction

The purpose of this chapter is to discuss the world programs in breeder blanket R&D, the mechanisms now in place for international cooperation and the Canadian capability for work in this field. The technical content of the programs to be discussed has already been covered in the preceding chapters; the intent here is to reorganize the material in a programmatic manner but not to repeat what has already been said. A remarkable feature of the programs is the contrast between the liquid metal and solid breeder options in forward planning; the future course of liquid metal work has not been well defined, whereas detailed plans for solid breeder work exist in the larger programs. This may be because the liquid metal work has historically developed in connection with projects extraneous to fusion, notably the LMFBR and also in the US, accelerator targets (e.g. FMIT). Thus, to some extent their directions have been beyond the control of the fusion community. This greater emphasis on the planning of solid breeder programs coincides with the thrust of the recommendations of this report.

In order to make the material in this chapter manageable, the discussion is restricted to topics of direct relevance to the blanket problem and only the main centres of blanket activity. Completeness is not possible; program size and future directions are stressed.

6.2 U.S. Program

6.2.1 Blanket Comparison and Selection Study

The Blanket Comparison and Selection Study (BCSS)[8] was initiated by the U.S. Department of Energy/Office of Fusion Energy (DOE/OFE) in 1982 October and is scheduled to be completed in 1984 September. The funding is US \$1.2 million for FY 1983 and US \$1.0 million for FY 1984. The BCSS is investigating the critical issues and the evaluation and comparison of fusion blanket concepts. The primary goal of the study is the selection of a limited number of

promising blanket concepts that should be the focus of blanket research and development over the next few years. This study will probably have a pivotal influence on the future direction of the U.S. breeder blanket program and thus, it is worth discussing in some detail[312].

The BCSS has a multidisciplinary team consisting of experts in specialized fields. The study is led by the Argonne National Laboratory (ANL) and other participants include: McDonnell Douglas Astronautics Company; GA Technologies, Inc.; TRW, Inc.; Hanford Engineering Development Laboratory (HEDL); Grumman Aerospace Corporation; Rensselaer Polytechnic Institute; University of Wisconsin; University of California-Los Angeles; and the Energy Technology Engineering Center. Additional input is being provided by several other U.S. laboratories.

The study has established a set of initial screening criteria and a concept selection procedure. The basic approach has been to use a three-stage process as follows:

- separation of blanket concepts into "mainline" and "alternate" categories at the beginning of the study based on expert judgement and results from previous studies;
- development of initial screening criteria; and
- development of a detailed evaluation procedure to systematically evaluate and rank the blanket concepts.

Two reactor designs, STARFIRE (Section 2.3.2) and MARS (Section 2.3.4), serve as the basis for comparing the blanket concepts. A set of design guidelines or parameter ranges was issued at the beginning of the study. For example, each of the different blanket concepts is being examined under the same boundary conditions at the first wall. Nominal first-wall total power load of 4-5 MW/cm², surface heat fluxes of 10-100 W/cm² and erosion rate of 1 mm/a are used. Other constraints such as temperature and stress limits for structural material and corrosion limits are set for all the blankets under evaluation.

Blanket concepts have been evaluated with respect to the following areas:

- safety and environment
- economics
- engineering feasibility
- R&D requirements.

Among the above four areas, the most readily quantified item is economics. The cost of energy (COE) has been used as the overall figure of merit for economic consideration. COE was determined for each blanket concept and the evaluation included factors such as the capital cost of the first wall/blanket/shield components, power conversion efficiency, power requirements, or total power output, blanket lifetime, and reactor availability.

The approach taken in "safety and environment" and "engineering feasibility" was to develop a set of indices for each, which was then combined into an overall figure of merit by calculating a weighted sum. For example, three of the safety and environment indices were radioactive emission rate, waste disposal and fault tolerance of containment integrity with weighting values of 20, 10 and 6, respectively. Each figure of merit for "safety and environment" and "engineering feasibility" had a maximum value of 100.

The R&D requirements for particular blanket concepts will be considered in the latter portion of FY 1984. This assessment, along with the ranking of various concepts with respect to engineering feasibility, safety and environment, and economics, will constitute the overall evaluation. It is anticipated that the final ranking of blanket concepts will be placed in the following three categories:

- M = 1 potentially attractive, recommended for further near term development;
- M = 2 set aside for possible further consideration;
- M = 3 rejected.

It is realized by those doing the study that there is some concern about the overall usefulness of this methodology for fusion blanket comparison and the

ranking of different blanket concepts. Other concerns involve the subjectiveness given to the various indices and weighting factors. And it is acknowledged that to find the best way to combine all these evaluation criteria into one "figure of merit" is somewhat difficult. Nevertheless, it is clear that some ranking system must be used in order to select the most viable blanket options.

At this point in the BCSS study, a temporary ranking system is being used. Categories 1 and 3 are the same as above i.e. M = 1 and M = 3; however, category 2 has been divided into 2A and 2B. The 2A rank means that no critical difficulty has been identified but that the concept is less attractive than those in category M = 1. The 2B rank indicates a candidate that does have potentially serious problems and would likely be set aside.

The BCSS preliminary rankings[313], as of 1983 December, are given in Tables 6-1 for liquid metal and molten salt concepts and in Table 6-2 for solid breeder blanket types. The concepts considered are denoted in the form breeder/coolant/neutron multiplier and arranged in columns by the structural alloy class (Section 2.2.1) used to construct the blanket. The molten salts FLIBE and HTS have been discussed in Sections 2.1.1 and 5.6.2 respectively; TC is used in Table 6-2 to mean a ternary lithium oxide. LM stands for an unspecified liquid metal breeder and similarly SB for a solid breeder; FS denotes a ferritic steel.

Table 6-1 shows that the self-cooled liquid metal blankets generally have higher ranking than separate cooled systems. This is a result of the emphasis in the evaluation criteria placed on simplicity of design. Coolant/breeder compatibility and reactivity is not a problem. Heat transfer requirements are also reduced because most of the nuclear heating is deposited directly in the breeder-coolant. For separately cooled liquid metal systems, helium is the preferred coolant largely for safety reasons. FLIBE with a Be neutron multiplier also gets a good ranking for heat transfer and material compatibility reasons. Note that the latter is the only case of a PCA structure having top ranking. The other concepts with M = 1 rely on the extrapolation of the

Table 6-1 BCSS preliminary rankings for tokamak blanket concepts as of
83 December: Liquid Metal and Molten Salt Breeders

CONCEPT	PCA	FERRITIC	VANADIUM
A. OUTBOARD BLANKET SAME AS INBOARD			
Li/Li	2B	2A	1
LiPb/LiPb	3	1	2A
Li/H ₂ O	3	3	3
Li/He	2A	1	2B
Li/Na	3	3	3
Li/HTS	3	3	3
LiPb/H ₂ O	2B	2A	2B
LiPb/He	2B	1	2B
LiPb/Na	3	3	3
LiPb/HTS	2B	2A	3
B. LM OUTBOARD BLANKET DIFFERENT INBOARD BLANKET			
Li/Li: -/He	2A	2A	1
LiPb/LiPb: -/He	2B	1	2A
LiPb/LiPb: -/H ₂ O	2B	1	2A
C. EITHER A OR B BUT USING MORE THAN ONE STRUCTURAL MATERIAL IN THE SAME BLANKET: (FS FOR LIQUID METAL CONTAINMENT)			
LiPb/He	2A	--	--
D. MOLTEN SALT BREEDER			
FLIBE/He	3	3	3
FLIBE/He/Be	1	1	2B
FLIBE/He/Pb	2B	2A	2B

Table 6-2 BCSS preliminary rankings for tokamak blanket concepts as of
83 December: Solid Breeders

CONCEPT	PCA	FERRITIC	VANADIUM
Li ₂ O/H ₂ O	2B	2B	2B
Li ₂ O/He	1	1	3
Li ₂ O/HTS	2A	1	3
Li ₈ ZrO ₆ /H ₂ O	2B	2B	2B
Li ₈ ZrO ₆ /He	2B	2B	3
Li ₈ ZrO ₆ /HTS	2B	2B	3
Li ₂ O/H ₂ O/Be	2A	2A	2A
Li ₂ O/He/Be	2A	2A	3
Li ₂ O/HTS/Be	2B	2B	3
Li ₈ ZrO ₆ /H ₂ O/Be	2B	2B	2B
Li ₈ ZrO ₆ /He/Be	2B	2B	3
Li ₈ ZrO ₆ /HTS/Be	2B	2B	3
Li ₂ O/H ₂ O/Pb	2B	2B	2B
Li ₂ O/He/Pb	2B	2B	3
Li ₂ O/HTS/Pb	2B	2B	3
TC/H ₂ O	3	3	3
TC/He	3	3	3
TC/HTS	3	3	3
TC/H ₂ O/Be	1	1	1
TC/He/Be	1	1	3
TC/HTS/Be	2B	2B	3
TC/H ₂ O/Pb	2B	2B	2B
TC/He/Pb	2A	1	3
TC/HTS/Pb	2A	1	3
SB WITH NEUTRON MULTIPLIER OUTBOARD, NONBREEDING INBOARD. SB/He/Be: -/H ₂ O	2A	2A	2B

favourable properties of the ferritic and vanadium alloys to fusion reactor conditions - the uncertainty of this procedure has been pointed out in Section 2.2.1.

Table 6-2 shows that helium cooling is viable for Li₂O without a neutron multiplier but water cooling in the same concept is not. Even with a Be multiplier, water cooled Li₂O achieves only a 2A ranking. Li₈ZrO₆ does somewhat worse than Li₂O. These rankings were largely made on the basis of neutronics, i.e. low tritium breeding ratios. A water-cooled ternary ceramic with a neutron multiplier, Be and Pb are both acceptable, gets a top ranking as do the same concepts with He cooling. The remarkable thing about this table, and indeed also Table 6-1, is that while a great many combinations have been winnowed out in the selection process, all of the main breeder materials remain as possibilities. Therefore, if these preliminary results are carried over to the final report of the BCSS, no existing line of blanket research is likely to be conclusively closed. Rather, the BCSS will at most pinpoint the best type of blanket concept (breeder/coolant/multiplier + structural material) to which a specific breeder material can be applied. As indicated in Section 2, no definitive choice of a blanket system can be made on the basis of current data; the BCSS is unlikely to change this situation.

6.2.2 U.S. R&D Program

In the U.S. no decision has been yet made on the next generation of fusion devices, although many concepts including FED (Section 2.3.6), TNS, ETR, TFCX, DCT, DEMO (Section 2.3.3), FPD (Section 2.3.5), etc. have been studied. Therefore, in contrast to the EEC where NET will probably follow JET and Japan where FER will come after JT-60, there is now no machine focus for the U.S. blanket program. Recently another study, FINESSE[314], has been initiated at UCLA to decide whether one near-term fusion machine can fulfil the dual requirements of plasma physics and engineering testing or if separate devices are required for each of these tasks. Superimposed on this, particularly in the US program, is the broader question of a future selection between the tokamak and mirror concepts as the main reactor type. Therefore, predictions of long-term directions for the US program must be treated with some caution.

The internal organization of breeder blanket work in the U.S. is largely determined by that of the primary sponsoring agency - the U.S. Department of Energy (DOE). The fusion development and technology program is divided among the Plasma Technologies, Reactor Technologies and Reactor Systems Design branches of the DOE; the last two are relevant to breeder R&D. Reactor Technologies covers fusion systems engineering including blanket/shield components and tritium processing, environment and safety, materials radiation facilities (ORR and RTNS-II) and materials. The latter task includes alloy development (with the "path" structure discussed in Section 2.2.1), radiation damage analysis and fundamental studies, plasma materials interaction (first wall effects) and special purpose materials which encompasses breeder materials. Reactor Systems Design includes projects such as the BCSS, the large reactor studies (e.g. MARS and STARFIRE) and support for the FED centre. An additional integrative term for the blanket components of the U.S. program is the first wall/blanket/shield program; this is a technical rather than an organizational terminology. The yearly budget for the U.S. breeder program is estimated to be in the order of \$8-10 M, excluding tritium management facilities and in-reactor tritium recovery experiments (e.g. TRIO)[315]. For solid breeder blanket work alone, the effort is in the order of 10 man-years/year. Since accounting policy varies from country to country and indeed, between organizations within a particular country, this and other such cost estimates below are only intended as rough guides to the magnitude of the programs.

The U.S. work on liquid metal breeders presents somewhat of an anomaly, since the major liquid lithium loop in the U.S., ELS (Section 4.2.5), has been constructed for another purpose, i.e. as the FMIT target system. Although a great deal of valuable data for breeders has been obtained from the ELS, its operating conditions are not those that would be required in a liquid lithium blanket; in particular, the temperature of the flowing lithium is very much lower. Work on corrosion and compatibility of liquid metal systems under more realistic conditions for fusion, but in very much smaller loops, is being done at ANL, ORNL and the University of Wisconsin (Section 4.3). There is also work on the safety of liquid metal systems being done at EG&G, Idaho and HEDL. It appears from the information now available that the situation on liquid

metal breeders in the U.S. will not change significantly in the near term; any such change will probably come as a result of planning arising from the conclusions of the BCSS study.

The U.S. solid breeder program was launched in 1980 as a result of a workshop held by the DOE [316]. Effort on lithium ceramics was initiated shortly thereafter and two in-reactor tests have now been done in the U.S. - FUBR-1A (Section 5.4.2) and TRIO-01 (Section 5.5.3.2). Figure 6-1 is a schematic of the U.S. solid breeder program based largely on [317]; it should be understood that this figure is illustrative only and is certainly not intended to be definitive. The U.S. solid breeder materials development program is conducted by ANL where fabrication, properties measurement, characterization and specification of lithium ceramics is done. ANL was also the lead laboratory for the TRIO-01 sweep gas test which was done in the ORR reactor at ORNL. HEDL is responsible for the FUBR test series of capsule irradiations of lithium ceramics including the design of the experiments and post irradiation examination. Two industrial organizations also participate in the program. MDAC does work on materials preparation and characterization, and is responsible for the compilation of data on fusion materials in handbook form. GA Technologies does thermal effects studies on lithium ceramics (Section 5.3.2) and has the responsibility for supplying the material for the LBM (Section 3.5).

A considerable part of the U.S. effort in solid breeders has concentrated on materials properties [317]. Major accomplishments thus far include the development of an analytical capability for determining the low-level moisture content in breeder materials, specifically important for Li_2O , and a technique for low-level lithium carbonate analysis. The latter is important since lithium carbonate is used as a starting material for the preparation of lithium ceramics (Section 5.2.1.1). It is anticipated that these activities will continue to play an important part in the future program. On the other hand, although another major capsule irradiation test, FUBR-1B, is now in the planning stage, no sweep gas tests further to TRIO-01 are scheduled. This is assumed to be due to budgetary restraints and it is not clear how this situation will be resolved in the longer term.

US-SOLID BREEDER R&D PROGRAM PLAN

YEAR TASK \	81	82	83	84	85	86	87	88	89	90
SYSTEMS	<u>BCSS</u> <u>Lithium Breeder Module(LBM)</u> <u>FINESSE Study</u>									
FABRICATION	<u>Preparation /Fabrication of Materials</u>									
PROPERTIES	<u>Thermophysical properties</u> <u>Mechanical Properties</u>									
IRRADIATION TESTS	<u>TRIO-01</u> <u>FUBR-1A</u> <u>FUBR-1B</u> <u>FUBR-2</u>									
FUNDAMENTAL STUDIES	(in conjunction with fusion materials program)									

Figure 6-1 Schematic of U.S. solid breeder program

The U.S. breeder program is the most varied anywhere but because of this diversity, its future course is more difficult to predict since no choice of options has yet been made.

6.3 EEC Program

The EEC blanket program, which is just beginning, has been planned in the context of NET and thus, it has a definite machine focus in contrast to the US program. Table 6-3 shows the categories of the blanket R&D program; the latter is one of several EEC programs in the fusion technology area, all of which are planned for a five year period with reviews at three year intervals. This particular plan is a result of a very recent EEC blanket study[318] which made recommendations along these lines; information about their proposed implementation has been obtained from other sources[317,319] to derive the picture presented in this section.

Project B-1 comprises the feasibility evaluation of blanket design concepts with the objectives of determining the best-suited materials for further investigation and assessing the impact of the experimental results, obtained in the other projects and elsewhere, on the proposed design concepts. In essence, this program component will tend to unify the total effort in evolving a feasible blanket design. B-2 and B-3 are supplementary to it. B-2 is the support of neutronics work through the improvement of computational tools and the nuclear data required, and B-3 is currently envisaged as a study to determine whether a benchmark experiment is necessary and if so, its cost, timing, etc. For the first five year program, the agreed expenditures for B-1 to B-3 respectively are 3.5, 1.79 and 0.27 MECU (where ECU means European Currency Unit $\approx \$1$ U.S.); additional funding of 3.5 and 2.2 MECU is possible but not confirmed for B-1 and B-2, respectively. To put these figures in perspective, 0.13 MECU is taken to be one man-year[318] and therefore, the 3.5 MECU over five years would imply an effort of about 5 man-years/year for B-1.

The liquid metal breeders are covered under projects B-4 to B-10. However, it appears that B-10 will receive no EEC financing in the current five-year plan. The funding levels are 1.0, 1.0, 2.0, 03., 0.7 and 1.7 MECU for tasks B-4 to

Table 6-3 EEC Blanket R&D Program Components for Current Five-Year Plan

- i) Design and Neutronics
 - B - 1 Blanket Design Studies
 - B - 2 Development of Computational Tools for Neutronics
 - B - 3 Neutronics Benchmark Experiment

- ii) Liquid Breeder Materials
 - B - 4 Development of Impurity Monitoring Devices for Use in Li and ^{17}Li - ^{83}Pb Environments
 - B - 5 Effect of Strong Magnetic Fields on Corrosion and Deposition Reactions in Flowing Liquid Breeder Systems
 - B - 6 Corrosion of Structural Materials in Flowing ^{17}Li - ^{83}Pb
 - B - 7 Mass Transfer in Dynamic Pure Lithium
 - B - 8 Tritium Extraction from ^{17}Li - ^{83}Pb : Inert Gas Bubbling
 - B - 9 Tritium Extraction Based on the Use of Solid Getters
 - B - 10 Safety Aspects of the Interaction Between ^{17}Li - ^{83}Pb and Water

- iii) Solid Breeder Materials
 - B - 11 Fabrication of Ceramic Breeder Materials
 - B - 12 Characterization of Ceramic Breeder Materials
 - B - 13 Measurement of Physical, Mechanical and Chemical Properties
 - B - 14 Compatibility with Cladding Materials
 - B - 15 Irradiation Testing
 - B - 16 Tritium Recovery

B-9 making a total of 6.7 MECU - an additional 1.0 MECU is also possible for B-8. As can be seen from these tasks and their budgets, the EEC emphasis in liquid metal breeders is on 17Li-83Pb as compared with liquid Li. The former has not only been judged to be a better prospect for a breeding material, but also because more R&D is required for it than for liquid Li[318]. Thus, this choice of 17Li-83Pb is a deliberate one in the EEC program plan. Section 4.2.5 discussed the liquid metal work at Mol laboratories in Belgium[159]. It was indicated during a visit that corrosion studies and development of impurity monitoring methods will continue to be a high priority. Future work will also include MHD studies, and some work on the use of the 17Li-83Pb eutectic, which is not commercially available and must be manufactured. The MHD studies will concentrate on the interactions between magnetic fields and magnetic corrosion products, using a test section of an existing liquid Li loop. The magnet coils to produce the field (≈ 2 Tesla over 1 metre) are already on site, and the core to concentrate the field lines is being designed. The direct MHD-thermalhydraulic interaction study, which requires larger piping than available in the lithium loop is not at present being supported, but will be performed in a future loop now being designed, and scheduled to start up in the summer of 1984. This new loop will also be designed mechanically to use 17Li-83Pb. There are plans to carry out 17Li-83Pb corrosion and purification studies in a smaller natural convection test stand at first. Clearly this laboratory can be expected to be heavily involved in the liquid metal tasks of the EEC program, with JRC/Ispra as another likely participant.

The solid breeder tasks B-11 to B-16 are budgeted to 16.1 MECU over the five-year period. As seen in Section 5.2.3.2, substantial EEC work has already been done in project areas B-11 to B-12 in the EEC, notably in France. These components include the manufacturing of Li ceramics (in the EEC the emphasis is on the lithium silicates and aluminates), the correlation of properties to fabrication methods and parameters, and reproducible production according to specifications. The main objective of these components is to produce formed Li ceramics (e.g. pellets) with well-defined densities, grain sizes, moisture contents and impurity levels for use in the irradiation experiments of B-15 and B-16. Having produced these specimens it is also necessary to investigate

their physical, mechanical and chemical properties (B-13), including compatibility with cladding materials (B-14). Physical properties measurements are intended to cover such items as heat capacity, thermal conductivity and thermal expansion. Mechanical properties to be investigated will include Young's modulus, thermal shock resistance, compressive strength, thermal creep, etc. Chemical properties will include thermodynamics of phase changes, volatility, chemical reactivity with water and air, tritium solubility, diffusion and release. The intention is to correlate these properties with the observed in-reactor behaviour of the Li ceramics. As indicated, the corrosion/compatibility component, B-14, is assigned its own category.

Task B-15 refers to capsule irradiations in the sense of FUBR-1A (Section 5.4.2). The objective is to irradiate Li silicates both in a thermal and in a fast neutron environment in order to evaluate their dimensional, structural and property changes under irradiation. Post-irradiation annealing would also be used to study tritium retention and release. Task B-16 comprises He - He gas tests analogous to TRIO-01 (see Section 5.5.3.2) where the objective is to study tritium release during irradiation and to do post-irradiation examination of the samples similar to B-15. At the time of the Albuquerque workshop[317], three EEC groups were competing for the solid breeder program: Springfields (UK)/Petten (Netherlands), Karlsruhe (Germany)/Saclay (France), and Mol (Belgium)/Casaccia (Italy). The execution of the tasks will, therefore, likely be divided among these labs in a somewhat complex manner. For example the German-French proposal included two experiments under B-15, one to be done in the OSIRIS (Saclay) reactor and the other to be done in the KNK II (Karlsruhe) reactor. For B-16, sweep gas tests were to be performed in the SILOE (Grenoble) reactor and the DIDO (Jülich) reactor. The OSIRIS work was scheduled to begin in 1984 May and the SILOE work would commence in the fall of 1984. How precisely the solid breeder program will be divided among the various EEC laboratories is not clear at this time.

6.4 Japanese Program

In contrast to the U.S. and EEC programs, which are pursuing the liquid metal and solid breeder options in parallel, the Japanese have opted for Li_2O as

their primary breeder material. And, since the late 70s, breeder research in Japan has been concentrated on this one substance, leading to a very well-focussed program. The FER reactor concept (Section 2.3.7) provides a machine objective for the program with a Li₂O breeder blanket (TBR ~ 1.0) slated for this device.

The lead agency for fusion materials R&D in Japan is JAERI (Japan Atomic Energy Research Institute), in particular its Department of Fuels and Materials Research. Work in the universities (Osaka, Nagoya, Tokyo, etc.) is supported by the Ministry of Science, Education and Culture and there is also extensive industrial involvement by firms such as Mitsubishi and Kawasaki[320]. A variety of coordinating mechanisms such as the Research Committee on Fusion Reactor Materials of JAERI, are used to organize the overall program. No official estimate of the funds specifically allocated to breeder blanket R&D is available. In 1982, some 19 teams were at work in the Japanese universities on fusion materials problems with some 125 M Yen (0.5 M\$) whereas JAERI's fusion budget was about 160 M\$ in the same year. Based on these and other figures in [320], a guess at the Japanese breeder program would be in the order of 2-3 M\$ per year.

The Japanese program, Figure 6-2, comprises fabrication of Li₂O, including materials characterization and specification, and investigation of its thermo-mechanical, physical and chemical properties. Notable work in this area has been an extensive investigation of H, D, and T solubility in Li₂O (Section 5.5.1.3) and weight loss measurements of Li₂O pebbles to clarify the mass transfer of Li₂O due to LiOH production in H₂O containing gas streams (Section 5.3.2). The compatibility of Li₂O with blanket structures under LiOH attack has also been studied (Section 5.3.4). At JAERI, there has also been a concentrated effort on research into fundamental radiation processes in Li₂O pellets and single crystals under both reactor irradiation and oxygen ion bombardment in accelerators. A continuing program in this area is planned using reactors, accelerators and neutron sources: FNS (Fast Neutron Source) in Japan and RTNS-II (Rotating Target Neutron Source-II) in the U.S.

JAPAN-SOLID BREEDER R&D PROGRAM PLAN

YEAR TASK	81	82	83	84	85	86	87	88	89	90
SYSTEMS	<u>FER Blanket Design</u>									
FABRICATION	<u>Lab. Scale Lithium Oxide Tests</u> <u>Advanced Lithium Oxide</u> <u>Fabrication and quality control kg scale</u>									
PROPERTIES	<u>Physical,chemical and mechanical properties and compatibility</u> <u>Engineering Test,Safety</u>									
IRRADIATION TESTS	<u>Initial</u> <u>0.2 % B.U.</u> <u> </u> <u>0.8 % B.U.</u> <u> </u> <u>0.8 % B.U. Grain</u> <u> </u> <u>1.0 % B.U.</u>									
FUNDAMENTAL STUDIES	<u>Radiation Damage,T and He behaviour,Transmutation</u> <u>(Reactor,ion accelerator,FNS,RTNS-II)</u>									

Figure 6-2 Schematic of Japanese solid breeder program

A series of in-reactor sweep gas tests is now underway in Japan and the results of the first one were recently reported[306] (Section 5.5.3.2). It is planned to do these tests at increasingly higher lithium burn-ups (B.U.) over the next few years, (see Figure 6-2), and also to study a variety of grain size effects. Overall, the Japanese program is a well coordinated effort concentrated on Li₂O.

6.5 International Collaboration in Blanket R&D

The framework for Canadian collaboration in fusion with other countries has been built up by the National Research Council of Canada (NRC) in its role as lead agency for the coordination of fusion activities. There are two fusion-relevant multinational bodies to which Canada belongs: the International Energy Agency (IEA) and the International Atomic Energy Agency (IAEA). These will be discussed in Sections 6.5.1 and 6.5.2, respectively. In addition, NRC has been active in negotiating bilateral agreements with the U.S., the EEC and Japan, to be discussed in Section 6.5.3. There has been a long-standing tradition of international collaboration in fusion that continues to the present time. This arises from the magnitude and complexity of the R&D problems involved and because no single fusion program has the capability of covering all areas of interest. Today, the general climate for Canadian collaboration in fusion is excellent, as will be seen in what follows.

6.5.1 IEA

The IEA was set up by the Western Allies in the early 1970s as a response to the Middle East oil embargo; it is an organ of the Organization for Economic Cooperation and Development (OECD) based in Paris. As such the OECD/IEA continues to play a central role in the Western Alliance as a mechanism for economic and scientific cooperation. For example, at the Versailles summit of Western leaders in 1982, fusion was specifically set out as an area for collaboration between the western nations. Therefore, the IEA route for multi-national cooperation on fusion has influential political backing, both in Canada and in other major western countries.

The coordination of fusion research between the partners (for fusion they are the U.S., the EEC, Japan and Canada with Australia likely to join in the near future) is done through the Fusion Power Coordinating Committee (FPCC). This body makes overall policy, whereas the detailed conduct of the collaborations is done through specific Implementing Agreements. At this time there are three such agreements; one refers to the Large Coil Project (LCP) which is a cooperative activity to build and test superconducting magnets for fusion applications - Canada doesn't participate in this effort. A second agreement covers the TEXTOR tokamak located at Jülich, Germany. Its goal is to investigate certain areas of fusion technology with emphasis on plasma-first wall problems. Canada has contributed 5 man-years to its construction and is entitled to about 7% of the experimental time of the machine.

It is the third implementing agreement, for a program of research and development on Radiation Damage in Fusion Materials, that is of most interest in the breeder blanket field. The stated aims of this agreement are to do cooperative research, development, demonstrations and information exchanges on fusion materials, including design and construction of radiation facilities, neutron irradiation experiments and related plasma irradiation experiments. The agreement is supervised by an executive committee with representatives from the U.S., the EEC, Japan, Switzerland and Canada. The work is organized under two annexes. Annex I concerns FMIT (Section 2.2.1) and covers its design, development, construction and preparation for use both at HEDL and Los Alamos. Specific topics in this annex are the design of the accelerator and its ion source, target physics including neutronics and lithium system engineering, and the preparation for its radiation damage testing program. The main provision for implementation is the assignment of personnel by the collaborating countries to the FMIT project - each participating country may assign up to three scientists at Los Alamos and up to five scientists at HEDL at the expense of the sending country. This, in effect, gives Canada a wide scope for participating in FMIT. Recently, as indicated in Section 2.2.1, the question of international funding for FMIT has arisen and was investigated by an IEA expert panel[14]. What effect, if any, this will have on the current operation of Annex I is uncertain.

Annex II is a mechanism for joint experimentation on fusion materials encompassing joint collaborative experiments, information exchange and the assignment of experts on radiation damage for up to one-year periods at the laboratories of the other participants. Since this annex is not based around a facility (and seems to be the only IEA program of this kind), a Working Group, reporting to the executive committee, has been set up to operate it. This body has coordinated an international experiment on radiation damage in stainless steel involving irradiations in several reactors in the U.S., the EEC and Japan; Canada does not participate in this experiment. The recent Albuquerque Workshop on Solid Breeder Materials, was sponsored by the Annex II group (Tables 6-4 to 6-6 were a result of this meeting)[317]. It was valuable not only for information exchange between the IEA countries on this topic but also more importantly was intended to pave the way for cooperative programs in solid breeders. Canada participated in the workshop and has an excellent opportunity to join in this particular collaboration at an early stage.

6.2 IAEA

The IAEA is a United Nations (UN) body dedicated to the peaceful uses of atomic energy. Because of its broad membership, it is unfortunately subject to a variety of political difficulties resulting from East-West tensions superimposed on a background of a North-South divergence of views on its objectives - these are the same problems that afflict most UN organizations at this time. Therefore, it is not likely to be as effective as the IEA in promoting fusion collaborations of interest to Canada. However, there are several useful IAEA activities in fusion.

The INTOR activity has already been discussed in Section 2.3.6. Canada does not have the personnel and financial resources to field a team capable of fully contributing to INTOR. Nor does Canada have a national next-stage tokamak design group, as do the other participating countries, that would form the nucleus for a Canadian INTOR team. Therefore, there has only been a small indirect contribution by means of the recent CFTP participation in some work with the U.S. FED/INTOR centre[321]. A similar possibility for work in the NET project of the EEC is also an opportunity for Canadian work on a blanket

Table 6-4

Solid Breeder Material Sources - Primary Materials (Powders) from [317]

Material	Source	Type	Particle Size (μm)	Purity
<u>US</u>				
Li_2O	ANL	Laboratory	3	Good
	GA	Laboratory	20	Good
	CERAC	Commercial	Varied	Good (?)
	LITHCOA	Laboratory	Varied	Good (?)
LiAlO_2	ANL	Pilot plant	1	Good
	GA	Laboratory	20	Good
Li_4SiO_4	MDAC	Laboratory	2	Good
	GA	Laboratory	20	Good
Li_2ZrO_3	MDAC	Laboratory	2	Good
Li_8ZrO_6	HEDL	Laboratory	?	Good
<u>EEC</u>				
Li_2SiO_3	KFK Karlsruhe	Laboratory	30	High
LiAlO_2	ENEA	Laboratory		?
LiAlO_2	CEA, Saclay	Laboratory	Several	Good
Li_2SiO_3	Springfields	Laboratory	0.8	Good
Li_2SiO_3	CEN (Mol)/ENEA	Laboratory		?
<u>Japan</u>				
Li_2O	CERAC (U.S.)	Commercial	Varied	Good
	Honjo	Laboratory	?	Good
	Tomiyama	Laboratory	?	Good
<u>Canada</u>				
No sources				

Table 6-5

Solid Breeder Material Sources - Formed Materials from [317]

Material	Form	Source	Process	Grain Size (μm)	Porosity (% TD)
<u>US</u>					
Li_2O	Pellet (2.5 cm x 2.5 cm)	GA	Pressing & sintering	45	75-85
	Pellet (~1 cm x 1 cm)	ANL	Sintering	60	85
	Pellet (~2 cm)	HEDL	Hot pressing	3	85
	Spheres Agglomerates	Research Dynamics Inc.	Molten LiOH	?	Porous ?
LiAlO_2	Pellets (~1 cm)	HEDL	Hot pressing	5	60-95
	Minipellets	ANL	Sintering	45	80
	Spheres	GA	Sintering	?	80
Li_4SiO_4	Pellets (~1 cm)	HEDL	Hot pressing	5	85
Li_2ZrO_3	Pellets (~1 cm)	HEDL	Hot pressing	5	85
Li_8ZrO_6	Pellets (~2 cm)	HEDL	Hot pressing	9	90
<u>EEC</u>					
LiAlO_2	Pellets	CEA, Saclay	Compression, sintering	1-30	60-80
Li_2SiO_3	Pellets	KFK Karlsruhe	Sintering	10-50	70
Li_2SiO_3	Pellets	Springfields	Hot pressing	0.8	70-100
<u>Japan</u>					
Li_2O	Pellets (1.1 cm x 1.1 cm)	JAERI	Pressing & sintering	5-50	80-86 (70-90)
	Pellets	Mitsubishi	Pressing & sintering	10	80-85
	Single crystal (~0.8 cm x 10 cm L)	JAERI	Floating zone Melting		100
<u>Canada</u>					
No sources					

Table 6-6

Solid Breeder Materials in R&D Programs from [317]

S = Sphere Pac P = Pellets C = Single crystal x = Done/in progress
 + = Proposed/planned Fab = Material fabricated Irrad. = Irradiation test

Country	US		EEC		Japan		Canada	
Material	Fab.	Irrad.	Fab.	Irrad.	Fab.	Irrad.	Fab.	Irrad.
Li_2O	S P C	x +		x		x +		
LiAlO_2	S P C	x +	x	+ x		x +		
Li_2SiO_3	S P C		x	+ x		x +		
Li_4SiO_4	S P C	+ +	x x	+ +				
Li_2ZrO_3	S P C		x x					
Li_8ZrO_6	S P C	+ +	x +					
$(\text{Li},\text{Be})_x$	S P C		+ +					

design concept now in a very early stage of development. It is probable that the main fusion nations will concentrate in future more on their own next-step designs in preference to INTOR. Hence, participation in NET and FED present the best paths for work by Canada in blanket systems rather than direct participation in INTOR itself.

A variety of other valuable fusion-related activities are undertaken by the IAEA. This includes the conference series "International Conferences on Plasma Physics and Controlled Nuclear Fusion Research", the tenth of which will be held in London in 1984 September. Various publications such as the journal "Nuclear Fusion", with its supplements and report series such as the "International Bulletin on Atomic and Molecular Data for Fusion", are products of the IAEA. Similarly, a variety of IAEA committees are used to periodically prepare a "Status of Fusion" report - the next is due in 1985. While the IEA is the best multilateral channel for Canadian collaboration in fusion at this time, the IAEA provides a useful mechanism for information exchange.

6.5.3 Bilateral Agreements

Bilateral agreements between Canada and other countries for cooperation on fusion are another means for enhancing Canadian access to the larger world fusion programs. At this time Canada is in the process of negotiating bilaterals with the US, the EEC and Japan. Although none of these has yet been signed, it is likely that the one with the EEC will be concluded first.

The EEC agreement is in the nature of an "umbrella" covering the general mechanisms for the exchange of personnel and information; no specific projects are named in it, but broad areas for cooperation are outlined. In the proposed agreement these would be:

- tokamak physics, including auxiliary heating, refuelling, diagnostics, data acquisition, and control instrumentation;
- fusion fuels, including requirements for the management of tritium and possible arrangements for its supply;
- remote manipulation;

- safety and environment problems related to fusion; and,
- high power electrotechnology.

The agreement would be supervised by a Joint Committee consisting of two representatives from Canada and two from the EEC. The proposed mechanisms for collaboration would be:

- exchange of information, including progress reports and other non-confidential scientific results which the parties have the right to disclose and which are either in their possession or available to them;
- mutual participation in scientific meetings organized by either party;
- exchange of experts for which each party shall bear the personnel expenses for the secondments of its own experts;
- conduct of joint experiments, studies and projects as agreed by the Joint Committee, especially with regard to NET and other facilities of both parties;
- exchange of materials, equipment and instrumentation.

Specific instances of collaboration would be approved by the Joint Committee in each case. The proposed agreement with the EEC is typical of bilaterals in that general principles are given for cooperation but individual approval of each project is required. Thus, a framework or "umbrella" for cooperation is set up with the advantage that the negotiations for each case do not have to start at a high level, since many of the broader issues have been settled in the agreement. Selection of a particular route for collaboration, i.e. multilateral or bilateral, will depend on the circumstances of the situation. What is clear is that there are ample mechanisms available, or soon to be put in place, which facilitate Canadian participation in the world's major fusion programs, including breeder blanket R&D.

6.6 Canadian Capabilities for Breeder Blanket R&D

There has been no Canadian program in fusion breeder blankets to date and liquid metal breeders do not appear to be a useful area for such a program. However, the experience and expertise generated largely by R&D for the CANDU

fission reactor forms a basis on which a solid breeder program could be launched. Here, this potential will be briefly outlined in general; a specific and detailed breeder blanket program for Canada will be given elsewhere[322].

6.6.1 Liquid Metal Breeders

Unlike some other countries pursuing fusion programs, Canada has had no substantial experience in the nuclear application of liquid metals, since there has been no Canadian LMFBR program. The work that has been done has involved the design of targets for accelerator-based neutron sources, in particular for proposed spallation-breeding concepts such as ING (Intense Neutron Generator)[323] and ZEBRA (Zero Energy Breeder Accelerator)[324]. Some liquid metal R&D for the former was done at CRNL in the 1960s (e.g. the work of [227]) and a small loop was operated[325]. These neutron sources envisaged flowing Pb-Bi eutectic targets with conditions not directly applicable to the fusion blanket case. Nevertheless, an enhanced R&D effort in neutron sources (e.g. [326]) would no doubt produce some useful by-product data in the liquid metal fusion breeder area, as has been the case in the FMIT program.

The initiation of a liquid metal facility in Canada purely for fusion work seems an unacceptable option at this time. In order to be competitive internationally, for instance with the loops at Mol (Section 4.2.5), would require catching up with a five- to seven-year lead in technology and would involve the construction of facilities costing several million dollars. Such facilities would have to be large enough to be capable of doing substantial engineering test work in order to make a significant international impact. This would have to be done with no existing base of expertise and experience to build upon and with little prospect of parallel funding. Opportunities for small laboratory-scale experiments in liquid metal compatibility and corrosion may exist in well-defined specific instances, and one such project has been initiated at the University of Western Ontario[327]. However, it should be recognized that the potential of this strategy for a breeder program is rather limited given the prevalence of this type of work internationally. Thus,

liquid metal breeders are not a viable basis for a Canadian breeder blanket program.

6.6.2 Solid Breeders

No specific expertise on lithium-bearing ceramics for fusion exists in Canada. However, substantial experience with ceramic nuclear fuels, i.e. especially uranium oxide, has been accumulated in the CANDU reactor program. This includes not only the fabrication and characterization of formed ceramics, but also sweep gas tests to study their in-reactor behaviour and post-irradiation examination to investigate the gross changes due to radiation damage[328]. These capabilities are now in place at CRNL. Therefore, the same technological base, i.e. experience with fission ceramic fuels, is present in Canada as in the other countries doing or contemplating such tests on lithium bearing ceramics.

Since the purpose of these irradiation tests is to study the evolution of tritium in the same manner as TRIO-01 (Section 5.5.3.2), it is essential to have capability in tritium handling and monitoring. In this aspect, Canada is particularly strong due to the nature of the CANDU reactor system. Both Ontario Hydro and AECL possess considerable expertise in tritium technology[329], thus enabling the investigation of the tritium-related properties of solid breeder materials.

A substantial capability for neutronics work has been built up in Canada, both in AECL and Ontario Hydro, and also in the universities. For solid breeder material irradiations it is necessary to calculate the radiation damage rate and the amount of tritium produced as a function of time for a given neutron spectrum (Chapter 3). Furthermore, it is essential to determine how well the conditions of the irradiation tests simulate those which would be present in a breeder blanket. Neutronics calculations also form the single most important tool for assessing blanket systems, i.e. in the determination of the tritium breeding ratios for given configurations (Chapter 3). Computer codes, nuclear data banks and the expertise needed to use them are all well established in Canada.

As was indicated in Section 5.4.1, investigations of the physical and chemical processes underlying the evolution of tritium from solid breeders has only just started, for example in Japan (Section 6.4). Such topics as the nature and type of defects produced under irradiation, the details of the trapping of tritium at these defects, the consequent effects on tritium mobility and surface phenomena all must be taken into account in modelling the macroscopic behaviour of solid breeder materials. This information at the atomic level is essential to the interpretation of the irradiation experiments. Such data can be obtained using ion beams from accelerators, and Canadian capability on this technique, and the relevant surface science methods, has already been surveyed by Kirkaldy et al.[330], in which the potential for significant Canadian contributions is shown to exist.

Expertise in the preparation of high-purity lithium compounds with low moisture levels, in the case of Li_2O , and very possibly with an enriched or depleted isotopic abundance, would have to be developed for a Canadian solid breeder program. It appears that lithium compound chemistry largely involves conventional methods, whereas experience in isotope separation techniques has already been established in the fission program although not specific to lithium isotopes. Therefore, it is anticipated that this aspect of work in solid breeder materials could be put into place in Canada without too great difficulty.

The discussion of Section 2.2.1 showed that an important factor in the design and assessment of a breeder concept is the choice of a structural material; neutron damage and helium generation by transmutation are fundamental limits on component lifetimes. Initial work on this topic is now underway at CRNL[331] which could be used to provide this essential component of a breeder blanket program.

A final program area for Canadian involvement in breeder blanket R&D would be in systems studies and engineering services. Technology developed for CANDU systems in such areas as tritium monitoring, heavy water and organic coolants, thermalhydraulics and low leakage valves and pump seals may well have

application to breeder blanket problems. The definition and elaboration of these applications should form part of a Canadian program in this area.

It is concluded that the scientific and technological nucleus of a Canadian solid breeder program is already in place and, as indicated above, this program will be presented in a separate report[322].

6.7 Summary

The three main world fusion programs with which Canada is likely to collaborate all have breeder blanket programs. The U.S. and EEC programs encompass both liquid metal and solid breeders, but that of Japan is entirely concentrated on lithium oxide. These foreign programs are still at a relatively early stage and a great deal of work remains to be done. The prospects for Canadian cooperation with these large programs in breeder blanket R&D are excellent, with a variety of multilateral and bilateral mechanisms available to facilitate collaboration. While liquid metal breeders do not appear to be a viable option for a Canadian program in this area, the scientific and technical resources for a solid breeder blanket program are largely now in place.

7. CONCLUSIONS AND RECOMMENDATION

7.1 Conclusions

The conclusions of the study may be summarized as follows.

- (a) The first generation of fusion reactors will use the deuterium-tritium fuel cycle. Since there is no feasible means of providing the required tritium from external sources, the production of tritium in a breeder blanket will be essential (Chapter 1 and appendices).
- (b) Lithium in the form of liquid metal or in lithium-bearing ceramics is the only element practical for tritium breeding in the near term. Both of these approaches are subject to substantial uncertainties in current knowledge and hence, no definitive choice of the best breeder system can be made at present (Chapter 2).
- (c) A large variety of breeder concepts have been investigated in conjunction with fusion reactor design studies that have brought to the fore the critical issues in the implementation of the two broad classes of breeders, thus setting the main themes for R&D. Neutronics calculations of the tritium breeding ratio and materials properties data are the major criteria used for determining the viability of proposed breeder configurations (Chapter 2).
- (d) The computer codes and data bases now available for neutronics calculations are sufficient to allow the initial screening of breeder concepts. However, the development of more sophisticated codes and the acquisition of more accurate nuclear data will be required to adequately assess the precise performance of practical breeder blankets (Chapter 3).
- (e) The critical issues for liquid metal breeders are safety, corrosion and compatibility, MHD effects and tritium control. The ultimate resolution of these problems will require the operation of large liquid

metal facilities to acquire the necessary engineering experience with these materials (Chapter 4).

- (f) For solid breeder materials, the critical issues are the tritium breeding ratio, tritium recovery, materials integrity, heat transport and corrosion and mass transport for lithium oxide. To a large extent, these problems can be investigated with existing facilities (Chapter 5).
- (g) Internationally, breeder blanket programs are still in an early stage and there is ample opportunity for Canadian collaboration with the larger programs. The funding levels of these activities are such that a Canadian program could have an international impact given the resources available (Chapter 6).
- (h) Existing Canadian expertise and experience indicate that a program in solid breeder materials could be pursued with reasonable assurance of success. However, a liquid metal breeder program is not a viable option for Canada at this time (Chapter 6).

7.2 Recommendation

It is recommended on the basis of these conclusions that Canada undertake a program in solid breeder materials (SBMs) consisting of (i) irradiation tests, (ii) fabrication of lithium ceramics, (iii) lithium compound chemistry, (iv) fundamental studies of SBMs, (v) neutronics, (vi) blanket structural materials, and (vii) blanket systems engineering.

8. REFERENCES

- [1] Bromberg, L., et al., "High Field Tokamaks with DD-DT Operation and Reduced Tritium Breeding Requirements", Nuclear Technology/Fusion 4, 264, 1983.
- [2] Gilligan, J.G., Evans, K. and Jung, J., "The Effective Cost of Tritium for Tokamak Fusion Power Reactors with Reduced Tritium Production Systems", Nuclear Technology/Fusion 4, 273, 1983.
- [3] Smith, D.L., "Blanket Materials for DT Fusion Reactors", Journal of Nuclear Materials 103/104, 19, 1981.
- [4] "Future Engineering Needs of Magnetic Fusion". A report on a workshop conducted by the Committee on Magnetic Fusion, National Research Council, Washington, 1982.
- [5] Abdou, M.A., "Tritium Breeding in Fusion Reactors", presented at the International Conference of Nuclear Data for Science and Technology, Antwerp, Belgium, 1982 September 6-10. Published as Argonne National Laboratory report ANL/FPP/TM-165, 1982 October.
- [6] Workshop on Fusion Blanket Technology, Erice, Italy, 1983 June 6-10.
- [7] Nygren, R.E., "Overview of First Wall/Blanket/Shield Technology and Progress", Nuclear Technology/Fusion 4, 1203, 1983.
- [8] Abdou, M.A., et al., "Blanket Comparison and Selection Study (Interim Report), Argonne National Laboratory, ANL/FPP/TM-177 (Draft), 1983 September.
- [9] Gold, R.E., et al., "Materials Technology for Fusion: Current Status and Future Requirements", Nuclear Technology/Fusion 1, 169, 1981.

- [10] Odette, G.R., Maziasz, P.J. and Spitznagel, J.A., "Fission-Fusion Correlations for Swelling and Microstructure in Stainless Steel", Journal of Nuclear Materials 103/104, 283, 1981.
- [11] Packan, N.H. and Farrell, K., "Simulation of First Wall Damage: Effect of the Method of Gas Implantation", Journal of Nuclear Materials 84/86, 677, 1979.
- [12] Grossbeck, M.L., et al., "Preparation of Nickel-Doped Alloys for HFIR Irradiation to Produce He", Alloy Development for Irradiation Performance, Quarterly Progress for Period Ending Dec. 31, 1979, Oak Ridge National Laboratory, DOE/ER-004511, p.100, 1980 April.
- [13] Klueh, R.L. and Bloom, E.E., "Radiation Facilities for Fusion Reactor First Wall and Blanket Structural Materials Development", Nuclear Engineering and Design 73, 101, 1982.
- [14] International Energy Agency "Report of the Panel on Fusion Materials and Testing", Paris, 1983 June.
- [15] Trego, A.L., "The FMIT Test Facility", presented at the 3rd Topical Meeting on Fusion Reactor Materials, Albuquerque, NM, 1983 September 19-22.
- [16] Yang, W.J.S. and Hamilton, M.L., "The Ductility and Microstructure of Precipitation - Strengthened Alloys Irradiated in HFIR", presented at the 3rd Topical Meeting on Fusion Reactor Materials, Albuquerque, NM, 1983 September 19-22.
- [17] Jung, J. and Abdou, M., "Assessments of Tritium Breeding Requirements and Breeding Potential for the STARFIRE/DEMO Design", Nuclear Technology/Fusion 4, 361, 1983.
- [18] Smith, D.L., et al., "Fusion Reactor Blanket/Shield Design Study", Argonne National Laboratory, ANL/FPP-79-1, 1979.

- [19] Carré, F., Proust, E. and Rocaboy, A., "Analysis of the Tritium Requirements for a Power Reactor", Nuclear Technology/Fusion 4, 93, 1983.
- [20] Baker, C.C., et al., "STARFIRE - A Commercial Tokamak Fusion Power Plant Study", Argonne National Laboratory, ANL/FPP-80-1, 1980 September.
- [21] Badger, B., et al., "NUMAK - A Tokamak Reactor Design Study", University of Wisconsin, UWFDM-330, 1979 March.
- [22] Iso, Y., "Fusion Reactor Design III", Nuclear Fusion 22, 671, 1982.
- [23] Abdou, M.A., et al., "A Demonstration Tokamak Power Plant Study (DEMO)", final report, Argonne National Laboratory ANL/FPP-82-1, 1982 September.
- [24] Abdou, M.A., "Demonstration Tokamak Power Plant", Nuclear Technology/Fusion 4, 579, 1983.
- [25] McCracken, G.M. and Stott, P.E., "Plasma-Surface Interactions in Tokamaks", Nuclear Fusion 19, 889, 1979.
- [26] "TASKA-Tandem Spiegelmaschine Karlsruhe - A Tandem Mirror Fusion Engineering Test Facility", Kernforschungszentrum Karlsruhe, KFK-331, 1982 June.
- [27] Henning, C.D., et al., "Fusion Power Demonstration", Nuclear Technology/Fusion 4, 67, 1983.
- [28] Kulcinski, G.L., et al., "A Commercial Tandem Mirror Reactor Design with Thermal Barriers - WITAMIR I", University of Wisconsin, UWFDM-375, 1980 October.
- [29] "Mirror Advanced Reactor Study - Interim Design Report", Lawrence Livermore National Laboratory, UCRL-53333, 1983 April.

- [30] Logan, B.G., "The Mirror Advanced Reactor Study (MARS)", Nuclear Technology/Fusion 4, 563, 1983.
- [31] Bullis, R., et al., "A Solid Breeder Blanket and Power Conversion System for the Mirror Advanced Reactor Study", Nuclear Technology/Fusion 4, 739, 1983.
- [32] Gordon, J.D., et al., "MARS High Temperature Blanket", Nuclear Technology/Fusion 4, 1233, 1983.
- [33] "International Tokamak Reactor: Zero Phase", International Atomic Energy Agency, Vienna, STI/PUB/556, 1980.
- [34] "International Tokamak Reactor: Phase One", International Atomic Energy Agency, Vienna, STI/PUB/619, 1982.
- [35] "The Fusion Engineering Device", General Atomic Company, DOE/TIC-11600, October 1981.
- [36] Tone, T., et al., "Conceptual Design of Fusion Experimental Reactor (FER)", Nuclear Technology/Fusion 4, 573, 1983.
- [37] "Japanese Contributions to IAEA INTOR Workshop, Phase IIA", Japan Atomic Energy Research Institute, JAERI-M-82-170 to 82-179, 1982 November.
- [38] "The Tokamak T-20 Demonstration Reactor", Kurchatov Institute Technical Report DLS-79-71, 1978.
- [39] Stacey, W.M., "Tokamak ETR Objectives, Characteristics and Critical Issues", Nuclear Engineering/Fusion 4, 46, 1983.
- [40] Head, C.R., "Nuclear Data Requirements of the Magnetic Fusion Power Program of the United States of America", Proceedings of the Advisory Group Meeting on Nuclear Data for Fusion Reactor Technology, International Atomic Energy Agency, Vienna, IAEA-TECDOC-223, p. 1, 1979.

- [41] Constantine, G., "Nuclear Data Requirements for Fusion Reactor Design - Neutronic Design, Blanket Neutronics and Tritium Breeding", Proceedings of the Advisory Group Meeting on Nuclear Data for Fusion Reactor Technology, International Atomic Energy Agency, Vienna, IAEA-TECDOC-223, p. 11, 1979.
- [42] Abdou, M.A., "Nuclear Data Requirements for Fusion Reactor Shielding", Proceedings of the Advisory Group Meeting on Nuclear Data for Fusion Reactor Technology, International Atomic Energy Agency, Vienna, IAEA-TECDOC-223, p. 91, 1979.
- [43] Bhat, M.R. and Abdou, M.A., "Nuclear Data Requirements for Fusion Reactor Nucleonics", Proceedings of the Fourth Topical Meeting on the Technology of Controlled Nuclear Fusion, King of Prussia, PA, October 14-17, 1980, Tenney, F.H. and Hopkins, C.C. (eds.). CONF-801011, p. 405, 1981 July.
- [44] Lee, J.D., Engholm, B.A., Dudziak, D.J. and Haight, R.C., "Fusion Reactor Nucleonics: Status and Needs", Proceedings of the Fourth Topical Meeting on the Technology of Controlled Nuclear Fusion, King of Prussia, PA, October 14-17, 1980, Tenney, F.H. and Hopkins, C.C. (eds.). CONF-801011, p. 367, 1981 July.
- [45] Abdou, M.A. and Maynard, C.W., "Calculational Methods for Nuclear Heating, Part I: Theoretical and Computational Algorithm", Nuclear Science and Engineering 56, 360, 1975.
- [46] Abdou, M.A. and Maynard, C.W., "Calculational Methods for Nuclear Heating - Part II, Applications to Fusion Reactor Blankets and Shields", Nuclear Science and Engineering 56, 381, 1975.
- [47] Muir, D.W. and Wyman, M.E., "Neutronic Analysis of a Tritium Production Integral Experiment", Proceedings of a Symposium on Technology of Controlled Thermonuclear Fusion Experiments and the Engineering Aspects of Fusion Reactors, Austin, TX, November 20-22, 1972. CONF-721111, p. 910, 1974 April.

- [48] Bachmann, H., et al., "Neutron Spectra and Tritium Production Measurements in a Lithium Sphere to Check Fusion Reactor Blanket Calculations", Nuclear Science and Engineering 67, 74, 1978.
- [49] Swinhoe, M.T. and Uttley, C.A., "Tritium Breeding in Fusion", Proceedings of the International Conference on Nuclear Cross-Sections and Technology, Knoxville, TN, 1979 October 22-26.
- [50] Lisowski, P.W., et al., "Cross-Sections for Neutron-Induced, Neutron Producing Reactions in ^6Li and ^7Li at 5.96 and 9.83 MeV", Los Alamos Scientific Laboratory, LA-8342, 1980 October.
- [51] Drake, D.M., Auchampaugh, G.F., Arthur, E.D., Ragan, C.E. and Young, P.G., "Double-Differential Beryllium Neutron Cross-Sections at Incident Neutron Energies of 5.9, 10.1 and 14.2 MeV", Nuclear Science and Engineering 63, 401, 1977.
- [52] Larson, D.C., "ORELA Measurements to Meet Fusion Energy Neutron Cross-Sections Needs", Proceedings of a Symposium on Neutron Cross-Sections from 10 to 50 MeV, 1980 May 12-14, Brookhaven National Laboratory, BNL-NCS-51245, 1980 May.
- [53] Haight, R.C. and Grimes, S.M., "Status of (n,charged particle) Measurements at LLL", Lawrence Livermore National Laboratory, UCRL-84341, 1980.
- [54] Dickens, J.K., et al., "Cross-Sections for Gamma Ray Production by Fast Neutrons for 22 Elements Between Z=3 and Z=82", Nuclear Science and Engineering 62, 515, 1977.
- [55] Drake, D.M., Arthur, E.D. and Silbert, M.G., "Cross-Sections for Gamma-Ray Production by 14 MeV Neutrons", Nuclear Science and Engineering 65, 49, 1978.
- [56] Ozer, O. and Garber, D., "ENDF/B Summary Documentation", Brookhaven National Laboratory, BNL-17541 and ENDF-201, 1973 May.

- [57] Howerton, R.J., "Evaluated Nuclear Cross-Section Library", Lawrence Livermore Laboratory, UCRL-50400, Vol. 4, 1971 April.
- [58] RSIC Data Library Collection, "VITAMIN-C, 171 Neutron, 36 Gamma-Ray Group Cross-Section Library in AMPX Interface Format for Fusion Neutronic Studies", Oak Ridge National Laboratory, DLC-41, 1977.
- [59] RSIC Data Library Collection, "MACKLIB-IV, 171 Neutron, 36 Gamma-Ray Group Kerma Factor Library", Oak Ridge National Laboratory, DLC-60, 1979.
- [60] Battat, M.E., LaBauve, R.J. and Muir, D.W., "The GAMMON Activation Library", Los Alamos Scientific Laboratory, LA-8040-MS, 1979 September.
- [61] Weisbin, C.R., Soran, P.D., Harris, D.R., LaBauve, R.J. and Hendricks, J.S., "MINX - A Multigroup Interpretation of Nuclear Cross Sections", Transactions of the American Nuclear Society 16, 127, 1973.
- [62] Wright, R.Q., et al., "SUPERTOG: A Program to Generate Finite Group Constant and P_N Scattering Matrices from ENDF/B", Oak Ridge National Laboratory, ORNL-TM-2679, 1969 September.
- [63] Greene, N.M., et al., "AMPX - A Modular Code System for Generating Coupled Multigroup Neutron-Gamma Libraries from ENDF/B", Oak Ridge National Laboratory, ORNL-TM-3706, 1976 March.
- [64] MacFarlane, R.E., Barrett, R.J., Muir, D.W. and Bricourt, R.M., "The NJOY Nuclear Data Processing System: User's Manual", Los Alamos Scientific Laboratory, LA-7584-M, 1978 December.
- [65] MacFarlane, R.E., "Energy Balance of ENDF/B-V", Transactions of the American Nuclear Society 33, 681, 1979.

- [66] Bartine, D.E., Oblow, E.M. and Mynatt, F.R., "Radiation Transport Cross Section Sensitivity Analysis - A General Approach Illustrated for a Thermonuclear Source in Air", Nuclear Science and Engineering 55, 147, 1974.
- [67] Gerstl, S.A.W., Dudziak, D.J. and Muir, D.W., "Cross Section Sensitivity and Uncertainty Analysis with Application to a Fusion Reactor", Nuclear Science and Engineering 62, 137, 1977.
- [68] Alsmiller, R.G., Jr., Santoro, K.T., Barisch, J. and Gabriel, T.A., "Comparison of the Cross Section Sensitivity of the Tritium Breeding Ratio in Fusion Reactor Blankets", Nuclear Science and Engineering 57, 122, 1975.
- [69] Gerstl, S.A., "SENSIT: A Cross Section and Design Sensitivity and Uncertainty Analysis Code", Los Alamos Scientific Laboratory, LA-8489-MS, 1980.
- [70] Bartine, D.E., "SWANLAKE, A Computer Code Utilising ANISN Transport Calculations for Cross Section Sensitivity Analysis", Oak Ridge National Laboratory, ORNL-TM-3809, 1973 May.
- [71] Weinberg, A.M. and Wigner, E.P., "The Physical Theory of Neutron Chain Reactors", The University of Chicago Press, 1958, Chapt. 9.
- [72] Dolan, T.J., "Fusion Research", Pergamon Press, 1982, Chapt. 7.
- [73] Engle, W.W., "ANISN--A One Dimensional Discrete Ordinates Transport Code with Anisotropic Scattering". Oak Ridge National Laboratory, Report ORNL-CCC-254, 1979.
- [74] Dupree, S.A., "Time Dependent Neutron and Photon Transport Calculations Using the Method of Discrete Ordinates", Los Alamos Scientific Laboratory, LA-4557, 1970 August.

- [75] Rhoades, W.A., "DOT 4.3 Two Dimensional Discrete Ordinates Radiation Transport Code", Oak Ridge National Laboratory, Report ORNL-CCC-320, 1979.
- [76] Henry, A.F., "Nuclear Reactor Analysis", The MIT Press, 1975, p.371-381.
- [77] Los Alamos Monte Carlo Group, "MCNP--A General Monte Carlo Code for Neutron and Photon Transport Version 2B". Los Alamos National Laboratory, LA-7346-M, Revised April 1981.
- [78] Emmett, M.B., "MORSE-CG-General Purpose Monte Carlo Multigroup Neutron and Gamma Transport Code with Combinational Geometry", Oak Ridge National Laboratory, ORNL-CCC-203, 1982.
- [79] Plechaty, E.F. and Kimlinger, J.R., "TARTNP: A Coupled Neutron-Photon Monte Carlo Transport Code", Lawrence Livermore Laboratory, UCRL 50400, Volume 14, 1976 July.
- [80] Leonard, B.R., "A Compendium of 14 MeV Neutron Source Experiments", Proceedings of the Magnetic Fusion Energy Blanket and Shield Workshop, Brookhaven National Laboratory, ERDA-76/117/1, p. 66, August 1975.
- [81] Maynard, C.W., "Integral Experiments for CTR Nuclear Data", Proceedings of a Symposium on Neutron Cross-Sections from 10~40 MeV, Brookhaven National Laboratory, BNL-NCS-50681, p. 375, 1977 July.
- [82] Kotov, V. and Shatalov, G.E., "Gas Cooled Blankets for a Hybrid Thermonuclear Reactor with Solid Lithium Containing Materials", Proceedings of the US-USSR Symposium on Fusion-Fission Reactors, Lawrence Livermore Laboratory, CONF 760733, p. 129, 1976 July.

- [83] Reupke, W.A. and Muir, D.W., "Neutronic Data Consistency Analysis for Lithium Blanket and Shield Design", Proceedings of a Conference on the Technology of Controlled Nuclear Fusion, CONF-760935, Volume 3, p. 861, 1976.
- [84] Weale, J.W., Goodfellow, H., McTaggart, M.H. and Mullendgr, M.L., "Measurement of the Reaction Rate Distribution Produced by a Source of 14 MeV Neutrons at the Centre of a Uranium Pile", Reactor Science and Technology 14, 91, 1961.
- [85] Haight, R.C., Lee, J.D. and Maniscalco, J.A., "Reaction Rates in a Uranium Pile Surrounding a 14 MeV Neutron Source: Calculations of the Weale Experiment", Nuclear Science and Engineering 61, 53, 1976.
- [86] Benjamin, P.W., Goodfellow, H., Gray, L. and Weale, J.W., "Measurements of Neutron Reaction Rates Produced by a 14 MeV Neutron Source at the Center of a Cylindrical Lithium Pile", Atomic Weapons Research Establishment, Aldermaston, AWRE NR4/64, 1964 September.
- [87] Cloth, P., et al., "Studies of the Space Dependent Tritium Production and the Fast Flux Distribution in a Lithium Blanket Experiment", Proceedings of the 8th Symposium on Fusion Technology, The Netherlands, p. 17, 1974 June.
- [88] Hall, R.J., "Measurement of 14 MeV Neutron Slowing Down in Graphite", BNL Annual Report for 1973 on Controlled Thermonuclear Reactor Technology, Battelle Pacific Northwest Labs., BNWL-1823, 1974 April.
- [89] Kappler, F., Rusch, D., Werle, H. and Wiese, H.W., "Determination of Neutron Spectra in a Lithium Sphere", Proceedings of the 8th Symposium on Fusion Technology, The Netherlands, 1974 June.
- [90] Maekawa, H., Seki, Y., Hiroaka, T. and Moriyama, M., "Uranium-238 to Uranium-235 Fission Ratio Distribution in Spherical Lithium-Metal Assemblies With and Without a Graphite Reflector", Nuclear Science and Technology 57, 335, 1975.

- [91] Johnson, R.J., Dorning, J.J. and Wehring, B.W., "Integral Tests of Nuclear Cross-Sections for Iron Above 1 MeV", *Transactions of the American Nuclear Society* 22, 799, 1975.
- [92] Smith, W.R., Jr. and Drapere, Linn, Jr., "Measured and Calculated Fast Neutron Spectra in a Graphite Medium", *Transactions of the American Nuclear Society* 22, 808, 1975.
- [93] Hasen, L.F., Wong, C., Komoto, T. and Anderson, J.P., "Measurements of the Neutron Spectra from Materials Used in Fusion Reactors and Calculations Using the ENDF/B III and IV Neutron Libraries", *Nuclear Science and Engineering* 60, 27, 1976.
- [94] Fritscher, V., Kappler, F. and Rusch, D., "Tritium Production Measurement in a Lithium Metal Sphere with New Techniques in Neutron Source Strength Determination", *Nuclear Instruments and Methods* 153, 563, 1978.
- [95] Guenther, C. and Kinnebrock, W., "The DTK One-Dimensional Transport Program", *Kernforschungszentrum Karlsruhe, EURFNR-927 (KFK-1381)*, 1971 March.
- [96] Goel, B., "Graphical Representation of the German Nuclear Data Library KEDAK, Part I: Non Fissile Materials", *Kernforschungszentrum Karlsruhe, KFK-2233*, 1975 December.
- [97] Reupke, W.A., "The Consistency of Differential and Integral Thermo-nuclear Neutronics Data", *Los Alamos Scientific Laboratory, LA-7067-*, 1978 January.
- [98] Hemmendinger, A., Ragan, C.E. and Wallace, J.M., "Tritium Production in a Sphere of ^6LiD Irradiated by 14 MeV Neutrons", *Nuclear Science and Engineering* 70, 274, 1979.
- [99] Carter, L.L., et al., "Monte Carlo Code Development in Los Alamos", *Los Alamos Scientific Laboratory, LA-5903-MS*, 1975 March.

- [100] Hansen, L.F., et al., "Neutron and Gamma-Ray Spectra from ^{232}Th , ^{235}U , ^{238}U and ^{239}Pu After Bombardment with 14 MeV Neutrons", Nuclear Science and Engineering 72, 35, 1979.
- [101] Hansen, L.F., Anderson, J.D., Wong, C. and Komoto, T., "Differential Integral Experiments for Testing Cross Section Evaluation for Fusion Reactors", Proceedings of a Symposium on Neutron Cross Sections from 10 to 40 MeV, Brookhaven National Laboratory, Upton, NY, 1977 May 3-5, BNL-NCS-50681, 1977 July.
- [102] Hansen, L.F., Wong, C., Komoto, T.T., Pohl, B.A. and Howerton, R.J., "Measurement and Calculation of the Neutron Emission Spectra from Materials Used in Fusion-Fission Reactors", Lawrence Livermore Laboratory, UCRL-84291, 1980.
- [103] Herzing, R., et al., "Experimental and Theoretical Investigations of Tritium Production in a Controlled Thermonuclear Reactor Blanket Model", Nuclear Science and Engineering 60, 169, 1976.
- [104] Iguchi, T., Nishitami, T., Takagi, J., Nakazawa, M. and Sekiguchi, A., "Neutron Spectra and Tritium Production Rate Measurements in the One-Dimensional LiF Slab Geometry as a Fusion Reactor Blanket Benchmark Experiment", Proceedings of the Fourth Topical Meeting on the Technology of Controlled Nuclear Fusion, King of Prussia, PA, October 14-17, 1980, Tenney, F.H. and Hopkins, C.C. (eds.). CONF-801011, p. 387, 1981 July.
- [105] Maekawa, H. and Seki, Y., "Absolute Fission-Rate Distributions in Lithium and Hybrid Fusion Blanket Assemblies, I - Experimental Method and Results", Journal of Nuclear Science and Technology 14, 97, 1977.
- [106] Seki, Y. and Maekawa, H., "Absolute Fission Rate Distribution in Lithium and Hydrid Fusion Blanket Assemblies, II Analysis and Evaluation", Journal of Nuclear Science and Technology 14, 210, 1977.

- [107] Seki, Y., Muir, D.W. and Maekawa, H., "Effect of Nonelastic Neutron Anisotropy on Fission Rates Measured in a Graphite Reflected Lithium Assembly", *Journal of Nuclear Science and Technology* 14, 680, 1977.
- [108] Nakamura, T., "Benchmark Experiments on Blanket Neutronics on Lithium Oxide System", presented at a Workshop on Fusion Blanket Technology, Erice, Italy, June 6-10, 1983.
- [109] Maekawa, H., Oyama, Y., Suzuki, T., Ikeda, Y. and Nakamura, T., "Measurements of Angular Flux on Surface of Li₂O Slab Assemblies and Their Analysis by a Direct Integration Transport Code BERMUDA", *Nuclear Technology/Fusion* 4, 1165, 1983.
- [110] Jassby, D.L., "Potential of the TFTR as a Fusion Neutron Test Facility", *Proceedings of a Conference on Fast, Thermal and Fusion Experiments*, Salt Lake City, UT, April 12-15, 1982.
- [111] Weikkinen, D.W. and Lagan, C.M., "Irradiations at RTNS-II", *Proceedings of a Conference on Fast, Thermal and Fusion Experiments*, Salt Lake City, UT, April 12-15, 1982.
- [112] Graumann, D.W., Creedon, R.L., Engholm, B.A., Lindgren, J.R. and Yang, L., "The TFTR Lithium Blanket Module Final Design and Materials Development", *Nuclear Technology/Fusion* 4, 1222, 1983.
- [113] Steiner, D., "The Nuclear Performance of Fusion Reactor Blankets", *Nuclear Applications and Technology*, 9, 83, 1970.
- [114] General Atomic Project Staff, "TFTR Lithium Blanket Module (LBM) Program", *Conceptual Design Report*. General Atomic, GA-A16226, 1981.
- [115] Sung, T.Y. and Vogelsang, W.F., "A Radioactive Calculation Code for Fusion Reactors", University of Wisconsin, UWFDM-170, 1976.

- [116] Jung, J., "Theory and Use of the Radioactive Code RACC", Argonne National Laboratory, ANL/FPP/TM-122, 1979 May.
- [117] Youssef, M.Z. and Conn, R.W., "On Isotopic Tailoring for Fusion Reactor Radioactive Reduction", Nuclear Technology/Fusion 4, 1177, 1983.
- [118] Conn, R.W., "The Engineering of Magnetic Fusion Reactors", Scientific American, 249, 60, 1983.
- [119] Gabriel, T.A., Amburgey, J.D. and Greene, N.M., "Radiation-Damage Calculations: Primary Recoil Spectra, Displacement Rates and Gas-Production Rates", Oak Ridge National Laboratory, ORNL/TM-5160, 1976 March.
- [120] Verschuur, K.A., "The Role of Neutronics in Blanket Design", Presented at the Workshop on Fusion Blanket Technology, Erice, Italy, June 6 - 10, 1983.
- [121] Lathrop, K.D., "THREETRAN: A Program to Solve the Multigroup Discrete Ordinates Transport Equation in (x,y,z) Geometry", Los Alamos Scientific Laboratory, LA-6333-MS, 1976 April.
- [122] Courtot, M., "Study of Some Numerical Schemes for Solving the Three-Dimensional Transport Equation", Proceedings of the International Topical Meeting on Advances in Mathematical Methods for the Solution of Nuclear Engineering Problems. Munich, FRG, April 27 - 29, 1981, Volume 1, p. 83, 1981.
- [123] Asaoka, T., Hyodo, T., Suzuki, T. and Kikuchia, S., "Summary Report on the Sixth International Conference on Radiation Shielding", Tokyo, Japan, May 16 - 20, 1981. Reported in the Radiation Shielding Information Center Newsletter No. 225, 1983.

- [124] Urban, W.T., Seed, T.J. and Dudyak, D.J., "Nucleonic Analysis of a Preliminary Design for the ETF Neutral-Beam-Injector Duct Shielding". Proceedings of the Fourth Topical Meeting on the Technology of Controlled Nuclear Fusion, King of Prussia, PA, October 14-17, 1980, Tenney, F.H. and Hopkins, C.C. (eds.). CONF-801011, p. 479, 1981 July.
- [125] Engholm, B.A., "Monte Carlo Neutronic Analysis for the TFTR Lithium Blanket Module", Nuclear Technology/Fusion 4, 381, 1983.
- [126] Filippone, W.Z., Woolf, S.A. and Lavigne, R.J., "Particle Transport Calculations with the Method of Streaming Rays", Nuclear Science and Engineering, 77, 119, 1981.
- [127] Daenner, W. "The Nuclear Performance of Various Breeding Materials", Presented at the Workshop on Fusion Blanket Technology, Erice, Italy, June 6 - 10, 1983.
- [128] Maroni, V.A., "A First Wall, Blanket and Shield Engineering Test Program for Magnetically Confined Fusion Power Reactors", Proceedings of the Fourth Topical Meeting on the Technology of Controlled Nuclear Fusion, King of Prussia, PA, October 14-17, 1980, Tenney, F.H. and Hopkins, C.C. (eds.). CONF-801011, p. 571, 1981 July.
- [129] Nygren, R.E., "Recent Developments in Fusion First Wall, Blanket and Shield Technology", Proceedings of the 7th International Conference on Structural Mechanics in Reactor Technology, Chicago, IL, 1983 August.
- [130] Sze, D.K., et al., "LiPb, a Novel Material for Fusion Applications", Proceedings of the Fourth Topical Meeting on the Technology of Controlled Nuclear Fusion, King of Prussia, PA, October 14-17, 1980, Tenney, F.H. and Hopkins, C.C. (eds.). CONF-801011, p. 1786, 1981 July.
- [131] Casini, G., et al., "Blanket Designs with Li-Pb Liquid Breeders", in "Fusion Technology 1982", Proceedings of the 12th Symposium on Fusion Technology, Jülich, 1982 September 13-17, Pergamon Press, Vol. 1, p. 623, 1983.

- [132] Farfaletti-Casali, F., et al., "Design of a Modular Blanket with Gas-Cooled Liquid Lithium", Proceedings of the 3rd Topical Meeting on the Technology of Controlled Nuclear Fusion, Santa Fe, NM, Vol. 1, p. 249, 1978 May.
- [133] Institution of Mechanical Engineers (London), "Pumps for Nuclear Power Plant", Convention papers, CP5, p. 149, 1974.
- [134] Atwood, J.M., private communication, Hanford Engineering Development Laboratory, 1983 July.
- [135] Baker, R.S., Blink, J.A. and Tessier, M.J., "Electromagnetic Pumping of Liquid Lithium in Inertial Confinement Fusion Reactors", Lawrence Livermore National Laboratory, UCRL-53356, 1983 March.
- [136] Kottowski, H.M., "Liquid Metal Experimental Facilities", Lecture Course on Thermohydraulics of Liquid Metals, Von Karman Institute for Fluid Dynamics, Brussels, 1983 June.
- [137] Grand, D., "Mixed Convection and Stratification Phenomena in Liquid Metals", Lecture Course on Thermohydraulics of Liquid Metals, Von Karman Institute for Fluid Dynamics, Brussels, 1983 June.
- [138] Kottowski, H.M., "Thermohydraulics of Liquid Metals", Lecture Course on Thermohydraulics of Liquid Metals, Von Karman Institute for Fluid Dynamics, Brussels, 1983 June.
- [139] Chao, J., Mikic, B.B. and Todreas, N.E., "A Parametric Study of a Lithium-Cooled Tokamak Blanket", Nuclear Technology 42, 22, 1979.
- [140] Carré, F., Tilliette, Z. and Remoleur, J., "Conceptual Study of a Lithium Lead Eutectic Blanket for a Power Reactor", Nuclear Technology/Fusion 4, 1101, 1983.
- [141] Wells, W.M., "ORNL Fusion Power Demonstration Study: Lithium as a Blanket Coolant", Oak Ridge National Laboratory, ORNL/TM-6214, 1978 April.

- [142] Misra, B., Smith, D.L. and Morgan, C.D., "Mechanical Design and Thermal Hydraulic Considerations for a Self-Cooled Lithium-Lead Blanket", Nuclear Technology/ Fusion 4, 1061, 1983.
- [143] Liu, Y.Y., et al., "Thermo-Structural and Thermal-Hydraulic Aspects of the STARFIRE/DEMO Tritium Breeding Blanket", Proceedings of the 7th International Conference on Structural Mechanics in Reactor Technology, Chicago, IL, 1983 August.
- [144] Bourque, R.F., "Flowing Pb₈₃Li₁₇ Liquid Metal Coolant in Fusion Reactors with High Power Densities and Magnetic Fields", Nuclear Technology/Fusion 3, 493, 1983.
- [145] Sutton, G.W. and Sherman, A., "Engineering Magnetohydrodynamics", McGraw-Hill, New York, 1965.
- [146] Kettani, M.A. and Hoyaux, M.F., "Plasma Engineering", Butterworths and Co., London, 1973.
- [147] Cairns, E.J., Cafasso, C.A. and Maroni, V.A., "A Review of the Chemical, Physical and Thermal Properties of Lithium that are Related to its Use in Fusion Reactors", The Chemistry of Fusion Technology, Proceedings of a Symposium on the Role of Chemistry in the Development of Controlled Fusion, D.M. Gruen, (ed.), Boston, 1972.
- [148] Hoffmann, M.A. and Carlson, G.A., "Calculation Techniques for Estimating the Pressure Losses for Conducting Fluid Flows in Magnetic Fields", Lawrence Radiation Laboratory, UCRL-51010, 1971 February.
- [149] Lielausis, O., "Liquid Metal Magnetohydrodynamics", Atomic Energy Review 13, 527, 1975.
- [150] Holroyd, R.J., "MHD Flow in a Rectangular Duct with Pairs of Conducting and Non-conducting Walls in the Presence of a Non-uniform Magnetic Field", Journal of Fluid Mechanics 96, 335, 1980.

- [151] Holroyd, R.J., "An Experimental Study of the Effects of Wall Conductivity, Non-uniform Magnetic Fields and Variable Area Ducts on Liquid Metal Flows at High Hartmann Number, Part 2, Ducts with Conducting Walls", *Journal of Fluid Mechanics* 96, 355, 1980.
- [152] Crocker, J.G. and Cohen, S., private communication, EG&G, Idaho Falls, ID, 1983 July.
- [153] Hagmann, D. and White, J., "Key Issues for Remote Inspection and Repair of a Tokamak", in "Fusion Technology 1982", Proceedings of the 12th Symposium on Fusion Technology, Jülich, 1982 September 13-17, Pergamon Press, Vol. 1, p. 57, 1983.
- [154] Spampinato, P.T., "Maintenance and Disassembly Considerations for the Technology Development Facility", *Nuclear Technology/Fusion* 4, 194, 1983.
- [155] Sviatoslavsky, I.N., Li, Y.T., Sze, D.K., "Mechanical and Thermal Design Aspects of the Blanket, and Maintenance Considerations of the Central Cell in MARS", *Nuclear Technology/Fusion* 4, 751, 1983.
- [156] Farfaletti-Casali, F., et al., "Mechanical Configuration and System Integration Studies of INTOR/NET", in "Fusion Technology 1982", Proceedings of the 12th Symposium on Fusion Technology, Jülich, 1982 September 13-17, Pergamon Press, Vol. 1, p. 581, 1983.
- [157] Fujisawa, N., Nishio, S. and Hiraoka, T., "Design Consideration and Remote Maintenance of INTOR J-11", in "Fusion Technology 1982", Proceedings of the 12th Symposium on Fusion Technology, Jülich, 1982 September 13-17, Pergamon Press, Vol. 1, p. 587, 1983.
- [158] Selander, W.N. and Carlick, E.C., information from a visit to Hanford Engineering Development Laboratory, 1983 July 11-12.
- [159] Selander, W.N., information from a visit to SCK/CEN, Mol, 1983 June 6.

- [160] Crocker, J.G. and Cohen, S., US Department of Energy Fusion Reactor Safety Research Program, Annual Reports, Fiscal Years 1980, 1981, 1982, EG & G, Idaho Falls, ID.
- [161] Rouhani, S.Z., Jones, J.L. and Merrill, B.J., "Application of ATHENA to STARFIRE Coolant- Blanket System Analysis", Nuclear Technology/Fusion 4, 465, 1983.
- [162] Roth, P.A. and Herring, J.S., "Pressurized-Water Cooling Tube Ruptures in a Fusion Blanket", Nuclear Technology/Fusion 4, 1121, 1983.
- [163] Jeppson, D.W. and Muhlestein, L.D., "Fusion Reactor Blanket Material Safety Compatibility Studies", EG and G, Idaho Falls, ID, unpublished report.
- [164] Whitlow, G.A., Wilson, W.L., Ray, W.E. and Down, M.G. "Materials Behaviour in Lithium Systems for Fusion Reactor Applications ", Journal of Nuclear Materials 85/86, 283, 1979.
- [165] Bazinet, G.D., Brehm, W.F., Down, M.G. and Matlock, D.K., "Corrosion Behaviour of Materials Selected for FMIT Lithium System", Nuclear Technology/Fusion 4, 718, 1983.
- [166] Olson, D.L., Reser, G.N. and Matlock, D.K., "Liquid Lithium Corrosion Rate Expressions for Type 304L Stainless Steel", Corrosion 36, 140, 1980.
- [167] Schlager, R.J., Patterson, R.A., Olson, D.L. and Bradley, W.L., "Stainless Steel Weight Loss in Nitrogen-Contaminated Liquid Lithium", Nuclear Technology 29, 94, 1976.
- [168] Barker, M.G. and Frankham, S.A., "The Effects of Carbon and Nitrogen on the Corrosion Resistance of Type 316 Stainless Steel to Liquid Lithium", Journal of Nuclear Materials 107, 218, 1982.

- [169] Casteels, F., et al., "Corrosion of Selected Materials in Dynamic Lithium", paper N3/3, Proceedings of the 6th International Conference on Structural Mechanics in Reactor Technology, Paris, August 17-21, 1981.
- [170] Rumbaut, N., et al., "Corrosion of Refractory Materials in Liquid Lithium", Conference on Material Behaviour and Physical Chemistry in Liquid Metal Systems, Karlsruhe, March 24-26, 1981.
- [171] Tortorelli, P.F., Devan, J.H. and Yonco, R.M. "Compatibility of Fe-Cr-Mo Alloys with Static Lithium", Journal of Materials for Energy Systems 2, 5, 1981.
- [172] Katsuta, H. and Furukawa, K., "On Contamination Effects on the Compatibility of Liquid Lithium with Mo, TZM, Nb, Stainless Steels, Ni and Hastelloy N in Stainless Steel Vessels at 600°C", Journal of Nuclear Materials 71, 95, 1977.
- [173] Shibata, K., et al., "Compatibility of Fusion Reactor Materials with Flowing Lithium", Presented at the 3rd Topical Meeting on Fusion Reactor Materials, Albuquerque, NM, 1983 September 19-22.
- [174] Casteels, F., et al., "Corrosion of Structural Materials in Dynamic Lithium", paper N2.5/3, Proceedings of the 5th International Conference on Structural Mechanics in Reactor Technology, Berlin, August 13-17, 1974.
- [175] Maniscalco, J.A., Berwald, D.H. and Meier, W.R., "The Material Implications of Design and System Studies for Inertial Confinement Fusion Systems", Journal of Nuclear Materials 85/86, 37, 1979.
- [176] Selle, J.E., "Corrosion of Iron-Base Alloys by Li", Proceedings of International Conference on Liquid Metal Technology in Energy Production, Champion, Pennsylvania, May 3-6, 1976, CONF-750503-P2.
- [177] Coen, V., et al., "Compatibility of AISI 316L Stainless Steel with the Li₁₇Pb₈₃ Eutectic", Journal of Nuclear Materials 110, 108, 1982.

- [178] Anderson, T.L. and Edwards, G.R., "The Corrosion Susceptibility of 2½Cr-1Mo Steel in a Lithium-17.6 wt. % Lead Liquid", Journal of Materials for Energy Systems 2, 16, 1981.
- [179] Wilkinson, B.D., Edwards, G.R. and Hoffman, N.J. "The Effect of Lead Concentration on the Corrosion Susceptibility of 2½Cr-1Mo Steel in a Lead-Lithium Liquid", Journal of Nuclear Materials 103/104, 669, 1981.
- [180] Sannier, J. et Santarini, G, "Etude de la Corrosion de Deux Aciers Ferritiques par le Plomb Liquide Circulant dans un Thermosiphon; Recherche d'un Modele", Journal of Nuclear Materials 107, 196, 1982.
- [181] Patterson, R.A., Schlager, R.J. and Olson, D.L., "Lithium Grain-Boundary Penetration of 304L Stainless Steel", Journal of Nuclear Materials 57, 312, 1975.
- [182] Reeves, J.A.Jr., Olson, D.L. and Bradley, W.L., "Grain Boundary Penetration Kinetics of Nitrided Type 304L Stainless Steel", Nuclear Technology 30, 385, 1976.
- [183] Ruedl, E., Coen, V., Sasaki, T. and Kolbe, H., "Intergranular Lithium Penetration of Low-Ni, Cr-Mn Austenitic Stainless Steels", Journal of Nuclear Materials 110, 28, 1982.
- [184] Chopra, O. and Smith, D.L., "Influence of a Flowing Lithium Environment on the Fatigue and Tensile Properties of Type 316 Stainless Steel", Presented at the 3rd Topical Meeting on Fusion Reactor Materials, Albuquerque, NM, 1983 September 19-22.
- [185] Chopra, O.K. and Smith, D.L., "Effects of Lithium Environment on the Fatigue Properties of Ferritic and Austenitic Steels", Journal of Nuclear Materials 103/104, 651, 1981.
- [186] Chopra, O.K., "Effects of Sodium and Lithium Environments on Mechanical Properties of Ferrous Alloys", Journal of Nuclear Materials 115, 223, 1983.

- [187] Chopra, O.K. and Smith, D.L., "Low-Cycle Fatigue Behaviour of HT-9 Alloy in a Flowing Lithium Environment", Presented at the Topical Conference on Ferritic Alloys for Use in Nuclear Energy Technologies, Snowbird, Utah, 1983 June 19-23, CONF-830659-4, 1983 June.
- [188] Chopra, O.K. and Smith, D.L., "Corrosion of Structural Alloys in Flowing Lithium and Eutectic Lead-Lithium Environments", Presented at the 3rd Topical Meeting on Fusion Reactor Materials, Albuquerque, NM, 1983 September 19-22.
- [189] Edwards, G.R., Matlock, D.K. and Olson, D.L., "Fatigue Crack Propagation Characteristics of Stainless Steel in Liquid Lithium in the Temperature Range of 200°C to 500°C", Hanford Engineering Development Laboratory, HEDL-TME-82-42, Section 3, 1983 April.
- [190] Edwards, G.R., Matlock, D.K. and Olson, D.L., "Evaluation of Fatigue Resistance in Lithium at 270°C of Seamless Type 321 Stainless Steel Bellows", Hanford Engineering Development Laboratory, HEDL-TME-82-42, Section 4, 1983 April.
- [191] Hammon, D.L., et al., "The Influence of Cyclic Loading on the Lithium Corrosion Behaviour of Reactor Materials", Journal of Nuclear Materials 103/104, 663, 1981.
- [192] Ferrici, F., et al., "Influence of Lithium Exposure on the Uniaxial Tensile Properties of a Cr-Mn Austenitic Stainless Steel", Journal of Nuclear Materials 103/104, 699, 1981.
- [193] Tortorelli, P.F. and DeVan, J.H., "The Effect of Nickel Concentration on the Mass Transfer of Fe-Ni-Cr Alloys in Lithium", Journal of Nuclear Materials 103/104, 633, 1981.
- [194] Burrow, G.C., Down, M.G. and Bagnall, C., "Corrosion Inhibition Experiments in Liquid Lithium", Journal of Nuclear Materials 103/104, 657, 1981.

- [195] Talbot, J.B., Fisher, P.W. and Clinton, S.D., "Recent Results on the Gettering of Tritium from Molten Lithium", Journal of Nuclear Materials 103/104, 681, 1981.
- [196] Borgstedt, H.U., "Material Problems Arising from Impurity Gettering of Lithium by Zirconium or Titanium", Journal of Nuclear Materials 103/104, 693, 1981.
- [197] Barker, M.G., et al., "The Interaction of Chromium with Nitrogen Dissolved in Liquid Lithium", Journal of Nuclear Materials 114, 143, 1983.
- [198] Natesan, K., "Influence of Non-metallic Elements on the Compatibility of Structural Materials with Liquid Alkali Metals", Journal of Nuclear Materials 115, 251, 1983.
- [199] Smith, D.L. and Natesan, K., "Influence of Non-metallic Impurity Elements on the Compatibility of Liquid Lithium with Potential CTR Containment Materials", Nuclear Technology 22, 392, 1974.
- [200] Meadows, G.E. and Keough, R.F., "Lithium Purity and Characterisation", Journal of Materials for Energy Systems 2, 44, 1981.
- [201] Hubberstey, P., "Silicon Behaviour in Liquid Lithium Systems", Presented at the 3rd Topical Meeting on Fusion Reactor Materials, Albuquerque, NM, 1983 September 19-22.
- [202] Ruedl, E. and Sasaki, T., "Effect of Lithium on Grain-Boundary Precipitation in a Cr-Mn Austenitic Steel", Journal of Nuclear Materials 116, 112, 1983.
- [203] Bagnall, C., "A Study of Type 304 Stainless Steel Containment Tubing from a Lithium Test Loop", Journal of Nuclear Materials 103/104, 639, 1981.

- [204] Konvicka, H.R. and Reithmayr, P., "Characterization of 304-SS and 316-SS Exposed to Liquid Lithium for 10,000 hours", Journal of Nuclear Materials 103/104, 645, 1981.
- [205] Ruedl, E., et al., "Corrosion and Phase Stability of Cr-Mn Austenitic Steels Exposed to Pure Lithium", Presented at the 3rd Topical Meeting on Fusion Reactor Materials, Albuquerque, NM, 1983 September 19-22.
- [206] Leavenworth, H.W. and Cleary, R.E., "The Solubility of Ni, Cr, Fe, Ti and Mo in Liquid Lithium", Acta Metallurgica 9, 519, 1961.
- [207] Pulham, R.J. and Hubberstey, P., "Comparison of Chemical Reactions in Liquid Lithium with Those in Liquid Sodium", Journal of Nuclear Materials 115, 239, 1983.
- [208] Hoffman, N.J., Darnell, A. and Blink, J.A. "Properties of Lead-Lithium Solutions", Proceedings of 4th ANS Topical Meeting on the Technology of Controlled Nuclear Fusion, King of Prussia, PA, October 14-17, 1980, CONF 801011.
- [209] Smith, D.L. Mattas, R.F., Clemmer, R.G. and Davis, J.W., "First-Wall/Blanket Materials Selection for STARFIRE Tokamak Reactor", Proceedings of the Fourth Topical Meeting on the Technology of Controlled Nuclear Fusion, King of Prussia, PA, October 14-17, 1980, Tenney, F.H. and Hopkins, C.C. (eds.). CONF-801011, p. 1714, 1981 July.
- [210] Nygren, R.E., "Materials Issues in the Fusion Engineering Device", Journal of Nuclear Materials 103/104, 31, 1981.
- [211] Blink, J.A., Krikorian, O.H. and Hoffman, N.J., "Use of Lithium in Fusion Reactors", in "Metal Bonding and Interactions in High Temperature Systems", Cole, J.L., and Stwalley, W.C. (eds.), ACS Symposium Series 179, American Chemical Society, Washington, 1982.
- [212] Tortorelli, P.F. and Chopra, O.K., "Corrosion and Compatibility Considerations of Liquid Metals for Fusion Reactor Applications", Journal of Nuclear Materials 103/104, 621, 1981.

- [213] Devan, J.H., "Compatibility of Structural Materials with Fusion Reactor Coolant and Breeder Fluids", *Journal of Nuclear Materials* 84/86, 249, 1979.
- [214] Weeks, J.R. and Isaacs, H.S., "Corrosion and Deposition of Steels and Nickel-Base Alloys in Liquid Sodium", *Advances in Corrosion Science and Technology* 5, 1, 1973.
- [215] Draley, J.E. and Weeks, J.R., (eds.), "Corrosion by Liquid Metals", Plenum Press, New York, 1970.
- [216] Tiltz, T.E. and Wilson, J.W., "Behaviour and Properties of Refractory Metals", Stanford University Press, Stanford, 1965.
- [217] Sze, D.K., "Mass Transfer Modelling of Corrosion of Steel by Lithium and Lead", Presented at the 3rd Topical Meeting on Fusion Reactor Materials, Albuquerque, NM, 1983 September 19-22.
- [218] Alden, T., Stevenson, D.A. and Wulff, J., "Solubility of Nickel and Chromium in Molten Lead", *Transactions of the Metallurgical Society of AIME* 212, 15, 1958.
- [219] Seebold, R.E., Birks, L.S. and Brooks, E.J., "Selective Removal of Cr from Type 304 Stainless Steel by Air-Contaminated Lithium", *Corrosion* 16, 468t, 1960.
- [220] Leavenworth, H.W. and Gregory, D.P., "Mass Transfer of Type 316 Stainless Steel by Liquid Lithium", *Corrosion* 18, 43t, 1962.
- [221] Scully, J.C., "The Role of Surface Films in Stress Corrosion Cracking and Corrosion Fatigue", *Proceedings of Conference on Environmentally-Sensitive Fracture of Engineering Materials*, 1977.
- [222] Warke, W.R., Johnson, K.L. and Breyer, N.N., "Liquid Metal Embrittlement of Steel by Lead and Lead Alloys", in reference[215], p. 417.

- [223] Asher, R.C., Davids, D. and Beetham, S.A., "Some Observations on the Compatibility of Structural Materials with Molten Lead", *Corrosion Science* 17, 545, 1977.
- [224] Friend, W.Z., "Corrosion of Nickel and Nickel-Base Alloys", J. Wiley and Sons, New York (1980), p. 187, 1980.
- [225] Distefano, J.R. and Litman, A.P., "Effects of Impurities in Some Refractory Metal-Alkali Metal Systems", *Corrosion* 20, 392t, 1964.
- [226] Klueh, R.L., "Oxygen Effects on the Corrosion of Niobium and Tantalum by Liquid Lithium", *Metallurgical Transactions* 5, 875, 1974.
- [227] Chalk River Nuclear laboratories, unpublished data, 1966.
- [228] Pierini, G. et al., "Tritium Recovery from Liquid Li₁₇Pb₈₃", in "Fusion Technology 1982", Proceedings of the 12th Symposium on Fusion Technology, Jülich, 1982 September 13-17, Pergamon Press, Vol. 1, p. 663, 1983.
- [229] Calaway, W.F., "Electrochemical Extraction of Hydrogen from Molten LiF-LiCl-LiBr and Its Application to Liquid Lithium Fusion Reactor Blanket Processing", *Nuclear Technology* 39, 63, 1978.
- [230] Buxbaum, R.E. and Johnson, E.F., "The Use of Yttrium for the Recovery of Tritium from Lithium at Low Concentrations", *Nuclear Technology* 49, 307, 1980.
- [231] Wu, C.H. and Ihle, H.R., "Thermochemistry of the Dimer Lithium Hydride Molecule Li₂H₂(g)", "Metal Bonding and Interaction in High Temperature Systems". Gole, J.L. and Stwalley, W.C. (eds.), ACS Symposium Series No. 179, American Chemical Society, Washington, 1982.
- [232] Ihle, H.R., "Thermochemistry of Fusion Reactor Breeding Materials and their Interaction with Tritium", Presented at the Fusion Breeder Blanket Workshop, Erice, Italy, 1983 June 6-10.

- [233] Velechis, E., Yonko, R.M. and Maroni, V.A., "The Current Status of Fusion Reactor Blanket Thermodynamics", Argonne National Laboratory, ANL-78-109, 1979 April.
- [234] Reiter, F., Rota, R. and Camposilvan, J., "Thermodynamic Properties of Li₁₇Pb₈₃", in "Fusion Technology 1982", Proceedings of the 12th Symposium on Fusion Technology, Jülich, 1982 September 13-17, Pergamon Press, Vol. 1, p. 671, 1983.
- [235] Wu, C.H. and Blair, A.J., "A Study of the Interaction of Tritium with Liquid Li₁₇Pb₈₃", in "Fusion Technology 1982", Proceedings of the 12th Symposium on Fusion Technology, Juelich, 1982 September 13-17, Pergamon Press, Vol. 1, p. 669, 1983.
- [236] Pierini, G., "Tests for Hydrogen Isotope Recovery from Liquid Pb₈₃Li₁₇ Alloy", Presented at the Fusion Breeder Blanket Workshop, Erice, Italy, 1983 June 6-10.
- [237] Weston, J.R., et al., "Chemical Processing of Liquid Lithium Fusion Reactor Blankets", Proceedings of the 14th Intersociety Energy Conversion Engineering Conference, Boston, MA, 1979 August, CONF-790803-52, 1979.
- [238] Van Deventer, E.H., et al., "A Review of Fusion Related Experimentation on Blanket/Tritium Processing and Hydrogen Isotope Migration at Argonne National Laboratory", Proceedings of the ANS National Topical Meeting on Tritium Technology in Fission, Fusion and Isotopic Applications. The American Nuclear Society, p.144, 1980.
- [239] Larsen, F.M., Ortman, M.S. and Plute, K.E., "Comments on the Hydrogen Solubility Data for Liquid Lead, Lithium, and Lithium-Lead Alloys and Review of a Tritium-Solubility Model for Lithium-Lead Alloys", University of Wisconsin, UWFDM-415, 1981 May.

- [240] Talbot, J.B. and Clinton, S.D., "Liquid Lithium Blanket Processing Studies", Proceedings of a Symposium on the Engineering Problems of Fusion Research, San Francisco, CA, 1979 November 13, CONF-791102-20, 1979.
- [241] Anantatmula, R.P. and Katsuta, A., "Hydrogen Trapping by Yttrium in Low Temperature Lithium", Presented at the 3rd Topical Meeting on Fusion Reactor Materials, Albuquerque, NM, 1983 September 19-22.
- [242] Mueller, W.M., Blackledge, J.P. and Libowitz, G.G., "Metal Hydrides", Academic Press Inc., New York, 1968.
- [243] Veleckis, E., Yonco, R.M. and Maroni, V.A., "Solubility of Lithium Deuteride in Liquid Lithium", Journal of the Less-Common Metals 55, 85, 1977.
- [244] Plute, K.E., Larsen, E.M. and Sze, D.K., "Tritium Recovery from Liquid Lithium-Lead by Vacuum Degassing", Nuclear Technology/Fusion 4, 407, 1983.
- [245] Natesan, K. and Smith, D.L., "Effectiveness of Tritium Removal from a CTR Lithium Blanket by Cold Trapping Secondary Liquid Metals Na, K and NaK", Nuclear Technology 22, 138, 1974.
- [246] Bull, P. (editor), IAEA Advisory Group, "Chemical Aspects of Fusion Technology - 1982", Nuclear Fusion 23, 955, 1983.
- [247] Johnson, C.E. and Hollenberg, G.W., "Recent Advances in the Development of Solid Breeder Materials", Presented at the 3rd Topical Meeting on Fusion Reactor Materials, Albuquerque, NM, 1983 September 19-22.
- [248] Johnson, C.E., Clemmer, R.G. and Hollenberg, G.W., "Solid Breeder Materials", Journal of Nuclear Materials 103/104, 547, 1981.
- [249] Roth, E., Presented at the Workshop on Fusion Blanket Technology, Erice, Italy, 1983 June 6-10.

- [250] Arons, R.M., Poeppel, R.B., Tetenbaum, M. and Johnson, C.E., "Preparation, Characterization, and Chemistry of Solid Ceramic Breeder Materials", Journal of Nuclear Materials 103/104, 573, 1981.
- [251] Suiter, D.J., Davis, J.W. and Kirkpatrick, B.A., "Preparation of Solid Tritium Breeding Compounds for Fusion Reactors", Journal of Nuclear Materials 103/104, 579, 1981.
- [252] Clemmer, R.G., Malecha, R.F. and Dudley, I.T., "The TRIO-01 Experiment", Nuclear Techology/Fusion 4, 83, 1983.
- [253] Wilson, C.N., "Fabrication of Lithium Ceramics by Hot Pressing", Hanford Engineering Development Laboratory, HEDL-SA-2594-FP, 1982 March.
- [254] Nakamura, T., "Experimental Program on Blanket Technology at JAERI". Presented at the Workshop on Fusion Blanket Technology, Erice, Italy, 1983 June 6-10.
- [255] Naruse, Y., et al., "Japanese Contributions to IAEA INTOR Workshop, Phase IIA, Chapter VIII: Tritium and Blanket", JAERI-M-82-175, 1982 November.
- [256] Hollenberg, G.W. and Baker, D.E., "Thermal Properties of Lithium Ceramics for Fusion Applications", HEDL-SA/2674-FP, 1982 March.
- [257] Christensen, A.O., Conway, K.C. and Kelley, K.K., U.S. Bureau of Mines Report of Investigations 5711, 1960.
- [258] Barin, I. and Knacke, O., "Thermochemical Properties of Inorganic Substances", Springer-Verlag, Berlin, 1973.
- [259] Tanifuji, T., Shiozawa, K. and Nasu, S., "Heat Capacity of Lithium Oxide from 306 to 1073 K", Journal of Nuclear Materials 78, 422, 1978.

- [260] Gurwell, W.E., "Characterization of Commercial Aluminates, Silicates, and Zero X Materials", Battelle Northwest Labs, Wa., BNW-CC-464, 1966 January.
- [261] Finn, P.A., Kurasawa, T., Nasu, S., Noda, K., Takahashi, T., Takeshito, H., Tanifuji, T. and Watanabe, H., "Solid Oxide Compounds - Properties Necessary for Fusion Applications", Proceedings of the 9th Symposium on Engineering Problems of Fusion Research, Chicago, IL, 26-29, October 1981.
- [262] Takahashi, T. and Kikuchi, T., "Porosity Dependence on Thermal Diffusivity and Thermal Conductivity of Lithium Oxide From 200 to 900°C", Journal of Nuclear Materials 91, 93, 1980.
- [263] Kurasawa, T., Takahashi, T., Noda, K. Takeshita, H., Nasu, S. and Watanabe, H., "Thermal Expansion of Lithium Oxide", Journal of Nuclear Materials 107, 334, 1982.
- [264] Kimura, H., Asuno, M. and Kubo, K., "Vaporization of Solid Lithium Nitride", Journal of Nuclear Materials 91, 200, 1980.
- [265] Ikeda, Y., Ito, H., Matsumoto, G. and Nasu, S., "A Mass Spectrometric Study of Vaporization of Li₂O with some Refractory Metal Cells", Mass Spectroscopy (Japan) 27, 263, 1979.
- [266] Kudo, H., Wu, C.H. and Ihle, H.R., "Mass-Spectrometric Study of the Vaporization of Li₂O(s) and Thermochemistry of Gaseous LiO, Li₂O, Li₃O, and Li₂O₂", Journal of Nuclear Materials 78, 380, 1978.
- [267] Ikeda, Y., Ito, H., Matsumoto, G. and Hayashi, H., "The Vaporization and Thermochemical Stability of Lithium Aluminates", Journal of Nuclear Materials 97, 47, 1981.
- [268] Nakagawa, H., Asano, M. and Kubo, K., "Mass-Spectrometric Study of the Vaporization of Lithium Metasilicate", Journal of Nuclear Materials 102, 292, 1981.

- [269] Guggi, D., Ihle, H.R. and Neubert, A., "Thermal Stability of Solid Lithium Compounds Proposed for Use in CTR Blankets". Proceedings of the 9th Symposium on Fusion Technology, Garmisch Partenkirchen, EUR 5602, p.635, 1976.
- [270] Finn, P.A., Breon, S.R. and Chellew, N.R., "Compatibility Study of Solid Ceramic Breeder Materials", Journal of Nuclear Materials 103/104, 1981.
- [271] Porter, D.L., et al., "Irradiation and Compatibility Testing of Li₂O Materials at EBR-II", Argonne National Laboratory, ANL/FPP/TM-167, 1982 December.
- [272] Chopra, O.K., Kurasawa, T. and Smith, D.L., "Compatibility of Ferritic Steels With Sintered Li₂O Pellets in a Flowing Helium Environment", Presented at the 3rd Topical Meeting on Fusion Reactor Materials, Albuquerque, NM, 1983 September 19-22.
- [273] Kurasawa, T., Takeshita, H. and Nasu, S., "Compatibility Between Several Heat Resistant Alloys and Sintered Li₂O in Static Helium Gas Environment", Journal of Nuclear Materials 92, 67, 1980.
- [274] Kurasawa, T., Takeshita, H., Muraoka, S., Nasu, S. Miyake, M. and Sano, T., "Reaction of Several Iron and Nickel Based Alloys with Sintered Li₂O Pellets", Journal of Nuclear Materials 80, 48, 1979.
- [275] Chopra, O.K. and Smith, D.L., "Interactions of Solid Ceramic Breeding Materials with Structural Alloys", Journal of Nuclear Materials 103/104, 555, 1981.
- [276] Noda, K., et al., "Irradiation Effects on Lithium Oxide", Presented at the 3rd Topical Meeting on Fusion Reactor Materials, Albuquerque, NM, 1983 September 19-22.
- [277] Noda, K., Uchida, K., Tanifuji, T. and Nasu, S., "Radiation Damage in Sintered Li₂O Pellets - ESR Study", Journal of Nuclear Materials 91, 234, 1980.

- [278] Uchida, K., et al., "Optical Absorption Spectra of Neutron-Irradiated Li₂O", *Physica Status Solidi(a)* 58, 557, 1980.
- [279] Noda, K., Uchida, K., Tanifuji, T. and Nasu, S., "Study of Radiation Damage in Li₂O by Means of Electron-Spin Resonance", *Physical Review B* 24, 3736, 1981.
- [280] Uchida, K., Akabor, M., Noda, K., Tanifuji, T. and Nasu, S., "Recoil Range of 2.7 MeV Tritons Produced by the $^6\text{Li}(\text{n},\alpha)^3\text{H}$ Reaction in LiO₂ Single Crystals", *Journal of Nuclear Materials* 89, 92, 1980.
- [281] Yang, L., Medico, R., Baugh, W. and Schultz, K., "Radiation Study of Lithium Compound Samples For Tritium Breeding Applications", *Journal of Nuclear Materials* 103/104, 585, 1981.
- [282] Hollenberg, G.W., "An Irradiation Experiment for Lithium Ceramics", Hanford Engineering Development Laboratory, HEDL-SA-2678-FP, 1982 March.
- [283] Hollenberg, G.W., "Fast Neutron Irradiation Results on Li₂O, Li₄SiO₄, Li₂ZrO₃, and LiAlO₂", Presented at the 3rd Topical Meeting on Fusion Reactor Materials, Albuquerque, NM, 1983 September 19-22.
- [284] Nasu, S., Fukai, K. and Tanifuji, T., "Microhardness and Microstructures of Neutron Irradiated Li₂O Pellets", *Journal of Nuclear Materials* 78, 254, 1978.
- [285] Takeshita, H., et al., "Reaction of Molybdenum and Molybdenum-Base Alloy With Sintered Li₂O Pellets", *Journal of Nuclear Materials* 80, 249, 1979.
- [286] Yang, L., Lindgren, J.R., Stetson, R.F. and Graumann, D., "Fabrication of Lithium Blanket Module (LBM) Components for TFTR. Part 1 - Lithium Oxide Pellets", Presented at the 3rd Topical Meeting on Fusion Reactor Materials, Albuquerque, NM, 1983 September 19-22.
- [287] Ortman, M.S. and Larsen, E.M., "Preparation, Characterization and Melting Point of High-Purity Lithium Oxide". *Journal of the American Ceramic Society* 66, 645, 1983.

- [288] Jeppson, D.W., Muhlstein, L.D. and Cohen, S., "Fusion Reactor Breeder Material Safety Compatibility Studies", Nuclear Technology/Fusion 4, 277, 1983.
- [289] Clemmer, R.G., "The Development of Tritium Breeding Blankets for DT-Burning Fusion Reactors", Proceedings of the Fourth Topical Meeting on the Technology of Controlled Nuclear Fusion, King of Prussia, PA, October 14-17, 1980, Tenney, F.H. and Hopkins, C.C. (eds.). CONF-801011, p. 526, 1981 July.
- [290] Guggi, D., et al., "Diffusion of Tritium in Single Crystal Li₂O". Journal of Nuclear Materials 118, 100, 1983.
- [291] O'Kula, K.R. and Vogelsang, W.F., "Aspects of Tritium Release from Neutron-Irradiated Lithium Oxide", Presented at the 3rd Topical Meeting on Fusion Reactor Materials, Albuquerque, NM, 1983 September 19-22.
- [292] Katsuta, H., Konishi, S. and Yoshida, H., "Solubility and Diffusivity of Hydrogen in Li₂O", Journal of Nuclear Materials 116, 244, 1983.
- [293] Okuno, K. and Kudo, H., "Thermal Release of Tritium Produced in Sintered Li₂O Pellets", Journal of Nuclear Materials 116, 82, 1983.
- [294] Kudo, H. and Okuno, K., "Kinetic Studies of the Tritium Release Process in Neutron-Irradiated Li₂O and LiOH", Journal of Nuclear Materials 101, 38, 1981.
- [295] Vasil'ev, V.G., et al., "Investigation of the Physical-Chemical Properties of Irradiated Inorganic Compounds of Lithium Oxides, Aluminates and Silicates", US/USSR Workshop on Engineering and Economic Problems of ETF, Moscow and Leningrad, USSR, 1979.
- [296] Nasu, S., et al., "Tritium Release from Neutron-Irradiated Li₂O Pellets", Journal of Nuclear Materials 68, 261, 1977.

- [297] Johnson, C.E. and Hollenberg, G.W., "Recent Advances in the Development of Solid Breeder Materials", Presented at the 3rd Topical Meeting on Fusion Reactor Materials, Albuquerque, NM, 1983 September 19-22.
- [298] Smith, D.L., et al., "Analysis of In-Situ Tritium Recovery From Solid Fusion Reactor Blankets", Proceedings of the Fourth Topical Meeting on the Technology of Controlled Nuclear Fusion, King of Prussia, PA, October 14-17, 1980, Tenney, F.H. and Hopkins, C.C. (eds.). CONF-801011, p. 560, 1981 July.
- [299] Norman, J.H. and Hightower, G.R., "Measurements of the Activity Coefficient of LiOH Dissolved in Li₂O(s) for an Evaluation of Li₂O as a Tritium Breeder Material", Presented at the 3rd Topical Meeting on Fusion Reactor Materials, Albuquerque, NM, 1983 September 19-22.
- [300] Ihle, H.R. and Wu, C.H., "The Solubility of Hydrogen Isotopes in Solid Li₂O", Presented at the 3rd Topical Meeting on Fusion Reactor Materials, Albuquerque, NM, 1983 September 19-22.
- [301] Morgan, G.D., IEA Workshop on Solid Breeder Materials, Albuquerque, NM, 1983 September 22-23.
- [302] O'Kula, K.R. and Sze, D.K., "Tritium Recovery from Solid Breeders: Implications of the Existing Data", Proceedings of the ANS Topical Meeting on Tritium Technology in Fission, Fusion and Isotopic Applications. The American Nuclear Society, p. 286, 1980.
- [303] Tanifugi, T., et al., "Tritium Release from Neutron-Irradiated Li₂O; Constant Rate Heating Measurements", Journal of Nuclear Materials 95, 108, 1980.
- [304] Bertone, P.C. and Jassby, D.L., "Tritium Recovery from Lithium Oxide Pellets", Presented at the 3rd Topical Meeting on Fusion Reactor Materials, Albuquerque, NM, 1983 September 19-22.

- [305] Clemmer, R.G. et al., "The TRIO-01 Experiment: In-Situ Tritium Recovery Results", Presented at the 3rd Topical Meeting on Fusion Reactor Materials, Albuquerque, NM, 1983 September 19-22.
- [306] Kurasawa, T., et al., "In-Situ Tritium Recovery Experiment from Lithium Oxide Under High Neutron Fluence", Presented at the 3rd Topical Meeting on Fusion Reactor Materials, Albuquerque, NM, 1983 September 19-22.
- [307] Krakowski, R.A. and Hagnson, R.L., "Compact Fusion Reactors," Los Alamos National Laboratory, LA-UR-83-930(Rev.), 1983.
- [308] Baker, L.J., "INTOR Test Sector: Neutronics", Presented at the Workshop on Fusion Blanket Technology, Erice, Italy, 1983 June 6-10.
- [309] Dittrich, H., Kuchle, M., Malang, S., Suppan, A. and Taczanowski, S., "A Breeding Ball Blanket Concept and the Integration into the INTOR Design", Presented at the Workshop on Fusion Blanket Technology, Erice, Italy, 1983 June 6-10.
- [310] Chevereau, G., "Solid Breeder Blanket Concepts", Presented at the Workshop on Fusion Blanket Technology, Erice, Italy, 1983 June 6-10.
- [311] Bond, A., "INTOR Test Sector: Overview and Design Choices", Presented at the Workshop on Fusion Blanket Technology, Erice, Italy, 1983 June 6-10.
- [312] Blanket Comparison and Selection Study, contractors' meeting, 1983 December.
- [313] Verrall, R.A. and Leung, T.C., Report of visit to attend the Blanket Comparison and Selection Study Workshop, Argonne National Laboratory, 1983 September 13-14.
- [314] Gierszewski, P.J., private communication, 1983 December.

- [315] Verrall, R.A., Information obtained at the Fusion Blanket Technology Workshop, Erice, Italy, 1983 June 6-10.
- [316] "Proceedings of the Workshop on Tritium Breeding Solids - Research and Development", McDonnell Douglas Astronautics Company, DOE/ET-52039/1, 1980.
- [317] Commission of the European Communities, document EUR FU BRU/XII-1099/83-MATIA 4, 1983 December.
- [318] Carré, F., et al., "Fusion Breeder Blanket Comparative Evaluation Study", CEA/Saclay, Report EMT/SERMA/BP/84/No. 584 "T" 3591-21-000, 1984.
- [319] Hancox, R., private communication, 1984 January 9.
- [320] Progress Report on Fusion Reactor Materials Research and Development in Japan, Japan Atomic Energy Research Institute, 1982.
- [321] Canadian Fusion Fuels Technology Project, private communication, 1983 December.
- [322] Jackson, D.P., et al., "A Review of Fusion Breeder Blanket Technology, Part II, CFFTP Report (in press).
- [323] Fraser, J.S., Hoffmann, C.R., Schriber, S.O., Garvey, P.M. and Townes, B.M., "A Review of Prospects for an Accelerator Breeder", Atomic Energy of Canada Limited, AECL-7260, 1981 December.
- [324] Schriber, S.O., "Canadian Accelerator Breeder System Development", Atomic Energy of Canada Limited, AECL-7840, 1982 November.
- [325] Carlick, E.C., private communication, 1983 August.
- [326] Lone, M.A., et al., "Characteristics of a Thermal Neutron Source Based on an Intermediate Energy Proton Accelerator", Atomic Energy of Canada Limited, AECL-7839, 1983 March.

- [327] Heinz, S., private communication, 1983 September.
- [328] Hastings, I.J., Hunt, C.E.L., Lipsett, J.J. and MacDonald, R.D., "Behaviour of Short-Lived Fission Products within Operating UO₂ Fuel Elements", Res Mechanica 6, 167, 1983.
- [329] Drolet, T.S., Wong, K.Y. and Diner, P.J.C., "Canadian Experience with Tritium - The Basis of a New Fusion Project", Nuclear Technology/Fusion 5, 17, 1984.
- [330] Kirkaldy, J.S., et al., "Tritium Surface Interactions - A Study to Define Current Understanding and Areas for Future R&D", Canadian Fusion Fuels Technology Project, CFFTP-83015, 1983 June.
- [331] MacEwen, S.R., Zee, R.H. and Birtcher, R.C., "Point Defect Production and Annihilation in Neutron-Irradiated Zr", Journal of Nuclear Materials (in press) 1984.

APPENDIX: TRITIUM PRODUCTION**A.1 Fission Reactors**

Both the projected tritium requirements of fusion reactors and current tritium production methods and facilities have been reviewed by Rhinehammer and Wittenberg[1]. A recent assessment of Ontario Hydro's CANDU reactors[2] estimates a total tritium production of ≈ 2 kg/a in their heavy water moderators. Studies of tritium production in CANDU reactor adjustor rods[3] indicate that additional tritium equivalent to 0.75 of the current moderator production could be manufactured in this manner. Preliminary investigation of enhanced tritium production in CANDU fuel rods[4] has also been undertaken. All of this work indicates that, while tritium produced in fission reactors will be valuable for initial experiments in D-T burning, fusion reactors must be self-sustaining in tritium.

A.2 Spallation Breeding

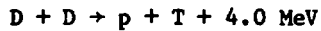
The history of the Canadian interest in accelerator-based breeders is briefly documented in the report of Fraser et al.[5], which reviews the prospects for an accelerator breeder within the Canadian fission reactor economy. The breeder envisaged in that report consists of an accelerator providing a 300 mA, 1 GeV proton beam and a high Z target, likely a liquid metal, on which the beam impinges and releases neutrons through spallation reactions. The anticipated neutron fluence from the target is $\approx 5 \times 10^{19}$ n/s. The breeding takes place in an appropriate blanket surrounding the target. The breeder could readily be converted to a tritium breeder by utilizing an appropriately designed breeder blanket containing lithium. A simplistic estimate of the annual production of tritium from such a facility yields a value of ≈ 10 kg.

The time scale being considered for development of the accelerator-based breeder has been selected to match predicted demands for make-up supplies of fissile fuel over the long term[5,6]. As a result the time frame is similar to that currently foreseen for fusion reactor development. The development scenario[6] envisages a staged development which would see a 70 mA, 1 GeV

pilot plant version of the breeder come on line in about 2005. This device could produce only ≈ 25 g/a of tritium. There is little doubt, however, that the development program could be speeded up very considerably if the necessary markets could be confidently identified.

A.3 DD Reactor Breeders

In a DD thermonuclear reactor the primary fusion reactions



occur with nearly equal probability. Most of the tritium which is generated as a product in the second of these reactions will be burned in situ by the reaction



It follows that the average fusion energy released per neutron produced will be ≈ 12.4 MeV. This is a much smaller value than the energy associated with neutron production using fission or spallation, and is such that a DD tritium breeder should be capable of fueling non-breeding DT reactors having a power output greater than that of the breeder itself.

Jassby and Katsurai[7] have considered the scenario in which a DD tritium breeder fuels non-breeding DT reactors. They estimate the thermal support ratio (the ratio of the thermal power output from the non-breeding DT reactors to that from the DD breeder) could be as high as 1.5. The minimum size of a DD reactor is considerably larger than that for a DT reactor. Jassby and Katsurai indicate a typical breeder power output of 10 GW. It is difficult to envisage a commitment to a machine of this enormous size and cost until one has gained considerable operating experience with breeding DT power reactors of more modest size.

A.4 References to the Appendix

- [1] Rhinehammer, T.B. and Wittenberg, L.J., "An Evaluation of Fuel Resources and Requirements for the Magnetic Fusion Energy Program", US DOE Mound Report MLM-2419, 1978.
- [2] Brereton, S., "Tritium Supply from Ontario Hydro's Nuclear Generating Stations", CFFTP Report 82001, 1982 (private communication).
- [3] Brereton, S., "Feasibility of Breeding Tritium Using Lithium in the Adjustor Rods of a CANDU Reactor", CFFTP Report 830014, 1983 (private communication).
- [4] Miller, J.M. and Douglas, S.R., "Tritium Production from Lithium Aluminate (LiAlO_2) in the NPD Reactor", Atomic Energy of Canada Limited, CRNL-2556, 1983 (private communication).
- [5] Fraser, J.S., Hoffmann, C.R., Schriber, S.O., Garvey, P.M. and Townes, B.M., "A Review of Prospects for an Accelerator Breeder", Atomic Energy of Canada Limited, AECL-7260, 1981.
- [6] Schriber, S.O., "Canadian Accelerator Breeder System Development", Atomic Energy of Canada Limited, AECL-7840, 1982.
- [7] Jassby, D.L. and Katsurai, M., "Fuel Provision for Non-Breeding Deuterium-Tritium Fusion Reactors", Journal of Fusion Energy 2, 197, 1982.